START

2710 0024896

ENGINEERING CHANGE NOTICE

Page 1 of 2

1. ECN 185093

Proj. ECN

2. ECN Category (mark one)	Supplemental	[]	Change ECN	[]	Supersedure	[]	
Cancel/Void []	Direct Revision	[X]	Temporary	[]	Discovery	[]	

3. Originator's Name, Organization, MSIN, and Telephone No. RD Crowe/SA&R/29120/H5-32/6-8343 ~~N239D~~ N336G		4. Date 7/24/92
5. Project Title/No./Work Order No. Waste Remediation Safety Programs	6. Bldg./Sys./Fac. No. 241-BX, 241-BY, 241-C, 241-T, and 241-TY	7. Impact Level 2 SQ
8. Document Number Affected (include rev. and sheet no.) WHC-SD-WM-RPT-032, Rev. 0, 1-237	9. Related ECN No(s). NA	10. Related PO No. NA

11a. Modification Work	11b. Work Package Doc. No.	11c. Complete Installation Work	11d. Complete Restoration (Temp. ECN only)
[] Yes (fill out Blk. 11b) [X] No (NA Blks. 11b, 11c, 11d)	NA	NA Cog. Engineer Signature & Date	NA Cog. Engineer Signature & Date

12. Description of Change

The purpose of the changes were to prepare the document for public release. All changes were editorial. No changes were made to the technical information presented in the document.

DEC 1992 RECEIVED EDMC

13a. Justification (mark one)	Criteria Change	[]	Environmental	[]	Facilitate Const.	[]	
Design Error/Omission []	Design Improvement	[X]	As-Found	[]	Const. Error/Omission	[]	

13b. Justification Details

Public release of the document requested by the Department of Energy.

14. Distribution (include name, MSIN, and no. of copies)

Onsite Distribution Sheet attached
Offsite Distribution list included at end of document

RELEASE STAMP

OFFICIAL RELEASE BY WHC
DATE NOV 09 1992
Sta. 21

A-7900-013-2 (11/88) {EF} GEF095
Engineering Change Notice

ENGINEERING CHANGE NOTICE

1. ECN (use no. from pg. 1): 185093

15. Design Verification Required	16. Cost Impact				17. Schedule Impact (days)	
	ENGINEERING		CONSTRUCTION			
[] Yes	Additional	[] $	Additional	[] $	Improvement	[]
[X] No	Savings	[] $	Savings	[] $	Delay	[]

18. Change Impact Review: Indicate the related documents (other than the engineering documents identified on Side 1) that will be affected by the change described in Block 12. Enter the affected document number in Block 19.

SDD/DD	[]	Seismic/Stress Analysis	[]	Tank Calibration Manual	[]
Functional Design Criteria	[]	Stress/Design Report	[]	Health Physics Procedure	[]
Operating Specification	[]	Interface Control Drawing	[]	Spares Multiple Unit Listing	[]
Criticality Specification	[]	Calibration Procedure	[]	Test Procedures/Specification	[]
Conceptual Design Report	[]	Installation Procedure	[]	Component Index	[]
Equipment Spec.	[]	Maintenance Procedure	[]	ASME Coded Item	[]
Const. Spec.	[]	Engineering Procedure	[]	Human Factor Consideration	[]
Procurement Spec.	[]	Operating Instruction	[]	Computer Software	[]
Vendor Information	[]	Operating Procedure	[]	Electric Circuit Schedule	[]
OM Manual	[]	Operational Safety Requirement	[]	ICRS Procedure	[]
FSAR/SAR	[]	IEFD Drawing	[]	Process Control Manual/Plan	[]
Safety Equipment List	[]	Cell Arrangement Drawing	[]	Process Flow Chart	[]
Radiation Work Permit	[]	Essential Material Specification	[]	Purchase Requisition	[]
Environmental Impact Statement	[]	Fac. Proc. Samp. Schedule	[]		[]
Environmental Report	[]	Inspection Plan	[]		[]
Environmental Permit	[]	Inventory Adjustment Request	[]		[]

19. Other Affected Documents: (NOTE: Documents listed below will not be revised by this ECN.) Signatures below indicate that the signing organization has been notified of other affected documents listed below.

Document Number/Revision	Document Number/Revision	Document Number Revision

20. Approvals

	Signature	Date		Signature	Date
OPERATIONS AND ENGINEERING			ARCHITECT-ENGINEER		
Cog./Project Engineer R. D. Crowe		7/24/92	PE		
Cog./Project Engr. Mgr. J. M. Grigsby		7/24/92	QA		
QA D. C. Board		7-30-92	Safety		
Safety M. N. Islam		7-30-92	Design		
Security			Other		
Proj. Prog./Dept. Mgr. J. C. Fulton		7-3-92			
Def. React. Div.					
Chem. Proc. Div.					
Def. Wst. Mgmt. Div.			DEPARTMENT OF ENERGY		
Adv. React. Dev. Div.					
Proj. Dept.					
Environ. Div.			ADDITIONAL		
IRM Dept.					
Facility Rep. (Ops.)					
Other for R. J. Cash		8/3/92			
M. H. Shannon		7/27/92			
J. L. Propson		8/4/92			

SUPPORTING DOCUMENT

1. Total Pages 260

2. Title

Ferrocyanide Waste Tank Hazard Assessment - Interim Report

3. Number

WHC-SD-WM-RPT-032

4. Rev No.

1

5. Key Words

ferrocyanide tank safety, waste tank safety, defense waste storage

APPROVED FOR PUBLIC RELEASE

U. Birkland 7/24/92

6. Author

Name: J. M. Grigsby

Ralph C. for J.M Grigsby

Signature

Organization/Charge Code 29120/~~N239D~~ N236G

7. Abstract

This report is an assessment of the prospects for energetic chemical reactions in ferrocyanide bearing waste tanks, based on currently available information as of the date of the original release of the document. Based on currently available data, the tank conditions appear to rule out such reactions. Additional information including tank waste sample data is needed to confirm this conclusion.

8. ~~PURPOSE AND USE OF DOCUMENT - This document was prepared for use within the U.S. Department of Energy and its contractors. It is to be used only to perform, direct, or integrate work under U.S. Department of Energy contracts. This document is not approved for public release until reviewed.~~

~~PATENT STATUS - This document copy, since it is transmitted in advance of patent clearance, is made available in confidence solely for use in performance of work under contracts with the U.S. Department of Energy. This document is not to be published nor its contents otherwise disseminated or used for purposes other than specified above before patent approval for such release or use has been secured, upon request, from the Patent Counsel, U.S. Department of Energy Field Office, Richland, WA.~~

DISCLAIMER - This report was prepared as an account of work sponsored by an agency of the United States Government. Neither the United States Government nor any agency thereof, nor any of their employees, nor any of their contractors, subcontractors or their employees, makes any warranty, express or implied, or assumes any legal liability or responsibility for the accuracy, completeness, or any third party's use or the results of such use of any information, apparatus, product, or process disclosed, or represents that its use would not infringe privately owned rights. Reference herein to any specific commercial product, process, or service by trade name, trademark, manufacturer, or otherwise, does not necessarily constitute or imply its endorsement, recommendation, or favoring by the United States Government or any agency thereof or its contractors or subcontractors. The views and opinions of authors expressed herein do not necessarily state or reflect those of the United States Government or any agency thereof.

9. Impact Level 2 SQ

10. RELEASE STAMP

OFFICIAL RELEASE BY WHC

DATE NOV 09 1992

Sta. 21

A-6400-073 (11/91) (EF) WEF124

RECORD OF REVISION	(1) Document Number WHC-SD-WM-RPT-032	Page 1

(2) Title
Ferrocyanide Waste Tank Hazard Assessment - Interim Report

CHANGE CONTROL RECORD

(3) Revision	(4) Description of Change - Replace, Add, and Delete Pages	Authorized for Release (5) Cog. Engr.	(6) Cog. Mgr.	Date
0	(7) EDT 131809 12/4/91			
1 RS	Completely replaces Rev. 0 with Rev. 1. This is a complete replacement of the earlier revision as per ECN 185093. No change bars are provided since changes were made to every page with the removal of the Predecisional label. All changes are editorial. No changes were made to the technical information presented in the document.	R. D. Crowe	J. M. Grigsby	7-24-92

A-7320-005 (08/91) (EF) WEF168

WHC-SD-WM-RPT-032 Rev. 1

FERROCYANIDE WASTE TANK HAZARD ASSESSMENT--INTERIM REPORT

Westinghouse Hanford Company

J. M. Grigsby
D. B. Bechtold
G. L. Borsheim
M. D. Crippen
D. R. Dickinson
G. L. Fox
D. W. Jeppson
M. Kummerer
J. M. McLaren
J. D. McCormack
A. Padilla
B. C. Simpson
D. D. Stepnewski

June 1992

Cleared for Public Release

This page intentionally left blank.

PREFACE

This report is published as a snapshot (as of November 1991) of what was known about the safety of continued in situ storage of ferrocyanide wastes at the Hanford Site. As such, it is not a final report and does not include research results that have become available during the review process this document has undergone. New information on ferrocyanide waste safety will be described and put into perspective in updated versions of this report and other reports used to report research findings.

One topic cited by several reviewers is the relative dearth of information regarding "In-Farm" waste. As described in the body of this report, these waste forms amount to roughly 20% of the total ferrocyanide waste. These waste forms are believed to be potentially more reactive than the remaining 80% of the waste.

Unfortunately, relatively little quantitative information was available earlier to characterize the reactivity of these waste forms. Because these waste forms were identified as being potentially more reactive than "U-Plant" and "T-Plant" waste, research efforts are now focused on the "In-Farm" wastes. Readers are alerted that tentative conclusions presented in this report for "U-Plant" and "T-Plant" waste do not necessarily apply to the "In-Farm" waste forms. Results of experimental programs designed to quantify the reactivity of "In-Farm" waste forms will be published when such results become available.

This page intentionally left blank.

CONTENTS

1.0 SUMMARY AND CONCLUSIONS 1-1
1.1 SUMMARY OF FERROCYANIDE HAZARD ASSESSMENT APPROACH 1-2
1.2 ASSESSMENT OF COMBUSTIBILITY (POTENTIAL FOR PROPAGATING EXOTHERMIC REACTIONS) 1-4
1.3 SUMMARY OF HOT SPOT ANALYSIS 1-11
1.4 INFORMATION NEEDED TO CONFIRM CONCLUSIONS AND RESOLVE THE SAFETY ISSUES 1-14

2.0 INTRODUCTION 2-1

3.0 SCOPE AND ASSESSMENT APPROACH 3-1
3.1 SCOPE 3-1
3.2 BACKGROUND 3-1
3.3 APPROACH TO THE FERROCYANIDE SAFETY ISSUE 3-2
3.3.1 Potential for Propagating Energetic Reactions 3-5
3.3.2 Potential for Energetic Chemical Runaway (Hot Spots) 3-6

4.0 METHODS TO ESTIMATE VALUES FOR KEY PARAMETERS 4-1
4.1 HISTORICAL DATA ON FERROCYANIDE PRECIPITATION AND FERROCYANIDE PREDICTIVE MODEL RESULTS 4-2
4.1.1 The Bismuth Phosphate and Uranium Recovery Processes 4-2
4.1.2 Scavenging Program 4-2
4.1.3 Processing in the 200 East Area 4-8
4.1.4 Processing in the 200 West Area 4-9
4.1.5 Estimated Ferrocyanide Tank Contents from Model Predictions 4-10
4.2 TANK SAMPLES AND ANALYSIS RESULTS 4-13
4.2.1 Tank 241-BY-104 4-15
4.2.2 Data Analysis and Interpretation of Samples Taken from Tanks 241-TY-101, -103, and -104 4-15
4.2.3 Recent Supernate Analyses from 200 East Area Ferrocyanide Tanks 4-19
4.2.4 Future Tank Sampling Activities 4-20
4.3 FLOWSHEET WASTE SIMULANTS AND ANALYSIS RESULTS 4-21
4.3.1 Composition of Synthetic U Plant Produced Sludge . . . 4-21
4.3.2 Synthetic In-Farm Produced Sludge 4-30
4.3.3 T Plant Decontamination Cycle Waste Produced Sludge 4-31
4.4 LIQUID LEVEL MEASUREMENTS 4-31
4.4.1 Liquid Level Measurement Locations 4-31
4.4.2 Liquid Level Determinations 4-31
4.5 GAMMA SCANS 4-35
4.5.1 Gross Gamma Scans--Routine Surveillance 4-40
4.5.2 Spectral Gamma Scans 4-40
4.5.3 Validation of Gamma Scan Readings 4-47
4.5.4 Application of Gamma Scans to Distribution of Ferrocyanide Within Waste Tanks 4-50
4.5.5 Lateral Maldistribution of Ferrocyanide Sludge 4-53

CONTENTS (continued)

4.6 ROUTINE TEMPERATURE MONITORING 4-53
4.7 THERMAL PROPERTY EVALUATIONS 4-60
4.7.1 Heat of Reaction 4-60
4.7.2 Fauske Adiabatic Calorimeter 4-61
4.7.3 Pacific Northwest Laboratory Testing 4-63
4.7.4 Los Alamos National Laboratory Thermal Testing . . . 4-72
4.8 NONTHERMAL SENSITIVITY TESTING 4-75
4.9 TANK HEAT LOAD BASED ON THERMAL MODELING EVALUATIONS 4-76
4.9.1 Thermal Model 4-76
4.9.2 Estimate of Heat Load 4-78
4.9.3 Distribution of Heat 4-80
4.9.4 Summary of Thermal Analysis 4-82
4.10 SUMMARY OF ESTIMATION OF KEY PARAMETERS 4-82
4.10.1 Ferrocyanide Concentration and Locations 4-82
4.10.2 Nitrate/Nitrite Concentrations 4-87
4.10.3 Organic Carbon Content/Concentrations 4-87
4.10.4 Water Content 4-91
4.10.5 Diluent Types and Concentrations 4-98
4.10.6 Decay Heat Load and Its Distribution 4-100
4.10.7 Reaction Initiation and Ignition Temperature 4-102
4.10.8 Waste Thermal Properties 4-103

5.0 POTENTIAL FOR ENERGETIC FERROCYANIDE REACTIONS 5-1
5.1 EVALUATION OF REACTIVITY 5-1
5.1.1 Basis of Calculation 5-1
5.1.2 Assumptions 5-1
5.1.3 Results of Calculations 5-4
5.1.4 Application to Ferrocyanide Tanks 5-12
5.1.5 Conclusions on Possible Combustibility of Tank Waste 5-15
5.1.6 Need for Experimental Measurements 5-16
5.2 POTENTIAL FOR ENERGETIC CHEMICAL RUNAWAY 5-16
5.2.1 Reactants and Heat Source Concentrated in a Layer 5-17
5.2.2 Reactants and Heat Source Concentrated in a Sphere 5-18
5.2.3 An Approach to Runaway Based on Tank Cooling Response Time 5-23

6.0 POTENTIAL FOR CHANGES IN TANK CONDITIONS 6-1
6.1 POTENTIAL FOR CONCENTRATION OF FERROCYANIDE DURING WASTE STORAGE 6-1
6.2 POTENTIAL FOR LOSS OF MOISTURE 6-2
6.2.1 Leakage 6-2
6.2.2 Evaporation 6-2
6.2.3 Moisture Loss Due to Radiolysis 6-4
6.2.4 Moisture Loss--Summary 6-4
6.3 POTENTIAL FOR CHANGES IN FERROCYANIDE REACTIVITY (CHEMICAL CHANGES/DEGRADATION) 6-4

7.0 REFERENCES 7-1

APPENDIXES

A FERROCYANIDE TANK LABORATORY RESULTS A-1
B FERROCYANIDE TANK GAMMA AND NEUTRON SCANS B-1
C SUPPORTING DOCUMENTATION C-1

LIST OF FIGURES

1-1 Approach to Assessing the Likelihood of Runaway Chemical Reactions in Ferrocyanide Waste Tanks 1-3

1-2 Reactivity Limits for Ferrocyanide Mixtures 1-7

3-1 Approach to Assessing the Likelihood of Runaway Reactions in Ferrocyanide Waste Tanks 3-4

4-1 Ferrocyanide Production by "U Plant" Flowsheet 4-5

4-2 Ferrocyanide Production by "T Plant" Flowsheet 4-6

4-3 Ferrocyanide Sludge Production by "In-Farm" Flowsheet 4-7

4-4 Thermogravimetric Analysis of U Plant Flowsheet Simulant Settled Sludge Composite 4-23

4-5 Thermogravimetric Analysis of U Plant Flowsheet Simulant Settled Sludge Composite Showing Reaction Release 4-24

4-6 Differential Scanning Calorimeter Analysis of U Plant Flowsheet Simulant Settled Sludge Composite 4-25

4-7 Reactive System Screening Tool Results of U Plant Flowsheet Simulant Solids 4-28

4-8 Reactive System Screening Tool Pressure Response for U Plant Flowsheet Simulant Solids 4-29

4-9 Neutron and Gamma Surveillance Scan Configuration 4-33

4-10 Liquid Levels Measured in Salt Wells 4-36

4-11 Interstitial Liquid Levels by Neutron Scan (1985-1991) for Tanks 241-BY-111, -112, 241-TX-118, and 241-TY-103 4-37

4-12 Interstitial Liquid Levels by Neutron Scan (1985-1991) for Tanks 241-BX-111, 241-BY-101, -103, and -104 4-38

4-13 Interstitial Liquid Levels by Neutron Scan (1985-1991) for Tanks 241-BY-105, -106, -107, and -110 4-39

LIST OF FIGURES (continued)

4-14 Collimated Cadmium Telluride Gamma Detector 4-41

4-15 Typical Gamma Energy Scan 4-42

4-16 Europium Scan for Tank 241-BY-104 4-45

4-17 Europium Scan for Tank 241-BY-106 4-46

4-18 Calculated Gamma Axial Profile--Uniform Source with Axial Material Density Variations 4-48

4-19 Calculated Gamma Axial Profiles--Variations in Source Distribution 4-49

4-20 Tank 241-BY-104 Temperature 4-55

4-21 Tank 241-BY-105 Temperature 4-56

4-22 Tank 241-BY-106 Temperature 4-57

4-23 Tank 241-BY-110 Temperature 4-58

4-24 Overall Reactive System Screening Tool Equipment Setup 4-62

4-25 Temperature History for Test A022-11, Fuel/Oxidant = 1 4-64

4-26 Pressure History for Test A022-11, Fuel/Oxidant = 1 4-65

4-27 Temperature Rate for Test A022-11, Fuel/Oxidant = 1 4-66

4-28 Temperature History for Test A021-25, Fuel/Oxidant = 0.45 4-67

4-29 Pressure History for Test A021-25, Fuel/Oxidant = 0.45 4-68

4-30 Temperature Rate for Test A021-25, Fuel/Oxidant = 0.45 4-69

4-31 Thermocouple Tree Data for Tank 241-BY-104 4-77

4-32 Comparison of Computer Prediction with Data, 2.46 kW 4-81

5-1 Combustibility Limits of Ferrocyanide Mixtures Reference Case . . 5-5

5-2 Combustibility Limits of Ferrocyanide Mixtures Effect of Initial Temperature 5-7

5-3 Combustibility Limits of Ferrocyanide Mixtures Effect of Ignition Temperature 5-8

5-4 Combustibility Limits of Ferrocyanide Mixtures Effect of Heat of Reaction 5-9

LIST OF FIGURES (continued)

5-5 Combustibility Limits of Dry Ferrocyanide Mixtures at High Temperatures. 5-10

5-6 Comparison of Combustibility Limits with Waste Tank Composition 5-13

5-7 Illustration of the Hot Spot Model in Tank 241-C-112 5-20

LIST OF TABLES

1-1 General Ferrocyanide Tank Waste Characteristics 1-4

1-2 Margin of Safety Between Ferrocyanide Reactivity Limits and Average Concentration in Sludge 1-8

1-3 Comparison of Upper-Bound Estimates of Heating Rates Required for Thermal Runaway Versus Available Heating Rates for Slab-Shaped Hot Spots 1-13

1-4 Illustration of Minimum Required Hot Spot Characteristics . . . 1-13

3-1 The 24 Single-Shell Tanks Declared to Involve the Ferrocyanide Unreviewed Safety Question 3-3

4-1 Key Parameters and Current Data Sources for Evaluating Reaction Propagation 4-3

4-2 Key Parameters and Data Sources for the Evaluation of Hot Spot Runaway 4-4

4-3 Comparison of Model Results with Baseline Values: Ferrocyanide Inventory at the End of Scavenging 4-11

4-4 Summary: Estimates of Tank Inventories, Adjusted for Post-Scavenging Transfer Activity 4-14

4-5 Analysis of Tank 241-BY-104 Core Sample Solids 4-16

4-6 Analysis of Tank 241-BY-104 Supernatant 4-17

4-7 Particle Size Distribution--Tank 241-BY-104 Solids 4-17

4-8 TY Tank Farm Summary Analysis 4-18

4-9 Cesium Distribution on Washing Single-Shell Tank Waste Samples 4-19

LIST OF TABLES (continued)

4-10 Analysis of BX and BY Tank Supernate Samples 4-20

4-11 Estimated Composition of Synthetic Composited U Plant Sludge Prepared from 0.0025 *M* Ferrocyanide Solution with Strontium Nitrate Addition to 0.004 *M* 4-27

4-12 Preliminary Analysis of Centrifuged, Dried, Synthetic U Plant Sludge 4-30

4-13 Analytical Content of the Most Concentrated Layer of Synthetic Centrifuged U Plant Sludge 4-30

4-14 Liquid Observation Well Locations in Ferrocyanide Tanks 4-32

4-15 Interstitial and Surface Liquid Levels in Ferrocyanide Tanks 4-34

4-16 Cesium Inventories and Heat Loads 4-43

4-17 Cesium Inventory in the Ferrocyanide Sludge Determined from the Spectral Gamma Scans 4-47

4-18 Upper-Bound Estimates of Peak Ferrocyanide Concentrations 4-52

4-19 Historic and Present Tank Temperature Averages 4-59

4-20 Calculated Heats of Reaction 4-61

4-21 Sensitivity Results 4-75

4-22 Ferrocyanide Tank Inventory Summary 4-83

4-23 Ferrocyanide Tank Historical Data Summary 4-85

4-24 Tanks Containing Significant Amounts of Organic Salts 4-88

4-25 Organic Content of Ferrocyanide Tanks 4-89

4-26 Comparison of Measured and Predicted Organic Content 4-91

4-27 Water of Hydration on Ferrocyanide Compounds 4-92

4-28 Water Content of Sludge Samples 4-94

4-29 Sludge Particle Size Parameters 4-94

4-30 Capillary Holdup in Porous Beds 4-95

4-31 Lowest Suggested Water Content 4-98

LIST OF TABLES (continued)

4-32 Synthetic U Plant Flowsheet Sludge 4-99

4-33 T Plant Sludge Analysis 4-99

4-34 Estimated Decay Heat Generation in Ferrocyanide Tanks 4-101

4-35 Ignition Temperature $Cs_2NiFe(CN)_6$ Stoichiometric Mix 4-103

4-36 Thermal Diffusivity 4-106

5-1 Differences in Internal Energy and Enthalpy 5-4

5-2 Margin of Safety Between Ferrocyanide Combustibility Limits and Average Concentration in Sludge 5-14

5-3 Maximum Temperature Versus Slab Thickness 5-17

5-4 Input Values for Upper-Bound Heat Rate Estimates 5-18

5-5 Comparison of Upper-Bound Estimates of Heating Rates Required for Thermal Runaway Versus Available Heating Rates for a Layer Concentration 5-19

5-6 Illustration of Required Hot Spot Characteristics with Hot Spot Diameter Equal to Nonconvective Sludge Height 5-22

5-7 Hot Spot Characteristics 5-23

5-8 Enveloping Ferrocyanide Tank Characteristics 5-24

5-9 Tank Characteristic Times 5-24

LIST OF TERMS

AC	adiabatic calorimetry
ARC	accelerating rate calorimetry
CW	coating waste
DSC	differential scanning calorimetry
DT	dip tubes
DTA	differential thermal analysis
EDTA	ethylenediaminetetraacetic acid
EIS	Environmental Impact Statement
FAI	Fauske and Associates, Inc.
FIC	Food Instrument Corporation
HEDTA	N-(hydroxyethyl)-ethylenediaminetriacetic acid
IC	first decontamination cycle
ITS	In-Tank Solidification
LOW	liquid observation wells
LANL	Los Alamos National Laboratory
LFL	lower flammability limit
MCNP	Monte Carlo neutron-photon
MT	manual tape
MW	metal waste
NPH	normal paraffin hydrocarbon
PNL	Pacific Northwest Laboratory
PSD	pulse shape discrimination
PUREX	Plutonium/Uranium Extraction (Plant)
RSST	Reactive System Screening Tool
SAR	safety analysis report
STG	scanning thermogravimetry
SST	single-shell tank
TBP	tributyl phosphate
TGA	thermogravimetric analysis
TOC	total organic carbon
TTX	time-to-explosion (testing)
USQ	Unreviewed Safety Question
VTS	vacuum thermal stability
Westinghouse Hanford	Westinghouse Hanford Company
ZC	zip cord

FERROCYANIDE WASTE TANK HAZARD ASSESSMENT--INTERIM REPORT

1.0 SUMMARY AND CONCLUSIONS

The purpose of this report is to document an assessment of the hazard represented by ferrocyanide-bearing chemical wastes stored in single-shell waste storage tanks on the Hanford Site. The tanks involved in this assessment were identified in an unusual occurrence report, and the uncertainties associated with the tanks were declared an Unreviewed Safety Question (USQ) (Deaton 1990). This assessment is a snapshot in time of the current understanding of the ferrocyanide hazard and should be recognized as an interim appraisal. It presents an integrated evaluation and interpretation of historical data and recently acquired information as of the time of the creation of this document.

This interim report will be revised and expanded as additional information becomes available through ongoing work in laboratory simulation, waste tank sampling, and chemical and thermocalorimetric analysis. Some of the issues presently being investigated, but not completed in time for this interim report, are the analyses of the In-Farm material, measurement of the burn propagation characteristics of all of the simulation materials, modeling of the aerosol generation and dispersion, and measurement of the hydraulic properties of the simulated material. The ultimate objective of the final version of this document is to provide the information needed for a technical basis to define the conditions for the safe storage of ferrocyanide-bearing waste.

The results of this study indicate that an uncontrolled, exothermic reaction in the ferrocyanide tanks is an unlikely event. This conclusion is tentative and is based on the current understanding of the contents of the waste tanks and the water-retention characteristics of the ferrocyanide-bearing sludge. Chemical reaction thermodynamics show that the waste compositions are noncombustible. The ferrocyanide sludges are moist (at least 40 wt% water) and contain little fuel. Approximately 80% of the ferrocyanide sludge was produced by processes (U Plant and T Plant processes) that left the material with low concentrations of ferrocyanide. This material is not expected to be combustible even if totally dry. The remainder (approximately 20%) of the ferrocyanide sludge was produced by a process (In-Farm) that resulted in fewer solid diluents in the waste. Additional information on the composition of In-Farm produced material is required for a definitive evaluation of combustibility. Conclusions on waste combustibility reached in this report do not apply to In-Farm produced material.

Review of the historical records and laboratory tests on flow characteristics led to the conclusion that sludge additions to the tanks spread across the entire tank diameter. This behavior suggests that potential segregation of material would occur in horizontal layers, if it occurred at all. Thus, local concentration variations or hot spots, if they exist, are predicted to occur as relatively thin layers that are readily cooled.

Hypothetical, spherical hot spots were analyzed and shown to require fission product concentrations that exceed any real possibility of occurring. This information leads to the tentative conclusion that thermal runaway in the ferrocyanide tanks is not possible.

In the process of evaluating available information to understand the hazard, further work needed to resolve data uncertainties has been identified. The sampling, laboratory, and surveillance programs that have been identified in the Ferrocyanide Program Plan (Cash and Mellinger 1991) should be continued to verify the tentative conclusions that are made in this document based on currently available information.

This summary outlines the basis for the foregoing tentative conclusions, discussing, in turn, the hazard assessment approach, review and evaluation of tank contents and waste properties, evaluation of combustibility, and the potential for thermal runaway reactions.

1.1 SUMMARY OF FERROCYANIDE HAZARD ASSESSMENT APPROACH

Ferrocyanide-bearing waste in underground tanks has been identified as a potential source for exothermic chemical reactions and subsequent dispersal of radioactive material to the environment. The hazard assessment approach used is to evaluate combustibility (the potential for the ferrocyanide waste to sustain propagating exothermic reactions) and the potential for thermal runaway (accelerating reaction rates due to chemical heating) due to hot spots. Waste material combustibility is assessed by developing propagation limits based on fuel, water, and diluent concentrations and on the chemical thermodynamics of the reactive system. The potential for thermal runaway by hot spots (local concentrations of fission products and ferrocyanide) is addressed by comparing calculated conditions required to form runaway hot spots to expected tank conditions. This assessment approach is shown in Figure 1-1.

An estimate of current tank conditions and key waste properties was developed from evaluations of available information including ferrocyanide scavenging and waste transfer records, monitoring data, and limited waste sample and simulant analysis results. The review of ferrocyanide scavenging and waste transfer records indicates that the ferrocyanide-bearing sludges were produced by three different processes: the U Plant, T Plant, and In-Farm processes. Sample data are available for T Plant processed waste. T Plant waste is stored in the TY Tank Farms. Waste simulant data are available for U Plant waste. U Plant waste is primarily stored in the BY Tank Farm. Little information is available for In-Farm waste. In-Farm waste is stored in the C Tank Farm. Based on the recent review, 7 of the 24 declared ferrocyanide tanks are believed to contain no significant (less than 1,000 mol) inventory of ferrocyanide.

The estimation of key tank and waste parameters is developed in Chapter 4.0 and summarized in Table 1-1. The requirements for initiating and sustaining energetic chemical reactions are developed in Chapter 5.0 based on the key parameters developed in Chapter 4.0. Finally, the potential for waste properties to change with time is discussed in Chapter 6.0. The hazard analyses and key parameters are summarized in Sections 1.2 and 1.3.

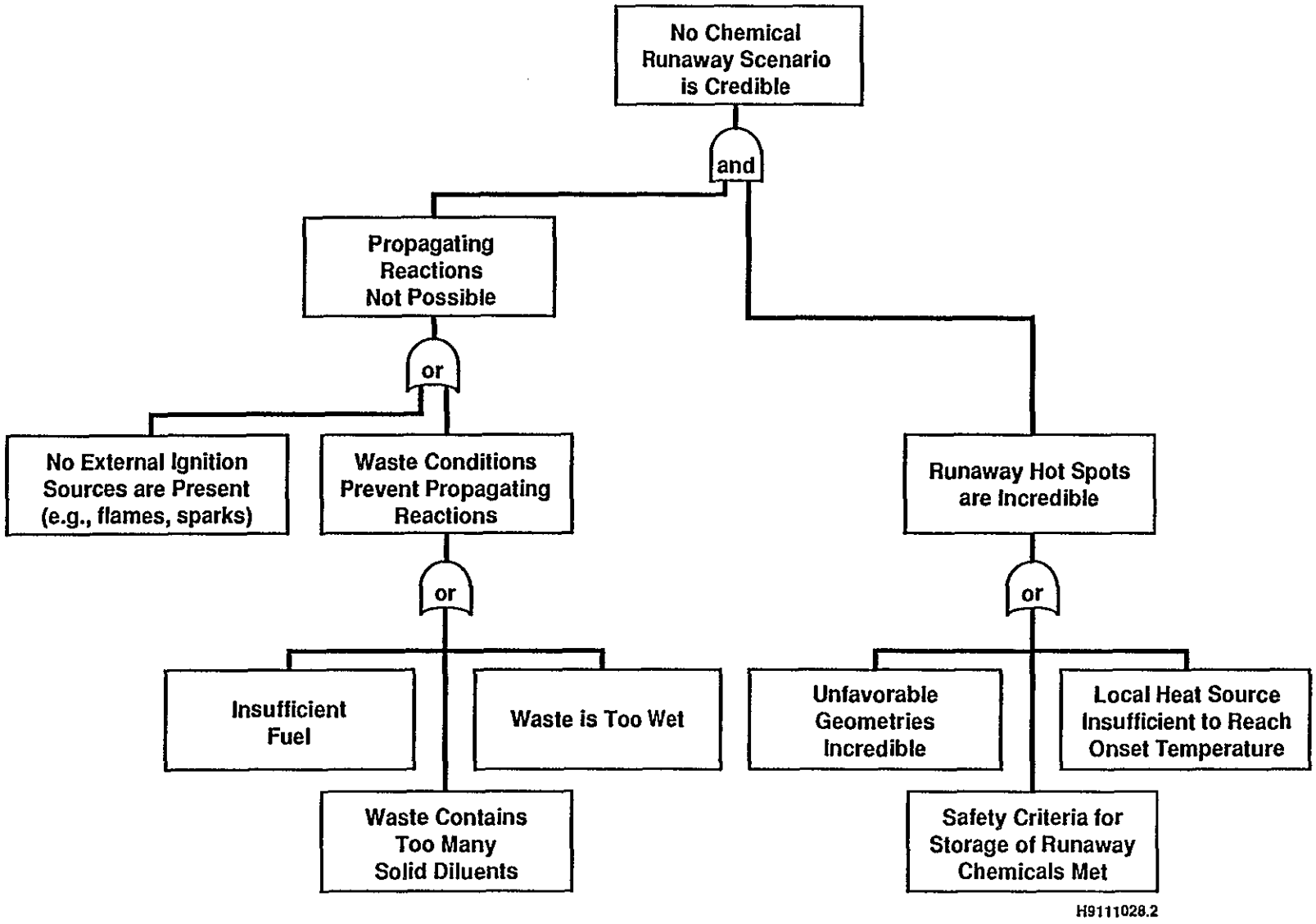

Figure 1-1. Approach to Assessing the Likelihood of Runaway Chemical Reactions in Ferrocyanide Waste Tanks.

Table 1-1. General Ferrocyanide Tank Waste Characteristics.

Parameter	Expected range of values
Bulk density	1.4 - 1.7 g/cm^3
Viscosity	Static viscosity >10,000 cP Apparent viscosity 100-200 cP
Thermal conductivity	Dry sludge: 0.17 W/m °C Wet sludge: 0.43-0.47 W/m °C
Specific heat	Dry sludge: 1,000 J/kg °C Wet sludge: 3,000 J/kg °C
Thermal diffusivity	Dry sludge: 7.2 E-08 to 9.1 E-08 m^2/s Wet sludge: 1.0 E-07 to 6.8 E-08 m^2/s
Concentration of ferrocyanide	0.004 to 0.10 *M*
Weight percent water	40% to 70%
Weight percent total organic carbon	<0.01% to 0.4%
Weight percent inerts	30% to 50%
Weight percent of ferrocyanide/oxidant mixture	0.5% to 6.0%
Waste temperatures	18 to 55 °C (64 to 130 °F)

The safety analysis process is intended to determine if and under what conditions the risk of continued storage of ferrocyanide-bearing waste is acceptable. Risk of continued storage must consider both the likelihood of runaway scenarios and, if credible, the consequences of such scenarios. This interim assessment addresses the potential for runaway. Consequences resulting from runaway scenarios will be addressed in a future report if credible scenarios are identified. It is recognized that the safety analysis process must continue until a conclusion is reached that has an adequate technical basis. Additional work needed to provide an adequate technical basis is discussed in Section 1.4.

1.2 ASSESSMENT OF COMBUSTIBILITY (POTENTIAL FOR PROPAGATING EXOTHERMIC REACTIONS)

The assessment of the potential for the ferrocyanide waste material to sustain propagating reactions compares the energy provided by the ferrocyanide-nitrate/nitrite reactions to the energy required to heat waste to the ignition temperature. Combustible material is defined as material that is able to maintain an exothermic reaction by producing sufficient heat to raise surrounding material to the ignition temperature. The ignition temperature is

defined as the minimum temperature at which material will flash or react vigorously. This is taken as the temperature where there is a significant increase in reaction rate from an Arrhenius-type to a propagating-type reaction. Limits on waste concentrations required to support propagation can be determined from chemical thermodynamics. Once the concentration limits are determined, waste compositions can be judged to be combustible or noncombustible.

If the material in the waste tanks contains a sufficient proportion of water or other substances that do not take part in an exothermic reaction, the material cannot sustain a reaction. If the available energy is insufficient to raise the reaction mass to the ignition temperature, propagation cannot occur. Therefore, it is possible by thermodynamic calculation to define compositions for which a sustained chemical reaction is impossible.

For the thermodynamic analysis, components of the waste were considered to belong to three general categories, based on their function as either heat producers or heat absorbers. The three categories are as follows.

1. The reacting species: A mixture of ferrocyanide and stoichiometric amounts of nitrate/nitrite that will react to produce heat. The heat of reaction must supply enough energy to the surrounding material to heat it to the ignition temperature.

2. Water: Present in the waste matrix, both as free water and water of hydration. The heat of reaction must supply enough energy to overcome both sensible heat and heat of vaporization for a reaction to take place.

3. Diluents: Inert materials, other than water, that do not participate in the reaction, including sodium nitrate/nitrite present in excess of the stoichiometric amount necessary for a reaction. Again, the heat of reaction must supply enough energy to heat the diluents to the reaction initiation temperature.

Two sets of thermodynamic conditions were considered, confined and unconfined:

- The first set of conditions assumed that the reaction took place in a confined volume within the waste without venting of product gases. As the gases accumulated in the confined space, the pressure would rise, and the vaporization of water would be suppressed. The effect is that the amount of heat that would otherwise be involved in the change of state would be available to contribute to the heatup of reactants. The confined case is not considered realistic because water vapor pressure would generate release pathways in the waste material.

- The second set of conditions allowed for the venting of product gases to a constant pressure sink, either through pathways in the material above the reacting region or because the reaction happens at the surface. The vented case is considered more realistic.

The theoretical range of combinations of ferrocyanide fuel and nitrate oxidant, water, and other inert compounds for which a reaction is thermodynamically possible was calculated using the following parameters.

- Heat of reaction--3,012 kJ/mol of ferrocyanide: This is the theoretical estimate calculated for the most energetic of the possible reactions involving sodium nitrate as the oxidant.

- Initial temperature--55 °C: This is approximately the maximum temperature measured in any ferrocyanide tank.

- Temperature to which the fuel must be heated to support propagation (ignition temperature)--275 °C: This is the temperature at which a stoichiometric mixture of ferrocyanide and sodium nitrate shows an abrupt increase in self-heating rate during adiabatic calorimetry testing. Tests supporting this temperature were conducted at Fauske and Associates, Inc. (FAI), Pacific Northwest Laboratory (PNL), and Los Alamos National Laboratory (LANL).

The results of the calculations were plotted on a triangular diagram (Figure 1-2) with each of the above-listed components (i.e., reactants, water, and diluents) represented by a side of the triangle. The reactivity limits for both the confined and the vented burn are represented as lines on the diagram. The compositions above the line can possibly sustain a propagating reaction; the compositions below the line cannot.

The tank compositions estimated in Chapter 4.0 may be compared to the reactivity limits shown on Figure 1-2. The shaded area shows the concentration of fuel plus oxidant as ranging from near zero to 6%, as indicated by tank composition estimates. The water concentration in the sludge is estimated to range from a minimum of 40 wt% to approximately 70 wt%. The ferrocyanide concentrations and water content are expected to be most representative of waste produced by the U Plant and T Plant processes. These wastes contain approximately 80% of the total ferrocyanide. Waste produced by the In-Farm process may be more concentrated in ferrocyanide and contain fewer solid diluents. Additional information on In-Farm produced waste is needed before its combustibility can be appropriately evaluated. The U Plant and T Plant waste compositions fall in the nonreactive region for both confined and vented burns.

It is tentatively concluded that the Hanford Site U Plant and T Plant ferrocyanide sludges cannot sustain a propagating exothermic reaction. Key waste properties supporting this conclusion include the following.

- **Ferrocyanide Concentration**--The ferrocyanide concentrations are dilute. Ferrocyanide concentrations in the sludge have been estimated from a predictive model that tracks scavenging campaign data and waste transfers. The model results have been compared to waste sample data where available, and the results compare favorably. Ferrocyanide concentrations are listed in Table 1-2 and range from 0.04 to 0.1 *M* (moles per liter) with the majority of the

Figure 1-2. Reactivity Limits for Ferrocyanide Mixtures.

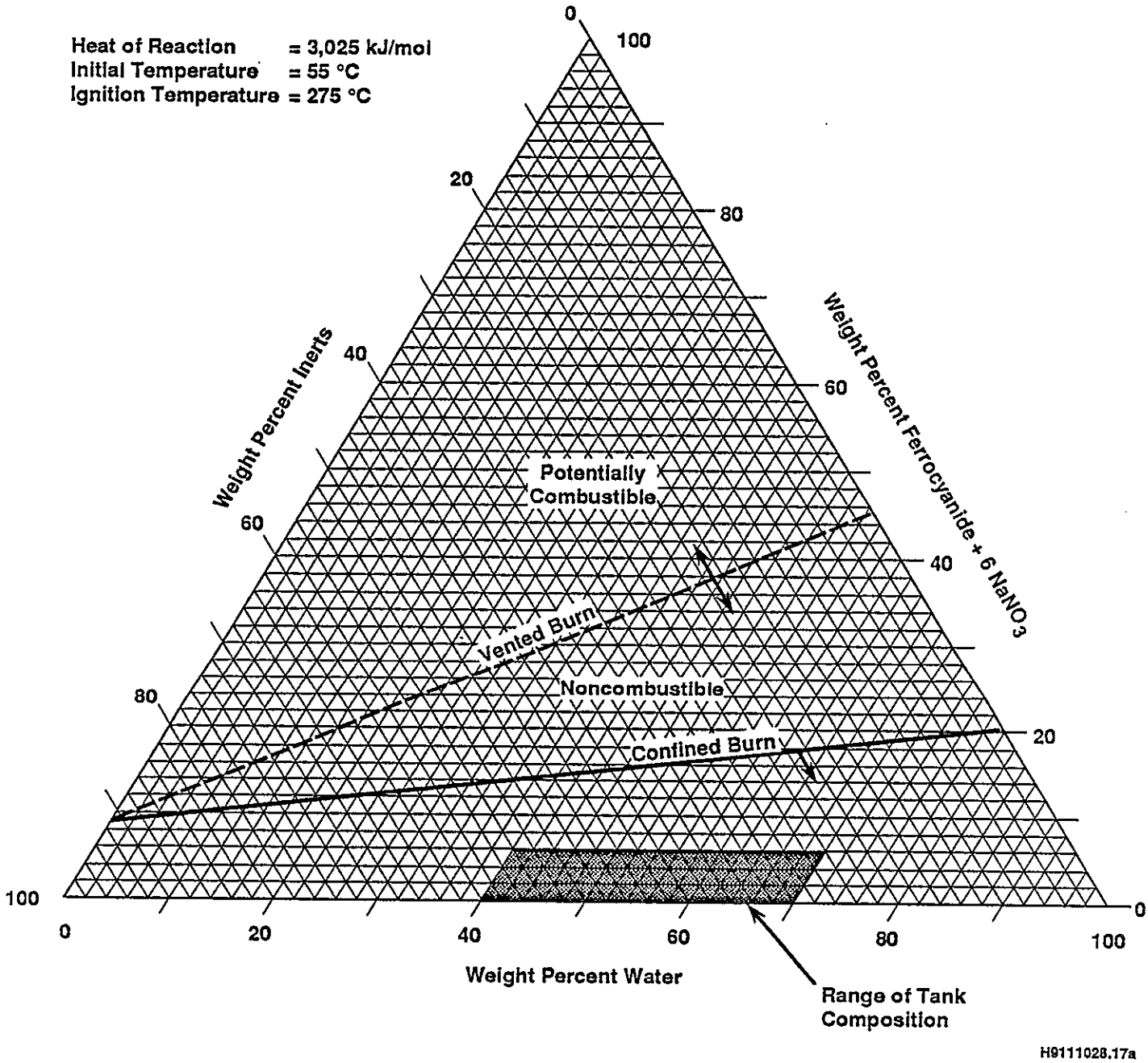

Table 1-2. Margin of Safety Between Ferrocyanide Reactivity Limits and Average Concentration in Sludge.

Tank	Average concentration[a] (mol $Fe(CN)_6^{-4}$/L)	Margin of safety for vented burn
241-BX-102	b	--
241-BX-106	b	--
241-BX-110	b	--
241-BX-111	b	--
241-BY-101	b	--
241-BY-103	0.082	7.4
241-BY-104	0.084	7.2
241-BY-105	0.099	6.1
241-BY-106	0.081	7.5
241-BY-107	0.070	8.6
241-BY-108	0.070	8.7
241-BY-110	0.080	7.6
241-BY-111	0.094	6.4
241-BY-112	0.076	8.0
241-C-108	0.086[c]	7.1
241-C-109	0.073[c]	8.3
241-C-111	0.089[c]	6.8
241-C-112	0.098[c]	6.2
241-T-101	b	--
241-T-107	0.006	98
241-TX-118	b	--
241-TY-101	0.042	14
241-TY-103	0.041	15
241-TY-104	0.042	14

[a]Based on predictive model (Borsheim and Simpson 1991) results.

[b]Ferrocyanide inventory predictive model (Borsheim and Simpson 1991) indicates no ferrocyanide sludges were transferred to these tanks.

[c]Predictive model concentrations are most representative of U Plant and T Plant waste. C Farm tanks contain waste produced by the In-Farm process, which may be more concentrated than current model predictions.

sludges less than 0.09 *M*. When combined with stoichiometric amounts of oxidant, this is a maximum 6 wt% fuel-oxidant mixture. Any additional oxidant would be considered an inert diluent. As indicated in Figure 1-2, a composition containing only 6 wt% fuel-oxidant mixture is noncombustible.

A margin of safety may be defined as the ratio of the maximum noncombustible ferrocyanide concentration to the average ferrocyanide concentration in the sludge. The margin of safety is thus the degree of concentration of ferrocyanide (ratio of peak-to-average concentration) that would have to exist to get a possibly reactive composition. The margin of safety for each tank is given in Table 1-2, assuming a minimum water content of 40 wt%, together with the average ferrocyanide concentrations on which it is based.

- **Organic Carbon**--The concentration of organic carbon in the ferrocyanide sludge, a potential fuel source, is insignificant. Analytical sample data available to date for total organic carbon (TOC) show the TOC to range from less than 0.1 to 0.4 wt%. (Tank 241-TX-118 is also classified as an organic tank and, as such, contains a higher TOC level than other ferrocyanide tanks contain.) This concentration of organic material is not considered capable of contributing significantly to the combustibility of the waste. In addition, several key conditions reduce the likelihood that the organic complexants contribute to the reactivity of the ferrocyanide sludge. The formation of the ferrocyanide sludge predates the addition of the organics by a number of years. The ferrocyanide compounds are very water insoluble, but the organic complexants are all highly water soluble. Thus, the organic complexants and the ferrocyanide precipitates would have been segregated. Because no significant mixing is expected in the tanks, the organics are probably not found in the sludge and do not contribute to its reactivity. In addition, the organic complexants may not exist in significant quantities in many of the single-shell tanks (SST) because they are subject to decomposition by radiolysis and, because of their solubility, were likely transferred to the double-shell tanks (DST) when the SSTs were interim stabilized. Therefore, the available sample data and solubility characteristics of the organic complexants strongly indicate that TOC is of no significance either as a fuel source or in increasing the reactivity of the ferrocyanide sludge.

- **Water Content**--The other constituents in the ferrocyanide sludge are composed of oxidant, water, and other inert diluents. The water content is high. A minimum content is estimated to be 40 wt%, but a range of 40 to 60 wt% may be more realistic. The water contained in the sludge is composed of chemical water (water of hydration), gel water from the flocculent precipitates formed during the scavenging process, and capillary water (water held between sludge particulates). This water is tightly held and will not be removed by jet pumping or leaks but may be removed by evaporation. In addition, tanks that have not been salt-well pumped will contain significant free (drainable) liquid. Based on available literature and thermogravimetric analysis (TGA) of waste simulants, three waters of hydration seem reasonable for ferrocyanide compounds expected in the sludge. Other precipitated compounds such as hydrous iron oxide are likely to be hydrated as well.

The insoluble ferrocyanide that formed to remove cesium is a flocculent precipitate that slowly settles to form a layer with a larger volume than that which would correspond to the density of the pure materials. Studies of ferrocyanide sludge and simulants indicated that a stable compacted sludge is formed that is approximately 4 vol% of the starting solution. U Plant simulants centrifuged under conditions that simulated 30 yr gravity settling contain approximately 55 to 65 wt% water. A typical granular solid would retain only about 30 wt% interstitial water. The interstitial liquid in the fine-particle ferrocyanide sludges will be held in place against gravity by capillary forces. The ferrocyanide surface mean particle size is quite small (approximately 14 μm) and is calculated to have a capillary holdup height greater than that of the ferrocyanide sludge heights. Interstitial liquid level measurements in sludges that have been salt-well pumped, in general, indicate liquid levels within 1 ft of the estimated sludge height. Given the accuracy of both measurements, these results seem to be consistent with the belief that sludges retain significant moisture due to capillary effects. Finally, results from available actual ferrocyanide waste tank samples indicate water content values from 43 to 63 wt%.

The potential for loss of moisture was evaluated. Chemical water, gel water, and capillary water will not be lost during jet pumping of drainable liquid from the tanks or lost due to leakage through new or existing tank leaks. Evaporation of water from the upper surface of the tank waste to the air in the dome space depends on the air exchange rate in the tanks. The ferrocyanide tanks are all passively ventilated; i.e., they breathe through filtered vents because of changes in barometric pressure. The water lost as a result of barometric breathing is expected to be insignificant, about 54 gal/yr. Some air exchange could possibly occur by convective air flow resulting from inleakage. Conservative calculations indicate convective flow could be as high as 21 ft^3/min, resulting in a conservative estimated water loss rate of about 1,400 gal/yr. This loss would be considered significant, amounting to as much as a 0.5-in. reduction in liquid level per year. The actual loss is probably much lower, and liquid level monitoring data indicate no loss in liquid levels.

- **Other Inert Diluents**--The ferrocyanide sludges are expected to contain significant inert diluents in addition to water. These would include inert solids and excess oxidant. Sludge simulants produced from the U Plant flowsheet were found to be incapable of supporting propagating reactions even when completely dry. Layers of more concentrated U Plant material may be possible due to more concentrated flowsheet recipes and layering during precipitate settling. These effects need to be studied further. Sludges produced by the U Plant flowsheet contain approximately 70% of the total ferrocyanide stored in the waste tanks. Samples of sludges produced by the T Plant flowsheet contain similar amounts of inert diluents as the U Plant flowsheet simulants. T Plant flowsheet wastes contain approximately 10% of the total ferrocyanide stored in

the waste tanks. Additional information is needed to estimate the inert diluents contained in the In-Farm flowsheet material.

1.3 SUMMARY OF HOT SPOT ANALYSIS

As indicated previously, the bulk of the ferrocyanide sludges is not expected to support propagating exothermic reactions. If the material cannot support propagation, the potential for energetic chemical reactions is limited to hot spots (local concentrations of ferrocyanide fuel and heat-producing fission products) that might reach a runaway condition. The hot spot analysis determined the waste conditions necessary to allow runaway chemical reactions and then compared the required conditions to possible waste properties. The analysis concluded that large concentrations of fission products would be necessary for hypothetical hot spots to run away. Such conditions are not considered credible in the Hanford Site storage tanks.

Chemical runaway scenarios require waste material to reach a temperature at which exothermic reactions are generating significant heat. Below a certain temperature (exothermic reaction onset temperature), no significant chemical heat is generated, and the only heat source available is from the decay of radioactive material, particularly the fission products ^{137}Cs and ^{90}Sr. The onset temperature for exothermic reactions in ferrocyanide-nitrate/nitrite mixtures was conservatively chosen to be 200 °C. Thermocalorimetic testing of synthetic ferrocyanide-nitrate/nitrite mixtures has indicated that no significant chemical activity is evident below this temperature. Waste temperatures approaching 200 °C are considered incredible for the following reasons.

- **Measured temperatures are all well below 200 °C.**

  The maximum measured waste temperature (tank 241-BY-104) is less than 55 °C, and most tanks have a maximum temperature of less than 32 °C. Although the waste temperatures are measured in only one radial location, they are considered likely to be representative of temperatures at other locations. The reasons for this are described as follows.

  Waste temperature is governed by the temperature difference between the waste and the environment necessary to dissipate the heat generated in the waste. The fission products settled with the precipitates that formed the sludge during the ferrocyanide scavenging operations. The settled sludge formed layers across the entire settling tanks. Sludges that were pumped to consolidation tanks had a low viscosity and would have rapidly formed uniform layers across the tank diameter. The sludge composition is therefore expected to be reasonably uniform across the tank. Thermal modeling analysis indicated that most of the heat generated in the waste is transferred vertically through the waste and out through the waste surface, the tank dome, and the earth overburden, with lesser amounts transferred out through the bottom and sides of the tank to the soil. Axial variations are expected, but radial variations should be small.

- **Slab-shaped hot spots cannot reach 200 °C.**

  Thermal modeling analyses of limiting axial fission product concentrations were performed. Slab geometry analysis was performed using the HEATING7 computer code (Childs 1991). The model representing tank 241-BY-104 used conservatively low heat-transfer properties [thermal conductivity of dry waste, 0.0017 W/cm-°C (0.10 Btu/h-ft-°F)], and the decay energy was concentrated in layers of various thicknesses. The analysis concluded that even when decay heat is concentrated by a factor of 30 over the average, the peak temperature is less than 100 °C. Another analysis of slab geometry calculated upper-bound estimates of the heat rate required at the bottom of each ferrocyanide tank for the waste to reach 200 °C. A one-dimensional model was used with all energy concentrated in the bottom node (approximately 1 ft of sludge) with the bottom of the tank taken as an adiabatic surface. The heat rate required to reach 200 °C therefore varies as a function of the waste height. The heat rate required to reach 200 °C is listed in Table 1-3 along with the total heat rate available in the tank. It is noted that the heat available is always less than that required even with this conservative model.

- **Bounding (spherical) hot spot geometries will not run away.**

  Even though concentrated regions other than layers are considered implausible, they were examined for the potential to produce runaway conditions. A spherical shape was chosen as the worst case because it has the lowest surface-to- volume ratio. The analysis determined the minimum volumetric heat rate that is required for waste to reach 200 °C. Several tanks of interest were evaluated, and the results are indicated in Table 1-4. The minimum heat rate required for a hot spot to reach 200 °C is 181 W/m^3 (tank 241-BY-104). This amounts to placing 55% of the fission products in the hot spot, while the hot spot contains only 0.7% of the total sludge volume. The fission product concentration factor (required heat rate divided by tank average heat rate) required for hot spots to reach 200 °C is 75 for tanks 241-BY-104 and -427 and 507 for tanks 241-C-112 and -109, respectively. There is no known mechanism for concentrating fission products in these tanks by such large factors. Table 1-4 provides a summary of calculated spherical hot spot characteristics. Although there is more uncertainty about the ferrocyanide concentration in the C Farm tanks (In-Farm processed material) than the remaining tanks, substantially larger margins are available to accommodate composition uncertainties.

Table 1-3. Comparison of Upper-Bound Estimates of Heating Rates Required for Thermal Runaway Versus Available Heating Rates for Slab-Shaped Hot Spots.

Tank	Depth of solid waste* (ft)	Heating rate required (W)	Available heating rate (W)	Ratio required/ available
241-BY-103	12.7	7.3 E3	2.3 E3	3.0
241-BY-104	12.9	7.3 E3	3.5 E3	2.1
241-BY-105	15.9	6.1 E3	2.5 E3	2.4
241-BY-106	20.1	5.3 E3	3.5 E3	1.5
241-BY-107	8.7	1.0 E4	2.0 E3	4.9
241-BY-108	7.5	1.1 E4	2.2 E3	5.3
241-BY-110	12.7	7.3 E3	3.8 E3	1.9
241-BY-111	14.5	6.4 E3	2.5 E3	2.6
241-BY-112	9.4	9.4 E3	4.7 E3	20
241-C-108	2.6	3.2 E4	2.4 E3	133
241-C-109	2.5	3.2 E4	5.3 E3	61
241-C-111	2.3	3.5 E4	5.9 E3	60
241-C-112	3.8	2.1 E4	4.7 E2	46
241-T-107	5.8	1.5 E4	1.8 E2	83
241-TY-101	4.2	2.0 E4	2.9 E2	68
241-TY-103	5.5	1.5 E4	9.7 E2	16
241-TY-104	1.9	4.4 E4	1.2 E2	360

*From Hanlon (1991).

Table 1-4. Illustration of Minimum Required Hot Spot Characteristics (for Spherical Hot Spots).

Tank	Average volumetric heating rate available (W/m^3)	Minimum volumetric heating rate to produce hot spot (W/m^3)	Percent of total heating rate in hot spot	Percent of total waste volume in hot spot
241-BY-104	2.4	181	55	0.7
241-C-109	<5.7	2,893	~24	0.05
241-C-112	<4.7	2,009	~28	0.07

1.4 INFORMATION NEEDED TO CONFIRM CONCLUSIONS AND RESOLVE THE SAFETY ISSUES

The following recommendations for future efforts are aimed at reducing uncertainties in waste properties that are key to assessing the ferrocyanide hazard. These recommendations are consistent with the Ferrocyanide Program Plan (Cash and Mellinger 1991).

- Tank waste sampling should continue to confirm key ferrocyanide waste property estimates. Waste samples should be analyzed for fuel concentration (e.g., ferrocyanides and organic carbon), water content, and fission product (heat load) concentrations. In addition, thermal analysis of waste samples should be performed to confirm that the onset temperature for exothermic reactions is well above waste storage temperatures and that no propagating exothermic reactions are indicated.

- Studies of ferrocyanide waste simulants should continue, particularly studies of In-Farm produced sludges. In-Farm sludges are higher in ferrocyanide concentration, contain fewer solid diluents, and contain small amounts of sulfides that need to be evaluated as an additional fuel source. Tank waste sampling results (for a number of representative tanks) will not be available for some time. The study of waste simulants, representative of the sludges actually produced, can provide near-term data to better estimate key waste properties. Waste simulants should provide valuable information regarding expected ferrocyanide concentration, water content, and thermokinetic behavior (exothermic reaction onset temperature, ignition temperature, and reaction rates as a function of temperature).

- Reaction propagation testing should be performed to better define the propagation limits. Parametric testing of ferrocyanide-nitrate/nitrite mixtures will define a realistic safety envelope of concentrations that preclude waste combustibility.

- The potential for ferrocyanide sludges to change properties under storage conditions should be investigated further. In particular, the potential for loss of moisture due to evaporation and the potential for the ferrocyanides to undergo chemical changes under existing tank conditions should be resolved.

2.0 INTRODUCTION

The background leading to the declaration of a USQ involving the ferrocyanide tanks has been summarized in a number of recent reports, including the program plan for ferrocyanide tanks (Cash and Mellinger 1991). Briefly, the USQ arose from a review of a hypothetical accident discussed in the Defense Waste Environmental Impact Statement (EIS) (DOE 1987). An issue was raised about the assumed radioactive material source term resulting from a postulated explosion of ferrocyanide in a waste tank. Further evaluation of this issue highlighted questions about uncertainties in the chemical content of the waste tanks. The tanks were known to contain ferrocyanide compounds added to remove radiocesium from the liquid chemical waste. The tanks were also known to contain sodium nitrite and sodium nitrate, which together with the ferrocyanide compounds can form explosive mixtures if present in appropriate concentrations. Even if reactive mixtures are present, energy sources are required to initiate a reaction.

As a result of the declaration of the USQ, restrictions on tank activities were established, and a major waste tank safety program was established (Leggett 1990, Gasper and Reep 1991).

All work involving the waste tanks is controlled by special requirements at the present time. No work may be performed within the tank boundary or in a location that could involve the contents without first performing a comprehensive safety assessment of that activity. The safety assessment must be approved by the appropriate authority before the activity can be conducted. The safety assessment considers the design, installations, and operations involved with the proposed activity and establishes mandatory controls to ensure that any risk associated with the activity is acceptable. To date, the activities authorized through review and acceptance of safety assessments have been limited to tank sampling aimed at resolving the waste composition/ concentration uncertainties.

The safety program plan (Cash and Mellinger 1991) defines the work proposed to resolve uncertainties associated with the USQ and to also provide a technical basis for waste remediation and ultimate disposal. That work includes the following elements:

- Accident modeling, risk analysis, and safety evaluations
- Chemical reaction studies
- Expanded tank monitoring and modeling
- Ferrocyanide waste characterization.

This report is a part of that work scope. Other activities related to the safety program plan work scope have been in progress since the declaration of the USQ. Information has been developed at a number of sites and in a number of key technical areas. This information includes detailed assessments of the tank contents from searches of historical records and chemical processing flowsheets conducted at Westinghouse Hanford Company (Westinghouse Hanford). The actual process flowsheets used to generate the stored wastes

have been used to create nonradioactive waste in the laboratory. These simulated wastes have provided valuable information on diluent concentrations, particularly water. Thermocalorimetric data have been obtained on chemical mixtures and simulated wastes at PNL, LANL, and FAI. Data from the tests have provided information on reaction onset temperatures and conditions required to obtain significant reactions. The data support the conclusion that there are large margins between current tank storage temperatures (less than 55 °C) and the reaction onset temperature (greater than 200 °C) for chemical compositions that are optimum for reaction. Historical data indicate that such optimally reactive compositions do not exist in the ferrocyanide waste tanks.

The foregoing information, mostly obtained since the declaration of the USQ, has been used as the basis for the tentative conclusions reached in this report. Data gathering is still in progress. This report will be revised as new information becomes available to improve the estimates of risk involved with the Hanford Site ferrocyanide waste storage tanks.

3.0 SCOPE AND ASSESSMENT APPROACH

3.1 SCOPE

The scope of this report includes the estimation of key parameters from available data sources and, based on these data, an assessment of the likelihood of runaway ferrocyanide reactions during continued waste storage. This report also identifies additional information needed to reduce uncertainties or to close out secondary issues. Risk of continued storage must consider both the likelihood of runaway reaction scenarios and, if scenarios are credible, the consequences. This interim assessment addresses the potential for runaway. Consequences resulting from runaway scenarios will be addressed in a future report if credible scenarios are identified.

The hazard assessment addresses all of the 24 Hanford Site ferrocyanide tanks to the extent data are available. The assessment, however, focuses on tanks containing waste produced by the U Plant and T Plant processes. These tanks are estimated to represent 80% of the ferrocyanide introduced in the cesium scavenging process. The remainder of the waste tanks (i.e., those containing In-Farm produced wastes) are thought to contain ferrocyanides in the highest concentrations. Although tank compositions have been estimated by the Ferrocyanide Inventory Predictive Model (Borsheim and Simpson 1991), the absence of corroborating data from synthetic or actual samples precludes conclusions on In-Farm material in this interim report.

Conclusions reached in this report are tentative and are based on the data available as of October 1991. The data are based largely on historical records of waste processing and transfers and routine tank monitoring data. Available data from waste simulants or tank waste samples are limited but also provided important input.

This report will be revised and updated as new information becomes available. New information may include waste sample data, waste simulant data, new tank monitoring data, and results from development of evaluation models.

3.2 BACKGROUND

Radioactive wastes from defense operations have been accumulated at the Hanford Site in underground waste tanks since the early 1940's. During the 1950's, additional tank storage space was required to support the defense mission. To obtain this additional storage space without constructing additional storage tanks, Hanford Site scientists developed a process to scavenge radiocesium from tank waste liquids. In implementing this process, approximately 140 metric tons of ferrocyanides was added to SSTs.

Ferrocyanides, in the presence of oxidizing material such as sodium nitrate/nitrite, can be combustible or explosive under certain conditions of concentration and high temperature. The explosive nature of ferrocyanide in the presence of an oxidizer has been known for decades, but the conditions under which the compound can undergo an uncontrolled exothermic reaction have not been thoroughly studied.

The effects of a postulated ferrocyanide explosion have not been considered in the safety analyses or safety analysis reports (SAR) applicable to the Hanford Site SSTs. The SARs have historically considered an explosion resulting from fuel/nitrate reactions as an incredible event.

Although not considered part of the safety analysis for the storage of waste in the SSTs, the 1987 EIS (DOE 1987) did include an environmental impact analysis of potential explosions involving ferrocyanide-nitrate mixtures. The EIS postulated that an explosion could occur during mechanical retrieval of salt cake or sludge from a waste tank. The EIS concluded that the ferrocyanide explosion could create enough energy to release radioactive material to the atmosphere through ventilation openings, exposing persons offsite to radiation doses approximately equivalent to the annual dose from natural and human-made radiation sources.

This conclusion had been questioned for two reasons. First, not enough was known about the tank contents or the ferrocyanide-nitrate reaction characteristics to conclude that an explosion would not breach the tank dome, releasing significantly more material than assumed in the EIS evaluation. Second, the EIS calculation assumed that the radioactive cesium (^{137}Cs) was distributed evenly throughout the tank. It is more likely that the ^{137}Cs is preferentially associated with the ferrocyanide compounds that might participate in the explosive reaction. As such, the ^{137}Cs might be vaporized and released to the atmosphere in a respirable particle size that might be greater than assumed in the EIS calculation.

In October 1990, the ferrocyanide hazard issue was reviewed and declared a USQ. This review indicated that the safety envelope for waste tanks that contain significant quantities (defined at that time as greater than 1,000 mol) of ferrocyanide may not be adequately described by the SAR (Smith 1986). Although available data indicated that the likelihood of an explosion is very low, insufficient data were available to deem such an event incredible or to determine the magnitude or consequences of a hypothetical explosion.

Records available in 1990 indicated that 24 SSTs might contain greater than 1,000 mol of ferrocyanide. These tanks are listed in Table 3-1. Based on more recent information, it is believed that 7 of the 24 tanks do not contain significant amounts of ferrocyanide.

3.3 APPROACH TO THE FERROCYANIDE SAFETY ISSUE

As indicated in the ferrocyanide USQ, the ferrocyanide nitrate/nitrite mixtures represent a hazard from the potential for runaway chemical reactions. The safety issue associated with the storage of ferrocyanide waste is whether the wastes are in a condition where runaway scenarios are possible and, if so, whether the consequences present significant risk.

Table 3-1. The 24 Single-Shell Tanks Declared to Involve the Ferrocyanide Unreviewed Safety Question.

BX Farm	BY Farm
241-BX-102*	241-BY-101*
241-BX-106*	241-BY-103
241-BX-110*	241-BY-104
241-BX-111*	241-BY-105
	241-BY-106
C Farm	241-BY-107
	241-BY-108
241-C-108	241-BY-110
241-C-109	241-BY-111
241-C-111	241-BY-112
241-C-112	
	T Farm
TY Farm	
	241-T-101*
241-TY-101	241-T-107
241-TY-103	
241-TY-104	TX Farm
	241-TX-118*

*Currently estimated to contain no significant amounts of ferrocyanide.

The potential for runaway ferrocyanide reactions depends on the energy available from the chemical reactions relative to the energy that would be absorbed by the material as its temperature is raised. If the waste material in the tanks includes a sufficient quantity of water and/or nonreactive diluents including excess oxidant, the material cannot sustain a propagating reaction. If reactions cannot propagate through the waste material, runaway scenarios would be confined to local concentrations of fuel and heat sources (hot spots).

This report evaluates the likelihood that conditions (chemical concentration and temperature) as currently existing in the ferrocyanide waste tanks are conducive to propagating reactions (Section 5.1). That evaluation is followed by an assessment of the likelihood of localized runaway scenarios, i.e., hot spots (Section 5.2). This assessment approach is shown in Figure 3-1.

The evaluation models used to perform this assessment are introduced in the following sections to identify key parameters. Values for these key parameters are estimated in Chapter 4.0. These estimates are based on various data currently available. These data are introduced in Sections 4.1 through 4.9. In Section 4.10, the various data for the key parameters are integrated into estimates that are used in the hazards evaluation presented in Chapter 5.0.

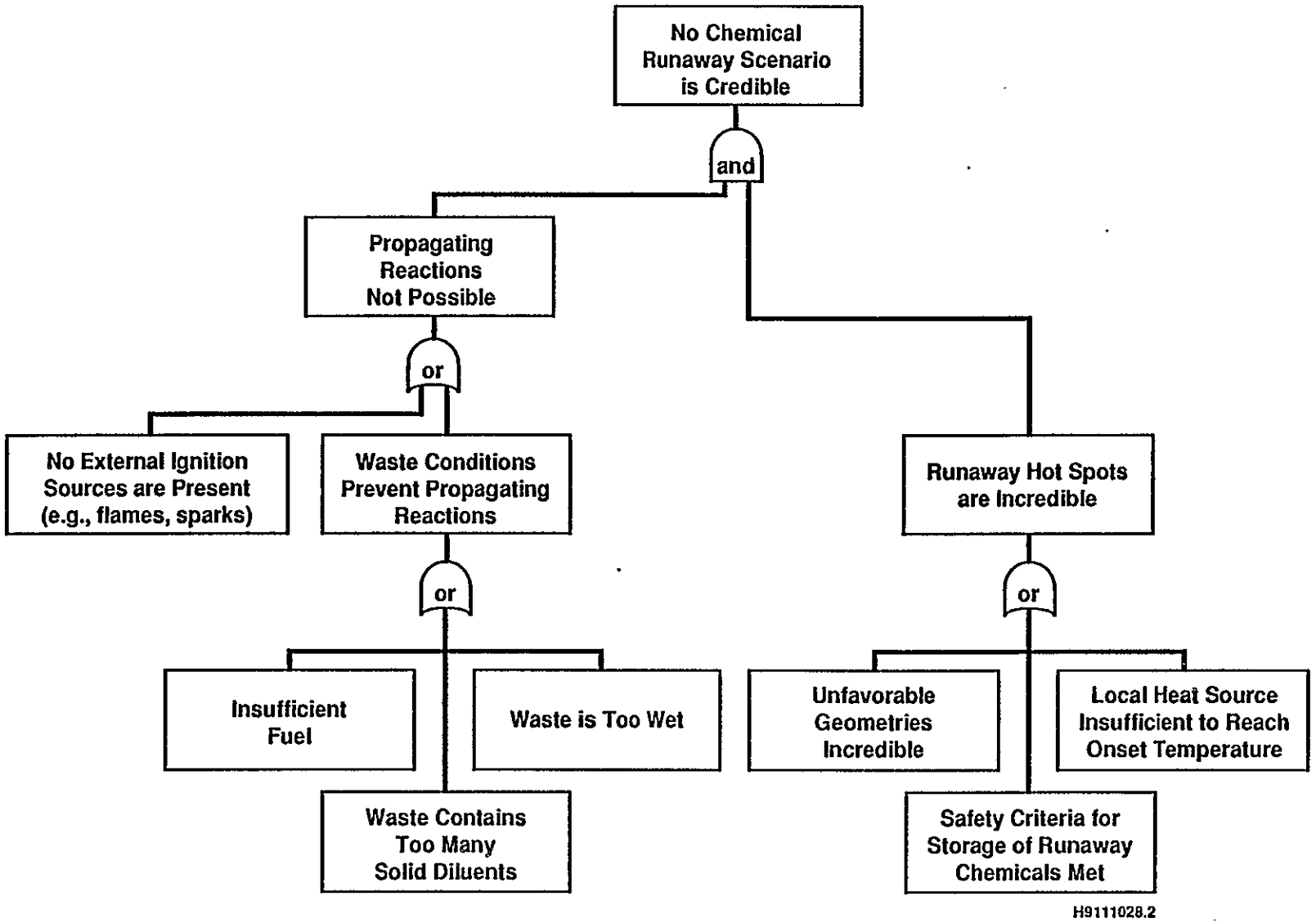

Figure 3-1. Approach to Assessing the Likelihood of Runaway Reactions in Ferrocyanide Waste Tanks.

3.3.1 Potential for Propagating Energetic Reactions

The ferrocyanide tanks, like most of the Hanford Site SSTs, contain abundant oxidizers in the form of sodium nitrate/sodium nitrite. The ferrocyanide tanks also contain potential fuels in the form of ferrocyanide compounds and small amounts of organic complexant compounds. In the proper quantities, and under certain conditions, the fuels and oxidizers could react causing an energetic propagating reaction. Several terms used in the assessment of propagating reactions are defined as follows.

Combustible--A material that is able to propagate an energetic reaction by releasing sufficient heat to raise surrounding material to the ignition temperature.

Energetic reaction--A reaction (or reaction rates) yielding sufficient energy to cause damage to containment boundaries from high temperatures or high pressures from the release of hot gases.

Ignition temperature--The minimum temperature at which a fuel/oxidant mixture will flash or react vigorously. This is taken as the temperature at which there is a significant increase in reaction rate from an Arrhenius-type reaction to a propagating-type reaction.

The potential for propagating reactions depends on several factors, especially the concentration of fuel and oxidant present and the concentration of diluents, especially water. If sufficient diluents are present, and/or if the fuel or oxidant concentration is low enough, the mixture is nonpropagating. The evaluation model that will be used to assess the combustibility of the wastes in the ferrocyanide tanks is described in the following paragraph. The discussion includes the identification of the key parameters needed for such an assessment.

Propagation Evaluation Model. The question of whether a ferrocyanide reaction could propagate if started may be evaluated by defining the range of conditions for which a sustained reaction is not possible, and then comparing the waste tank contents to these conditions. If the ferrocyanide is too dilute, the large heat sink provided by the inert material will render it impossible to sustain the temperature required for ignition. The reactivity limit may thus be calculated by setting the heat of reaction equal to the heat required to raise fresh fuel plus accompanying inert material to its ignition temperature. This limit can be calculated from the following parameters, as discussed more fully in Section 5.1:

- Concentration of fuel (ferrocyanides)
- Concentration of oxidant (nitrates/nitrites)
- Concentrations of diluents (especially water and excess nitrate/nitrite)
- Initial temperature
- Ignition temperature

- Heat of reaction
- Heat capacities of materials present
- Pressure (is vaporization of water suppressed?).

3.3.2 Potential for Energetic Chemical Runaway (Hot Spots)

Even if the general waste conditions will not support propagating reactions, the potential exists for localized concentrations of heat-producing fission products to cause hot spots. Under certain conditions of concentration, geometry, and temperature, hot spots could cause thermal runaway. Several of the key terms used in the hot spot analysis are defined as follows.

Thermal runaway--The condition of accelerating exothermic reaction rate and increasing temperature resulting from heat production in excess of heat dissipation in the material/system.

Onset temperature--The temperature below which no significant exothermic chemical activity is evident. The temperature where evident exothermic activity begins.

Based on conservative simulant mixtures of ferrocyanide wastes (stoichiometric mixes of fuel and oxidant), an onset temperature of 200 °C is used. A hot spot must reach 200 °C before heating from chemical reactions is a contributor. The only heat source below this temperature is radioactive decay heat. The temperature reached in a postulated hot spot depends on the heat balance between the heat produced from radioactive decay of fission products (primarily ^{137}Cs and ^{90}Sr) and the heat dissipated. Heat dissipation is dependant of the waste thermal properties (density, heat capacity, and conductivity); tank/waste boundary conditions (temperature, heat transfer); and hot spot geometry (surface/volume ratio).

The assessment approach is to determine the volumetric heat generation (due to decay of fission products) required to drive various hot spot geometries to 200 °C. Geometries considered include slabs and spheres. The required heat-generation rate is then compared to the decay energy available in the tank. A judgment can then be made of the plausibility of the required concentration of energy sources occurring in the tanks. This procedure is discussed in Section 5.2.

Values for the key parameters used in the hot spot assessment are developed in Chapter 4.0, including the following:

- Likelihood of various hot spot geometries
- Waste thermal properties

- Decay heat source available
- Waste temperature boundary conditions
- Ferrocyanide-nitrate/nitrite onset temperature.

This page intentionally left blank.

4.0 METHODS TO ESTIMATE VALUES FOR KEY PARAMETERS

Key parameters involved in assessing the hazards in the ferrocyanide tanks were discussed in Sections 3.2 and 3.3. Providing accurate values for these key parameters for in-tank conditions is not possible without data from waste samples and analyses. However, an estimate of expected values is possible by reviewing available data and studying waste simulants. An estimate of each key parameter is made based on currently available data as discussed below. Data currently available include historical records such as the chemical flowsheets used for the various scavenging campaigns and waste transfer records. A limited amount of tank waste sample data are currently available, including core samples and analysis from three ferrocyanide tanks and supernate sample analysis from six ferrocyanide tanks. Some tank monitoring data are available including temperature data, historical measurements of sludge and liquid levels, and neutron and gamma probe scans from tanks with liquid observation wells (LOW). In addition to these waste and tank data, key parameters can be estimated based on information provided by testing waste simulants. Waste simulants are being produced using the chemical flowsheets for the scavenging campaigns. These and other simulants are being tested to determine key chemical, thermal, and physical properties and the behavior of various reactions. Testing has included chemical analysis, thermal analysis such as calorimetry, thermal gravimetric analysis, time-to-explosion testing (TTX), propagation rate testing, safe handling testing, and physical testing. Available data sources discussed in this chapter include the following:

Data Source	Report Section
Bulk ferrocyanide inventory based on ferrocyanide scavenging history and a ferrocyanide waste predictive model	4.1
Waste sample analysis results (sludges and supernates)	4.2
Waste simulant analysis	4.3
Liquid level measurements	4.4
^{137}Cs gamma scan data	4.5
Tank waste temperature measurements	4.6
Ferrocyanide-nitrate/nitrite mixture thermal property analyses	4.7
Ferrocyanide-nitrate/nitrite safe handling testing	4.8
Tank/waste thermal hydraulic modeling	4.9

The data sources used to estimate key parameters for the reaction propagation evaluation are indicated in Table 4-1. The data sources used to estimate key parameters for the hot spot runaway evaluation are indicated in Table 4-2.

4.1 HISTORICAL DATA ON FERROCYANIDE PRECIPITATION AND FERROCYANIDE PREDICTIVE MODEL RESULTS

Several ferrocyanide tank key parameters can be estimated based on studying the ferrocyanide scavenging campaign history. These key parameters include the amount of ferrocyanide expected to be contained in each tank, the volume of settled ferrocyanide sludge expected (based on laboratory work that estimated the settled solids volume as a percent of the slurry volume), and some indication of where the ferrocyanide sludge would be located in the tanks (based on what other waste was in the tank when the ferrocyanide sludges were transferred in or wastes placed in the tanks subsequent to the ferrocyanide sludge transfers). A ferrocyanide sludge predictive model has been developed to predict sludge properties based on this historical information (Borsheim and Simpson 1991).

4.1.1 The Bismuth Phosphate and Uranium Recovery Processes

The bismuth phosphate process used in B Plant and T Plant was a plutonium recovery/purification process that did not recover uranium from its waste streams. The extraction waste, called metal waste (MW), contained the uranium and approximately 90% of the fission products. This waste was stored in underground waste tanks in the 200 Areas. In addition, first decontamination cycle (IC) waste was also stored in other underground waste tanks in the 200 Areas. The IC waste contained approximately 10% of the fission products.

The U Plant was built as a third bismuth phosphate plant but was never used as such. To recover uranium from the MW, U Plant was converted to a solvent extraction Uranium Recovery (UR) plant. The alkaline MW solution was sluiced from the underground waste tanks, transferred to the UR plant for processing, and acidified. After extracting the uranium, UR plant waste was neutralized and returned to the underground waste tanks.

The UR process, also called the tributyl phosphate (TBP) process because TBP was the active solvent extractant, began production in November 1952. The process efficiently recovered uranium from the sluiced, acidified MW, but the overall process generated almost 2 gal of waste to be stored for every gallon of stored MW processed. Methods to reduce the volume of stored waste were studied and resulted in the implementation of the ferrocyanide scavenging process.

4.1.2 Scavenging Program

The principal long-lived fission products in the waste were ^{90}Sr (28.6 yr half-life) and ^{137}Cs (30.2 yr half-life). The objective of the ferrocyanide scavenging process was to remove the soluble, long-lived fission product (^{137}Cs) from the UR and IC liquid wastes as a precipitate; ^{90}Sr was already

Table 4-1. Key Parameters and Current Data Sources for Evaluating Reaction Propagation.

Key parameter	Data sources
Ferrocyanide inventory and concentration	• Historical records for tank scavenging and transfers • Sludge volume measurements • Analysis of core samples and supernate samples • Waste simulant analysis • ^{137}Cs gamma scan data and ferrocyanide chemistry
Organic fuel concentrations	• Analysis of supernate samples • Analysis of core samples
Nitrate/nitrite (oxidant) concentrations	• Sample analysis and porosity measurements • Simulant analysis • Flowsheet chemistry
Moisture (water) content of sludges	• Core sample analyses • Simulant analyses • Liquid level measurements, capillary action predictions, porosity and chemical water
Diluent types and concentrations	• Core sample analyses • Simulant analysis • Flowsheet chemistry
Waste temperature	• Tank monitoring temperature data
Ferrocyanide/nitrate sludge simulant ignition temperature	• Calorimetry (AC, DSC, ARC) • LANL: DTA, and Henkin Tests • PNL: TTX tests

AC = adiabatic calorimetry.
ARC = accelerating rate calorimetry.
DSC = differential scanning calorimetry.
DTA = differential thermal analysis.
LANL = Los Alamos National Laboratory.
PNL = Pacific Northwest Laboratory.
TTX = time-to-explosion testing.

Table 4-2. Key Parameters and Data Sources for the Evaluation of Hot Spot Runaway.

Key parameter	Data sources
Waste geometry	• Waste scavenging and transfer histories • Tank surveillance data
Waste thermal properties	• Core sample data • Handbook values • Thermal hydraulic analysis
Decay heat source and location	• Waste scavenging and transfer histories • Gamma scan data • Thermal hydraulic analysis
Ferrocyanide-nitrate/ nitrite onset temperature	• Calorimetry (adiabatic, DSC, ARC)
Waste/tank temperatures (heat transfer boundary conditions)	• Tank monitoring temperature data

ARC = accelerating rate calorimetry.
DSC = differential scanning calorimetry.

essentially insoluble in the neutralized UR waste. This enabled the disposal of the supernate to the ground, reducing the stored waste volume in the tanks.

Three scavenging campaigns were conducted to treat three different types of wastes. The corresponding flowsheets have been termed "U Plant," "T Plant," and "In-Farm" flowsheets (Borsheim and Simpson 1991). In general, aqueous waste was pumped to large process tanks (approximately 50,000 gal) where the precipitating agents were added. Ferrocyanide ion [$Fe(CN)_6^{-4}$] was added to acid waste, the pH of the solution was adjusted to a pH of 9 ± 1, and then an equal molar amount of Ni^{+2} ion was added to coprecipitate radiocesium with the $Na_2NiFe(CN)_6$ precipitates. Other added chemicals included $Ca(NO_3)_2$, $Sr(NO_3)_2$, and Na_2HPO_4. The nickel ion was added as the sulfate and the ferrocyanide as the sodium or potassium salt. The target concentrations of $Fe(CN)_6^{-4}$ and Ni^{+2} ranged from 0.0025 *M* to 0.005 *M*. Two batches of "In-Farm" wastes used ferrocyanide and nickel target concentrations of 0.0075 *M*. The treated waste was stirred to ensure thorough mixing and then pumped to receiver tanks where the flocculent precipitate was allowed to settle for a minimum of 7 days. Supernatant liquid was then disposed of, if scavenging was shown to be successful based on supernatant sample results. When sludge layers built up in the receiver tanks, they were sometimes transferred by means of sludge transfer pumps to other tanks for storage. Simplified flowsheets and flow diagrams for the three processing campaigns that produced ferrocyanide precipitates are provided in Figures 4-1 through 4-3.

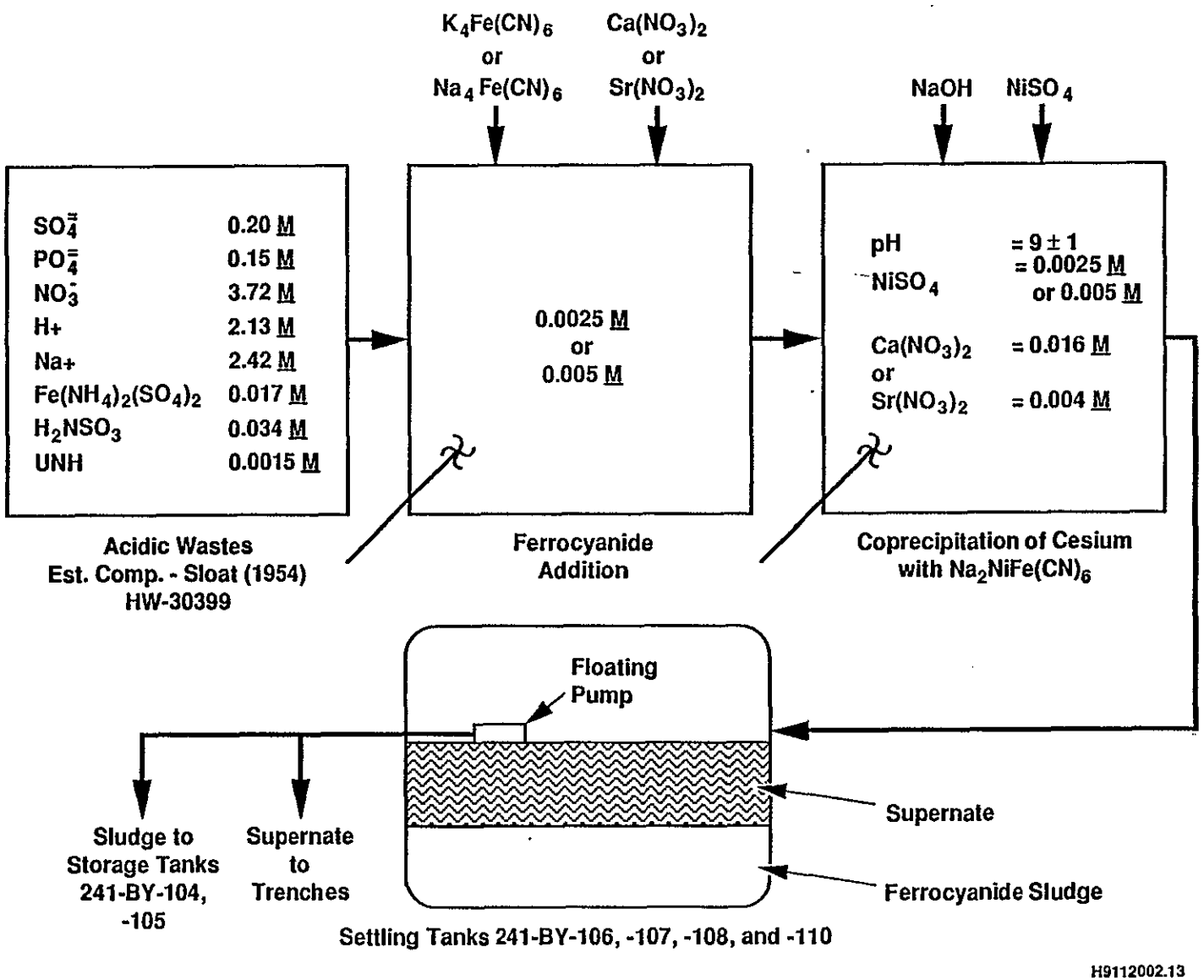

Figure 4-1. Ferrocyanide Production by "U Plant" Flowsheet.

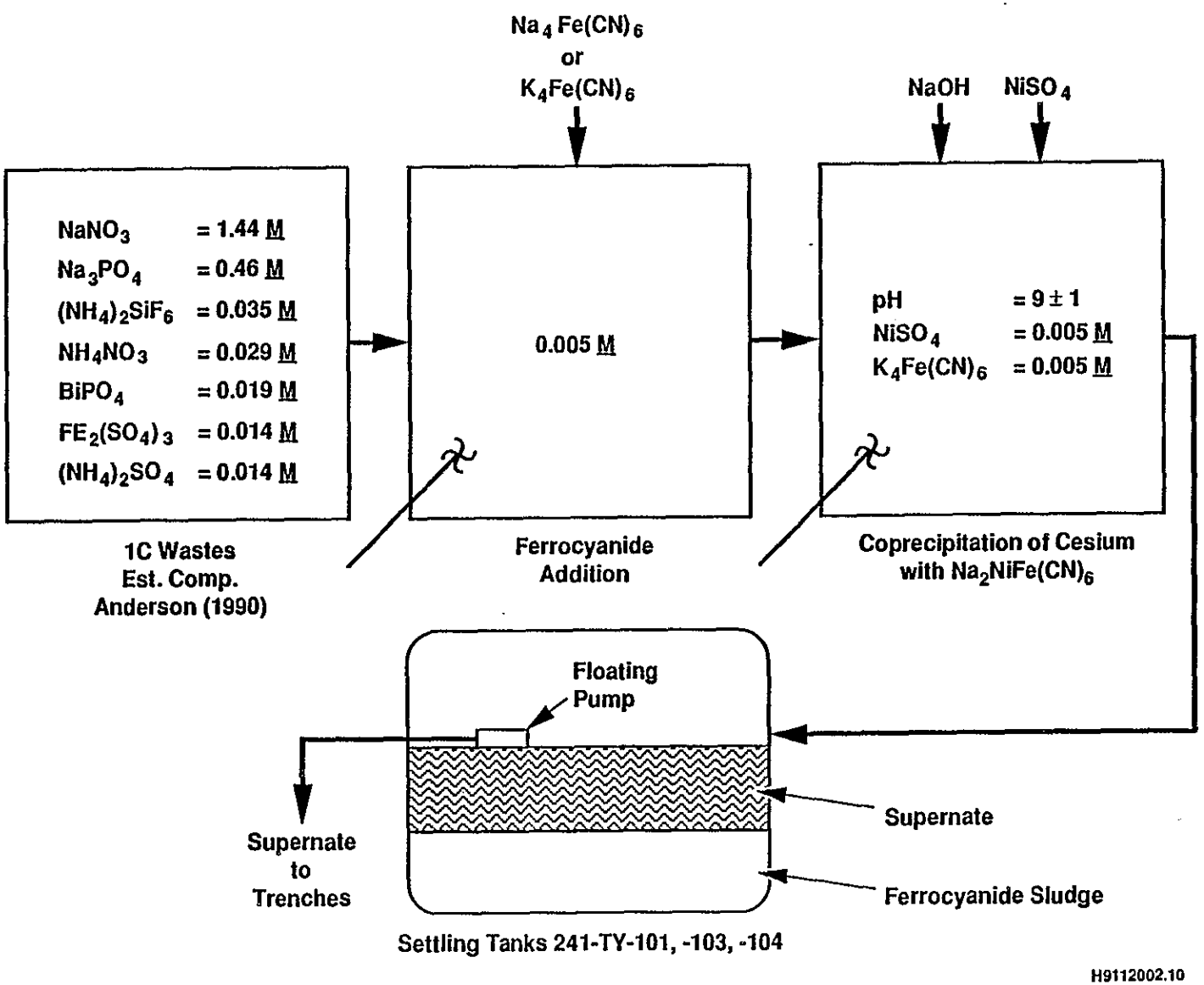

Figure 4-2. Ferrocyanide Production by "T Plant" Flowsheet.

Figure 4-3. Ferrocyanide Sludge Production by "In-Farm" Flowsheet.

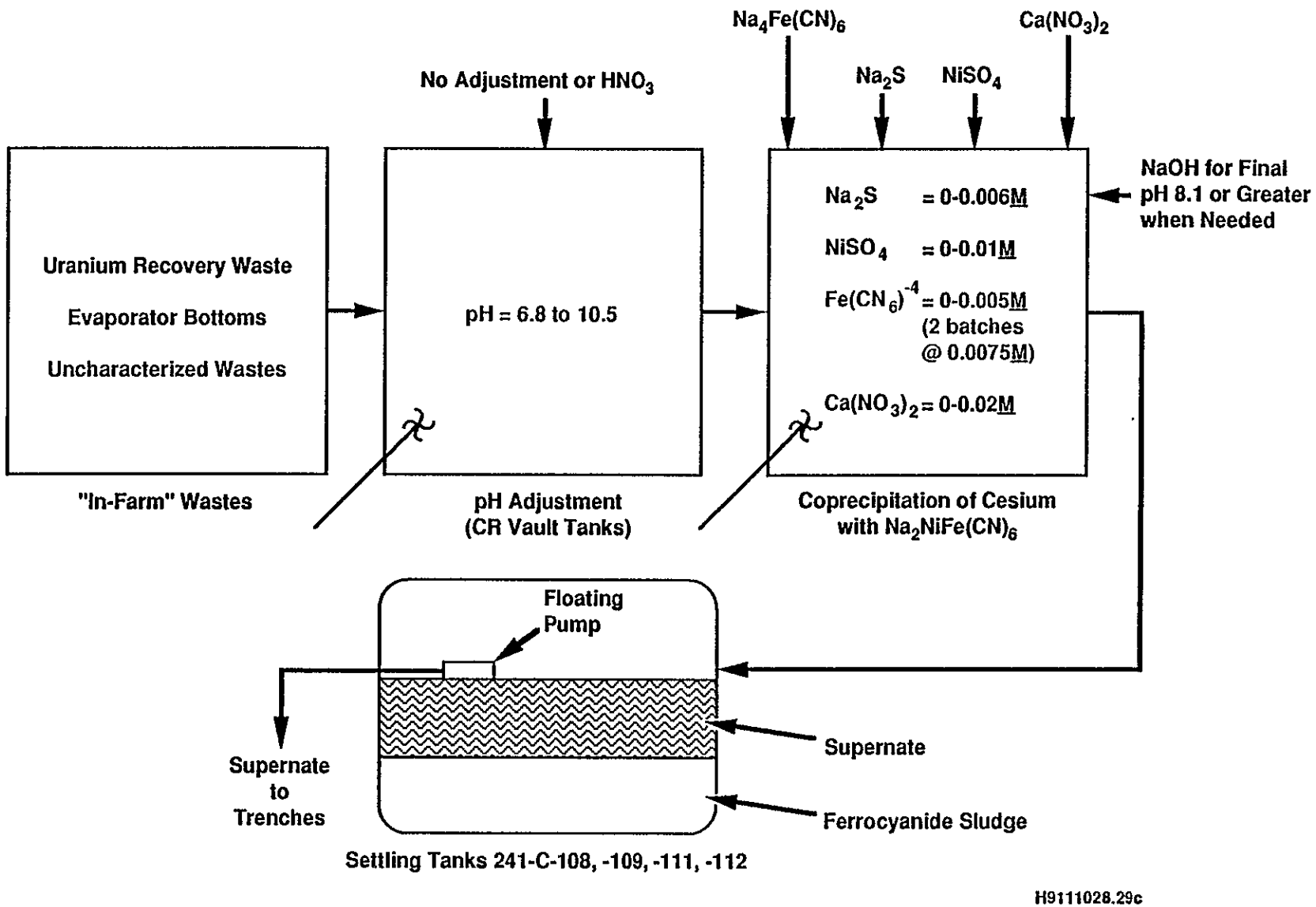

Production scavenging of the UR wastes began in late September 1954. At that time there was a total of approximately 21.2 Mgal of unscavenged UR waste in the tank farms. Approximately 13.1 Mgal of waste was located in the 200 East Area, and approximately 7.9 Mgal was located in the 200 West Area (Stedwell 1957).

4.1.3 Processing in the 200 East Area

4.1.3.1 BY Farm Tanks. Production scavenging of U Plant waste began in September 1954. Scavenged UR waste was routed to a settling tank in the BY Tank Farm in 200 East Area (usually tank 241-BY-106, -107, -108, or -110) at a rate up to approximately 50,000 gal/day. When a tank was full, the waste stream was switched to another settling tank. The filled tank was allowed to settle for a minimum of 7 days before sampling. The scavenged waste was then sampled at several incremental depths and analyzed for ^{137}Cs, ^{90}Sr, total beta, total gamma, and PO_4^{-3}. If the cesium and strontium were below limits, the supernate was pumped to a crib/trench via a floating suction pump. Grab samples were taken from the discharge line to the crib/trench for every 50,000 gal cribbed. The grab samples were composited and analyzed routinely for the previously mentioned components. In addition, several other analyses were performed intermittently. In June 1955 the sampling procedure was changed to every 100,000 gal cribbed. The pump discharge line had a continuous gamma monitor mounted on it. The pump was to be shut off when a sudden increase in the monitor signal indicated the tank sludge level had been reached (Clukey 1955). The accumulated sludge in the settling tanks was periodically transferred to tank 241-BY-104 or -105. The sludge volume was expected to be 7% to 10% of the treated supernate volume (Sloat 1954, Carpenter 1954). The UR wastes were scavenged throughout the remainder of the MW recovery program. The last scavenged waste from U Plant was received in the BY Tank Farm in June 1957.

The BY Farm tanks remained in service after the ferrocyanide scavenging program was completed. Most of these tanks received Plutonium/Uranium Extraction (PUREX) Plant aluminum decladding waste [coating waste (CW)] in the early 1960's and were incorporated into the In-Tank Solidification (ITS) systems as bottoms/recycle tanks in the late 1960's (Anderson 1990). The ITS systems consisted of a feed tank, a tank with installed heating equipment [either a heated air lift recirculator (ITS-1) or electric immersion heaters (ITS-2) in an air lift recirculator], and downstream bottom/recycle tanks. The hot concentrated solutions from the ITS tanks were batch transferred to the bottoms/recycle tanks. These tanks were at lower temperatures and connected to an active exhauster system for heat removal. The solutions were expected to cool in the bottoms/recycle tanks; salt cake solids would crystallize out, and the saturated solution was batch transferred to the next bottoms/recycle tank, which was at an even lower temperature. This process was repeated through several "bottoms loop" tanks and the residual supernatant eventually returned to the ITS feed tank for further concentration. The ITS systems were shut down in the mid-1970's, and the drainable liquid in several of the tanks was salt-well pumped into DSTs.

4.1.3.2 C Farm Tanks. Beginning in May 1955, unscavenged UR waste already stored in 200 East Area tanks was routed to the 244-CR vault for scavenging

using the In-Farm process. A ^{60}Co scavenging flowsheet was used on some In-Farm scavenging campaigns. This procedure involved adding Ni^{+2} ion to 0.005 *M* and Na_2S to 0.0025 to 0.006 *M* in the waste after ensuring that the pH ranged from 6.8 to 9.5, and then proceeding with $Na_4Fe(CN)_6$ and $NiSO_4$ additions. If laboratory analysis of the feed tank indicated additional ^{90}Sr decontamination was necessary, calcium nitrate was also added (Sloat 1955). Before settling, the pH was adjusted to greater than 8.1, and the scavenged waste was routed to another tank for settling, sampling, and decantation to a crib. Note that this procedure may have left much of the original alkaline-insoluble solids [e.g., $Fe(OH)_3$] produced from neutralizing the UR waste in the original UR waste storage tanks. The primary settling tanks for this In-Farm scavenged waste were tanks 241-C-108, -109, -111, and -112. The sludge volume expected from the In-Farm scavenging was 10% of the treated supernate volume. In-Farm scavenging was completed in December 1957.

The original plans called for cribbing the scavenged supernate. However, in 1956 it was found that ^{60}Co in the supernate would go to the groundwater and exceed allowable limits. Considerable effort was expended trying to develop a cobalt scavenging procedure while disposal to ground was held up. In October 1956, a decision was made to dispose the high ^{60}Co wastes to the ground on a specific retention basis. The BC trenches/cribs were built for specific retention disposal of the scavenged supernatant.

4.1.3.3 BX Farm Tanks. These tanks were originally placed on the ferrocyanide watch list because inventory values from the TRAC model indicated that these tanks contained greater than 1,000 mol of ferrocyanide. However, the records from the scavenging program show that supernate destined for the cribs was occasionally diverted to other tanks for interim storage or "side pocketed" to accommodate volume and curie disposal limits for the cribs. Generally, the scavenged waste met the ^{137}Cs and ^{90}Sr disposal limits; however, ^{60}Co sometimes exceeded its limit. If a crib was approaching its ^{60}Co limit, or the scavenged supernate had an excess of ^{60}Co, the supernate was moved to a nonsettling tank for further ^{60}Co decontamination or disposal to a specific retention crib. Tanks 241-BX-102 and -106 were used to interim store scavenged supernates in this manner. Tanks 241-BX-102 and -106 were not, however, used to store or settle ferrocyanide sludges. There is no record of tanks 241-BX-110 and -111 receiving ferrocyanide wastes. The BX Farm tanks, therefore, are not expected to contain any ferrocyanide sludges.

4.1.4 Processing in the 200 West Area

Records for scavenged waste in the 200 West Area include the U Plant test in late 1953, during which the treated waste was routed to tank 241-T-101, and U Plant scavenging of T Plant IC wastes, which were subsequently routed to TY tanks 241-TY-101, -103, and -104. A total of six batches, with a total of 2.93 Mgal of scavenged supernate, were disposed to the TY cribs. There were plans at the time to continue In-Farm ferrocyanide treatment of the unscavenged UR waste stored in the 200 West Area. Studies for the addition of chemical treatment facilities at the 242-T Evaporator and laboratory were completed. However, no In-Farm scavenging in 200 West Area was performed. Examination of records for waste disposed to the ground for both the 200 East and 200 West Areas does not show ground disposal of scavenged wastes in the 200 West Area other than those noted.

The T Plant test added $K_4Fe(CN)_6$ to the acid waste to a concentration of 0.005 *M*, adjusted the pH to 9 ± 1, and then added $NiSO_4$ to 0.005 *M*. Coating waste was to be combined with the scavenged waste either in T Plant or in the underground waste tanks. It was planned to scavenge 750,000 gal of IC wastes in the initial plant test (Schmidt and Stedwell 1954). The two waste types were segregated because later information indicated that incorporation of the CW into the IC scavenged waste gave poor ^{90}Sr decontamination (Anderson 1990).

Routine scavenging of T Plant IC wastes started on December 31, 1954, and continued until T Plant was shut down in March 1956. The effective reduction in waste volume, as discharged from the building, was approximately 88% (Anderson 1990). Note that the IC waste would contain less than 10% of the fission products ^{137}Cs and ^{90}Sr originally present, because the MW contained greater than 90% of the fission products.

4.1.5 Estimated Ferrocyanide Tank Contents from Model Predictions

The identification of SSTs that contain significant quantities of ferrocyanide is ultimately based on the records of 59 U Plant UR waste scavenging campaigns, 29 In-Farm campaigns, 6 T Plant bismuth phosphate waste scavenging campaigns, and 1 PUREX Plant test. The identification utilized the TRAC computer database (Jungfleisch 1984) to evaluate the process history and estimate the amounts of ferrocyanide in the SSTs used as receivers of scavenging waste. A listing of 14 SSTs identified in 1984 (Pickett 1984) was expanded in 1989 to include all the SSTs that may contain greater than 1,000 mol of ferrocyanide ion (Nguyen 1989). Approximately 90% of the ferrocyanide is estimated to be in eight tanks that were primary receivers for the scavenging waste (tanks 241-BY-106, -107, -108, and -110 and 241-C-108, -109, -111, and -112) and two other tanks in which scavenging waste was consolidated (tanks 241-BY-104 and -105).

The scavenging process was well documented, and records for most of the campaigns still exist. A recent study (Borsheim and Simpson 1991) developed a spreadsheet model of the scavenging program from the historical records. This modeling effort was quite extensive and used the available documentation to develop several assumptions about the scavenging program. Using these assumptions and the existing transfer records as data inputs, the spreadsheet model was able to monitor the addition, accumulation, and transfer of ferrocyanide, ^{137}Cs, ^{90}Sr, and their associated solids. During the development of the model, the records search also resulted in adding two tanks, 241-T-107 and -104, to the ferrocyanide tank listing. The results of that study are shown in Table 4-3 for moles ferrocyanide. Also shown and compared in the table are the ferrocyanide values predicted by Nguyen (1989) based on TRAC (Jungfleisch 1984). Note that the model values represent waste amounts stored in the tanks at the end of the scavenging campaign. The TRAC values shown in the table include the input of ^{137}Cs and ^{90}Sr from subsequent processing and includes soluble ^{137}Cs in addition to precipitated ^{137}Cs. The model predicts more ferrocyanide inventory than Nguyen predicted for 6 tanks and no significant inventory (less than 1,000 mol) for 7 of the 24 ferrocyanide tanks.

Table 4-3. Comparison of Model Results with Baseline Values: Ferrocyanide Inventory at the End of Scavenging. (sheet 1 of 2)

Tank	Date (yr/qtr)	Model value	Baseline value[a]
		Amount $Fe(CN)_6^{-4}$ (mol)	Amount $Fe(CN)_6^{-4}$ (mol)
241-BX-102[b]	1956/4	<1	0 to 3,000
241-BX-106[b]	1956/1	<1	0 to 1,000
241-BX-110[b]	1958/1	<1	0 to 1,000
241-BX-111[b]	1958/1	<1	0 to 1,000
241-BY-101[b]	1955/1	<1	0 to 1,000
241-BY-103[b]	1955/3[c]	<1	0 to 2,000
241-BY-104	1957/3[c]	124,000	100,000 to 200,000
241-BY-105	1957/3[c]	89,000	70,000 to 100,000
241-BY-106	1956/4[c]	45,000	30,000
241-BY-107	1957/1	42,000	30,000 to 80,000
241-BY-108	1957/3	55,000	30,000 to 70,000
241-BY-110	1957/3	68,000	50,000 to 90,000
241-BY-111	1956/4	5,000	0 to 3,000
241-BY-112	1957/2	2,000	2,000 to 3,000
241-C-103[b]	1958/1	<1	0 (TRAC)
241-C-104[b]	1958/1	<1	0 (TRAC)
241-C-108	1958/1	25,000	9,000 to 20,000
241-C-109	1958/1	30,000	30,000 to 50,000
241-C-111	1957/4	33,000	10,000 to 30,000
241-C-112	1958/1	31,000	50,000 to 70,000
241-T-101[d]	1953/4[c]	10,000 5,000	0 to 10,000
241-T-107[d]	1953/4	5,000	0 (TRAC)
241-TX-118	1958/1	Not estimated	0 to 3,000
241-TY-101	1956/4	24,000	0 to 30,000

Table 4-3. Comparison of Model Results with Baseline Values: Ferrocyanide Inventory at the End of Scavenging. (sheet 2 of 2)

Tank	Date (yr/qtr)	Model value	Baseline value[a]
		Amount $Fe(CN)_6^{-4}$ (mol)	Amount $Fe(CN)_6^{-4}$ (mol)
241-TY-103	1956/4	28,000	0 to 30,000
241-TY-104	1955/3	12,000	0 (TRAC)

TRAC = Jungfleisch (1984).

[a]From Nguyen (1989).

[b]Tank did not receive significant amounts of scavenged solids; therefore, the amount of ferrocyanide in the tank was assumed to be insignificant.

[c]It is believed that except in the instances noted, ferrocyanide that was precipitated or transferred to a tank remained in that tank after the scavenging campaign.

[d]After cribbing half of the supernate, 50% of the solids from tank 241-T-101 were transferred to tank 241-T-107.

Several key assumptions of the model are as follows.

- Sludge formation in the BY, C, and T Farms was 4.25% of the original waste volume. Sludge formation in the TY Farm was 12%.
- All of the ferrocyanide added to the tank precipitated.
- The sludge was completely settled, and sludge was not routinely transferred to the cribs.
- Sludge was uniformly distributed throughout the tank.
- The porosity value used to estimate the nitrate inventory associated with the ferrocyanide was 71 vol%.

The remaining assumptions and their rationale, the results of the model, and a more in-depth treatment of the model's development can be found in Borsheim and Simpson (1991).

Both the TRAC computer program and the recent study assumed that during the scavenging program, the ferrocyanide sludge remained in the settling tanks unless special efforts were made to transfer sludge (e.g., to the 241-BY-104 and -105 sludge collection tanks). The ferrocyanide tanks remained in use after the scavenging program and were used for the receipt and processing of waste until the SSTs were removed from active service in 1980. Table 4-4 provides estimates of the concentration of ferrocyanide in the scavenging sludge and the ratio of moles ferrocyanide to moles of nitrate/nitrite in the sludge. The bases for these estimates are the spreadsheet model values for ferrocyanide and solids accumulation and the flowsheet or analytical data for nitrate concentrations in the supernate. However, Table 4-4 also includes the effects of large post-scavenging transfers from ferrocyanide tanks that could be expected to transfer some of the settled sludge to another tank. A summary of other pertinent historical and tank farm data about the ferrocyanide tanks is tabulated in Table 4-23.

4.2 TANK SAMPLES AND ANALYSIS RESULTS

Ultimately, much of the data needed to finalize a hazard evaluation of the ferrocyanide tanks must come from waste samples and analyses. However, some information is available from samples taken and analyzed in the past. These samples were not originally analyzed for ferrocyanide but have recently been analyzed for total cyanide. Several other key parameters can also be estimated based on the sample analysis data including moisture content, oxidant concentrations, organic carbon content, diluents present, sludge particle size, and waste density.

Few sample analyses of solids in the ferrocyanide tanks are available. In general, the samples and analyses were secured several years ago and did not include ferrocyanide or total cyanide analyses. Analyses have been located for tanks 241-BY-104 and 241-TY-101, -103, and -104 as presented in the following sections. These tanks contain sludges produced from T Plant and U Plant flowsheets.

Table 4-4. Summary: Estimates of Tank Inventories, Adjusted for Post-Scavenging Transfer Activity (radionuclides decayed to 1991).

Tank	$Fe(CN)_6$ (mol)	^{90}Sr (Ci)	^{137}Cs (Ci)	Vol sludge containing $Fe(CN)_6$ (gal)	Molarity of $Fe(CN)_6$ in sludge (M)	Molar ratio $Fe(CN)_6/NO_3/NO_2$
241-BX-102[a]	NE	NE	NE	NE	NE	DNA
241-BX-106[a]	NE	NE	NE	NE	NE	DNA
241-BX-110[a]	NE	NE	NE	NE	NE	DNA
241-BX-111[a]	NE	NE	NE	NE	NE	DNA
241-BY-101[a]	NE	NE	NE	NE	NE	DNA
241-BY-103[a]	6.59 E+04	2.32 E+05	1.55 E+05	2.12 E+05	0.0823	1.0/28.6/9.5
241-BY-104	8.32 E+04	3.03 E+05	1.98 E+05	2.60 E+05	0.0843	1.0/30.9/10.3
241-BY-105	3.62 E+04	1.26 E+05	8.82 E+04	9.60 E+04	0.0991	1.0/26.3/8.8
241-BY-106	7.00 E+04	3.31 E+05	2.15 E+05	2.28 E+05	0.0811	1.0/32.2/10.7
241-BY-107	4.24 E+04	2.19 E+05	1.31 E+05	1.58 E+05	0.0702	1.0/37.1/12.4
241-BY-108	5.80 E+04	2.59 E+05	2.12 E+05	2.08 E+05	0.0699	1.0/37.3/12.4
241-BY-110	7.07 E+04	3.16 E+05	1.90 E+05	2.25 E+05	0.0798	1.0/32.7/10.9
241-BY-111	5.50 E+03	1.85 E+04	1.11 E+04	1.40 E+04	0.0944	1.0/27.6/9.2
241-BY-112	2.00 E+03	8.06 E+03	5.09 E+03	7.00 E+03	0.0755	1.0/34.6/11.5
241-C-108	2.50 E+04	5.93 E+02	6.50 E+04	7.70 E+04	0.0858	1.0/45.7/15.2
241-C-109	3.00 E+04	3.84 E+03	1.06 E+05	1.09 E+05	0.0727	1.0/53.9/18.0
241-C-111	3.30 E+04	8.15 E+02	1.37 E+04	9.80 E+04	0.0890	1.0/44.0/14.7
241-C-112	3.10 E+04	1.25 E+03	1.44 E+05	8.40 E+04	0.0975	1.0/40.2/13.4
241-T-101[b]	0	0	0	0	0	D.N.A
241-T-107	5.00 E+03	1.30 E+04	7.83 E+03	2.12 E+05	0.0062	1.0/112.3/37.4
241-TX-118[a]	NE	NE	NE	NE	NE	DNA
241-TY-101	2.29 E+04	3.67 E+04	4.17 E+04	1.51 E+05	0.0420	1.0/16.7/5.6
241-TY-103	2.80 E+04	4.54 E+04	5.16 E+04	1.79 E+05	0.0413	1.0/16.9/5.6
241-TY-104	1.20 E+04	1.88 E+04	2.13 E+04	7.50 E+04	0.0423	1.00/16.6/5.5

NOTE: Values in this table reflect the impact of post-1958 transfers on tank inventories. Nitrates/nitrites counted in this inventory are only those intimately mixed with the ferrocyanide in the interstitial liquid space. Nitrite amount is assumed to be one-third nitrate amount from radiolytic degradation of nitrate.

DNA = Does not apply.

NE = not evaluated. Records show tank did not receive ferrocyanide solids.

[a]Tank did not receive significant amounts of scavenged solids during or after the scavenging campaign; therefore, this relationship has no meaning.

[b]Tank 241-T-101 was sluiced in 1956 after it received ferrocyanide solids; thus, it is considered emptied and no longer contains ferrocyanide.

4.2.1 Tank 241-BY-104

The analyses from a core sample containing both solids and supernate taken in 1976 were reported by Horton (1976) and are reproduced in Tables 4-5, 4-6, and 4-7. This was a split-barrel core sample, and the depth at which the sample was taken is unknown. The reported solid's nitrate concentration is so high that the sample is probably composed of salt cake (predominantly sodium nitrate). In addition, the water content of the solids was 28.3 wt%, which is also indicative of salt cake. Salt cake forms the top several feet of the waste in this tank and in most of the other BY Farm tanks.

Several reported values in this report are suspect, although the general trend of the data is reasonable for salt cake. For example, pure dry sodium nitrate with a density of 2.26 g/cm^3 would be 26.6 *M*; thus, the reported 24.1 *M* NO_3^- is unreasonably high. Note that nitrite is not reported in the sludge analysis, but the supernate analysis shows it to be a factor of 25 times greater than the nitrate on a molar basis and yet only twice the nitrate on a weight basis. The nickel concentration reported in the sludge also appears too high. It is approximately four to nine times higher than the nickel values listed for the TY samples discussed in Section 4.2.2. Other reported values appear within reason. The similarity of ^{137}Cs concentration values between the solids and the supernate also indicates that the sample was taken from the salt cake and is probably a result of the ITS-2 program processing.

4.2.2 Data Analysis and Interpretation of Samples Taken from Tanks 241-TY-101, -103, and -104

Tanks 241-TY-101, -103, and -104 were core sampled in August and September 1985. The six TY Farm tanks were rotary core sampled in 1985 as part of the effort to develop reliable techniques for achieving full-depth core samples. One core from tank 241-TY-101, two from 241-TY-103, and four from 241-TY-104 were composited and analyzed. Information from an earlier core sample of tank 241-TY-101 taken in October 1979 was also available. The full analytical results for these core samples are in Appendix A. The most relevant data have been summarized in Tables 4-8 and 4-9.

These analytical results and the process histories of these tanks strongly suggest that the majority of the waste in the TY farm ferrocyanide tanks consists of water and nitrate salts (sodium nitrate in particular) on a weight-percent basis. The ^{137}Cs in tanks 241-TY-101 and -103 was not readily soluble in water (less than 0.1% dissolution) but was liberated in acid dissolution solutions. It appears that the cesium in these tanks is strongly associated with the ferrocyanide. The cesium in tank 241-TY-104 appears to be much more soluble; however, tank 241-TY-104 only received a single transfer of solids containing ferrocyanide. Other wastes received later in the tank's process history likely contributed significantly more ^{137}Cs to the tank inventory than the ferrocyanide scavenging waste.

Table 4-5. Analysis of Tank 241-BY-104 Core Sample Solids.

Component	Value	Units
Bulk density	1.61	g/cm^3
Particle density	2.09	g/cm^3
$\%H_2O$	28.3	wt%
Al	2.3	*M*
Fe	0.1	*M*
NO_3	24.1	*M*
Ca	0.06	*M*
Ba	<0.004	*M*
Mg	0.04	*M*
Mn	0.03	*M*
Ni	0.5	*M*
PO_4	0.1	*M*
Si	<0.3	*M*
Pu	1.13×10^{-3}	g/L
$^{89,90}Sr$	1.74×10^{5}	$\mu Ci/L = 1.18 \times 10^{-3}$ W/L
^{137}Cs	4.40×10^{5}	$\mu Ci/L = 2.11 \times 10^{-3}$ W/L

*From Horton (1976).

Table 4-6. Analysis of Tank 241-BY-104 Supernatant.

Component	Value	Wt. (%)
Density	1.45 g/cm^3	
H_2O	--	48.0%
Al	2.48 *M*	14.0%
Fe	1.07×10^{-3} *M*	4.1%
NO_2	2.46 *M*	11.7%
NO_3	0.11 *M* (1.10 *M*)*	6.4%
OH	3.74 *M*	10.3%
CO_3	0.43 *M*	3.1%
Si	$<3.25 \times 10^{-3}$ *M*	<0.6%
PO_4	9.79×10^{-3} *M*	0.1%
$^{89,90}Sr$	2.01×10^2 μCi/L	
^{137}Cs	5.30×10^5 μCi/L	
Total Wt. Recovery		98.3%

*Typographical error suspected; wt% falls in line with 1.0 *M* NO_3.

Table 4-7. Particle Size Distribution--Tank 241-BY-104 Solids.

Particle size (μm)	Average diameter (μm)	Wt. (%)	Cumulative wt.(%)
5 to 10	8.25	4.0	99.4
10 to 20	16.5	68.3	95.4
20 to 30	25.9	19.2	27.1
30 to 40	35.7	3.1	7.9
40 to 50	45.5	1.0	4.8
50 to 60	55.4	1.3	3.8
60 to 70	65.4	0.8	2.5
70 to 80	75.3	0.8	1.7
80 to 90	85.3	0.4	0.9
90 to 100	95.3	0.5	0.5

Source: Horton (1976).

Table 4-8. TY Tank Farm Summary Analysis.

Tank	Water (wt%)	Bulk density (g/cm^3)	Particle density	Ni (µg/g)	CN^- (µg/g)*	Total organic carbon		^{90}Sr (µCi/g)	^{137}Cs (µCi/g)	NO_3^- (µg/g)	Free OH^- (µg/g)	pH
						µg/g	wt%					
241-TY-101	43.5	1.64	0.924	5,100	NA/ 3,300-3,800	663	<0.1	12.4	0.284	14,500	0.212	8.2
241-TY-103	52.5	1.70	0.754	2,530	NA/ 2,300-3,000	1,490	0.1	105	24.7	13,500	87-168	10.9-11.2
241-TY-104	55.5	1.48	1.19	1,730	NA	907	0.4	236	47	62,300	1,580	12

Source: Weiss (1986).
NOTE: Samples not originally analyzed for cyanide.
NA = not originally analyzed, but archived samples were analyzed for total cyanide in 1988.

Table 4-9. Cesium Distribution on Washing Single-Shell Tank Waste Samples.

Tank	Riser	Total ^{137}Cs ($\mu Ci/g$)	^{137}Cs in water wash (%)	^{137}Cs in acid wash (%)	^{137}Cs in dissolution test (%)
241-TY-101*	R-3	0.3	0.09	57	43
241-TY-103*	R-8	25	0.002	8	92
241-TY-103	R-8	11	0.01	8	91
241-TY-104*	R-5	47	84	15	1.6
241-TY-104	R-3	93	12	17	70
241-TY-104	R-5	26	30	38	31
241-TY-104	R-5	15	47	52	2

*Cesium-137 core composite analytical result reported in Table 4-8.

The TY Farm core samples were all composited before analysis, and the initial characterization effort did not include analysis for cyanide or ferrocyanide. Two of the tanks sampled, 241-TY-101 and -103, were predicted (in 1988) to contain ferrocyanides. During 1988, archive samples from tanks 241-TY-101 and -103 were analyzed for total cyanide. For tank 241-TY-101, the CN^- concentration results ranged from 3,300 to 3,800 $\mu g/g$ (wet solids). For tank 241-TY-103, the CN^- concentration results ranged from 2,300 to 3,000 $\mu g/g$ (Winters 1988). These results, coupled with the bulk density measured on the samples and the measured solids volumes in the tanks, indicate that these tanks now contain approximately 17,000 mol (241-TY-101) and 15,000 to 20,000 mol (241-TY-103) of ferrocyanide. These inventories compare favorably with the estimated input of $Fe(CN)_6$ into tanks 241-TY-101 and -103 of 23,000 and 28,000 mol, respectively (Borsheim and Simpson 1991). The measured values do not suggest that large quantities of ferrocyanide have been solubilized. Supernates with pH values greater than 12 may possess relatively high concentrations of soluble CN^- (over 100 p/m) from ferrocyanide resolubilization. All core samples and supernate samples taken in the tank farms are now routinely analyzed for CN^-. In addition, the inventories determined from the Borsheim and Simpson (1991) model give the upper bound for ferrocyanide inventories in these tanks and thus are conservative.

4.2.3 Recent Supernate Analyses from 200 East Area Ferrocyanide Tanks

Archived supernate samples were analyzed in the Process Chemistry Laboratories in 1990. Table 4-10 reports available relevant values for the soluble species in the ferrocyanide tanks.

Table 4-10. Analysis of BX and BY Tank Supernate Samples.

Tank	Sp. gr.	pH	Water (%)	Total organic carbon (g/L)	CN^- (µg/g)	NO_x^- (M)	^{90}Sr (µCi/L)	^{137}Cs (µCi/L)
241-BX-106	1.33	13.28	63.8	4.4	NA	2.62	5.16 E+02	1.81 E+05
241-BX-110	1.37	12.5	56.6	5.6	NA	5.04	1.50 E+01	1.35 E+05
241-BX-111	1.44	12.7	53.3	5.7	NA	2.62	2.00 E+01	2.60 E+05
241-BY-103	1.45	13.29	52.0	2.73	6.73	4.37	2.33 E+02	2.00 E+05
241-BY-105	1.39	13.24	54.3	2.93	14.57	8.42	1.30 E+01	7.40 E+04
241-BY-106	1.46	13.47	49.6	3.16	45.38	4.05	1.20 E+02	3.11 E+05

NA = not available.

The data in Table 4-10 indicate that the supernate (and the associated salt cake) are highly alkaline, composed primarily of water and soluble nitrate salts. Relatively high concentrations of soluble ^{137}Cs are found in all of the supernate samples, and the reported concentrations are within a narrow range of values. This behavior is not unexpected because all but one of these tanks (tank 241-BX-106) were in the ITS-2 program. In the ITS-2 process, the supernate was evaporated at atmospheric pressure in a tank with a heating element in it. The hot supernate was cooled by running it through each tank that was connected in the series, allowing it to precipitate salts from the saturated solution. As time went on, this process also allowed the supernate to become more and more homogeneous. In the time elapsed since the end of the ITS-2 process, however, the initial differences in the tanks, as well as the effect of further processing, have caused some differentiation in the solutions' composition. The anomalous ^{137}Cs value for tank 241-BY-105 may be the result of a waste solidification experiment. In 1966, 63 tons of cement was added to tank 241-BY-105. This material may have fixed a large amount of soluble ^{137}Cs in place. Because ^{90}Sr was much less soluble under the solution conditions, the homogenizing effect is much less pronounced, and its solution concentrations are significantly lower. The relatively small amount of soluble CN^- indicates that the majority of ferrocyanide added to these tanks has not dissociated and remains in the sludge.

4.2.4 Future Tank Sampling Activities

The Waste Characterization Plan for the Hanford Site SSTs (Winters et al. 1990) calls for securing two core samples from each of the 149 SSTs by September 1998. The ferrocyanide watchlist tank sampling program has been given a high priority. However, core sampling of many of the ferrocyanide tanks is complicated by a relatively hard salt cake layer overlying the sludge. The salt cake layer requires core sampling to be done in a rotary mode. The rotary core sampling techniques must first be shown to be safe; i.e., it must not generate an unacceptably high temperature in the waste that might initiate a ferrocyanide-nitrate/nitrite reaction. The rotary core sampling safety demonstration is expected to be completed in fiscal year 1992.

Initial solids samples to be obtained from the ferrocyanide tanks will be auger surface samples of the tanks with salt cake and push-mode core samples of tanks without overlying salt cake. The analyses for these samples will include differential scanning calorimetry (DSC) to detect potential exothermic reactions. Adiabatic calorimetry will also be performed if a significant low-temperature exotherm is seen by DSC. Additionally, cyanide and ferrocyanide speciation will be performed. The ferrocyanide speciation procedure is being developed, and it may be necessary to archive samples pending certification of the procedure. Many of the analyses will be performed on 11.4-cm (4.5-in.) individual core sample segments to identify the location (depth) of the ferrocyanide solids in the waste tanks. The sampling and analysis procedure for ferrocyanide tanks is described in detail in WHC-EP-0210 Rev. 3, Appendix I (Winters et al. 1991), and is subject to modification.

4.3 FLOWSHEET WASTE SIMULANTS AND ANALYSIS RESULTS

The nickel ferrocyanide scavenging flowsheet used to remove cesium from tank farm wastes varied as a function of waste feed, process improvements with time, and changing process requirements during 1954 to 1957. Section 4.1 and Abrams (1956) contain a chronological sequence of flowsheet uses and adjustments. The scavenging flowsheet, a modified Sloat flowsheet, was used for processing three general waste types (U Plant, In-Farm, and T Plant). The modified Sloat flowsheet used to produce a synthetic U Plant sludge for characterization studies is shown in Figure 4-1.

The first nine batches of U Plant waste were treated to 0.005 *M* nickel sulfate and 0.005 *M* potassium ferrocyanide for cesium scavenging, but no calcium nitrate or strontium nitrate was added for strontium scavenging. Thereafter, about nine batches were treated to 0.005 *M* nickel sulfate, 0.005 *M* sodium ferrocyanide, and 0.016 *M* calcium nitrate for cesium and strontium scavenging. The addition of calcium nitrate was expected to result in an additional source of inert solid diluents in the final sludge. The sludge produced by this second process would be expected to be less reactive than the previous sludge produced without calcium nitrate addition. The remaining batches (32) were treated to 0.0025 *M* nickel sulfate, 0.0025 *M* sodium ferrocyanide, and 0.004 *M* strontium nitrate. Because most of the waste stored in the tank farms (including tank 241-BY-104, the ferrocyanide tank believed to contain the most ferrocyanide) was produced using this process, it was decided to first test synthetic ferrocyanide sludge produced by this process. Synthetic sludge produced by the process used for the first nine U Plant batches will also be evaluated for reactivity because it may contain less of the solid diluents. Excess oxidant appears to be present in all of the ferrocyanide sludges produced by the three flowsheets.

4.3.1 Composition of Synthetic U Plant Produced Sludge

Synthetic flowsheet material was produced in the chemical engineering laboratory by a modified Sloat (Sloat 1955) flowsheet (Figure 4-1) to produce sludge (excluding uranium and radioactive isotopes) similar to the bulk of the ferrocyanide waste added to the BY and T farm tanks. The exclusion of uranium and fission products as solid diluents is a conservative condition for reactivity determination in that there would be slightly fewer chemically

inert diluents present in the prepared precipitate. For uranium, this typically would amount to less than 1 wt% of the sludge, because plant uranium losses had a typical value of 1%. If there were plant process upsets, uranium losses would be greater than 1%, and inert uranium diluents would be present in greater amounts in the ferrocyanide sludge. This circumstance would make the tank farm sludge less reactive than the synthetic material produced for testing.

Synthetic U Plant flowsheet material preparation, to represent the bulk of the U Plant sludge, consisted of adding sodium ferrocyanide and strontium nitrate to the Figure 4-1 synthetic waste feed solution to form a solution of 0.0025 *M* ferrocyanide and 0.004 *M* strontium nitrate, mixing and digesting at 40 °C for 1 h, adjusting the pH to 9.3 by adding sodium hydroxide, adding nickel sulfate to 0.0025 *M*, mixing and digesting for an additional hour at 40 °C, allowing the precipitate to settle for 10 days, removing the supernate, and centrifuging the sludge. The batch size was with an initial feed solution volume of 75 L in a stainless steel tank of 0.44 m diameter and 0.7 m high. The ratio of liquid depth-to-settling surface area was 3.1 m/m^2 for the synthetic sludge produced in the chemical engineering laboratory and ranged from about 0.0003 to 0.003 m/m^2 for actual sludge in the tank farm. Settling characteristics of the synthetic sludge are expected to be similar to that experienced in the waste tanks even with the large difference in size.

The sludge formed after a settling time of 2 weeks consisted of 19% of the original feed solution volume. This sludge was observed to consist of three separate layers: (1) a blue layer on top, (2) a thin tan layer in the middle, and (3) a grey-green layer on the bottom. Initial infrared analysis of the three layers indicated that cyanide was present in all three layers. Methods to quantify the amounts of cyanide in each layer are being developed. The supernatant was determined to have a density of 1.19 to 1.20 g/cm^3 and a water content of 72 wt%. The settled solids were determined to have a density of 1.27 g/cm^3; a water content of 71 wt%; a viscosity of between 100 and 200 cP at low shear rates (less than 200 s^{-1}), decreasing to 20 cP at high shear rates (greater than 700 s^{-1}); and were very pourable.

Thermogravimetric analysis and DSC analysis of the settled sludge simulant were completed and indicate that free water and hydrated water are released by heating to 170 °C. The mass change as a function of temperature is indicated in the TGA shown in Figure 4-4. The TGA shows that there is about 67.5 wt% free water and 13.1 wt% bound water in the settled sludge. The free water appeared to be released up to 96 °C and the bound water up to 170 °C. Some weight release is also indicated by the slow mass decrease between 225 °C and 500 °C, as shown in Figure 4-5. This small mass change amounted to about 0.9 wt% and indicated that some offgasing was occurring. Exotherms are very weak or nonexistent as shown by the DSC trace in Figure 4-6. Three endotherms are shown by this DSC at onset temperatures of 61, 159, and 290 °C corresponding to free-water release, bound-water release, and oxidant melting, respectively. This settled sludge, when heated to dryness, has a greater fraction of solids present than actual waste may have, because it has additional liquid with soluble species associated with it. The centrifuged sludge would be expected to have a greater dry weight fraction of ferrocyanide and to be more representative of the waste in the waste tanks.

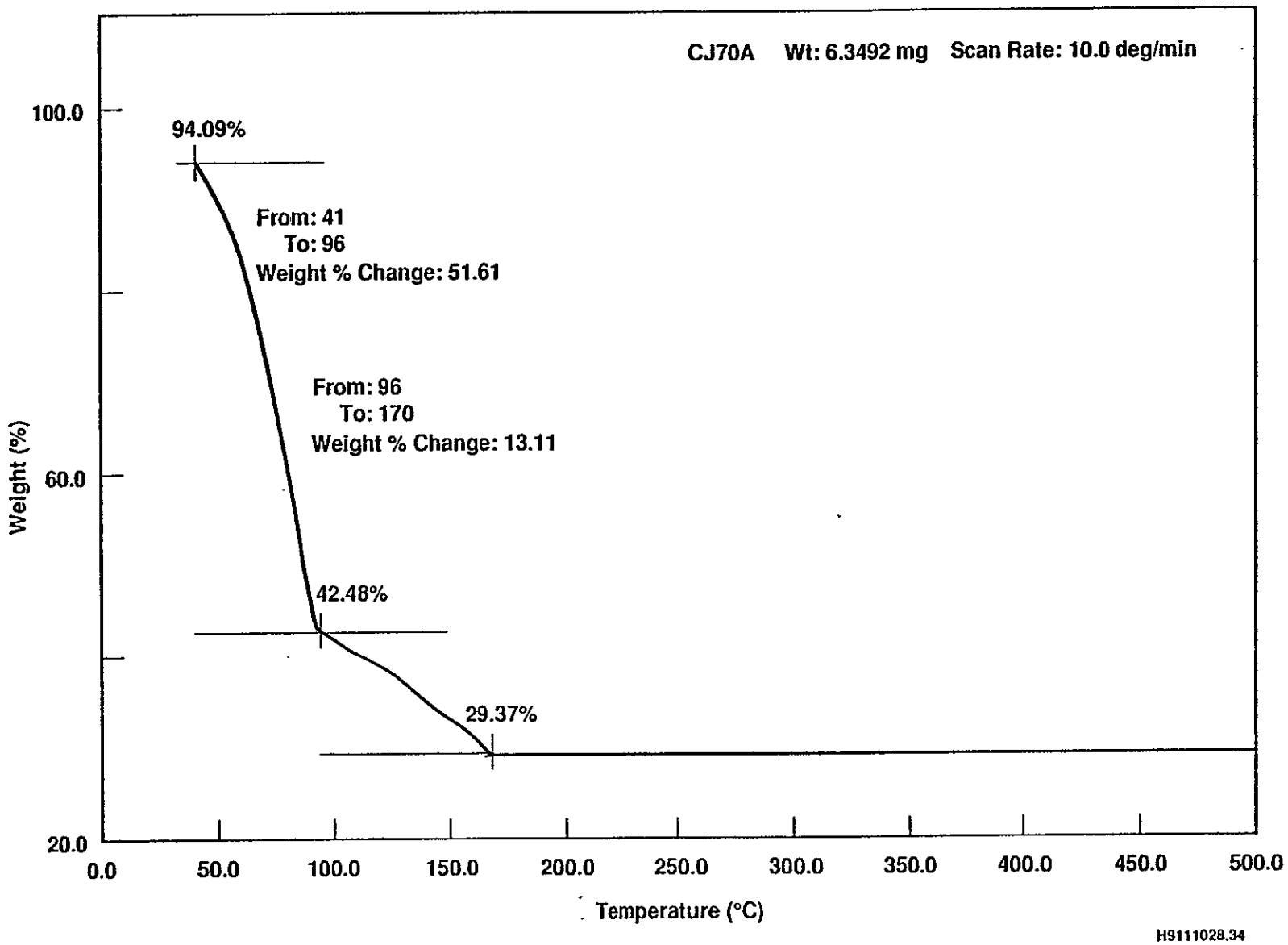

Figure 4-4. Thermogravimetric Analysis of U Plant Flowsheet Simulant Settled Sludge Composite.

Figure 4-5. Thermogravimetric Analysis of U Plant Flowsheet Simulant Settled Sludge Composite Showing Reaction Release.

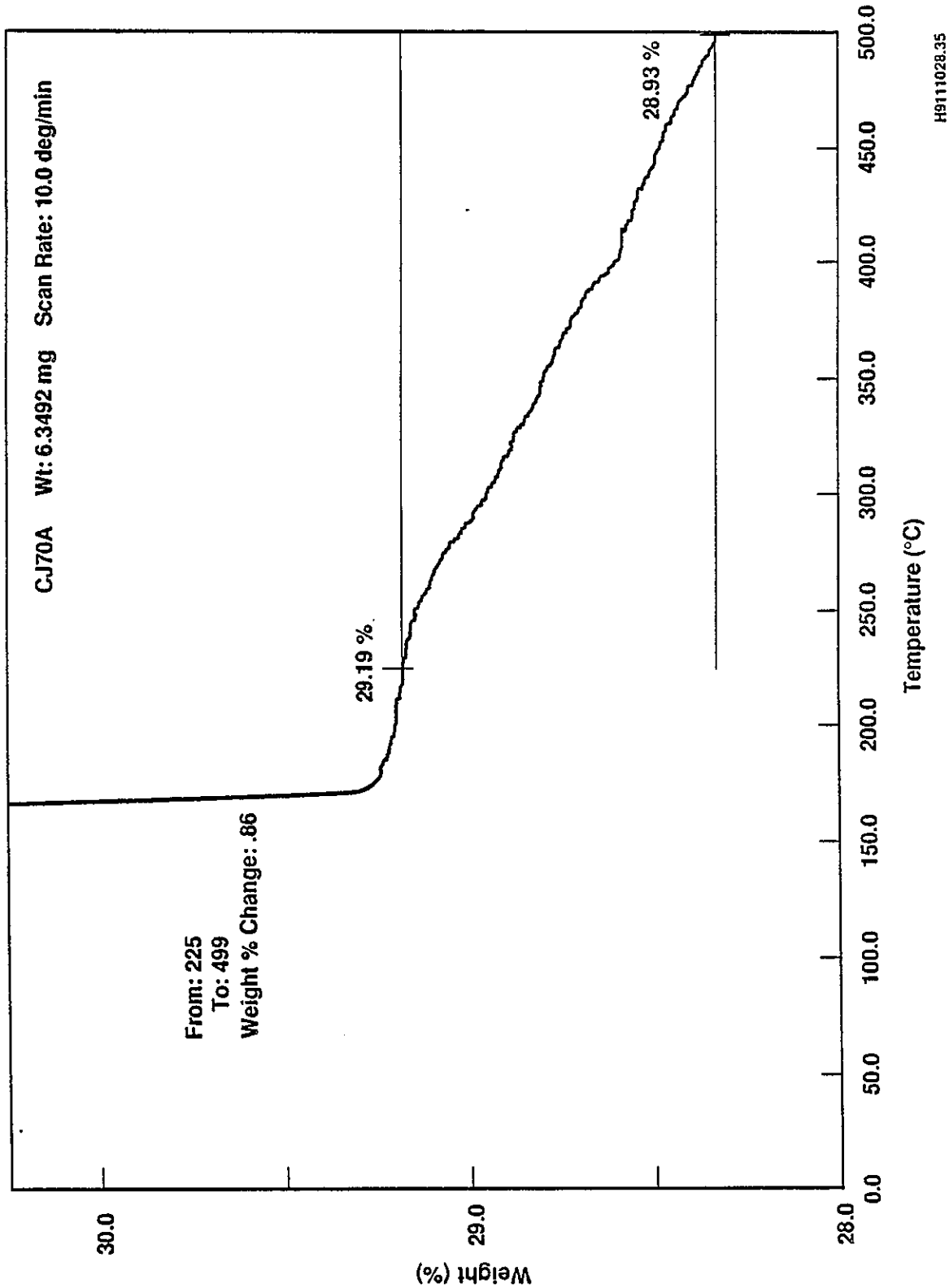

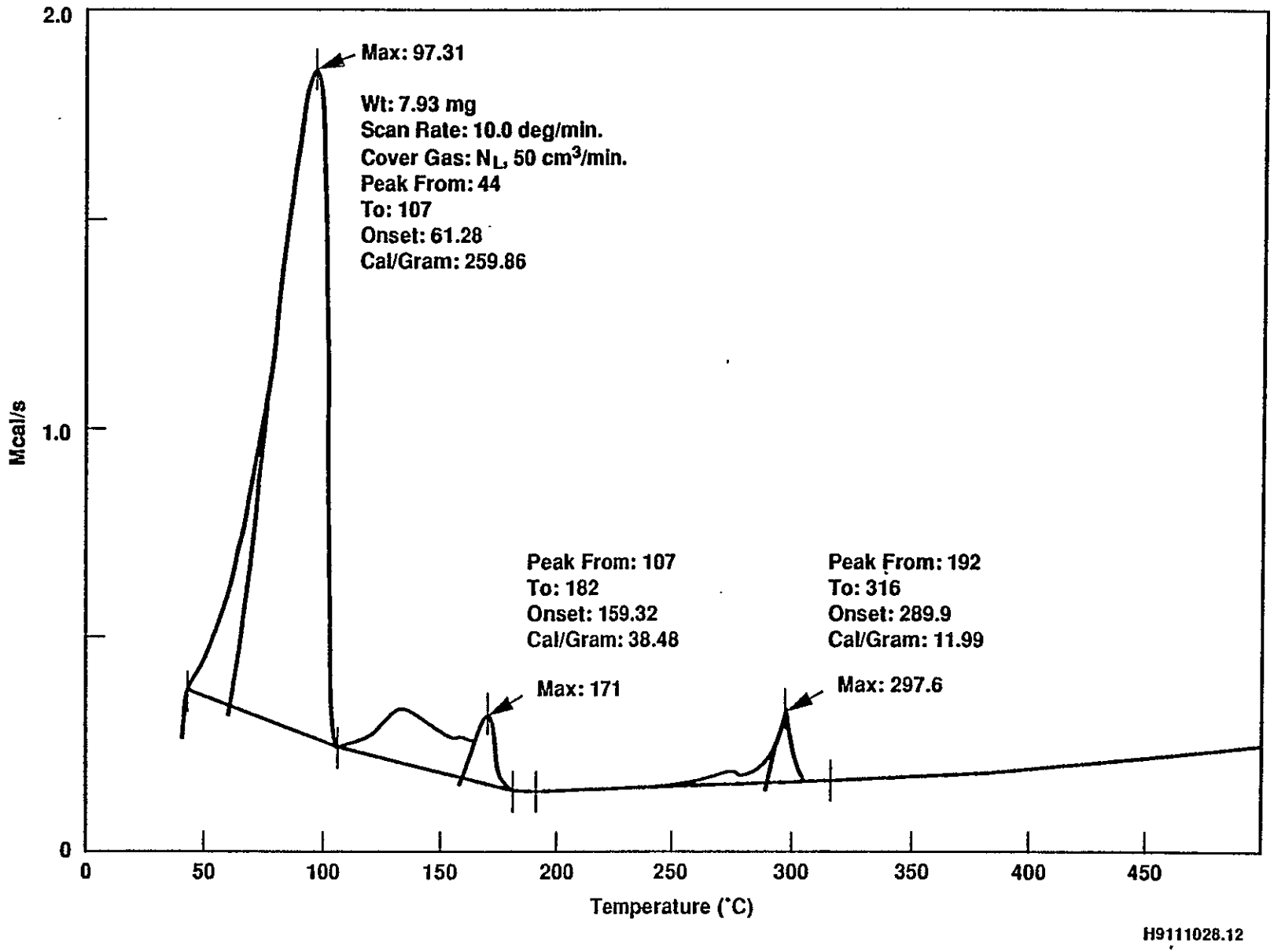

Figure 4-6. Differential Scanning Calorimeter Analysis of U Plant Flowsheet Simulant Settled Sludge Composite.

Additional chemical analyses of the settled sludge and supernatant are being made to quantify the solid diluents, cyanide content, metal atoms, and cations present and composition of the three different layers of precipitate in the settled sludge.

Some settled sludge simulant material was reslurried and centrifuged for 17 h at 2,000 r/min and radius of 8.5 in. (equivalent to 1.9 gravity years) to obtain a sludge product at 4.18% of the original waste volume. It was determined to have a density of 1.30 g/cm^3 and a water content of 64.6 to 67.1 wt% (including both free water and waters of hydration).

Additional settled sludge simulant was also slurried and centrifuged for 10.67 days to simulate 30 gravity-years settling; this produced a solids product with 65.7 to 67.0 wt% water and 1.38 to 1.42 sp gr. The solids produced were a pseudoplastic and had an initial viscosity of 10,000 cP or greater and an apparent viscosity of 200 to 300 cP after sufficient shear stress had been applied to the solids to mobilize them. These centrifuged solids were not pourable. An estimate of the composite composition of the centrifuged synthetic sludge prepared from 0.0025 *M* ferrocyanide solution with strontium nitrate addition to 0.004 *M* is listed in Table 4-11. These calculations were based on measured water content, specific gravity, and volume of the centrifuged solids produced and the flowsheet values of the interstitial liquid within the sludge. A listing of components considered as diluents is included in the table.

Composited material prepared in this manner was tested by FAI in the Reactive System Screening Tool (RSST) adiabatic calorimeter (Appendix C). It was observed to have only very weak exotherms. The self-heating rate for 10 g of this material with an imposed self-heat rate of 1 °C/min is shown in Figure 4-7 for the temperature range of 20 to 380 °C. There is no runaway reaction and only slight internal heating observed. The pressure response of the contained (370 mL) reaction is shown in Figure 4-8 and shows no pressure increase. This prepared material, representing the bulk of the U Plant ferrocyanide sludge, was shown to not generate any appreciable heat and would not support a propagating reaction (even in a completely dried-out state).

Infrared analysis of the noncomposited (layered) centrifuged solids confirm the presence of $NiFe(CN)_6^{=}$, hydroxide, sulfate, phosphate, ammonium, nitrate, and water. Preliminary quantitative analyses are listed in Table 4-12. Table 4-12 presents the analytical results for the top and middle layers formed in the centrifuged sludge. The values are presented for dried material. Table 4-13 presents an estimated composition for the upper (more concentrated) layer assuming the wet sludge contained 50 wt% water.

Table 4-11. Estimated Composition of Synthetic Composited U Plant Sludge Prepared from 0.0025 *M* Ferrocyanide Solution with Strontium Nitrate Addition to 0.004 *M*.

Sludge component	Weight fraction
Disodium mononickel ferrocyanide	0.018
Iron hydroxide	0.030
Strontium phosphate	0.012
Sodium phosphate	0.017
Sodium and ammonium sulfates	0.028
Sodium nitrate	0.235
Water	0.661
Total	1.001
Diluents	**Weight fraction**
Iron hydroxide	0.030
Strontium phosphate	0.012
Sodium phosphate	0.017
Sodium sulfate	0.014
Sodium nitrate	0.217
Water	0.661
Total	0.951

Figure 4-7. Reactive System Screening Tool Results of U Plant Flowsheet Simulant Solids (Centrifuged, Composited, and Dried) (Appendix C).

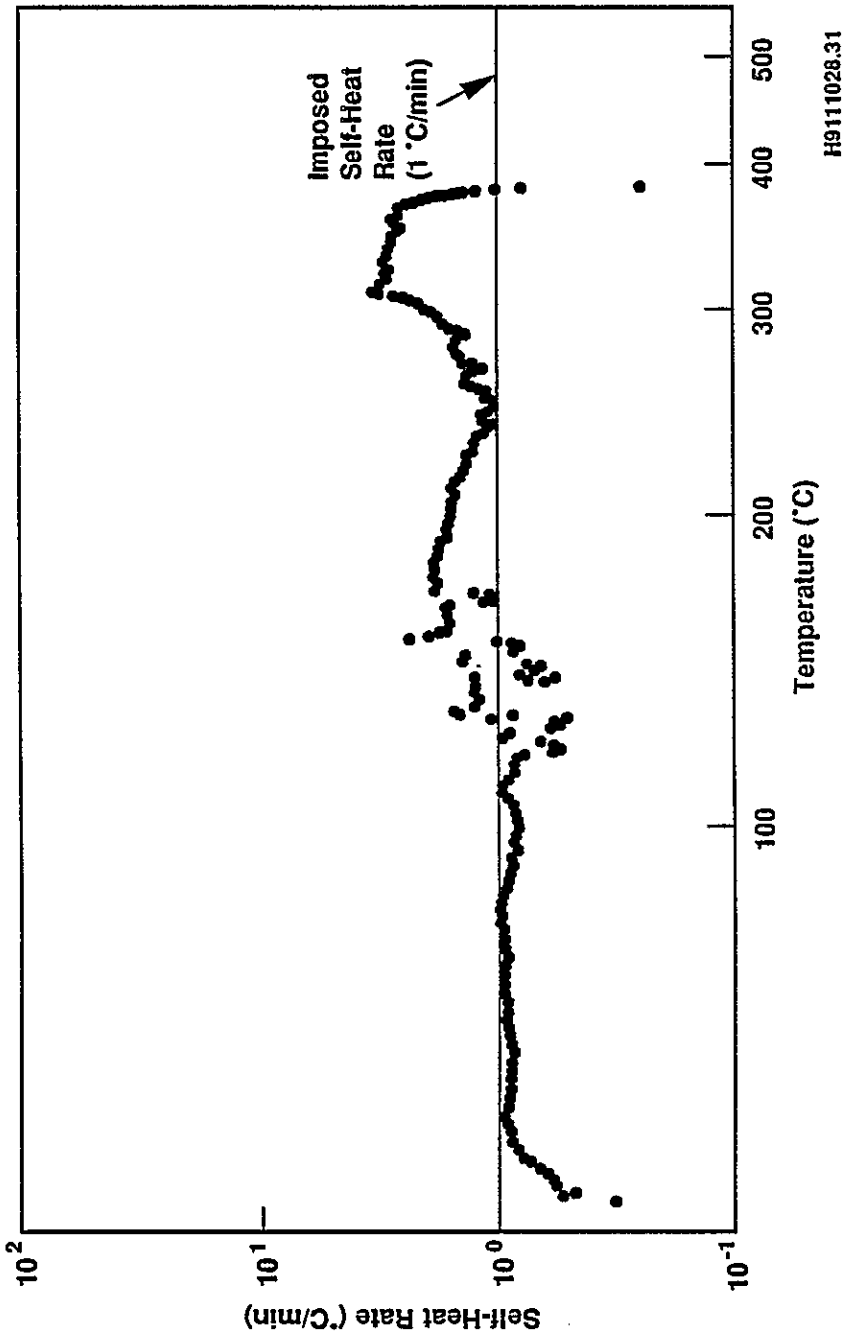

Figure 4-8. Reactive System Screening Tool Pressure Response for U Plant Flowsheet Simulant Solids (Centrifuged, Composited, and Dried) (Appendix C).

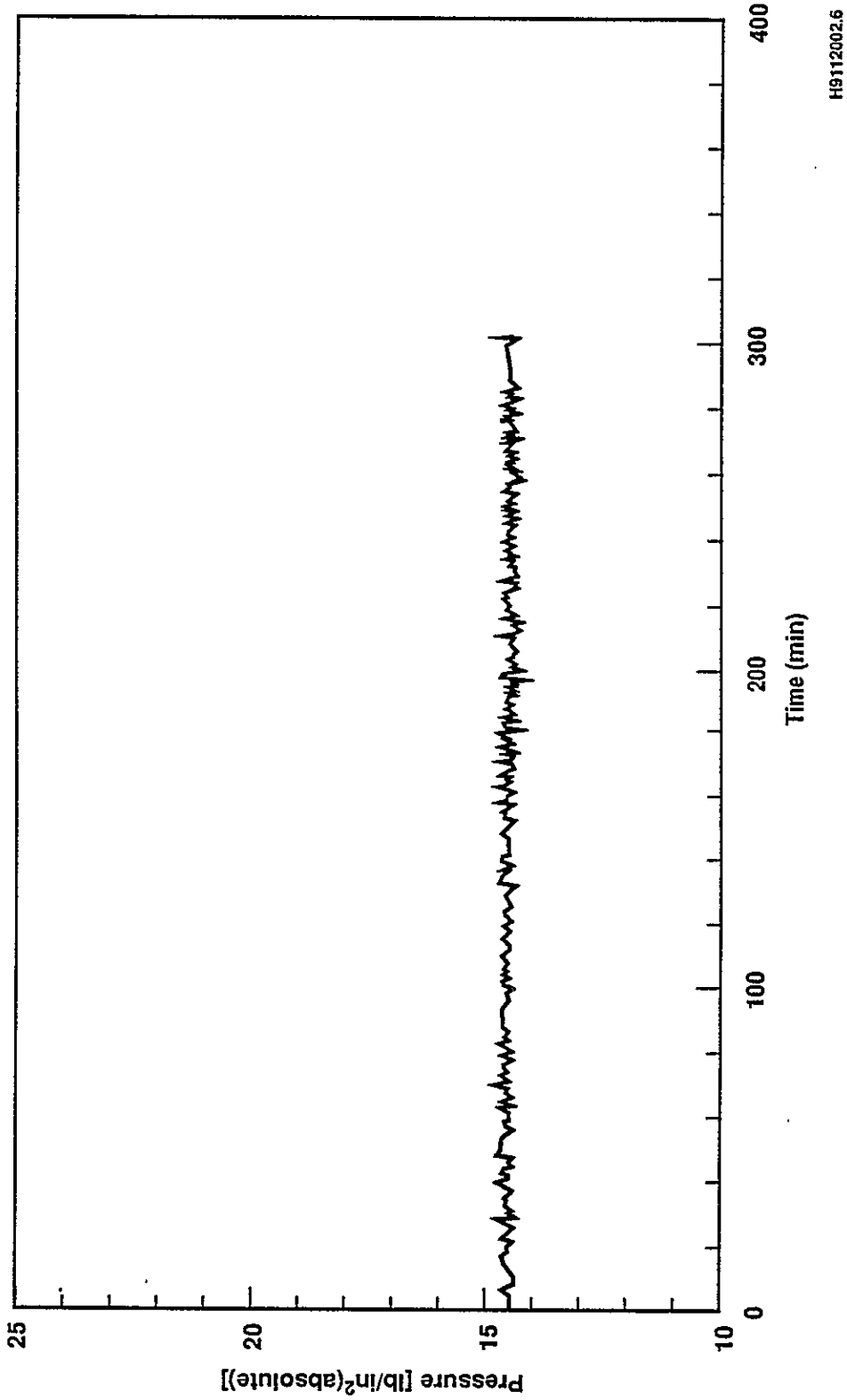

Table 4-12. Preliminary Analysis of Centrifuged, Dried, Synthetic U Plant Sludge.

Centrifuged dried sludge	Weight (%)			
	$NaNO_3$	$Na_2NiFe(CN)_6$	Na_2SO_4	$Sr_3(PO_4)_2$
Upper layer	50	7.5-8	3-4	4-5
Middle layer	50	4.4-5.0	4-5	5-6
Bottom layer	--	--	--	--

NOTE: Iron hydroxide is expected to account for most of the remaining mass in the dried mixture. Results from the iron analysis are not yet available.

Table 4-13. Analytical Content of the Most Concentrated Layer of Synthetic Centrifuged U Plant 1 Sludge.

	Flowsheet (weight fraction)
Disodium mononickel $Fe(CN)_6$	0.027
Iron hydroxide	--
Sodium sulfate	0.014
Strontium phosphate	0.018
Sodium nitrate	0.175
Water	0.66*
Total	0.884

*Water content estimated based on composite analysis value (0.66 weight fraction) of all layers. Iron hydroxide analysis not completed yet but expected to make up most of the difference in mass between the 0.88 and 1.00 weight fraction.

4.3.2 Synthetic In-Farm Produced Sludge

Synthetic In-Farm ferrocyanide sludges have been produced to determine their compositions and reactivity characteristics. Analysis results for the In-Farm simulant were not available at the time of this interim report. The presence of sulfide in some of the In-Farm ferrocyanide waste will be evaluated as an additional fuel source and to determine if it has an effect on the ignition temperature of the waste. Determination of diluents present in these synthetic materials will be made. The Hanford Site waste produced by the In-Farm flowsheet is stored in the C Farm tanks.

4.3.3 T Plant Decontamination Cycle Waste Produced Sludge

Synthetic T Plant ferrocyanide sludge will be produced and characterized. This sludge is expected to be more dilute than the In-Farm sludge. Sample analysis of actual stored T Plant sludge from tanks 241-TY-101 and -103 have been completed (see Section 4.2) and indicate that the ferrocyanide concentrations are low enough that no propagating reactions are expected.

4.4 LIQUID LEVEL MEASUREMENTS

Interstitial liquid level measurements are routinely taken by neutron and gamma scans in ferrocyanide tanks that have LOWs. Liquid level measurements have been obtained by using manual tapes or Food Instrument Corporation (FIC) gauges in some ferrocyanide tanks where liquid is exposed at a location below the tank salt-well riser. The salt-well locations, where available, are near the center of the tanks. Neutron and gamma scans are obtained at a monthly or quarterly frequency, and the manual tape and FIC liquid level readings are obtained on a weekly or continuous frequency.

4.4.1 Liquid Level Measurement Locations

Liquid observation wells are located in 12 of the 24 ferrocyanide tanks. The ferrocyanide tank, LOW riser, riser radius, and method of determining tank liquid level and solids level are included in Table 4-14. A schematic of a LOW riser, monitoring van, and typical BY Farm tank is shown in Figure 4-9. The LOWs in the ferrocyanide tanks are all constructed of fibercast material.

4.4.2 Liquid Level Determinations

Neutron and gross gamma scans are made routinely in 12 of the 24 ferrocyanide waste tanks to identify interstitial liquid levels in the tanks. The scans have been made since the LOWs were installed. Neutron and gross gamma scans obtained in 1985 and in 1991 are shown in Appendix B, Figures B-1 through B-24, for each of the 12 ferrocyanide tanks. Current interstitial liquid levels determined by neutron and gross gamma scans are listed in Table 4-15 along with liquid level values determined by the manual tapes and FIC gauges. In general, the neutron and gamma scan interstitial liquid levels are in fair agreement. The level determined by neutron scanning is considered to be more reliable. The magnitude of the neutron scan is highly dependent on the hydrogen concentration. Calculations using a Monte Carlo code for neutron and photon transport in sludge and salt cake waste show that readings above 2,000 counts per minute indicate the presence of interstitial liquid.

The FIC and manual tape readings were obtained at the tank salt wells near the center of the tanks and may indicate a liquid level less than the actual tank average interstitial liquid level because a hydraulic gradient is expected. Liquid levels for five ferrocyanide tanks for which the surface

Table 4-14. Liquid Observation Well Locations in Ferrocyanide Tanks.

Tank	Riser	Riser radial location (ft)	Method of determination
Liquid observation well interstitial liquid level readings			
241-BX-111	R-5	33.25	Neutron and gamma scans
241-BY-101	R-9A	20.75	Neutron and gamma scans
241-BY-103	R-10A	8.0	Neutron and gamma scans
241-BY-104	R-10C	20.75	Neutron and gamma scans
241-BY-105	R-10B	20.75	Neutron and gamma scans
241-BY-106	R-10B	20.75	Neutron and gamma scans
241-BY-107	R-7	5.0	Neutron and gamma scans
241-BY-110	R-3	8.0	Neutron and gamma scans
241-BY-111	R-1	8.0	Neutron and gamma scans
241-BY-112	R-15	29.35	Neutron and gamma scans
241-TX-118	R-5	29.35	Neutron and gamma scans
241-TY-103	R-3		

Figure 4-9. Neutron and Gamma Surveillance Scan Configuration.

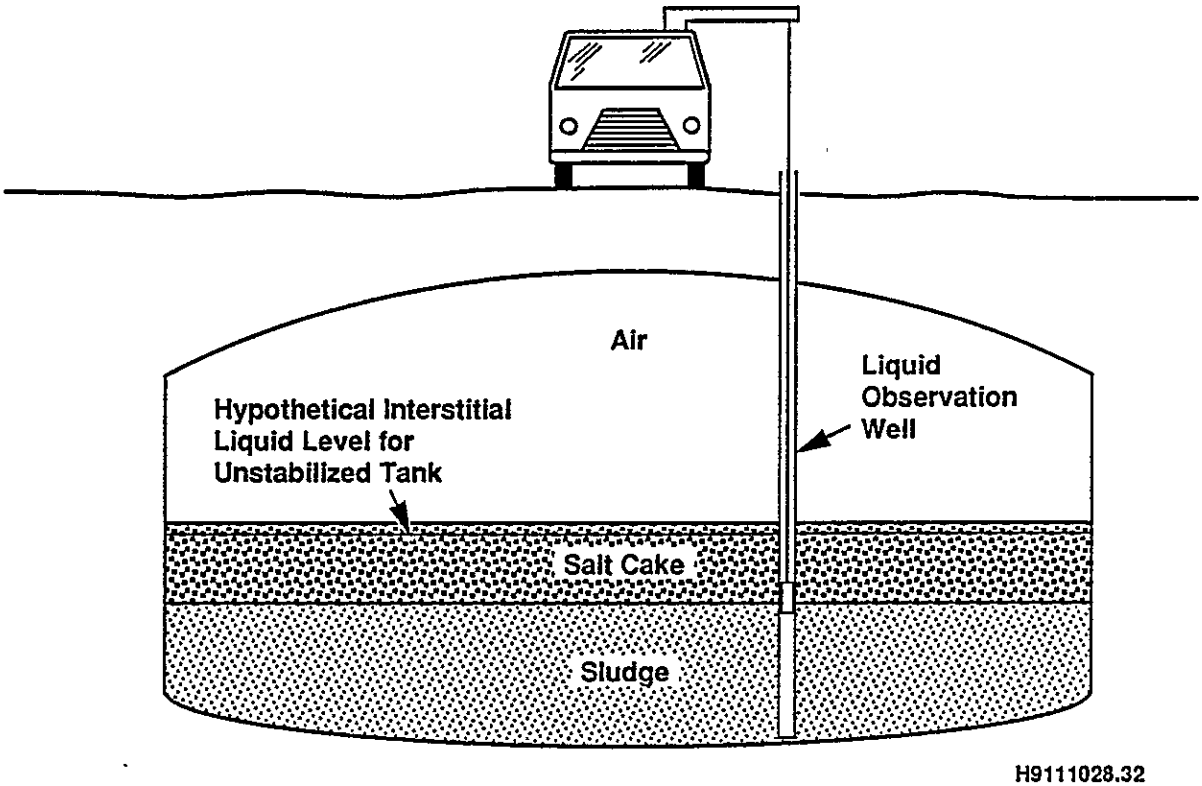

Table 4-15. Interstitial and Surface Liquid Levels in Ferrocyanide Tanks (readings obtained July through September 1991).

Interstitial and Surface Liquid Level Height (feet from bottom center of tank)			
Tank	Neutron	Gamma	Food Instrument Corporation gage/manual tape
	Interstitial liquid levels		Surface liquid levels
Tanks containing liquid observation wells			
241-BX-111	7.6	7.5	6.6
241-BY-101	5.2	5.7	--
241-BY-103	11.9	11.3	--
241-BY-104	6.8	6.5	--
241-BY-105	13.8	14.8	--
241-BY-106*	18.6	18.6	--
241-BY-107*	5.2	5.6	--
241-BY-110*	6.2	5.9	--
241-BY-111	6.8	4.0	--
241-BY-112	2.9	3.2	--
241-TX-118	4.5	4.4	--
241-TY-103	5.0	3.9	--
Tanks without liquid observation wells			
241-BX-102	--	--	--
241-BX-106	--	--	1.1
241-BX-110	--	--	--
241-BY-108	--	--	--
241-C-108	--	--	--
241-C-109	--	--	--
241-C-111	--	--	--
241-C-112	--	--	--
241-T-101	--	--	3.7
241-T-107	--	--	5.1
	Interstitial liquid levels		Surface liquid levels
Tanks without liquid observation wells			
241-TY-101	--	--	--
241-TY-104	--	--	2.0

Reference: Tank Farm Operations Log Sept 1991.

NOTE: Liquid observation wells are located at various radii, and Food Instrument Corporation and manual tape are located near the tank center in salt wells. The interstitial liquid level readings are expected to be greater at the liquid observation wells than the liquid level at the salt well because of capillary forces in the waste solids.

Reference elevations are being investigated, which may result in different interstitial liquid levels.

liquid level is measurable from the salt-well riser are shown in Figure 4-10 for the time period from 1985 to 1991. Slight liquid level increases for these five tanks are indicated by the surface liquid level readings over the 5.5-yr time period.

The interstitial liquid levels determined by neutron scanning are shown in Figures 4-11 through 4-13 for the time period 1985 to 1991.

The water content of the waste in the ferrocyanide waste tanks has remained essentially constant. This observation was confirmed by the interstitial liquid levels determined by neutron scans and surface liquid levels measured by manual tapes and FIC gauges from 1986 to 1991. An exception to this behavior is the increase in interstitial liquid level indicated by the neutron scans in tank 241-BY-111, which shows a substantial increase in liquid level in 1990 due to the apparent downward movement of interstitial liquid above the previously established interstitial liquid level. Neutron scans over the last several years appear to indicate downward migration of moisture from the 7-ft level to raise the interstitial liquid level as shown in Appendix B, Figures B-25 through B-27, by the gradual disappearance of the valley near the old interstitial liquid level. The decrease in interstitial liquid level for tank 241-BY-103 in 1987 was due to salt-well pumping from April 8 through September 9.

In general, these liquid levels indicate that there is negligible water loss from the waste in the tanks and that the ferrocyanide sludge does not appear to be drying out as a function of time in these passively vented tanks. It should be noted that there are eight ferrocyanide tanks for which there are no liquid level measurements made. Provisions for monitoring the moisture content of the waste in these eight tanks should be considered.

Modeling is currently being done in an attempt to determine moisture concentration as a function of elevation in the waste by neutron scanning.

4.5 GAMMA SCANS

Gross gamma scans are used to identify interstitial liquid levels in the waste tanks and to observe movements of cesium over time. Spectral gamma scans were used to measure the concentrations of cesium, europium, and cobalt in the waste tanks; total cesium, europium, and cobalt inventories; and further evaluation of isotope layering (Subrahmanyam et al. 1991). Gross and spectral gamma energy scans have been obtained in all 12 of the 24 ferrocyanide waste tanks that contain LOWs.

The method of installation used in placing the LOWs in the tank waste leaves some question about the validity of relating the isotope density measurements obtained in the LOW to the respective waste layer throughout the tank. A water lance was used to wash through the salt cake and sludge layers so that the LOW could be inserted to near the bottom of the tank. The calculated cesium inventories from the gamma scan data, however, tend to suggest that the waste is closely represented because the inventories calculated agree reasonably well with the TRAC (Jungfleisch 1984) and Borsheim and Simpson (1991) reported values.

Figure 4-10. Liquid Levels Measured in Salt Wells.

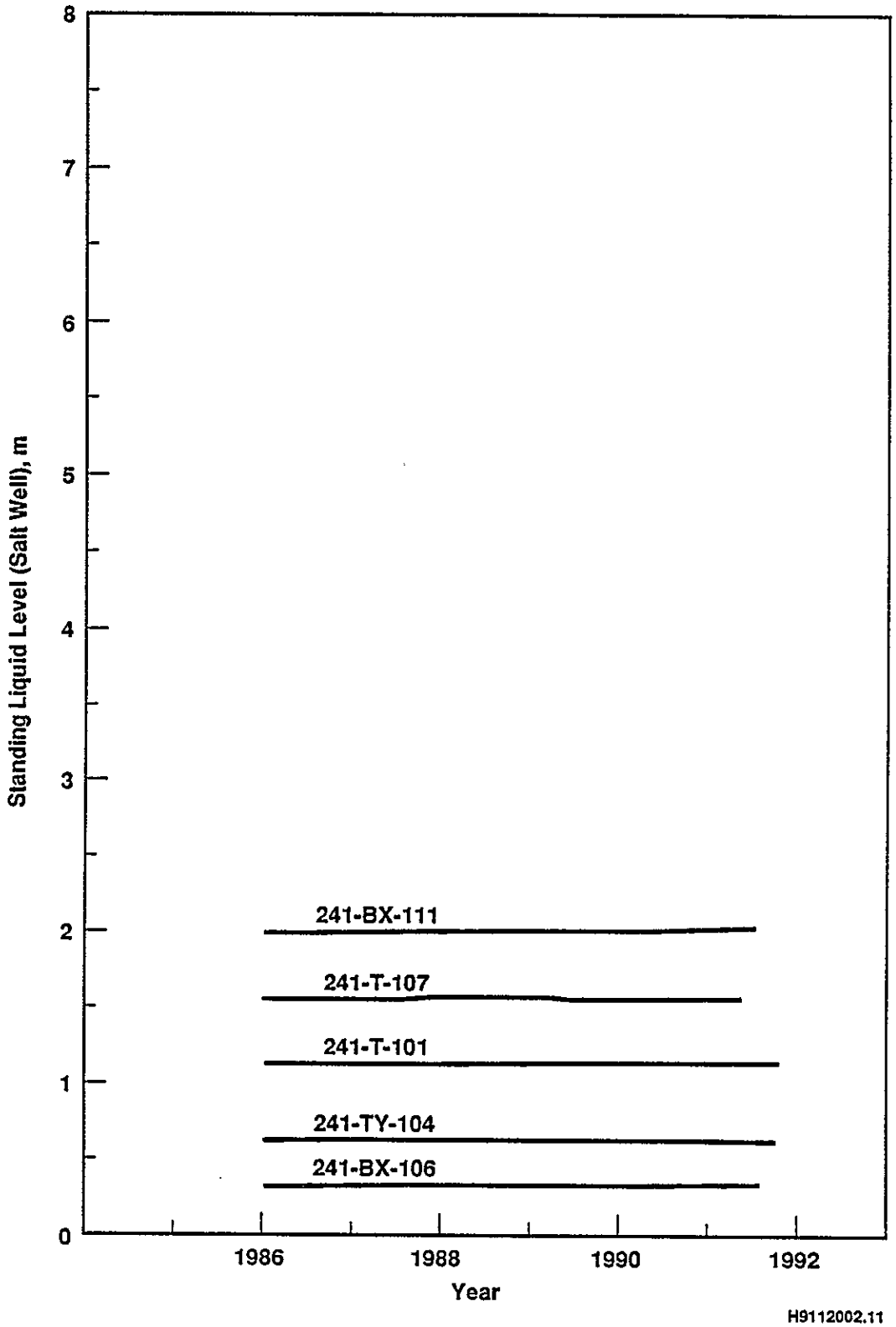

Figure 4-11. Interstitial Liquid Levels by Neutron Scan (1985-1991) for Tanks 241-BY-111, -112, 241-TX-118, and 241-TY-103.

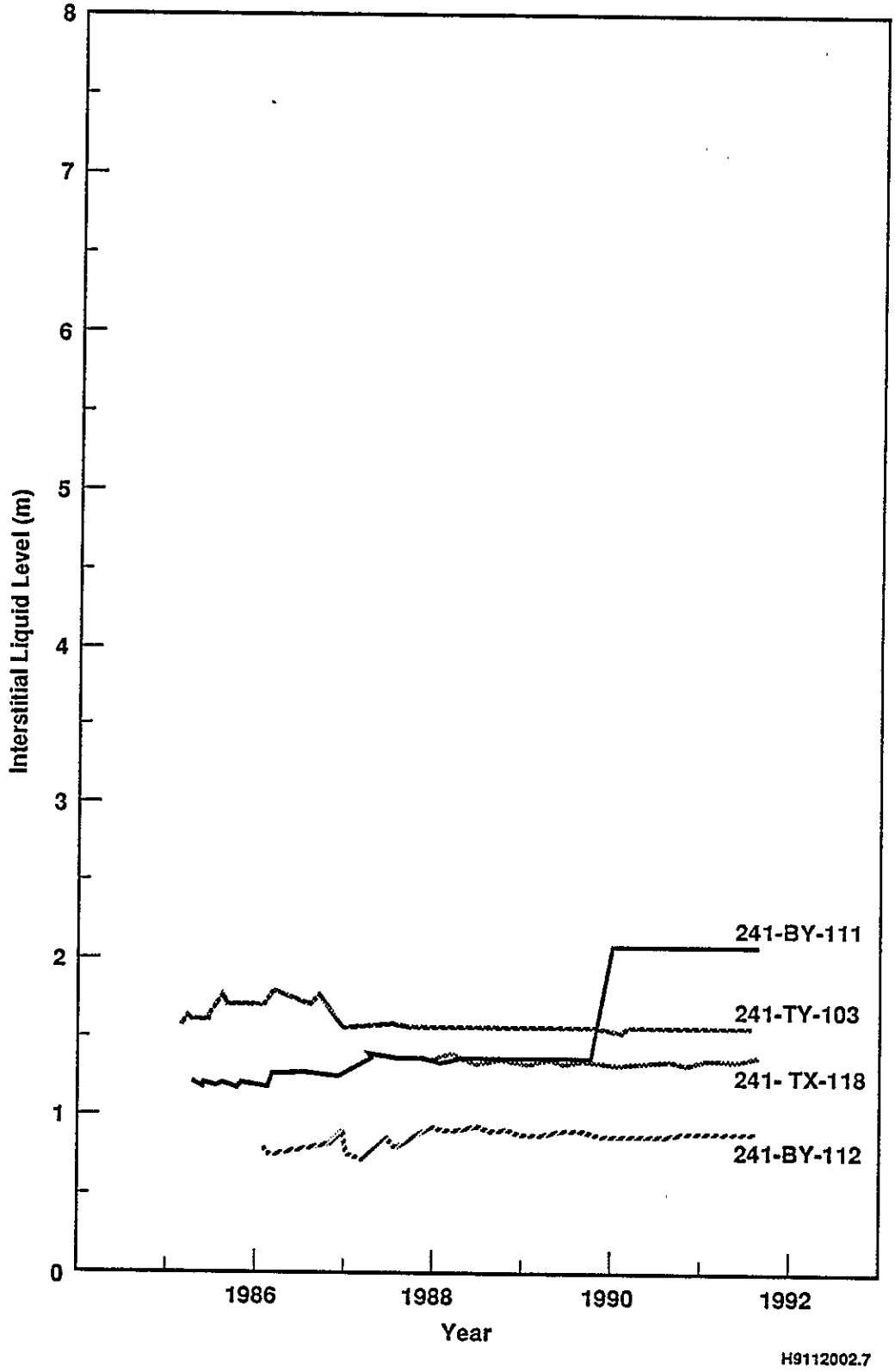

Figure 4-12. Interstitial Liquid Levels by Neutron Scan (1985-1991) for Tanks 241-BX-111, 241-BY-101, -103, and -104.

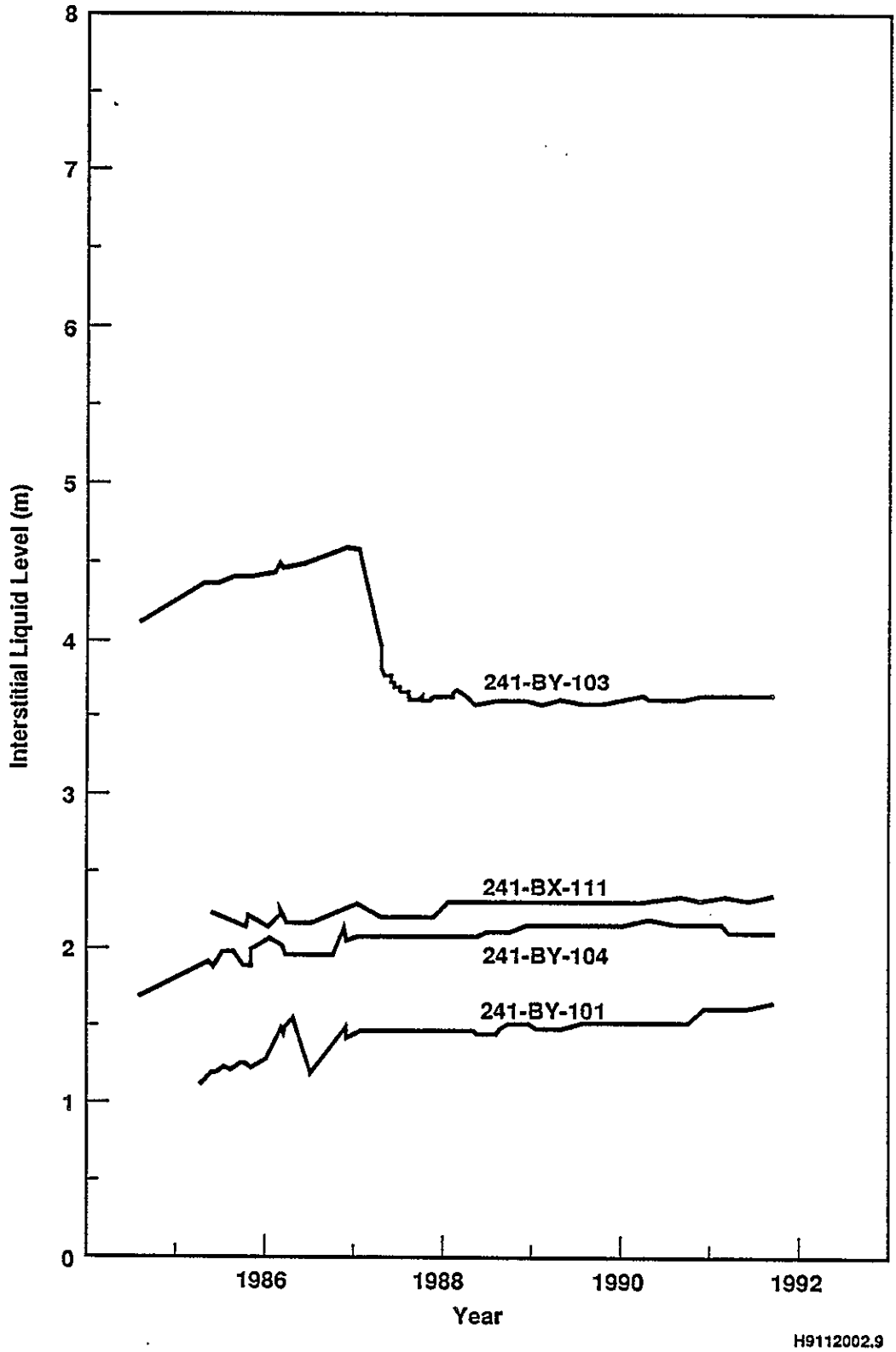

Figure 4-13. Interstitial Liquid Levels by Neutron Scan (1985-1991) for Tanks 241-BY-105, -106, -107, and -110.

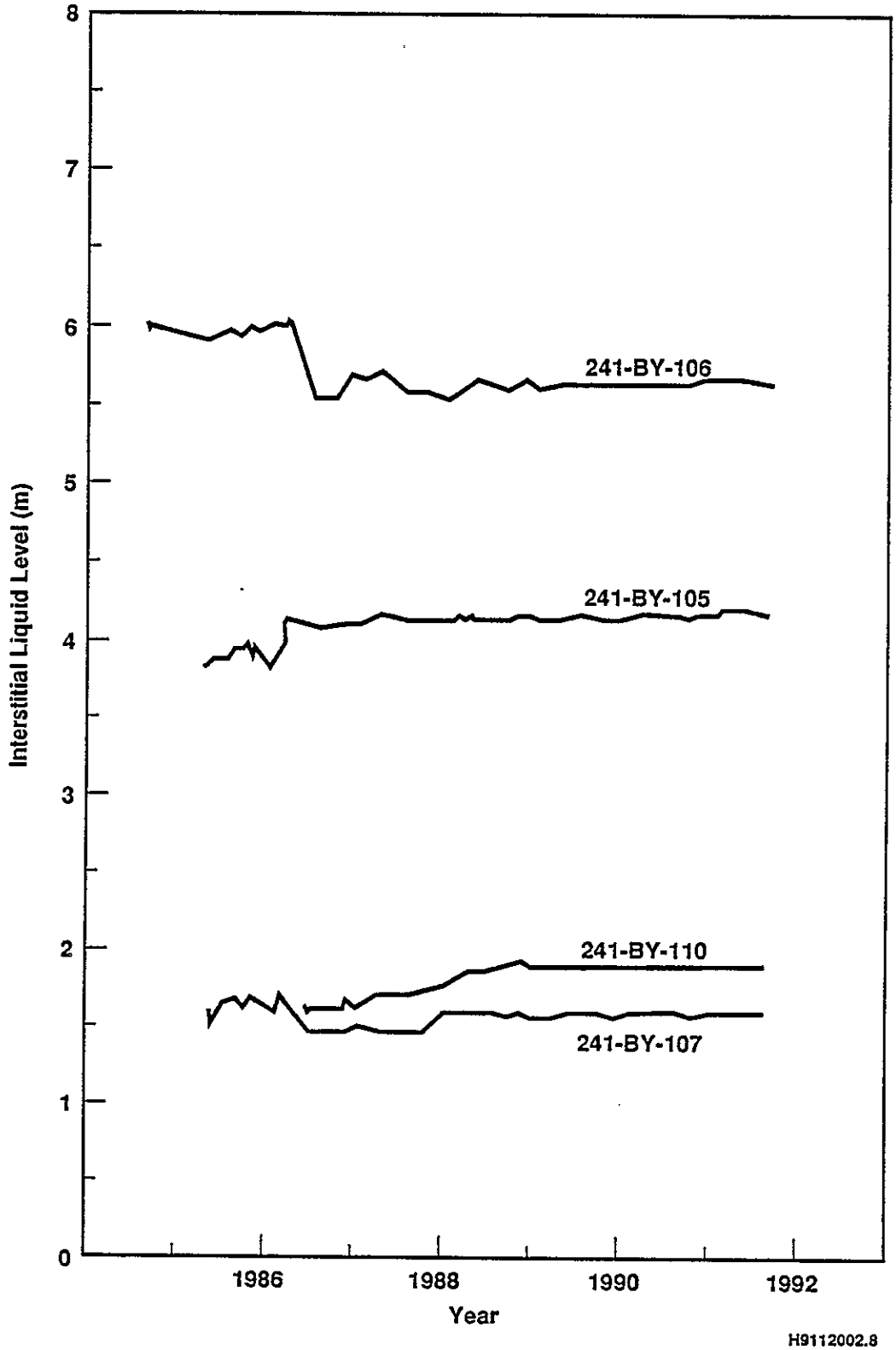

4.5.1 Gross Gamma Scans--Routine Surveillance

Gross gamma scans are obtained quarterly in each of the 12 ferrocyanide tanks. Scans have been obtained since the LOWs were installed. The scans were used to identify the liquid level and changes in cesium location over time. Current liquid levels determined by gamma scans are listed in Table 4-15 along with the values determined by neutron scan and other methods. In general, they are in good agreement. Current gamma scans are shown in Appendix B, Figures B-1 through B-23 (odd-numbered figures), along with the scans obtained early in the history of the LOWs. Many factors influence the scan readings, including liquid content, waste density, void spaces, and cesium concentration. Interpretations of the gamma scans are discussed in RHO-SD-WM-TI-237 (Stong 1986).

4.5.2 Spectral Gamma Scans

A spectral gamma scan cadmium telluride (CdTe) detector assembly was developed in 1991. Spectral gamma scans were made with this detector assembly to determine concentrations of gamma-emitting isotopes (^{137}Cs or ^{154}Eu and ^{60}Co) in the ferrocyanide waste, the associated heat load, and the total gamma-emitting isotope inventories in 12 of the 24 ferrocyanide tanks. Variations in gamma-emitting isotope concentrations measured at different elevations indicate that there is layering of these isotopes in the waste and imply that only limited mixing has occurred over the lifetime of the collected waste.

4.5.2.1 Detector Description. A small CdTe detector (2 by 2 by 2 mm) was encased in a tungsten shield with a partially open slot to allow measurements of gamma energy from discrete horizontal layers of the tank waste near the existing LOWs. A schematic of this collimated detector assembly is shown in Figure 4-14. A cooling coil, thermocouple, and insulation were provided as part of the detector assembly. This assembly was fabricated to allow insertion in the 3-in.-inside-diameter LOWs while maintaining the detector temperature within operating temperature specifications during waste tank readings. The slot in the tungsten was 0.125 in. wide, which allowed the detection of 95% of the gamma energy in the waste at a distance of 8 in. from the LOWs assuming a waste specific gravity of 1.6 and a visual maximum vertical waste thickness of 0.70 in. at 8 in. from the LOW.

A preamplifier, main amplifier, pulse shape discriminator, and multichannel analyzer were used to process the data. Pulse shape discrimination (PSD) provides complete charge collection of the full energy photopeak pulses over unwanted electrical pulses. Pile-up rejection was used to diminish the effects of radiation striking the detector in close time proximity. A typical gamma energy scan is shown in Figure 4-15. The ^{137}Cs peak (30-yr half life) at approximately 0.662 MeV, the ^{60}Co peaks (5.27-yr half life) at 1.17 and 1.33 MeV, and the ^{154}Eu peak (8.59-yr half life) at 1.28 Mev are clearly shown in the typical scan.

Figure 4-14. Collimated Cadmium Telluride Gamma Detector.

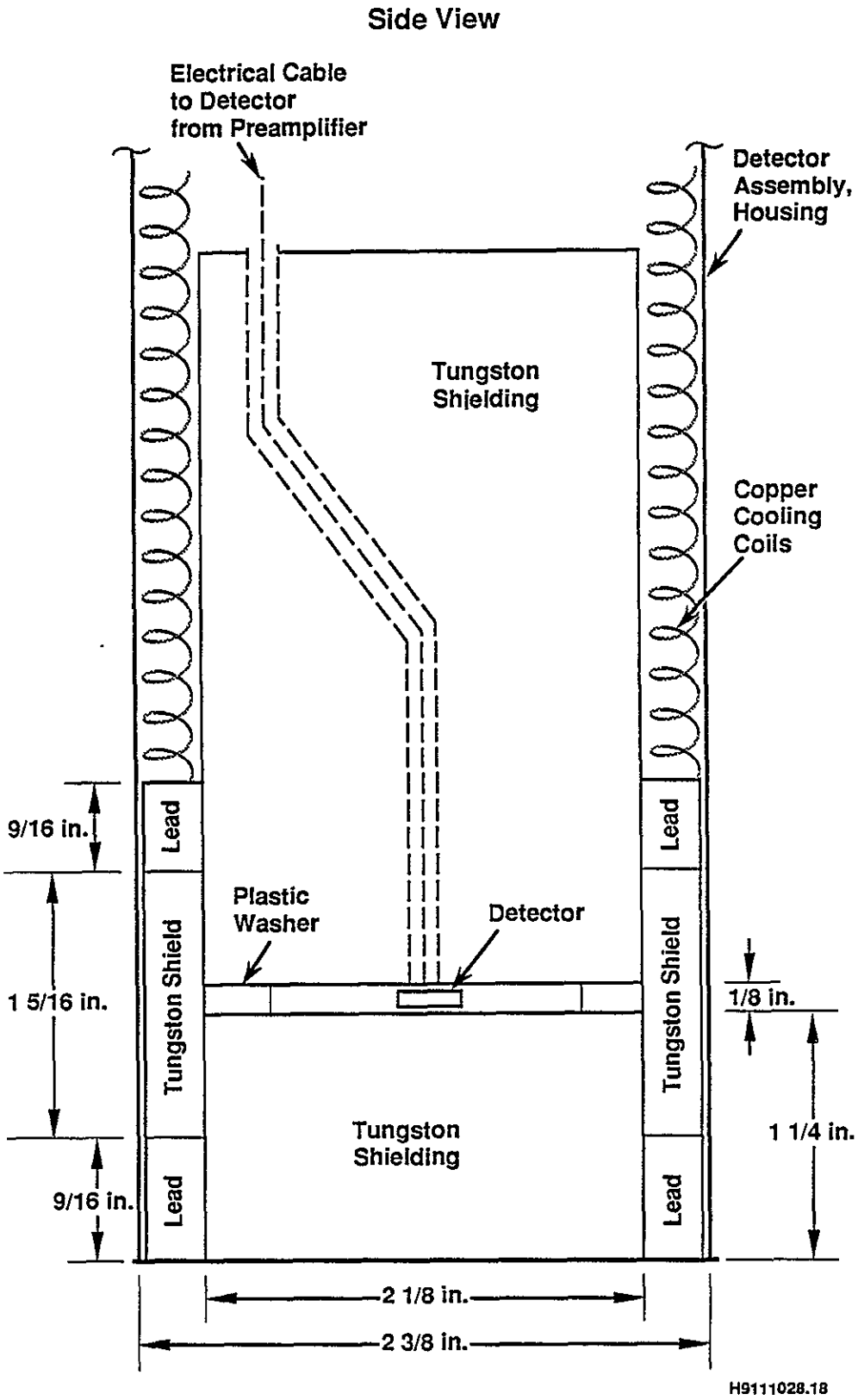

Figure 4-15. Typical Gamma Energy Scan (Subrahmanyam et al. 1991).

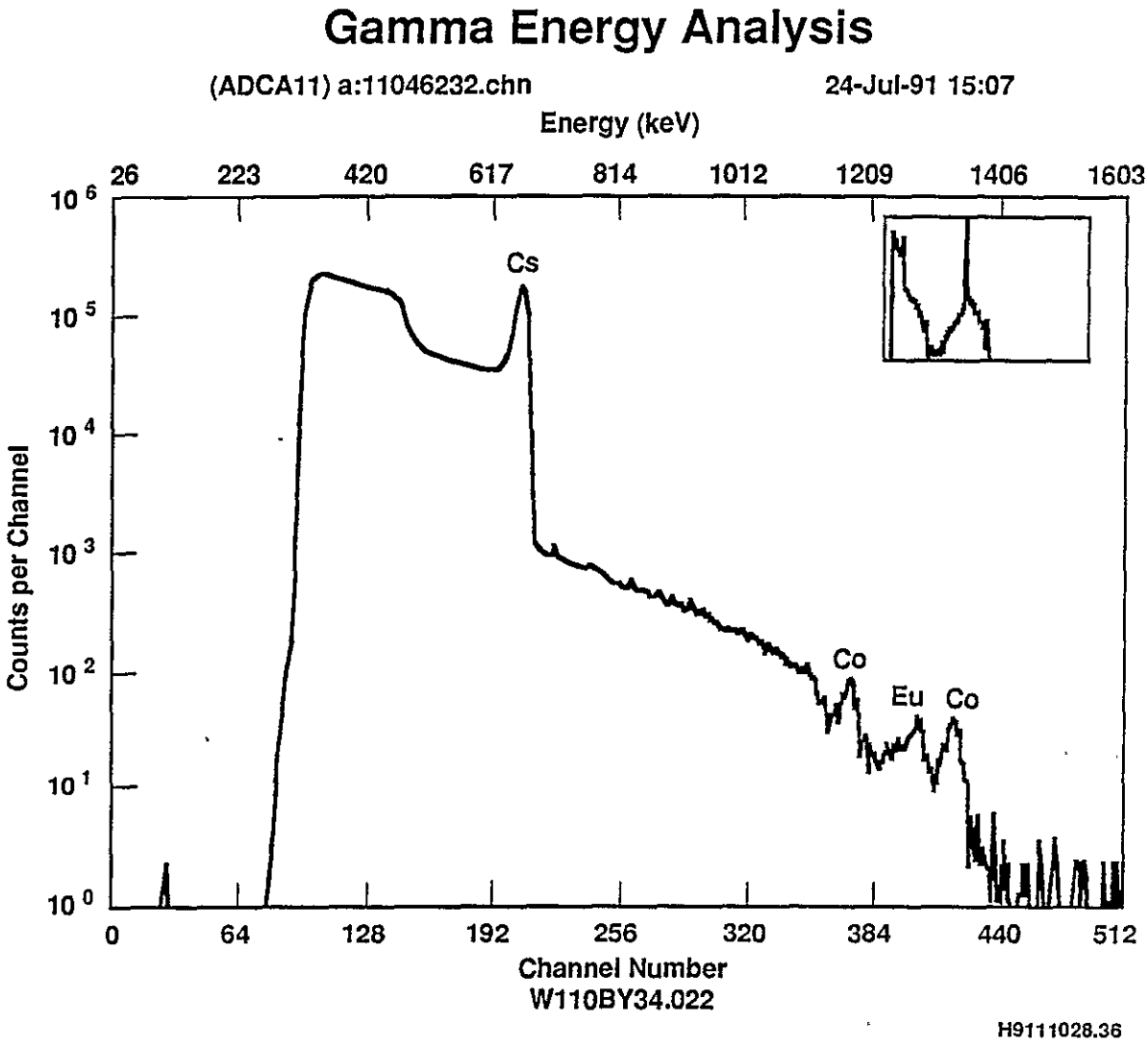

The data for each of the various gamma-emitting isotopes are based on the total area under spectral photopeaks corresponding to their respective energy peaks. The collimated detector was calibrated with the use of the 4-pi environmental calibration facility at the Hanford Site.

4.5.2.2 Collimated Spectral Gamma Scans. The collimated gamma scans made in September 1991 are shown in Appendix B, Figures B-28 through B-39, for tanks 241-BY-101, -103, -104, -105, -106, -107, -110, -111, and -112; 241-BX-111; 241-TX-118; and 241-TY-103. The scans show various concentrations of cesium at different vertical elevations through the tank waste. The collimated scans indicate a maximum cesium concentration of 270 μCi/g near the bottom of tank 241-BY-106. It must be noted that not all of the ferrocyanide tanks have been scanned, and there may be some that may contain a higher concentration of cesium. The cesium inventory estimated by integrating the spectral gamma scan data is compared to TRAC (Jungfleisch 1984) inventories in Table 4-16. In general, TRAC values compare within a factor of 1.7, with the spectral gamma scan values generally being lower. The heat load from ^{137}Cs decay based on the gamma scan values is indicated in the table. The heat conversion factors were obtained from Brown (1986). Assumptions used in making the isotope calculations include (1) waste density of 1.6 g/cm^3 and (2) constant lateral composition. The four waste tanks (241-BY-104, -105, -106, and -110) that had greater than 3,000 Btu/h heat associated with cesium correspond to the tanks with waste temperatures above 100 °F.

Table 4-16. Cesium Inventories and Heat Loads.

Tank	Cesium spectral scan (Ci)	Cesium Inventory TRAC[a] (Ci)	Cesium decay heat[b] (Btu/h)
241-BX-111	1.5 E5	4.4 E5	2,500
241-BY-101	3.9 E4	5.2 E5	650
241-BY-103	1.4 E5	2.6 E4	2,300
241-BY-104	2.1 E5	5.2 E5	3,500
241-BY-105	1.8 E5	4.4 E5	3,000
241-BY-106	4.5 E5	5.2 E5	7,400
241-BY-107	1.7 E5	1.7 E5	2,800
241-BY-110	2.3 E5	5.2 E5	3,800
241-BY-111	1.0 E5	5.2 E5	1,700
241-BY-112	7.5 E4	7.8 E4	1,200
241-TX-118	5.3 E4	9.0 E5	880
241-TY-103	3.7 E4	1.7 E5	610

[a]Decayed to January 1, 1991.
[b]Calculated from spectral scan.

Collimated spectral gamma scans have been obtained for europium and cobalt concentration measurements in two of the ferrocyanide waste tanks. The detector is in the process of being calibrated for europium and cobalt so that concentrations can be obtained. Initial results show that the europium is located near the bottom of the waste tanks. This implies that the transuranics would also be expected to be located near the bottom. The location of the transuranics will be important in any model that predicts aerosol releases. Additional europium measurements could be obtained in the remaining ferrocyanide tanks with LOWs. The europium scans for tanks 241-BY-104 and -106 are shown in Figures 4-16 and 4-17.

The collimated gamma scans made for ^{137}Cs were graphically integrated over the ferrocyanide sludge depths, given in Tables 4-16 and 4-17, to obtain a measure of cesium in the sludge. The average concentration, the peak-to-average concentration ratio, and the cesium in the sludge are all given in Table 4-17 for the seven tanks that contain significant sludge. A comparison with the cesium in the sludge as calculated by the Borsheim/Simpson model (Borsheim and Simpson 1991) is also given.

As noted previously, several tanks show increasing cesium concentrations near the tank bottom. The inventory and peak-to-average ratios given in Table 4-17 assume a constant cesium concentration from the bottom end of the scan to the bottom of the tank.

From Table 4-17 it can be seen that the sludge cesium inventory determined from the gamma scans averages 71% of the cesium inventory estimated by the Borsheim/Simpson model. The average agreement between the two methods is satisfactory, but an apparent difference is observed because gamma scan results are always less than the model values.

The following are possible reasons for the differences:

(1) Use of a sludge density of 1.6 when calculating the cesium inventory from the spectral scan data. This value is supported by the Horton (1976) analysis and by synthetic waste characterization but may be low.

(2) Some cesium may have dissolved and migrated out of the sludge to the salt cake or may have been removed from the tank by salt-well pumping or post-ferrocyanide campaign transfers. This could result in the Borsheim and Simpson (1991) model being biased high.

(3) Dilution of the tank contents near the LOW from lance water used to install the LOW.

(4) A systematic error in the gamma calibration or the assumed 4.25% volume of sludge used in the Borsheim/Simpson model calculation.

In spite of these comments, the agreement between the two methods is considered to be good and supports the idea of lateral uniformity in the sludge layer.

Figure 4-16. Europium Scan for Tank 241-BY-104 (Subrahmanyam et al. 1991).

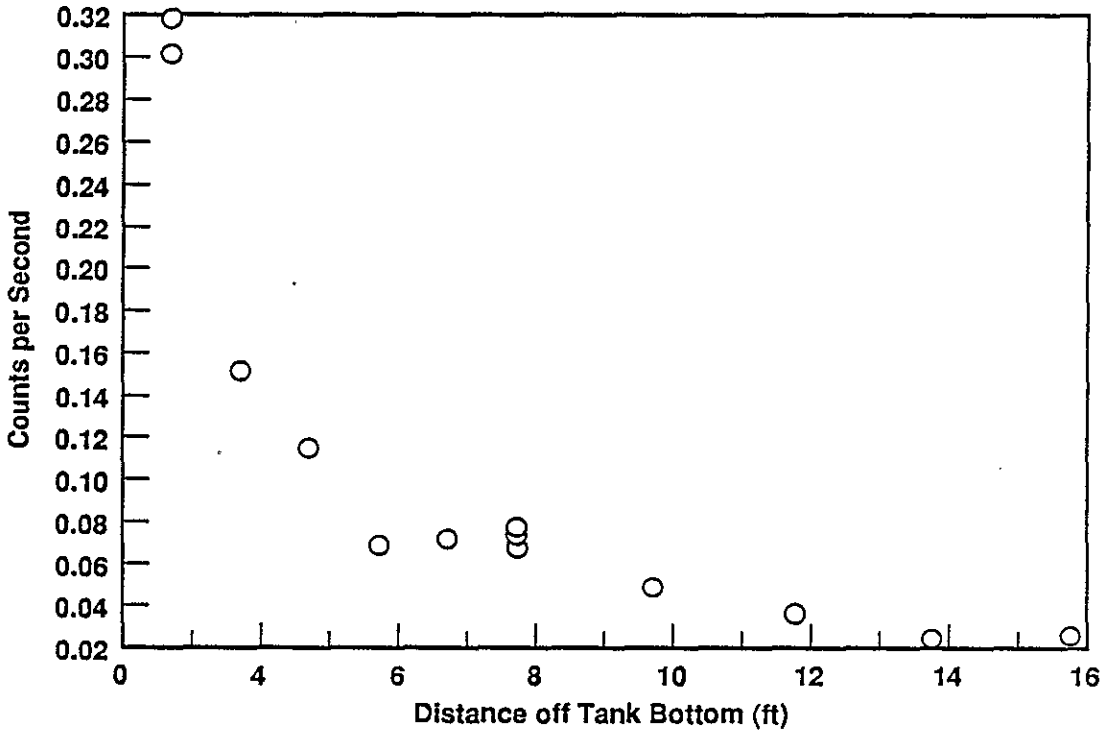

Relative Europium Location in BY-104 Waste Showing an Increased Concentration at the Bottom of the Tank (europium acts as a tracer for transuranics)

H9112002.14

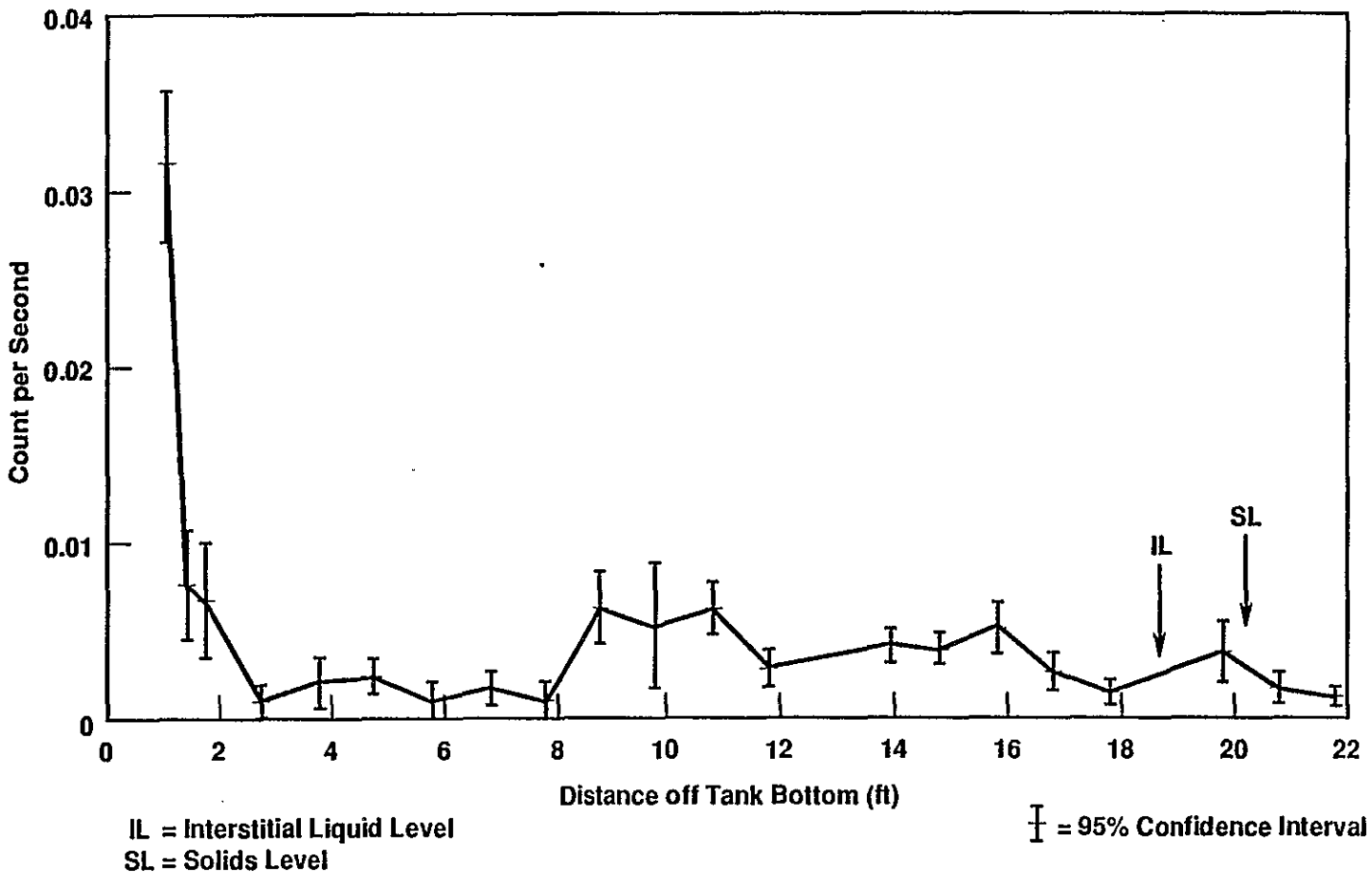

Figure 4-17. Europium Scan for Tank 241-BY-106 (Subrahmanyam et al. 1991).

Table 4-17. Cesium Inventory in the Ferrocyanide Sludge Determined from the Spectral Gamma Scans.

Tank	Spectral scan in sludge			Model value for ^{137}Cs[b] (Ci)	^{137}Cs Inventory ratio scan/model
	Average concentration (μCi/g)	Ratio $\frac{\text{peak conc}}{\text{avg conc}}$	Total[a] ^{137}Cs (Ci)		
241-BY-103	55	1.8	7.1 E4	1.6 E5	0.44
241-BY-104	93	1.2	1.5 E5	2.0 E5	0.75
241-BY-105	104	1.2[c]	6.0 E4	8.8 E4	0.68
241-BY-106	85	3.1[c]	1.2 E5	2.2 E5	0.67
241-BY-107	103	1.4[c]	9.8 E4	1.3 E5	0.75
241-BY-110	135	1.3[c]	1.8 E5	1.9 E5	0.95
241-TY-103	32	2.9	3.8 E4	5.2 E4	0.73
				Average	0.71

[a]Calculated from average concentrations using density = 1.6 g/cm^3 and sludge volume from Table 4-4.
[b]From Borsheim and Simpson (1991) for sludge, Table 4-4.
[c]These tanks show increasing cesium concentration at the bottom limit of the scan.

4.5.3 Validation of Gamma Scan Readings

The condition of having a significant percentage of cesium activity concentrated in a narrow layer of waste could cause local temperatures to exceed average or measured values. Significant concentrations of cesium are expected to result in substantial peaks in the gross and collimated gamma profiles. A Monte Carlo neutron-photon (MCNP) analysis was performed for the gross gamma scans to support this supposition. The effect of waste composition was included in the model based upon approximate tank 241-BY-104 waste content.

Figure 4-18 shows the axial gamma profile calculated for a uniform source and axial material density variation. Changes in the gamma profile can clearly be seen as a consequence of the material density changes. Note that the calculational uncertainties associated with each data point are indicated with the error bars on the gamma profile curve.

Figure 4-19 shows four bulk gamma scan profiles obtained by MCNP calculations for varying source distribution. The four cases presented are (1) uniform distribution, (2) 25% cesium localized in a 30-cm-thick layer, (3) 50% cesium localized in a 30-cm-thick layer, and (4) 90% cesium located in a 30-cm-thick layer. This modeling shows that for the case with only 25% of the activity located in the concentrated layer, the resulting peak is twice the surrounding average and would be easily detected.

Figure 4-18. Calculated Gamma Axial Profile--Uniform Source with Axial Material Density Variations.

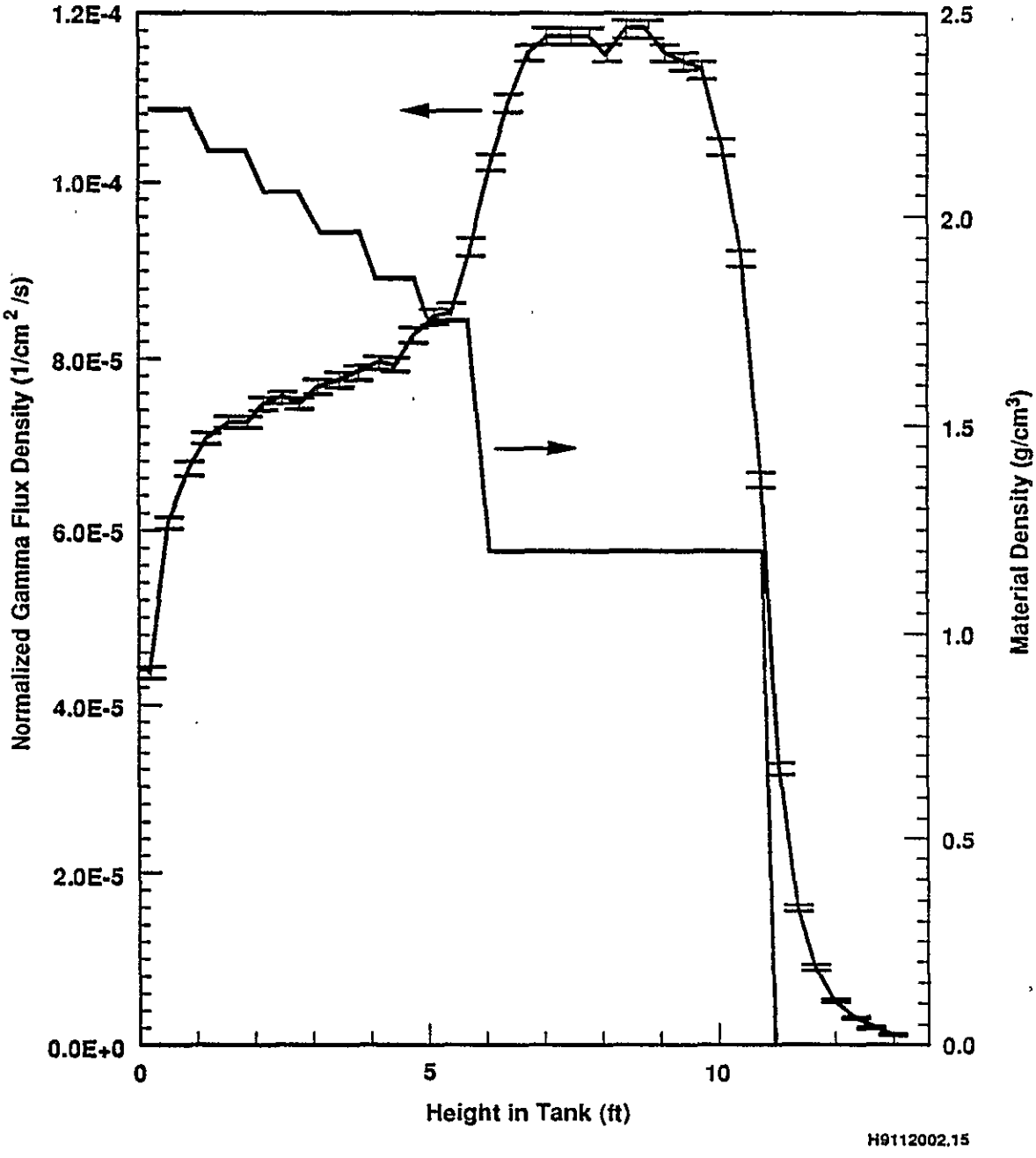

Figure 4-19. Calculated Gamma Axial Profiles--Variations in Source Distribution.

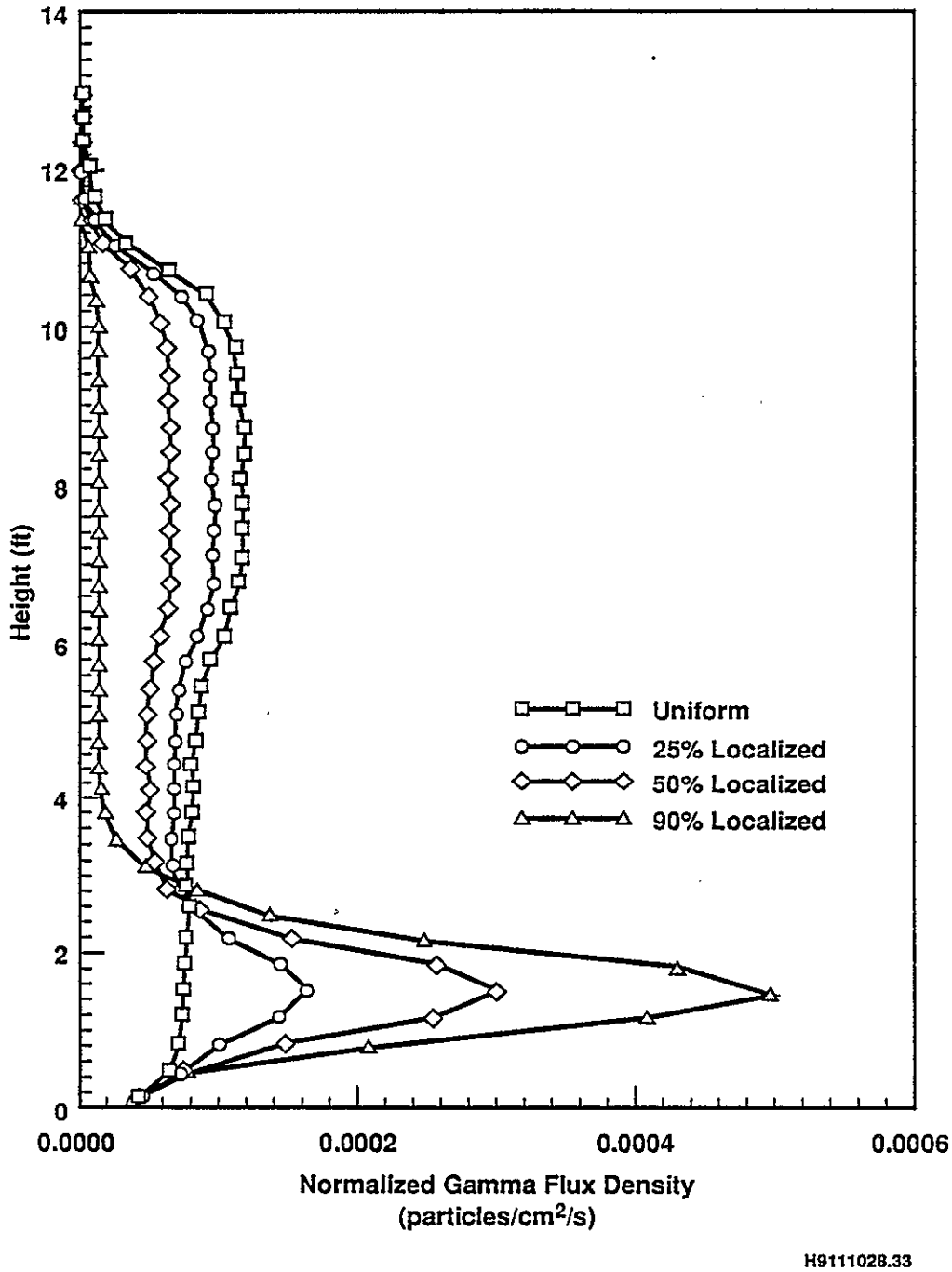

4.5.4 Application of Gamma Scans to Distribution of Ferrocyanide Within Waste Tanks

The total amount and average concentration of ferrocyanide in each of the waste tanks from a scavenging campaign history has been discussed in Section 4.1.6. However, the degree of uniformity of the ferrocyanide distribution within each tank and the peak local ferrocyanide concentrations must also be determined to assess the possibility of layers of material with higher-than-average reactivity. The ^{137}Cs gamma scans can provide valuable information on the ferrocyanide distribution, as discussed below.

It will be useful to review some of the chemistry of the ferrocyanide tanks to understand the relationship between cesium and ferrocyanide. The initial scavenging resulted in the following equation:

$$Cs^{+} + 1999Na^{+} + 1000Ni^{+2} + 1000Fe(CN)_6^{-4} \text{ ---> } 999[Na_2NiFe(CN)_6] + [NaCsNiFe(CN)_6]. \quad (4\text{-}1)$$

where the [ ]'s denote a solid precipitate. Note that a very high excess of ferrocyanide over cesium was used (Borsheim and Simpson 1991).

Historically, other types of waste such as evaporator bottoms and cladding waste were added to the tanks already containing the ferrocyanide sludge. These added wastes contained both cesium and caustic. If the ferrocyanide salts came in contact with strong caustic, there could be some dissolution of both cesium and ferrocyanide as follows:

$$2OH^{-} + [NaCsNiFe(CN)_6] \text{ ---> } Na^{+} + Cs^{+} + Fe(CN)_6^{-4} + [Ni(OH)_2]. \quad (4\text{-}2)$$

When examining the consequences of adding evaporator bottoms, it is necessary to know that the progression of solubilities for these ferrocyanide salts is Na >K >Cs (Loos-Neskovic and Federoff 1989), which means that new cesium would displace sodium from old salts as follows:

$$Cs^{+} + [Na_2NiFe(CN)_6] \text{ ---> } Na^{+} + [NaCsNiFe(CN)_6]. \quad (4\text{-}3)$$

If most of the disodium salt were consumed, the reaction would tend to be:

$$Cs^{+} + [NaCsNiFe(CN)_6] \text{ ---> } Na^{+} + [Cs_2NiFe(CN)_6]. \quad (4\text{-}4)$$

That is, extremely dilute radiocesium is scavenged from solution by coprecipitation with $Na_2NiFe(CN)_6$. Soluble cesium added (as in evaporator

bottoms) subsequent to ferrocyanide precipitation will be removed from solution by "sorption" (in an ion exchange-like reaction) on the ferrocyanide precipitation.

Thus, although it is possible that both cesium and ferrocyanide were rendered soluble by the caustic present in later additions, it is not possible for precipitated cesium to become soluble and capable of migration while the ferrocyanide remained insoluble.

It may be concluded from the following reasoning that the maldistribution of the cesium forms a conservative upper bound for the maldistribution of the ferrocyanide.

1. The ferrocyanide was at least as well distributed in the initial sludge as the cesium. Any mechanisms that concentrated the ferrocyanides relative to water or the inert materials would similarly concentrate the cesium, because the cesium was efficiently bound to the ferrocyanide. Concentration of cesium ferrocyanide relative to the much larger quantity of sodium ferrocyanide is credible (e.g., by more rapid settling), but in this case, the ferrocyanide would remain more uniformly distributed than the cesium. The same reasoning applies to any settling or compaction of the sludge with time.

2. Dissolution of ferrocyanide by high pH and transport of dissolved materials would deplete the ferrocyanide in the initial sludge at least as much as the cesium. No credible mixing mechanisms are available in the waste tanks that could have produced a high degree of intimate contact between ferrocyanide and caustic. However, to the extent that the caustic present in the later additions to the tank may have migrated into the ferrocyanide region, some ferrocyanide could have been rendered soluble, as previously discussed. This could lead to diffusion of ferrocyanide ion into the new material or to possible removal of some ferrocyanide from those tanks that were pumped. However, because the cesium ferrocyanide is the least soluble, it would not be possible for the cesium to dissolve and migrate out of regions of high concentration without the ferrocyanide also doing so.

3. Mixing of the initial ferrocyanide sludge with the material added later would dilute the ferrocyanide at least as much as the cesium. The later additions contained cesium but no ferrocyanide. Therefore, the peak ferrocyanide concentrations in the original sludge would be reduced more by mixing than the corresponding cesium peaks. The large excess of $Na_2NiFe(CN)_6$ could act as an attractor for cesium present in the added liquid. This could create a large cesium peak but would not affect the ferrocyanide concentration.

It may be concluded that there are no peaks in the ferrocyanide concentration that are more pronounced than the cesium peaks. This fact permits using the cesium gamma scans to estimate an upper bound for the local peak ferrocyanide concentration in each tank containing a LOW. The average ferrocyanide concentration in the initial sludge (Table 4-4) is multiplied by the ratio of the peak-to-average cesium concentrations from Table 4-17.

The results of such a calculation are shown in Table 4-18 for the tanks for which cesium scans have been made. (Tanks 241-BY-111, -112, and 241-TX-118 were not considered because the original sludge depth in Table 4-22 was below the bottom of the gamma scans.)

Table 4-18. Upper-Bound Estimates of Peak Ferrocyanide Concentrations.

Tank	Average concentration[a] of ferrocyanide (*M*)	Peak/average[b] from cesium scans	Peak ferrocyanide concentration (*M*)
241-BY-103	0.082	1.8	0.15
241-BY-104	0.084	1.2	0.10
241-BY-105	0.099	1.2	0.12
241-BY-106	0.081	3.1	0.25
241-BY-107	0.070	1.4	0.10
241-BY-110	0.080	1.3	0.10
241-TY-103	0.041	2.9	0.12

[a]From Table 4-4.
[b]From Table 4-17.

Note that both the average ferrocyanide concentration and the average ^{137}Cs concentration used in this calculation apply to the original ferrocyanide sludge and are therefore comparable. The ferrocyanide concentration is that in the initial ferrocyanide sludge before any mixing with later additions. The ^{137}Cs was averaged over a distance at the bottom of the tank equal to the estimated depth of the ferrocyanide sludge, which would be the layer occupied by the ferrocyanide sludge without mixing.

The peak ferrocyanide concentration calculated at the bottom of tank 241-BY-106 (0.25 *M*) is significantly higher than in the other tanks because of the strong peaking of the cesium measured at the bottom of this tank. There are likely causes of such a cesium peak that do not imply a high ferrocyanide concentration. It is likely that the variation in cesium concentration resulted in variations in the cesium content of the scavenged waste. The ferrocyanide added remained at the flowsheet values and therefore would not have a corresponding variation. However, the existence of a high ferrocyanide concentration at the bottom of tank 241-BY-106 cannot be ruled out, and it will be appropriate to give this tank particular attention in an assessment of ferrocyanide reaction hazard.

The above calculation of peak ferrocyanide concentrations assumes, of course, that the cesium concentrations measured near the LOW are valid over the entire lateral area of the tank. That is, the insertion of the LOW did not significantly perturb the local concentrations, and higher concentrations do not exist in other parts of the tank. The possible effects of LOW

insertion are discussed in Section 4.5. Higher concentrations at other lateral positions are unlikely because there were no mechanisms that could cause significant lateral maldistribution, as discussed in Section 4.5.5.

4.5.5 Lateral Maldistribution of Ferrocyanide Sludge

If a highly viscous sludge were pumped into a waste tank, one can imagine that a conical pile would accumulate beneath the outfall. This conical pile, if it could persist, would represent a departure from horizontal layering expected for more fluid sludges and would be by definition a case of lateral maldistribution of ferrocyanide sludge. As shown in the following paragraphs, ferrocyanide sludges, as pumped into waste tanks, were very likely to have had viscosities much too low to retain the conical profile conjectured above.

Evidence for the fluidity of the settled sludges can be seen from the observation of the behavior in the field and in the laboratory. The accumulated sludges in the tanks were pumped between tanks (Section 4.1.2), sometimes for several miles. Settled synthetic In-Plant sludges made in the laboratory were observed to be readily pourable. Viscosities in the range of 100 to 200 cP (Section 4.3.1) were measured. [10 weight motor oil has a viscosity of approximately 100 cP (Perry and Chilton 1973, p. 1202)]. These low viscosities will allow rapid leveling even in the large waste tanks.

Fluid behavior in the sludge transfer process is expected to be governed by Reynolds number and Froude number (Knudsen and Katz 1958). When a relative time is defined by distance/velocity, it was found that Reynolds/Froude scaling led to relative time that scaled with size. Thus, an event that occurred in 1 s in a 1-ft tank would take 75 s in a 75-ft tank. The handling of freshly prepared synthetic In-Plant ferrocyanide sludges provides an independent way to predict conical pileup in tanks. Although a carefully controlled and scaled test was not done, incidental observations indicated that sludge poured into transparent plastic containers formed a level surface in a matter of seconds after pouring was terminated. Based on the observation that a level surface was achieved within seconds in 0.3-m- (1-ft-) diameter container, a level surface would be expected within minutes in a 23-m- (75-ft-) diameter tank.

Based on the preliminary calculations presented above, it is concluded that ferrocyanide pumped into storage tanks, for example, would form a horizontal surface within minutes. Fresh sludge would be expected to mix with sludge already in the tank in the immediate vicinity of the outfall. This mixed sludge would spread on top of the preexisting sludge surface. Therefore, while horizontal layers having compositions corresponding to specific batches would be possible, it appears that localized vertical piles of sludge are highly improbable.

4.6 ROUTINE TEMPERATURE MONITORING

The SSTs were all originally equipped with thermocouples for temperature measurement. The thermocouples (contained on a multiple thermocouple "tree") can be replaced when they fail, but installing a new thermocouple tree into a tank with several feet of solids (sludge and salt cake) is difficult and

generally requires "sluicing-in" the new tree with added liquid. Adding liquid to a tank, which may be a confirmed or suspect leaker, is undesirable. Therefore, failed thermocouples have not been replaced except in high-heat tanks. Procedures now require that the temperatures of the ferrocyanide-containing tanks be measured weekly.

The lowest thermocouple probe is nominally 10 cm (4 in.) from the bottom of the tank, with additional thermocouples located at approximately 0.6-m (2-ft) intervals. There are typically enough thermocouples so that the top thermocouple(s) is above the waste and reading the vapor space temperature. The thermocouple tree is often located near the center of the tank; however, in many tanks, the only available riser is near the tank wall. Typically, the highest temperature reading is at the second lowest thermocouple [approximately 0.7 m (2.3 ft) above tank bottom]. Temperature profiles within the waste are consistent with models of the transfer of heat from the solids with more heat transferred to the air in the vapor space than to the soil below the tank.

The four highest temperature ferrocyanide tanks are tanks 241-BY-104, -105, -106, and -110. (These temperature data were obtained from Tank Farm Surveillance Analysis data records.) A plot of the temperatures for the past several years shows a typical temperature decrease of approximately 1 °C/yr (approximately 1.7 °F/yr) (Figures 4-20 through 4-23). Note that the higher temperatures shown in the mid-1970's for these tanks occurred because the tanks received hot liquid from the In-Tank solidification system. The tanks have been cooling since that system was shut down in 1974. Many of the early temperature spikes were related to the operation of this system. Also noticeable is the reduced variation in the recorded temperature during the last year, because of improved operational procedures and system maintenance. This improved precision will allow detection of smaller temperature changes. A continuous temperature monitoring system now being installed will further reduce the scatter noted in Figures 4-20 through 4-23.

The recent decrease in tank temperatures is consistent with the expected change in fission products over time. Because of the radioactive decay of the major heat producers in the tanks, ^{137}Cs and ^{90}Sr, the head load in the tank is going to decrease. For a tank such as tank 241-BY-104, which can be assumed to lose heat from a present temperature of approximately 54 °C (approximately 130 °F) to an average ambient temperature of 13 °C (55 °F), the expected temperature decline will be approximately 1 °C/yr (1.7 °F/yr). Other tanks at lower temperatures will cool at slower rates. For example, a tank at 27 °C (80 °F) under similar conditions would cool at an estimated rate of 0.3 °C/yr (0.6 °F/yr).

These cooling rates are low. The temperature measuring systems are subject to various reading errors and ambient temperature influences. Thermocouple system repeatability errors are estimated to be approximately 2 °C (4 °F); thus, repeated measurements over a significant time interval must be examined to determine actual tank temperature changes.

Table 4-19 presents the historic tank temperature data in the form of average readings for selected thermocouples (located in the sludge, when possible). All tanks except tanks 241-BY-103 and 241-C-111 show decreasing

Figure 4-20. Tank 241-BY-104 Temperature.

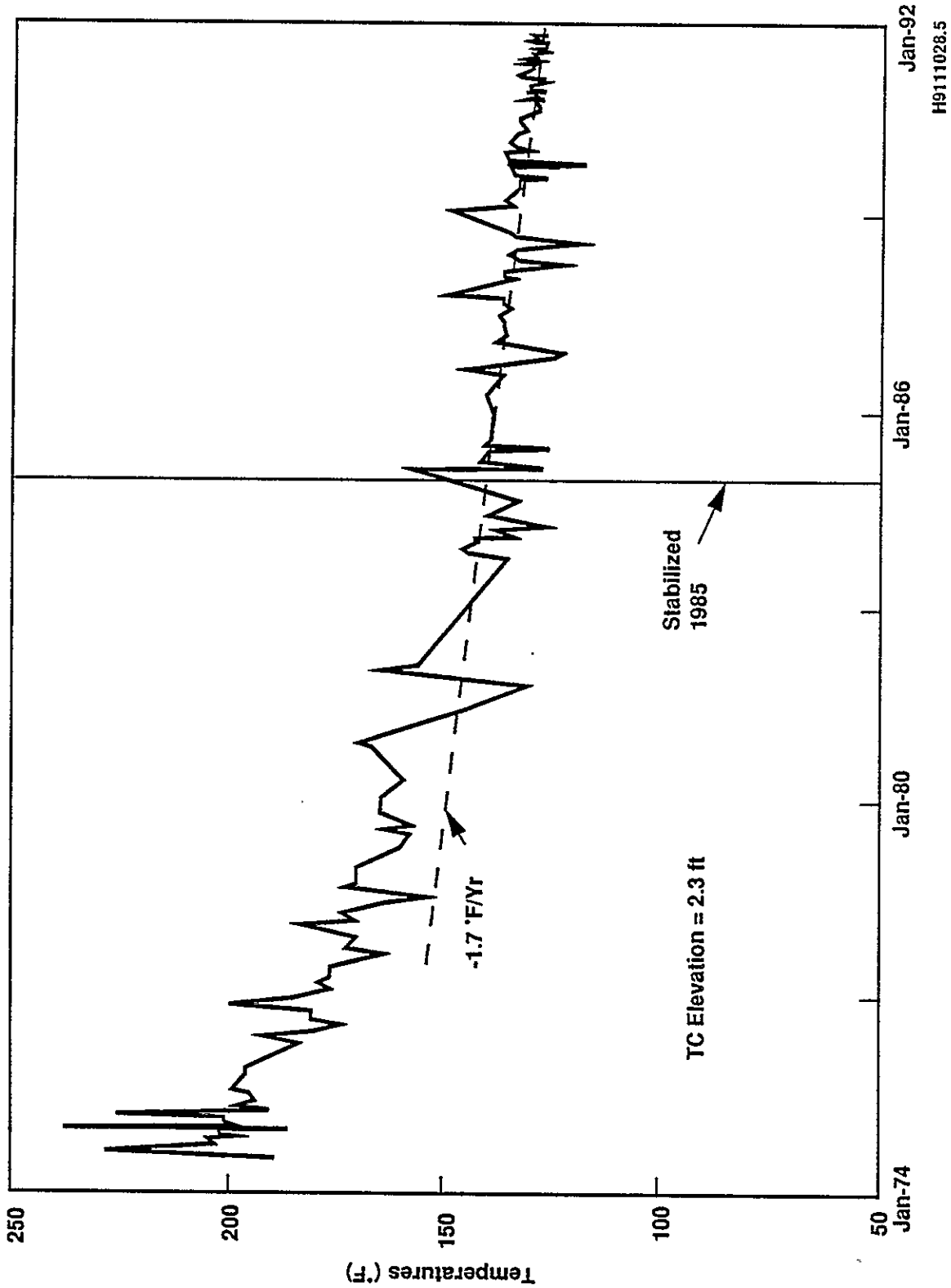

Figure 4-21. Tank 241-BY-105 Temperature.

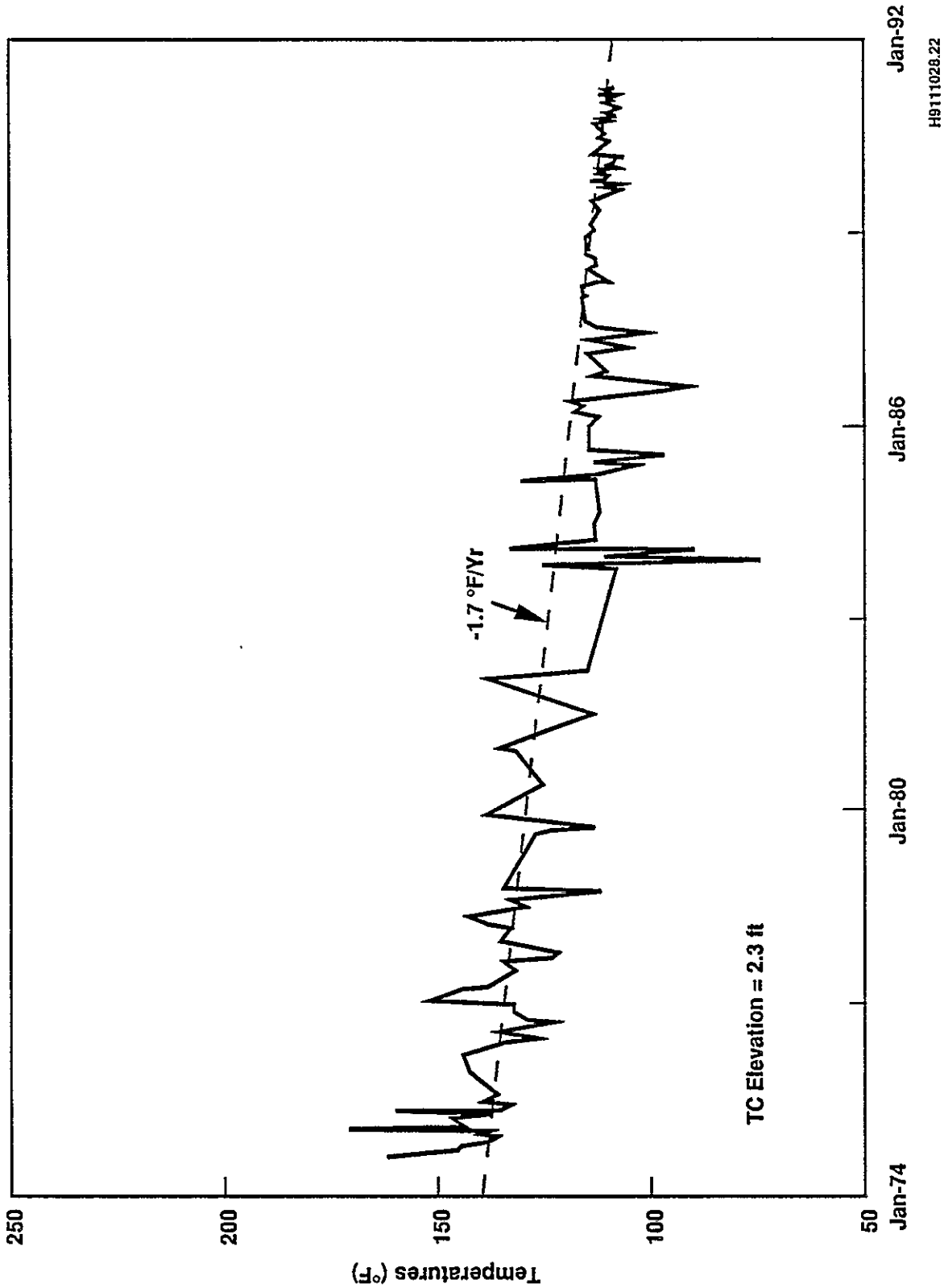

Figure 4-22. Tank 241-BY-106 Temperature.

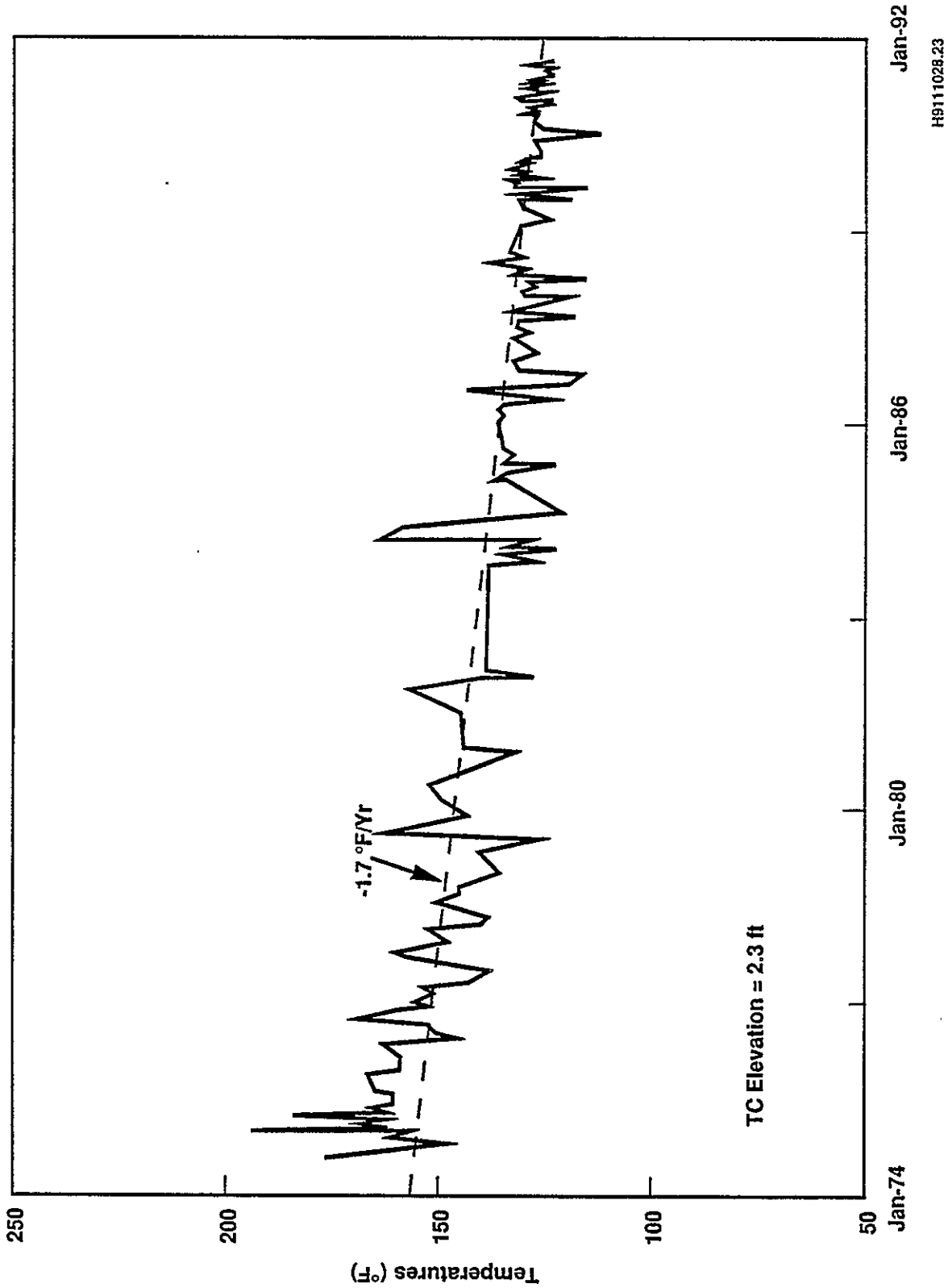

Figure 4-23. Tank 241-BY-110 Temperature.

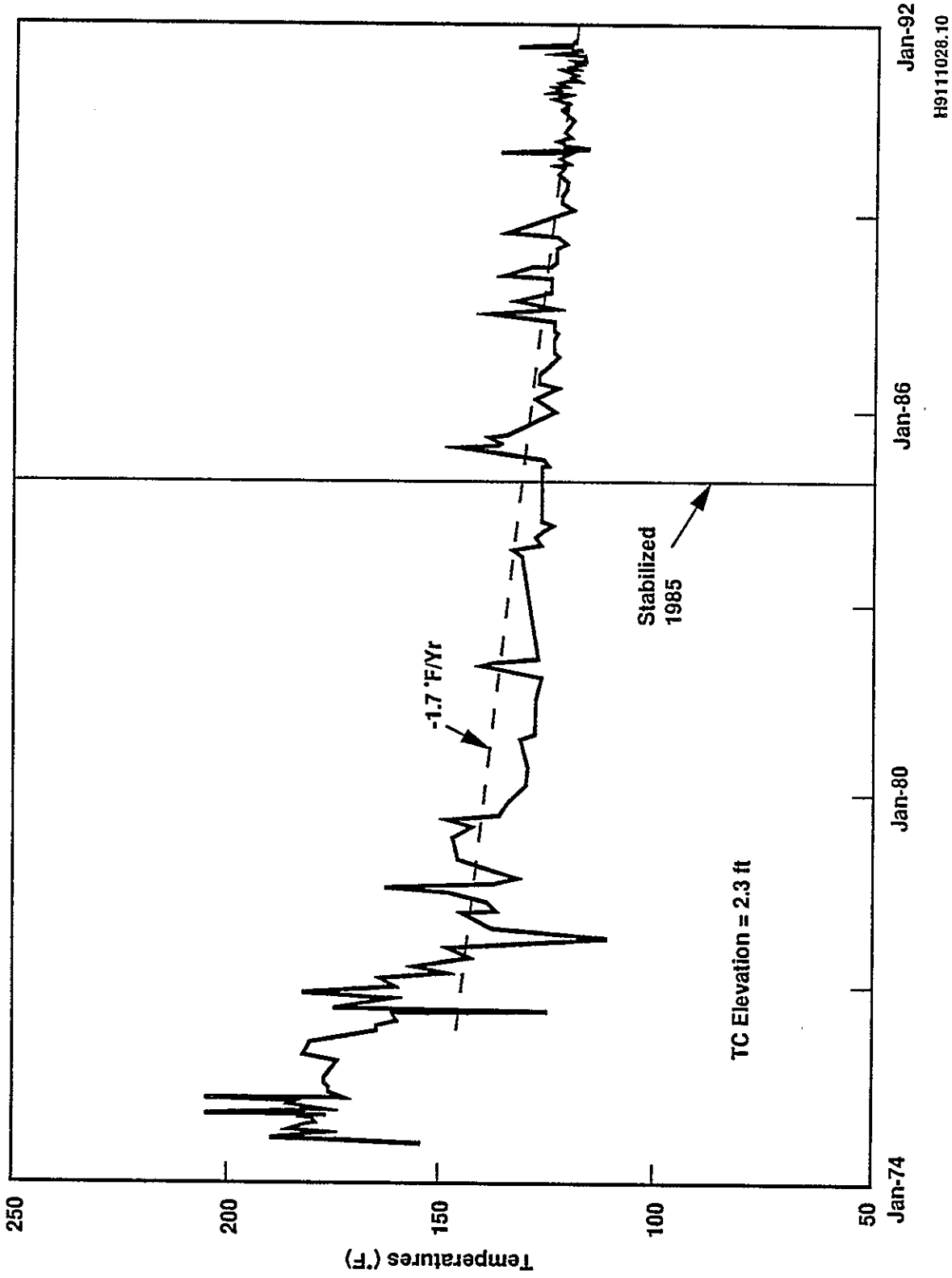

Table 4-19. Historic and Present Tank Temperature Averages.

Tank	Thermocouple elevation (ft)	Temperature (°F)		
		Historic, 1975 to 1985	Present, April 1991 to September 1991	Change
241-BX-102	2.3	68	65	-3
241-BX-106	0.3	78	65	-13
241-BX-110	2.3	73	63	-10
241-BX-111	2.3	79	67	-12
241-BY-101	2.3	87	73	-14
241-BY-103	0.3	77	80[a]	+3[c]
241-BY-104	2.3	172	129	-43
241-BY-105	2.3	134	110	-24
241-BY-106	2.3	151	126	-25
241-BY-107	2.3	74	72	-2
241-BY-108	2.3	109	82	-27
241-BY-110	0.3	148	120	-28
241-BY-111	0.3	95	85[a]	-10
241-BY-112	0.3	124	78[a]	-46
241-C-108	2.3	79	74	-5
241-C-109	2.3	83	76	-7
241-C-111	0.3	77	80	+3[c]
241-C-112	0.3	88	80	-8
241-T-101	2.3	72	66	-4
241-T-107	0.3	73	64[b]	NA
241-TX-118	2.3	95	74	-21
241-TY-101	2.3	71	63	-8
241-TY-103	0.3	66	64[a]	-2
241-TY-104	2.3	72	62	-10

[a]Current temperatures are measured by thermocouple in liquid observation wells at 1-ft elevation.

[b]No operating thermocouple in waste. Gas temperature at 8.3 ft reported.

[c]These small positive deviations are not significant (see text).

NA = not applicable.

temperatures, and the temperature change for these two tanks is not significant because of the scatter in the data and repeatability errors previously discussed.

4.7 THERMAL PROPERTY EVALUATIONS

This section discusses the potential effects of the chemical reactions that may occur in a ferrocyanide/oxidant system. Chemical heating and the associated rates are needed to determine tank consequences. The results of various test programs at FAI, PNL, and LANL are used to determine key reactive chemical properties for stoichiometric and near-stoichiometric mixtures.

4.7.1 Heat of Reaction

The amount of heat generated by a ferrocyanide reaction affects both the rate of thermal runaway and the ability of a dilute mixture to sustain combustion. The heat of reaction is defined as the enthalpy that must be added when the reaction proceeds to completion at constant temperature. Exothermic reactions reject heat and thus have a negative heat of reaction. The heat of reaction depends on the exact reactants and products involved in the reaction. One likely reaction is as follows:

$$Na_2NiFe(CN)_6 + 6\ NaNO_3 \text{ ---> } NiO + FeO + 4\ Na_2CO_3 + 2\ CO_2 + 6\ N_2. \quad (4\text{-}5)$$

Other possible reactants or products include the following:

- Nitrite in place of nitrate as an oxidant
- Na_2O in place of Na_2CO_3, or NaOH if water is present
- CO in place of CO_2
- Oxides of nitrogen in place of N_2.

The heats of reaction for several possible reactions have been calculated from the published heats of formation of the reactants and products (Scheele et al. 1991) and are listed in Table 4-20. They contain an estimated uncertainty of at least 200 kJ/mol in estimating the heat of formation of $Na_2NiFe(CN)_6$.

At temperatures below approximately 1,700 °C, the carbonate product is the thermodynamically stable form and should predominate (Scheele et al. 1991). Note that considerably lower values are obtained if the reaction is incomplete, and NO is formed rather than N_2 or CO rather than CO_2. There is no reason to expect that equilibrium will be reached among the products formed. Recent measurements by R. D. Scheele of PNL in a differential scanning calorimeter have given an enthalpy of reaction of -2,150 to -2,470 kJ/mol, using an equimolar ratio of $NaNO_3$ and $NaNO_2$. Heats of reaction of 1,180 and -1,330 kJ/mol ferrocyanide were estimated by LANL from tests in an accelerating-rate calorimeter (Scheele and Cady 1992).

Table 4-20. Calculated Heats of Reaction.

Oxidant	Products	Energy (kJ)
$NaNO_3$	Na_2CO_3, CO_2, N_2, FeO, NiO	-3,012
$NaNO_3$	Na_2O, CO_2, N_2, FeO, NiO	-1,722
$NaNO_3$	Na_2O, CO, N_2, FeO, NiO	-240
$NaNO_3$	Na_2CO_3, Na_2O, NO, FeO, NiO	+230
$NaNO_2$	Na_2CO_3, N_2, FeO, NiO	-3,708

4.7.2 Fauske Adiabatic Calorimeter

As discussed in the previous section, knowledge of the chemical heat-generation rate becomes a key factor in analysis of thermal runaway conditions. One method of measuring this parameter is to maintain a sample without heat losses (adiabatic) during the exothermic heat release. All the heat generated goes to producing a temperature increase. The temperature-time history, along with knowledge of the specific heat, can provide the necessary parameters. If the system is truly adiabatic, sample size is not important, and all sizes will give the same result.

The adiabatic calorimeter used for testing ferrocyanide samples is referred to as the RSST (Creed and Fauske 1990).

4.7.2.1 Experimental Description. The basic features of the RSST are shown in Figure 4-24. An open, small (approximately 10-mL), spherical glass test cell with low thermal mass (ϕ factor $\approx$1.04) is placed in a high-pressure containment vessel that serves as both a pressure simulator and a safety vessel. The apparatus measures the temperature and containment pressure. The test cell is well insulated and holds a single heating element that compensates for heat losses and adds heat to initiate the runaway reaction if the potential exists. The heater is controlled by feedback from the sample temperature measurement to ensure sufficient heater power to overcome heat losses and produce a specified linear temperature-increase rate at that temperature. For a reactive system, this same linear heat-up rate is added to the reaction energy release; i.e., the heat loss from the test cell to the surroundings does not affect the measurement of the chemical energy release. The imposed linear ramp rate can be varied from 0.1 °C/min to ramp rates approaching those required to simulate exposure to fire. This rate can be either fixed or varied within a given test run.

The overall RSST equipment setup is shown in Figure 4-24. Connections are made to a regulated inert gas supply and vent. The control box contains the temperature/pressure amplifiers and heater power supply. This box typically rests near and is connected to a computer that records the time, temperature, and pressure during the test. Data-handling programs produce hard copies of the data and plots of the following: (1) pressure versus temperature, (2) temperature versus time, (3) pressure versus time, (4) the rate of temperature rise versus the inverse of temperature, and (5) the rate

Figure 4-24. Overall Reactive System Screening Tool Equipment Setup (Creed and Fauske 1990).

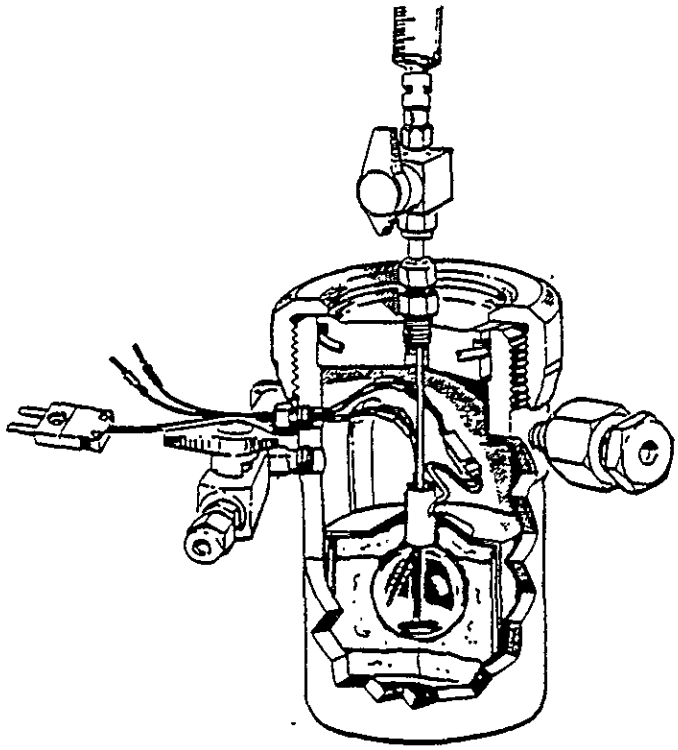

(a) Reactive System Screening Tool Vessel

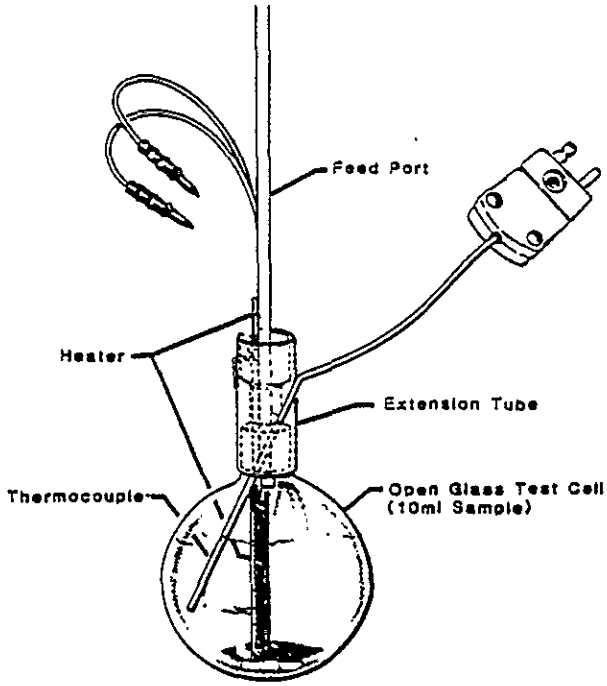

(b) Test Cell and Associated Equipment

of pressure rise versus the inverse of temperature. Arrhenius parameters for the exponential form of chemical heat release may be evaluated from these data.

The RSST determines the potential for runaway reactions and measures the rates of temperature and, in case of gas-phase reactions, pressure increases to allow reliable determinations of the energy and gas release rates.

4.7.2.2 Reactive System Screening Tool Test Results. Cesium nickel ferrocyanide was prepared by Westinghouse Hanford and shipped, along with bottles of sodium nitrate and sodium nitrite, to Fauske & Associates in Burr Ridge, Illinois (Appendix C). The chemicals were then mixed with the oxidizer, 50% sodium nitrate and 50% sodium nitrite on a molar basis, and tested in the RSST adiabatic calorimeter described earlier. Two tests were performed, the first having a near stoichoiometric fuel/oxidant ratio of 1 (weight basis) and the second having a ratio of 0.45. A description of these tests follows.

4.7.2.2.1 Test A022-11, Fuel/Oxidant Ratio of 1. A 9.92-g sample was heated from room temperature at an imposed rate of between 1 and 2 °C/min. An energetic propagating reaction occurred around 280 °C (553 K). This resulted in a temperature exceeding 1,350 °C (1623 K) and pressure of about 2.27 MPa (330 lbf/in^2) (absolute) in the RSST containment vessel.

Figures 4-25, 4-26, and 4-27 show the sample temperature history, pressure history, and temperature rate versus 1/T respectively. After cooldown, the measured containment pressure was approximately 0.76 MPa [111 lb/in^2 (gage)].

4.7.2.2.2 Test A021-25, Fuel/Oxident Ratio of 0.45. A 9.98-g sample was heated from room temperature at an imposed rate of approximately 1 °C/min. A data set similar to that described above is included in Figures 4-28 to 4-30. An energetic propagating reaction occurred at approximately 275 °C (548 K). This is similar to the previous test except the peak temperature and pressure are lower [i.e., 870 °C (1,143 K) and 0.52 MPa (75 lb/in^2 [absolute])]. After cooldown, the pressure was 0.22 MPa [approximately 32 lb/in^2 (gage)]. These lower values appear consistent with the lower fuel weight.

It is appropriate to reexamine these data considering the concept of ignition temperature. Both of these tests indicate the mixtures switch to a propagating reaction when temperatures reach about 280 °C (553 K). The abrupt increase in energy and gas release rates indicates that an autoignition process has occurred. These results are somewhat lower than the temperature of 330 °C (603 K) measured in the modified Henkin tests discussed later.

4.7.3 Pacific Northwest Laboratory Testing (Thermogravimetric Analysis, Differential Scanning Calorimetry, Time-to-Explosion)

Pacific Northwest Laboratory undertook a series of studies to evaluate how changes in composition of ferrocyanide and oxidant mixtures would affect reaction and explosion temperatures. All the tests used cesium nickel

Figure 4-25. Temperature History for Test A022-11, Fuel/Oxidant = 1 (Cesium Nickel Ferrocyanide, Nitrate/Nitrite) (Appendix C).

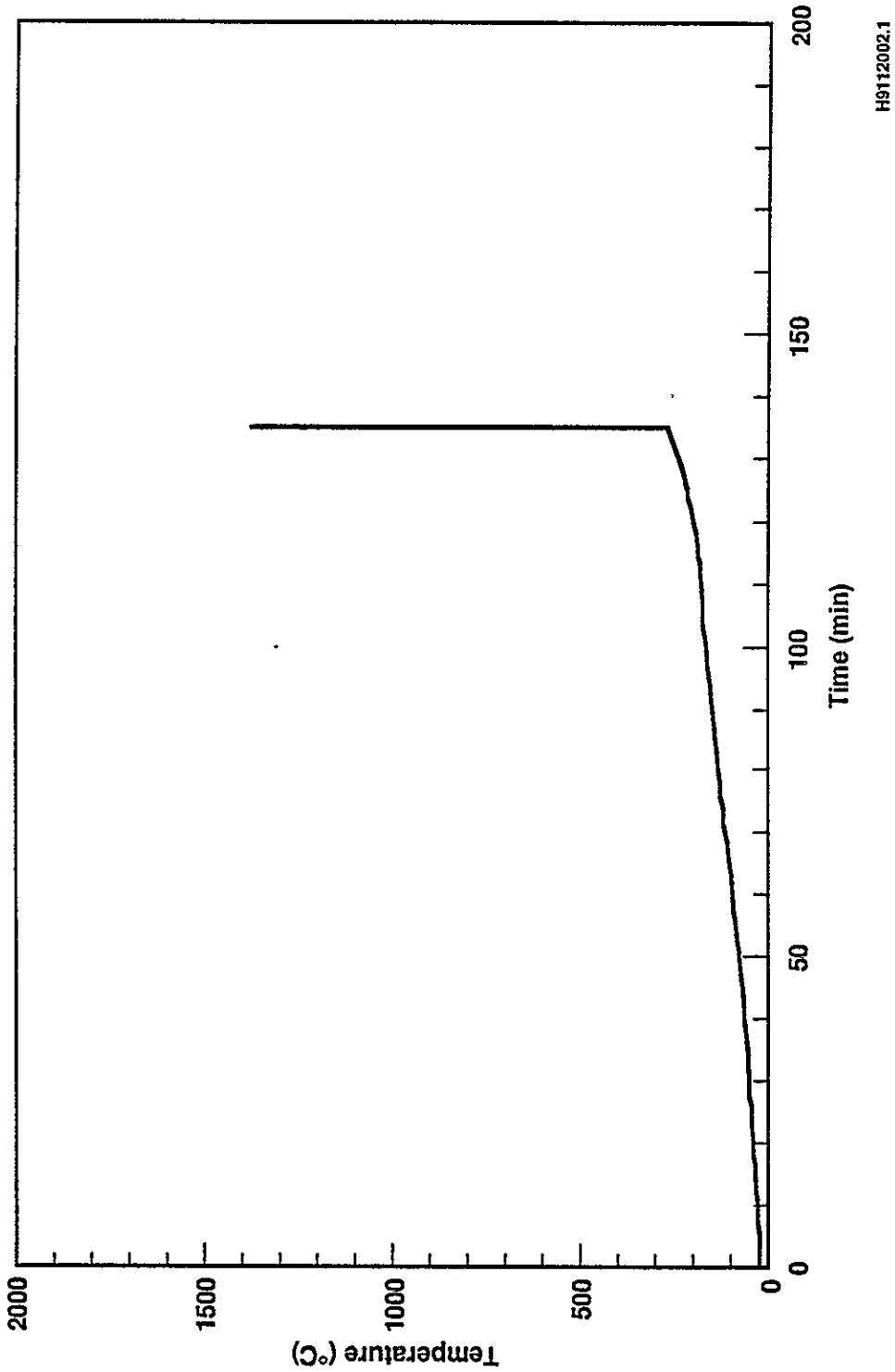

Figure 4-26. Pressure History for Test A022-11, Fuel/Oxidant = 1 (Cesium Nickel Ferrocyanide, Nitrate/Nitrite) (Appendix C).

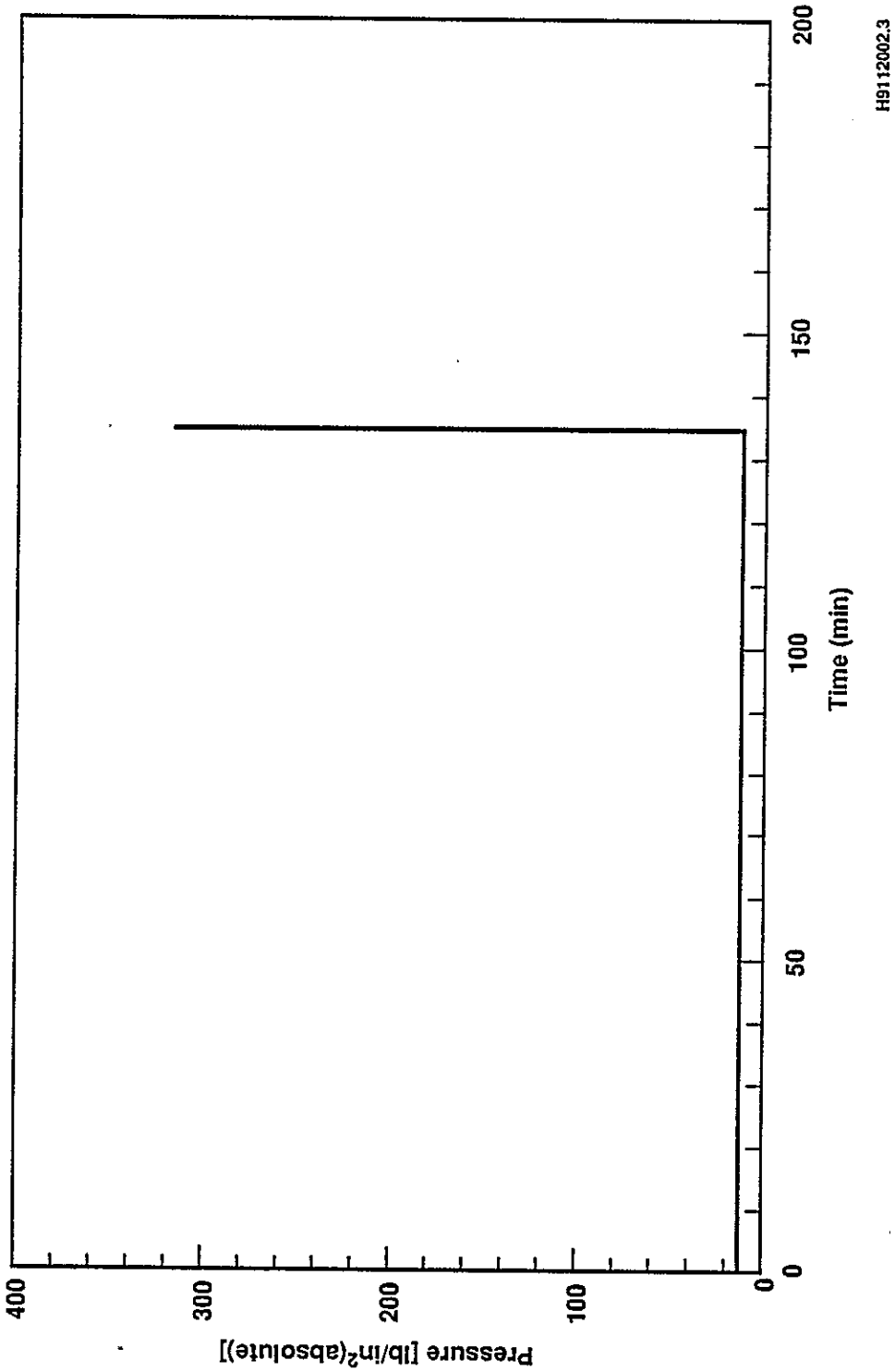

Figure 4-27. Temperature Rate for Test A022-11, Fuel/Oxidant = 1 (Cesium Nickel Ferrocyanide, Nitrate/Nitrite) (Appendix C).

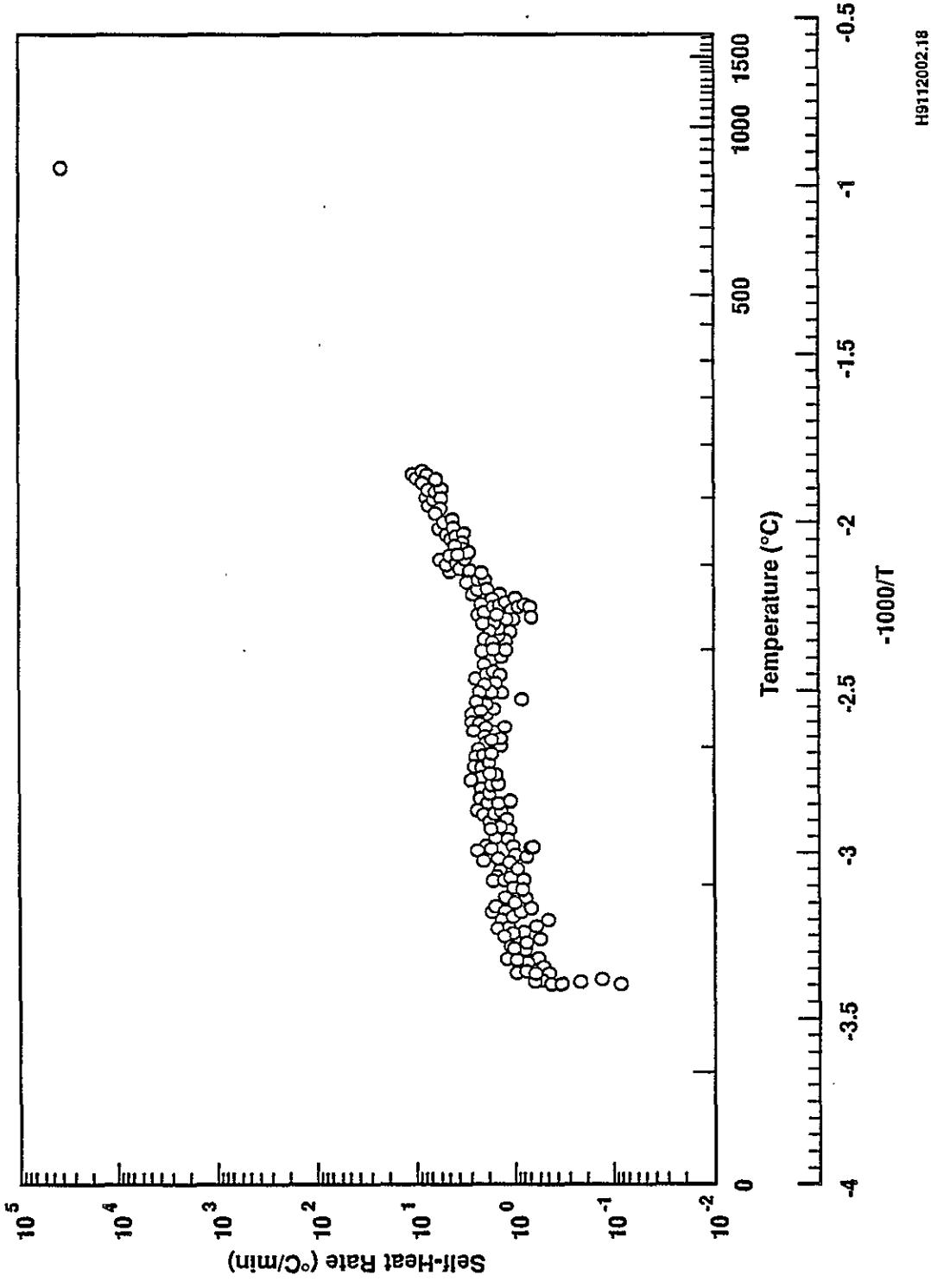

Figure 4-28. Temperature History for Test A021-25, Fuel/Oxidant = 0.45 (Cesium Nickel Ferrocyanide, Nitrate/Nitrite) (Appendix C).

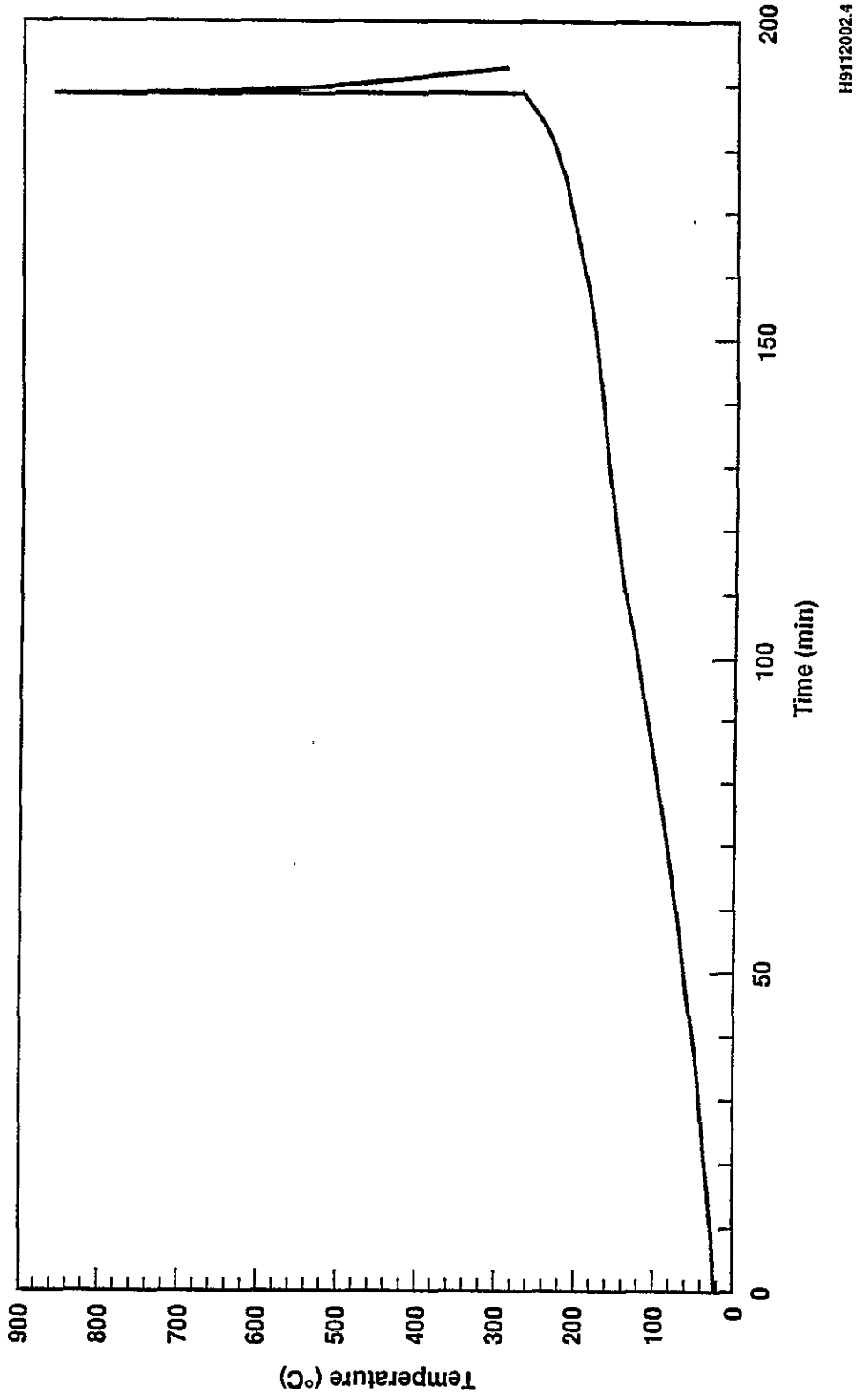

Figure 4-29. Pressure History for Test A021-25, Fuel/Oxidant = 0.45 (Cesium Nickel Ferrocyanide, Nitrate/Nitrite) (Appendix C).

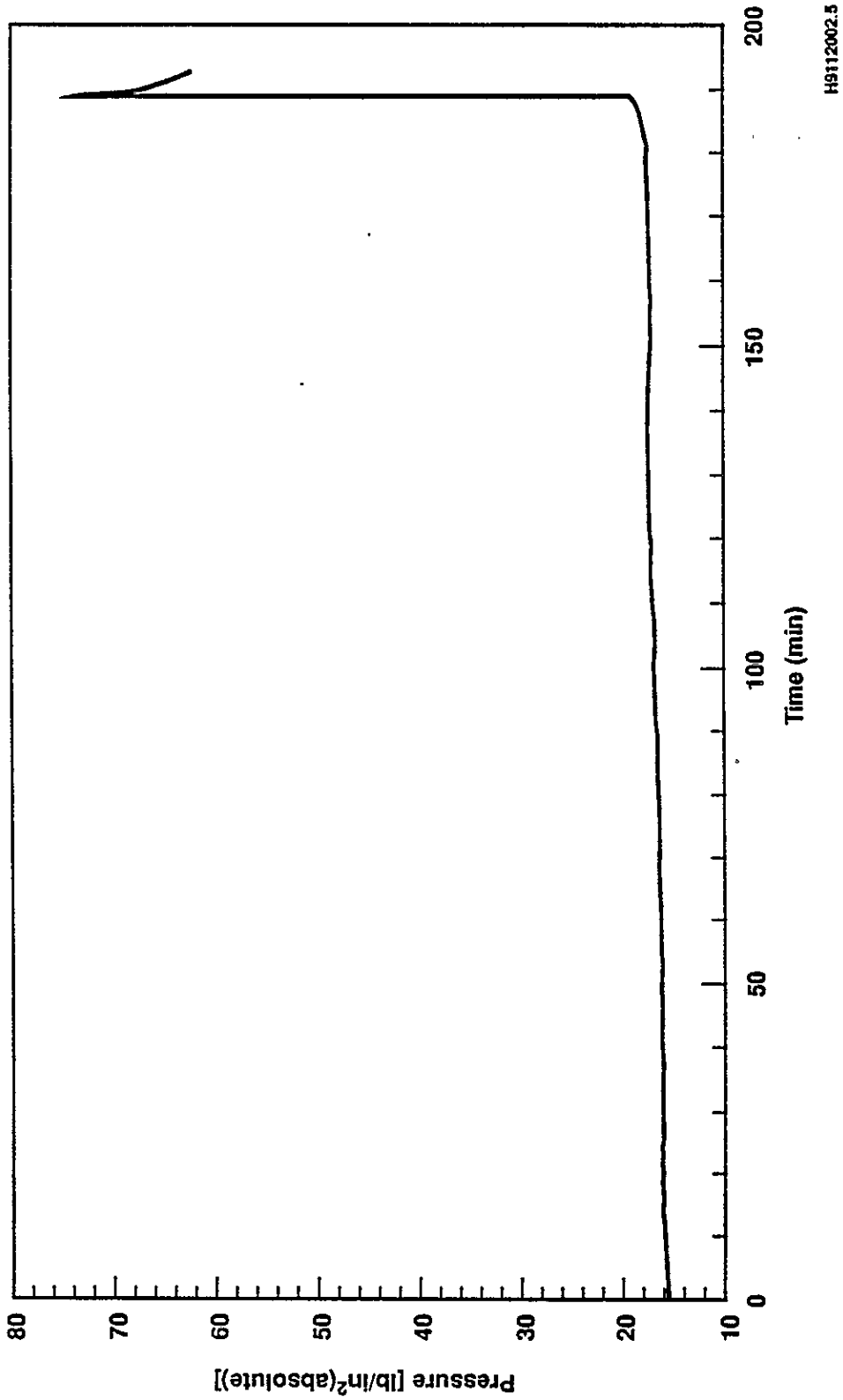

Figure 4-30. Temperature Rate for Test A021-25, Fuel/Oxidant = 0.45 (Cesium Nickel Ferrocyanide, Nitrate/Nitrite) (Appendix C).

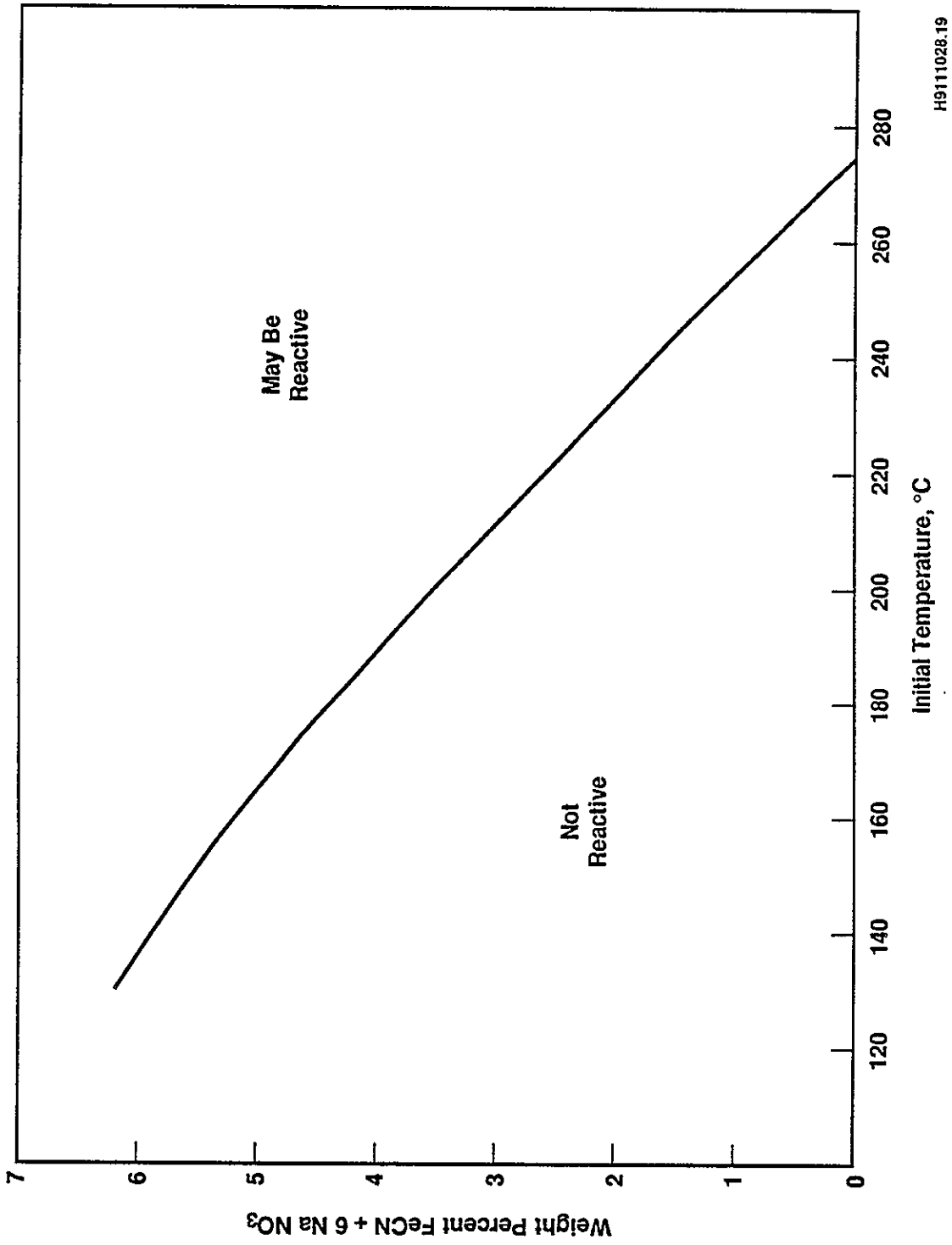

ferrocyanide ($Cs_2NiFe(CN)_6$) with various combinations of nitrate/nitrite mixtures as oxidant. At the time of testing, the cesium salt was the only complex ferrocyanide salt available. The cesium salt is believed to possess chemical properties similar to the sodium nickel ferrocyanide that is more common in the tanks. The sodium salt properties will be evaluated in future tests. Some of the tests included the addition of potential catalysts and/or initiators to the oxidant mixtures. The catalysts/initiators chosen were compounds that are potential waste constituents.

The parameters tested focused on the influence on reaction energetics of the following: (1) oxidant melting point, (2) nitrate/nitrite ratio in the oxidant, (3) ratio of oxidant to ferrocyanide, and (4) presence of catalysts or initiators. Analyses included DSC, scanning thermogravimetry (STG), and small-scale TTXs. Burger and Scheele (1991) report the results of analyses performed to date. The following paragraphs summarize their results.

4.7.3.1 Materials Tested. Cesium nickel ferrocyanide was prepared in the laboratory by a procedure similar to the cesium scavenging operation used in the waste tanks. The exception was that an excess of cesium was used to ensure the formation of $Cs_2NiFe(CN)_6$. The oxidants were prepared by mixing reagent grade chemicals, premelting to ensure uniform mixing, and then grinding with a mortar and pestle. Mixtures of oxidants and catalysts or initiators were mechanically blended.

4.7.3.2 Thermal Analysis Testing. Differential scanning calorimetry measures enthalpy changes in a sample as temperature is changed at a constant rate. Reaction starting and onset temperatures can be observed, and the enthalpy of the reaction can be measured. Scanning thermogravimetry measures weight change in a sample as temperature is changed at a constant rate. A negative weight change can occur by the loss of volatile reaction products from the sample; a positive change would occur if the reaction produced solids formed by combination with components of the air.

These techniques are related and can be used together to provide increased understanding of the reaction of interest. An enthalpy change during a reaction will not necessarily involve a weight change. However, it is highly unlikely that a weight change observed by STG will occur without an accompanying enthalpy change. Because onset temperatures are determined differently by the two methods, they are not expected to agree exactly when compared. However, trends should be similar.

The STG and DSC results failed to show a correlation between oxidant melting point and reaction temperatures. The results of varying the nitrate/nitrite ratio in the oxidant were inconclusive. The STG results show a decrease in reaction temperatures with an increased proportion of nitrite in the oxidant. This is consistent with previous tests (Burger and Scheele 1992) that indicated that nitrite reacted more rapidly with ferrocyanide than did nitrate. However, the DSC results showed an unexpected increase in onset temperature when the oxidant was all nitrite. The overall trend of the onset temperatures was reversed from those of the STG. The minimum observed reaction temperature from the samples that contained only nitrates and/or nitrites with the ferrocyanide was 230 °C.

To study the effects of catalysts or initiators on reaction temperature, the composition of the oxidant was held constant at equimolar quantities of sodium nitrate and sodium nitrite. With one exception, the potential catalyst or initiator was added to the oxidant to make the mixture 5 mol% in the additive. The exception was 30% TBP/normal paraffin hydrocarbon (NPH), which was added to make 1% by weight of the mixture. The other additives that were tested were sodium hydroxide, ammonium nitrate, hydrous ferric oxide, nickel(II)hydroxide, and the sodium salt of ethylenediaminetetraacetic acid (EDTA). The results showed that the presence of sodium hydroxide or EDTA reduced the start and onset temperatures of the mixture. The remaining results either showed no obvious effect or were inconclusive because the decomposition of the additive masked the start of the ferrocyanide reaction.

4.7.3.3 Explosion Tests. Explosion tests were performed on small quantities of samples, 25 to 100 mg. By measuring the time required for an explosion to occur at various temperatures, a minimum explosion temperature for that sample size and geometry was derived.

Of the oxidant mixtures tested without the presence of catalysts or initiators, the ones with the lowest melting temperatures (those containing calcium or lithium) showed the lowest explosion temperatures and the shortest time to explosion. Higher ratios of nitrite to nitrate in the oxidant without catalyst gave lower explosion temperatures, but the time to explosion was not significantly changed. Tests of the effect of varying the oxidant to ferrocyanide ratio showed that a stoichiometric mix is more reactive than one that is lean in oxidant. Higher ratios tested at 400 to 410 °C showed a decrease in reaction violence. Of the catalysts/initiators tested, the nickel and iron hydroxides and the sodium salt of EDTA lowered both the explosion temperature and the explosion time. The effect of the EDTA was most dramatic, lowering the measured explosion temperature from 350 to 280 °C and reducing time to explosion at 360 °C from 50 to 8 s.

4.7.3.4 Conclusions from Pacific Northwest Laboratory Testing. The thermal analysis testing discussed previously (Burger and Scheele 1991) failed to show any strong dependence of reaction temperature on the melting point of the oxidant mixture used in the sample. However, the lower the melting temperature of the oxidant, the lower was the observed explosion temperature for the small samples used in explosion testing.

Changes in the progress of the reaction with variations in the nitrite/nitrate ratio of the oxidant mixture were observed. However, the two methods used for thermal analysis gave conflicting results. The minimum observed reaction temperature for pure oxidant, either nitrite or nitrate, was 230 °C. Onset temperatures decreased as the proportion of nitrite in the oxidant increased.

The stoichiometric mixture of oxidant and ferrocyanide seemed to be most reactive under explosion testing. Of the catalyst/initiators tested, the sodium salt of EDTA showed a marked effect in reduced reaction temperatures in the thermal tests as well as lowered critical temperature and time-to-explosion in the explosion tests. Sodium hydroxide also produced lower reaction times in the thermal tests, and the nickel and iron hydroxides lowered explosion temperatures and explosion times.

4.7.4 Los Alamos National Laboratory Thermal Testing

Los Alamos National Laboratory performed tests (Scheele and Cady 1992) to estimate thermal properties of a ferrocyanide/oxidant mixture provided by PNL. The test mixture consisted of 12 g of hydrated cesium nickel ferrocyanide and 13 g of an equimolar mixture of sodium nitrate and sodium nitrite. The tests performed are typically used to evaluate the thermal stability of explosives. They include differential thermal analysis (DTA), pyrolysis, vacuum thermal stability, Henkin critical temperature, and accelerating rate calorimetry (ARC). The following sections summarize the nature of the tests performed and the conclusions to be drawn from them.

4.7.4.1 Differential Thermal Analysis. The DTA is used to observe temperatures at which exothermic and endothermic changes occur in a sample. This information contributes to an understanding of the phase changes and chemical reactions that a sample may undergo as it is heated.

The sample and an inert reference are heated simultaneously in a controlled environment at a known rate. Temperature increase of both the sample and reference will progress in tandem until a heat-related change in the sample takes place. The deviation of the sample temperature from the reference temperature is measured and indicates that heat is being either evolved or absorbed. The sample size used for all analyses reported here was 9 to 10 mg.

All DTA of the ferrocyanide/oxidant mixture showed three endothermic regions between 100 and 240 °C. The locations of these endotherms were the same for all the tests, regardless of the heating rate. It was suggested by the analysts that the first two endotherms (approximately 155 °C, 185 °C) are associated with the loss of water. The third endotherm (225 °C) may be caused by the heat required to melt the nitrate/nitrite oxidant mixture, because it occurred near its eutectic temperature.

Two exothermic regions are found at higher temperatures than the endotherms. The temperatures at which they occurred varied with the heating rate. At slower heating rates, the exothermic phenomena shifted to lower temperatures. The onset of the lower temperature exotherm was abrupt and occurred at temperatures between approximately 300 and 380 °C.

A further run using a different DTA apparatus and a dried sample showed behavior similar to those reported above. However, the first endotherm was absent. This substantiates the supposition that the lowest temperature endotherm was caused by the evaporation of free water in the sample.

No attempt was made to quantify the heat changes observed in the DTA. The analyses show this sample mixture undergoes energetic exothermic reactions above the melting point of the $NaNO_2/NaNO_2$ mixture. The reactions for this sample size were controlled and did not lead to explosions.

4.7.4.2 Pyrolysis. Pyrolysis in a flowing gas stream is used to study the thermal stability and compatibility of explosive mixtures. A sample is heated at a constant rate as a gas flow is passed over it. The gas stream picks up any gaseous reaction products. The rate of gas evolution is detected by comparing the thermal conductivity of the effluent gas with that of the gas

upstream of the sample chamber. Curves showing gas evolution versus temperature are generated. Comparing these curves to DTA results gives an indication of the relationship of gas evolution from a sample to thermal reactions.

The pyrolysis output for the ferrocyanide/oxidant mixture reveals four significant gas evolution peaks. The first peak, between 150 and 190 °C, corresponds to the second DTA endotherm. It is probably due to the loss of water of hydration. The second small peak between 270 and 330 °C does not seem to be associated with any recognizable thermal event. The third peak is well defined at 368 °C and corresponds to the lowest temperature exotherm. The fourth peak at 436 °C comes at the tail of the second exotherm. This indicates that the second exotherm is not caused by a simple chemical reaction.

4.7.4.3 Vacuum Thermal Stability. Vacuum thermal stability (VTS) testing is a method used to determine the stability of explosives at processing temperatures. The function of the VTS testing is to look for the evolution of gases at temperatures that are at the upper limit of temperatures used during processing. A small sample is sealed in a test bulb attached to a mercury manometer. The test bulb is then immersed in an oil bath of controlled temperature. After equilibration, the gas volume, converted to standard conditions, is taken. The sample remains in the hot bath for a period of time, after which the final gas volume is determined from the change in height of the manometer reading. This also is converted to standard conditions. The difference between the initial and final standard volumes gives the amount of gas evolved.

The ferrocyanide/oxidant mixture was tested at 120 °C for 48 h. The amount of gas evolved under these conditions is calculated to be 0.07 mL of gas per gram of sample. This is considerably less than conventional explosives and indicates that the sample did not react detectably to give permanent gases at 120 °C.

4.7.4.4 Henkin Critical Temperature. The lowest temperature at which a thermal explosion occurs in a material is called its critical temperature. The method used for determining the critical temperature of the ferrocyanide/oxidant mixture is based on a time to explosion. Approximately 40 mg of sample is compressed to approximately 90% of its crystal density in an aluminum blasting cap shell with a hollow, skirted aluminum plug. The assembly is placed in a preheated, liquid metal bath, and the time to explosion is observed. Explosion is determined by rupture of the blasting cap shell or unseating of the plug. Many tests must be made at different temperatures to determine critical temperature with confidence, and sufficient time must be allowed on each test to ensure time for the reaction to occur.

The critical temperature for the sample size and geometry was estimated to be 367 °C. Explosion temperature is expected to be substantially lower for large masses of material. However, the estimated critical temperature of the tested ferrocyanide/oxidant mixture was significantly higher than those of standard explosives tested in the same configuration (286 °C for trinitrotoluene).

4.7.4.5 Accelerating Rate Calorimetry. The ARC is a device to measure the time-temperature relationship for a runaway process. As exothermic decomposition occurs under adiabatic conditions, the heat evolved will cause a temperature rise in the sample that will, in turn, cause an acceleration of the reaction rate and the subsequent heat evolution. The instrument used for the tests on the ferrocyanide/oxidant mixture is capable of providing heat to the sample in steps, with pauses in between to allow equilibration and search for exothermic behavior. If an exotherm is detected during this pause (0.01 °C/min temperature rise with no external heat added), the instrument switches to the adiabatic mode. In this manner, the sample can be brought up to a desired temperature, and observations can be started from that point onward.

A series of ARC tests were performed on the ferrocyanide/oxidant mixture to further observe the exothermic behavior of this mixture. The analysts concluded that, at very slow heating rates, a decomposition exotherm can be detected at 200 °C. The experiments are not sufficient to predict the heating rates for pure samples, but the heating rate should be slow while the temperature is below 240 °C because both exothermic and endothermic processes are taking place simultaneously. A self-heat rate of approximately 0.4 °C/min at 250 °C is measured.

4.7.4.6 Conclusions from Los Alamos National Laboratory Testing. It is evident from the DTA and ARC results that the mixture of ferrocyanide and oxidant displays the most energetic exothermic behavior at temperatures above 300 °C. However, the DTA results indicate that the heating rate affects the temperature at which this exothermic behavior will begin. Slowing the heating rates lowers the onset of the exotherm. The ARC detects some exothermic behavior as low as 209 °C. However, in the region of the melting temperature of the oxidant (218 to 240 °C from the DTA), the heat yield will be offset by the heat required to overcome the heat of fusion of the oxidant.

All the tests reported in this section were made on small samples of the ferrocyanide/oxidant mixture. Without confirmation from large-scale tests, it is not possible to use the results to predict the lowest safe temperature for this mixture. The Henkin critical temperature test is a measure of the temperature at which heat is produced faster than it can be conducted away. Therefore, it is highly dependent on sample size and geometry. A large mass of sample, or one in a disadvantageous geometric configuration, is expected to react at a lower temperature.

Preliminary thermal parameters on optimum stoichiometric mixtures from this work that may contribute to the body of knowledge for future work are the following:

- Henkin critical temperature--367 °C
- Lowest temperature of observed exothermic behavior (ARC)--209 °C
- Self-heat rate at 250 °C--0.4 °C/min.

4.8 NONTHERMAL SENSITIVITY TESTING

Reactive mixtures can possibly be initiated by mechanisms other than increasing temperatures, and it is common to test experimental explosives for sensitivity to shock, impact, friction, and electric sparks in addition to heat. Standardized empirical tests are used for such sensitivity evaluations. The results are expected to be highly dependent on the composition of the mixture tested; i.e., the amounts of oxidizer, solid diluents, and water are all expected to be important.

Measuring the sensitivity of a range of so many parameters would require an extensive test program. To reduce the work, initial testing has been confined to representative, conservative mixtures comprised of dry stoichiometric amounts of ferrocyanide fuel and oxidizers. Later, testing can be expanded to mixtures more typical of the tank contents.

The LANL has also performed nonthermal sensitivity tests (Scheele and Cady 1992) of $Cs_2Ni[Fe(CN)_6]\cdot x\ H_2O$ mixed with stoichiometric amounts of oxidizer (50 mol% $NaNO_3/NaNO_2$). This mixture, identified as FECN-1, is 52 wt% fuel and also contains a small (approximately 2%), variable amount of water, probably as water of hydration.

The use of this test mixture is expected to be conservative in that the mixture is at or near the optimum reaction proportions and contains no diluents as would actual tank mixtures. The tank mixture is expected to contain mostly $Na_2NiFe(CN)_6$ rather than the cesium form, but the reactions are expected to be similar. This expected reaction behavior will be confirmed in later tests.

The test report concludes ". . . that the test mixture is safe to handle from an explosives point of view. It does not react under the most severe conditions available in our impact or friction tests . . . Reactions are observed in the spark-sensitivity tests at energies much higher than are required to ignite all but the most insensitive explosives." (Scheele and Cady 1992). Table 4-21 summarizes the reported test results and compares these results with two common explosives.

Table 4-21. Sensitivity Results.

Test method	Units	Material		
		FECN-1	TNT	TATB
Impact (2.5 kg)	cm	>320	157	>320
Impact (2.5 kg), roughened surfaces	cm	>320	>320	>320
Friction, BAM	kg	>36	>36	Not listed
Spark, 3-mil foil	J	2.8	0.46	4.25
Spark, 10-mil foil	J	19 to 26	3.75	18.1

BAM = bundesanstalt fur materialprufungen.
FeCN = ferrocyanide test mixture.
TATB = triaminotrinitrobenzine.
TNT = trinitrotoluene.

Briefly summarized, the ferrocyanide/oxidant test mixture does not react to impact or friction when tested to the machine limits.

The spark sensitivity also is very low. Note that the maximum static charge likely to be accumulated on a human body is 0.015 J.

The LANL work reported did not address the question of shock and the ease with which high-order detonation can be established in the FECN-1 mixture; however, the summary did note that "FECN-1 did not show any unusual tendency for small reactions to grow easily to large reactions . . ." (Scheele and Cady 1992).

4.9 TANK HEAT LOAD BASED ON THERMAL MODELING EVALUATIONS

Thermal analyses using the HEATING7 computer code (Childs 1991) were conducted on models of tank 241-BY-104 to determine the heat load of the tank, the thermal conductivity of its contents, and the distribution of the heat generation in the tank. The published radioactive decay heat load for tank 241-BY-104 (Hanlon 1991) is 4.89 kW (17,000 Btu/h). It is necessary to confirm this value or determine a value more consistent with expected thermal conductivities and measured temperatures.

This section describes the thermal model and the calculations performed and provides estimates of the heat load and distribution of heating rates.

4.9.1 Thermal Model

This section describes the measured temperatures for the tank contents, the HEATING7 heat transfer model, and the parametric studies that result in establishing the heat load and thermal conductivities.

4.9.1.1 Measured Temperatures. The temperature of the contents of tank 241-BY-104 is measured by a thermocouple tree that is located 3.658 m (12 ft) from the centerline of the tank and contains six thermocouples. A curve of temperatures taken from this tree (Reynolds 1990) is used for the analysis and shown in Figure 4-31. The temperatures in this tank have been decreasing slowly since the tank was filled as discussed earlier in Section 4.6. From 1982 to 1983, the tank was stabilized by removing the supernate above the salt cake and as much liquid as could be removed from the sludge. This liquid also contained heat-generating radionuclides in solution. The temperature readings before and after stabilization show a drop of 16.7 °C (30 °F) in the maximum temperature of the tank due to the reduction of the heat load.

4.9.1.2 Description of Model. The three-dimensional thermal analysis model was developed for the HEATING7 code. It consists of regions, connected together by boundaries, with the appropriate heat transfer conditions describing these boundaries and regions. The heat sources are described by tabular functions and can represent a uniform or nonuniform distribution. Because of symmetry, the model was described only for 180°.

Figure 4-31. Thermocouple Tree Data for Tank 241-BY-104 (Reynolds 1990).

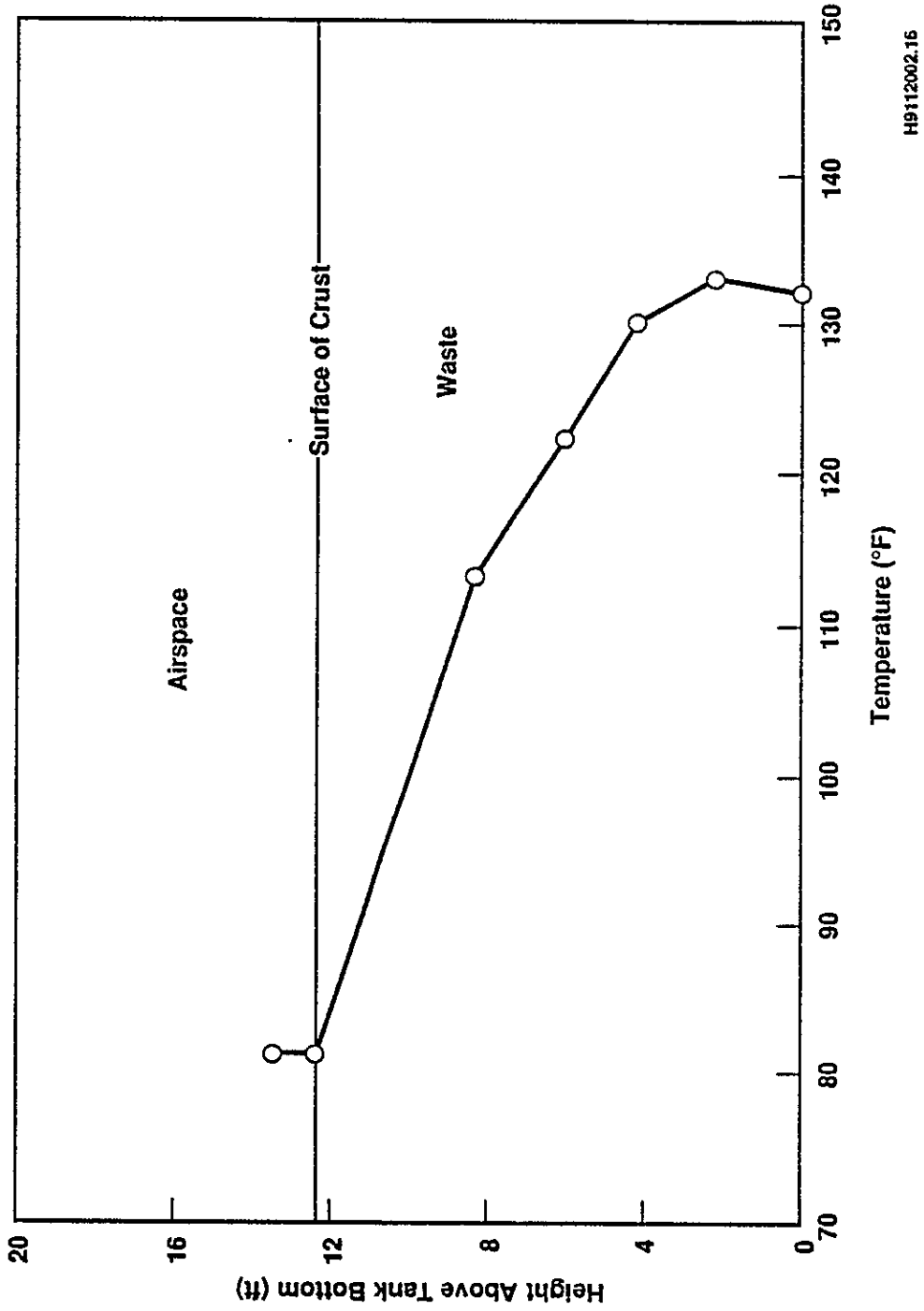

The model is made up of nine regions and four boundary conditions. Three regions describe the soil over the tank, around the tank, and under the tank. Three regions describe the concrete bottom and sides of the tank. The concrete tank top was not separately modeled. Its volume was included in the dirt top cover. This is conservative because the dirt has a lower thermal conductivity than the concrete. One region describes the air space in the tank. Anther region describes the salt cake of the waste in the tank. The sludge is divided into two volumes vertically, considered "damp" and "wet." The heat generation due to radioactive decay is assumed to be only in the wet and damp sludge layers.

The first boundary condition is a constant temperature surface that describes the temperature of the soil at the water table (considered to be 55 °F at 200 ft below the surface). The second boundary is a surface-to-boundary condition, with forced convection heat transfer to a constant temperature boundary, that describes the soil-to-atmospheric air interface. A forced convection heat transfer coefficient is used because there is nearly constant wind at the tank farms. The third boundary condition is a surface-to-surface condition with convective and radiative heat transfer coefficients that describe the interfaces between the waste salt cake and the air space in the tank and between the air space and the tank top. The fourth boundary condition is a surface to insulator (i.e., a reflection) that describes the boundary in the soil between one tank and another.

4.9.1.3 Method of Analysis. During the initial phases of the thermal analysis, it was found that a unique combination of thermal conductivities and heat load was required to match the thermocouple temperature data. The thermal conductivity of the soil over and around the tank bound the heat load within certain limits, and the thermal conductivities of the sludge and salt cake defined the shape of the temperature versus height curve. The heat generation and conductivities of the tank contents were adjusted to fit the data curve. The conductivity of the crust layer has a considerable effect on the temperature profile in the waste. The conductivity of the waste is a major factor in the shape of the temperature profile, with the magnitude of heat generation also being a major factor. However, there is an interrelationship between the two variables, which is why the solution of conductivity and heat load can be considered unique. When high heat loads were investigated, the conductivity of the soil was required to be increased beyond reasonable limits in order to maintain the tank temperatures within the data. Once the heat load and thermal conductivities within the tank were established, the effect of uneven heat distributions could be investigated by moving the point of the concentrated heat source to different locations.

4.9.2 Estimate of Heat Load

The radioactive decay heat load was determined two different ways. First, the heat transfer analysis, including ventilation effects, provides one estimate. Second, the radioactivity measurements, with corrections for decay and isotope losses when pumping out supernate, provides another. These two approaches provide reasonably consistent results.

4.9.2.1 Computer Thermal Analysis. The published heat load of tank 241-BY-104 is 4.89 kW (17,000 Btu/h) (Hanlon 1991). This heat load was determined from psychrometric analysis of the atmospheric conditions versus the air exhausted from the tank while under forced ventilation prior to stabilizing the tank. The results of the computations varies greatly, from 11.30 kW (38,555 Btu/h) to 2.29 kW (7,815 Btu/h). A thermal model utilizing a heat load of 4.89 kW was created, and the thermal conductivity of the tank contents and the soil over the tank were adjusted until the computed temperature distribution in the tank matched the observed temperatures from the thermocouples. The results indicate that a thermal conductivity of 2.60 W/m-K (1.5 Btu/h-ft-°F) for the soil is required to match the temperature in the tank air space. This value is considered to be unreasonable, as laboratory analysis indicated that a conductivity value of 0.433 W/m-K (0.25 Btu/h-ft-°F) is to be expected (McLaren 1991). As a result of this analysis and comparison with laboratory data, the published heat load is considered to be in error. An examination of the published heat loads of the ferrocyanide-bearing tanks does not reveal a good correlation with their measured maximum temperatures. Accordingly, all the published heat loads are suspect, and their values should be determined by analysis and verified by new tank measurements.

After stabilization, tank 241-BY-104 was taken off forced ventilation and the piping sealed. It was expected that the tank was isolated from the atmosphere except for a breather pipe with a filter. The breathing rate due to atmospheric pressure changes was expected to be very low and the resulting heat loss to be negligible. Using this assumption, the boundary conditions of an annual average temperature of 12.2 °C (54 °F) for the atmosphere, and a groundwater temperature of 12.8 °C (55 °F), the conductivities of the sludge and salt cake and the heat load of the tank were determined. The heat load for the tank was determined to be 1.61 kW (5,500 Btu/h). This is markedly less than the published value of 4.89 kW. However, during a study of tank 241-C-103, it was determined that if as little as 1 in^2 of an air inlet opening was allowed, the resulting natural convection airflow could remove up to 440 W (1,500 Btu/h) of heat. These calculations used an outlet pipe of 10.16 cm (4 in.) diameter with a heat trace that augmented the chimney effect. The air velocity in this pipe was calculated to be just under 122 cm/s (4 ft/s). Inspection of the engineering drawings of tank 241-BY-104 showed that it was very possible that air infiltration was occurring in the tank and had to be accounted for. Accordingly, a method of approximating the effect of natural convection airflow was developed.

Using the 18.9-cm/s maximum air velocity in the vent pipe as a basis, it was found that the maximum expected airflow through the tank was 9.91 L/s (21 ft^3/min). It was determined that the average wet bulb temperature for the site was 8.9 °C (48 °F) and that the dry bulb temperature was 12.2 °C. With these values and assuming that the exiting air was at the temperature of the air in the tank and saturated, psychrometric analysis indicated that the heat removed by ventilation was less than 716 W (2,300 Btu/h). Although the exiting air is most probably not saturated, assuming that it is saturated maximizes the heat removal, which is conservative. This was added to the tank heat load that had been determined for the unventilated case. The resulting heat generation rate is thus approximately 2.34 kW (8,000 Btu/h). The conductivities of the tank contents and the heat generation fractions were then adjusted to fit the data curve. The thermal conductivities determined by

the parametric analysis are as follows: the salt cake equals 0.277 W/m-K (0.16 Btu/ft h°F), the damp layer under the salt cake equals 0.364 W/m-K (0.21 Btu/ft-h°F), and the wet layer at the bottom of the tank equals 0.467 W/m-K (0.27 Btu/ft-h°F). The salt cake is 1.18 m (3.88 ft) thick, the damp layer is 1.22 m (4 ft) thick, and the wet layer is 1.34 m (4.4 ft) thick. The heat generation of the damp layer was 40% of the total, and the heat generation of the wet layer was 60% of the total. Using these conductivities and heat generation rate, the computer prediction matched the data, shown in Figure 4-32. These conductivities, heat generation rate, and heat generation fractions were used in the upper-bound analysis calculations.

4.9.2.2 Analysis of Radioactivity. An alternative method of calculating the heat load in the tank is to evaluate the radioactive nuclide data from previous sampling. In March 1976, a letter report gave values of the radioactivity of the sludge and supernate in the tank (Horton 1976). The values for the sludge were 1.74×10^5 μCi/L of ^{90}Sr and 4.40×10^5 μCi/L of ^{137}Cs. The values for the supernate were 2.01×10^2 μCi/L of ^{90}Sr and 5.30×10^5 μCi/L of ^{137}Cs. The heat generation resulting from radioactive decay in the sludge was 1.18×10^{-3} W/L for the ^{90}Sr and 2.11×10^{-3} W/L for the ^{137}Cs. If the ratio of watts to curies in the sludge is used for the supernate, the heat load for a sludge volume of a cylinder 22.86 m (75 ft) in diameter and 2.25 m (7.4 ft) high, with 757,219 L of supernate calculates to be 4.98 kW in 1976. The 757,219 L of supernatant on top of the sludge was pumped out in 1983. With the supernate removed and accounting for radioactive decay, the heat load in 1990 is 2.20 kW (7,500 Btu/h). This is within the upper and lower bounds of heat load determined by the thermal analysis. This calculation assumes that the heat load of the tank is being generated in the sludge only. Gamma scans of the vertical profile of the tank indicate that the bulk of the radioactivity in the tank comes from the sludge volume, with only a small contribution from the salt cake. See Appendix B, Figure B-5.

4.9.3 Distribution of Heat

One of the problems in developing a thermal model is determining the distribution of heat generation within the tank. The possibility that the ferrocyanide with its bound cesium settled in a layer at a position commensurate with its density was considered. Two-dimensional modeling of the tank with the heat source concentrated in a layer was investigated. The results required matching the observed temperature values in a critical area. Figure 4-31 shows a lower temperature on the bottom of the tank than at the next point above it. This temperature difference exists in all the recorded temperature data. The shape of the temperature versus height curve indicates a homogeneously distributed heat source. Layers containing the heat source were placed at various levels in the tank. The only way a layer was found to approximate the data curve was when a layer heat source was placed with its centerline just above the height of the maximum observed temperature. If this is the actual distribution of the heat, it should be shown as a spike on the plot of gamma counts per second versus tank height at about 1.2 m (4 ft) (see Appendix B, Figure B-5). This spike does not exist. Figure B-5 shows that for the sludge region, the counts of gamma activity are quite uniform versus the depth of the sludge. The available evidence indicates that the heat source is homogeneously distributed throughout the sludge layer in the tank. The computer model uses a heat source distribution that is slightly

Figure 4-32. Comparison of Computer Prediction with Data, 2.46 kW (8,000 Btu/h) (Reynolds 1990).

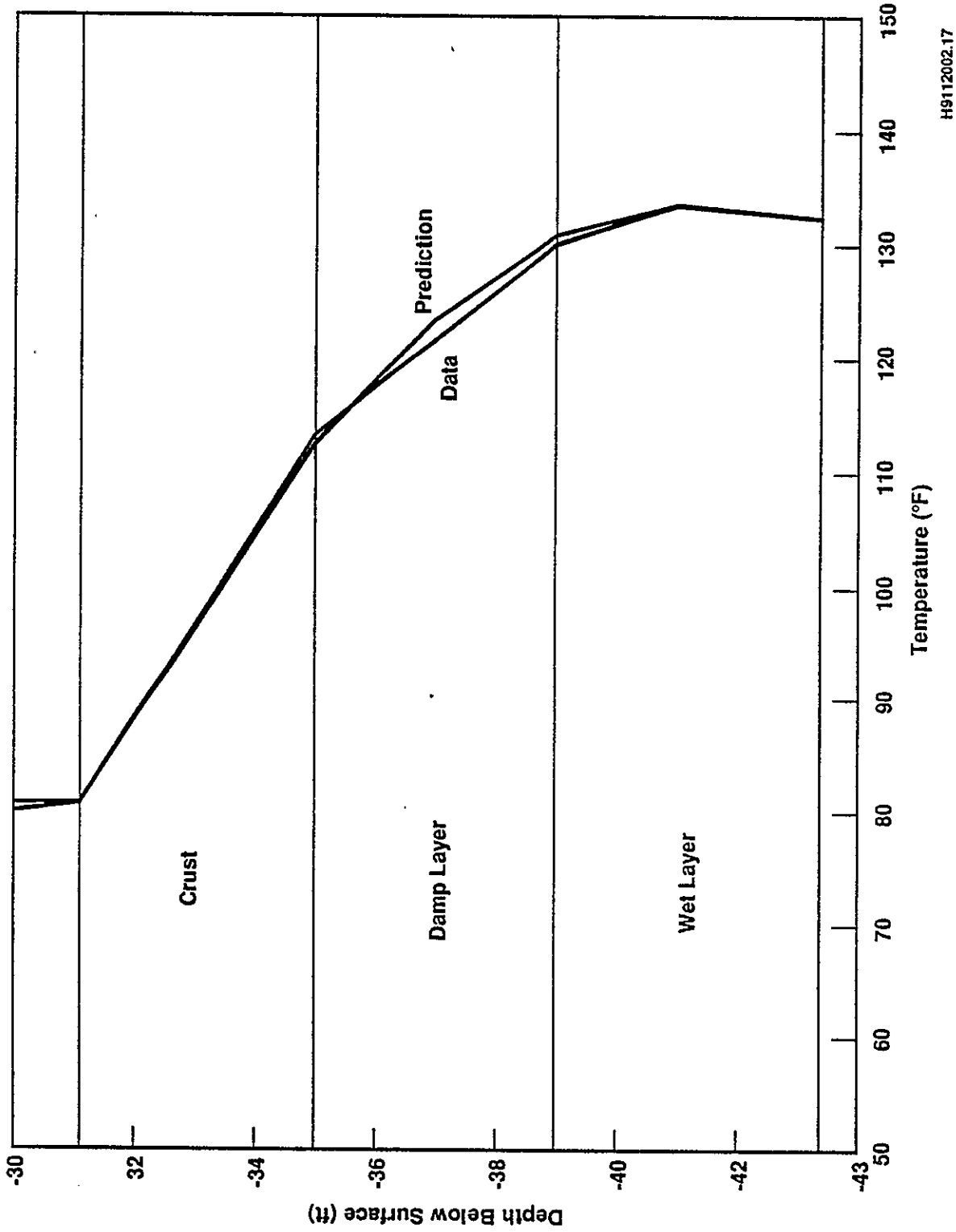

skewed towards the bottom; i.e., 60% of the heat source was placed in the bottom 52% of the sludge volume, and 40% of the heat source was placed in the top 48% of the sludge volume.

4.9.4 Summary of Thermal Analysis

Section 4.9 contains the basis for establishing the heat load for tank 241-BY-104 from thermal analysis. This thermal analysis, made with a three-dimensional heat transfer model of tank 241-BY-104 using measured waste temperatures, shows the heat load to be 1.6 kW to 2.3 kW, which is less than the previously published value of 4.9 kW. These values are constant with the 2.2-kW heat load calculated from the decay heat of the tank contents. In addition, thermal conductivities for the salt cake and the heat-generating sludge are estimated. These values are compared to values obtained via other means in Section 4.10.6.

4.10 SUMMARY OF ESTIMATION OF KEY PARAMETERS

The evaluation of the hazards associated with ferrocyanide sludges requires values for a number of key parameters. Various data sources were discussed in Sections 4.1 through 4.9. This section attempts to estimate the values for several key parameters based on an integration of these various data sources. Estimates are provided for ferrocyanide concentration, organic carbon fuel present, water content of sludges and salt cakes, diluent types and concentrations, decay heat amounts and locations, reaction indication, and ignition temperature and waste thermal properties (conductivity, heat capacity, and thermal diffusivity).

4.10.1 Ferrocyanide Concentration and Locations

The scavenging process formed insoluble ferrocyanide complexes, strontium salts, and other precipitates from the UR and IC wastes in process tanks in U Plant or in CR Vault. These solids formed a slurry that was routed and settled in tanks that were previously emptied. The slurry was estimated to have a relatively low viscosity, because it was pumped for several miles across the site from the process tanks to the settling tanks. The solids were assumed to be uniformly distributed in the slurry and, after several days, to have settled in relatively similar layers across the bottom of the settling tanks. After the solids had settled out of the slurry, the supernatant was then pumped out of the tank and disposed to the ground.

The best available estimate of the specific tank volume and concentration of ferrocyanide sludge is obtained from the sludge predictive model (Borsheim and Simpson 1991) discussed in Section 4.1. Table 4-22 lists the bulk inventory of ferrocyanide for each tank and the concentration of ferrocyanide in the sludge. Table 4-23 summarized the remaining ferrocyanide tank historical data. The ferrocyanide concentration (molarity) shown was calculated by determining the total amount of ferrocyanide remaining in the tank and dividing that value by its occupying volume. The volume and amount

Table 4-22. Ferrocyanide Tank Inventory Summary (using model values).

Tank	$Fe(CN)_6^{-4}$ (mol)	NO_3 (mol)	NO_2 (mol)	$Fe(CN)_6$ Sludge (gal)	$Fe(CN)_6^{-4}$ in sludge (M)	Molar ratio $Fe(CN)_6^{-4}/NO_3/NO_2$
241-BX-102a	NE	DNA	DNA	NE	NE	DNA
241-BX-106a	NE	DNA	DNA	NE	NE	DNA
241-BX-110a	NE	DNA	DNA	NE	NE	DNA
241-BX-111a	NE	DNA	DNA	NE	NE	DNA
241-BY-101a	NE	DNA	DNA	NE	NE	DNA
241-BY-102b	9.00 E+02	3.40 E+04	1.13 E+04	2.30 E+03	0.10	1.0/38.4/12.8
241-BY-103a	6.59 E+04	2.12 E+06	7.08 E+05	2.12 E+05	0.08	1.0/32.2/10.7
241-BY-104	8.32 E+04	2.60 E+06	8.68 E+05	2.60 E+05	0.08	1.0/31.3/10.4
241-BY-105	3.62 E+04	9.61 E+05	3.20 E+05	9.60 E+04	0.10	1.0/26.6/8.9
241-BY-106	7.00 E+04	2.28 E+06	7.61 E+05	2.28 E+05	0.08	1.0/32.6/10.9
241-BY-107	4.24 E+04	1.58 E+06	5.27 E+05	1.58 E+05	0.07	1.0/37.3/12.4
241-BY-108	5.80 E+04	2.08 E+06	6.94 E+05	2.08 E+05	0.07	1.0/35.9/12.0
241-BY-109b	NE	DNA	DNA	NE	NE	DNA
241-BY-110	7.07 E+04	2.25 E+06	7.51 E+05	2.25 E+05	0.08	1.0/31.9/10.6
241-BY-111	5.50 E+03	1.40 E+05	4.67 E+04	1.40 E+04	0.09	1.0/25.5/8.5
241-BY-112	2.00 E+03	7.01 E+04	7.34 E+04	7.00 E+03	0.08	1.0/35.0/11.7
241-C-108	2.50 E+04	1.16 E+06	3.86 E+05	7.70 E+04	0.09	1.0/46.3/15.4
241-C-109	3.00 E+04	1.64 E+06	5.46 E+05	1.09 E+05	0.07	1.0/54.7/18.2
241-C-111	3.30 E+04	1.47 E+06	4.91 E+05	9.80 E+04	0.09	1.0/44.7/14.9
241-C-112	3.10 E+04	1.26 E+06	4.21 E+05	8.40 E+04	0.10	1.0/40.8/13.6
241-T-101	1	DNA	DNA	1	.01	DNA
241-T-107	5.00 E+03	6.16 E+05	2.05 E+05	2.12 E+05	0.01	1.0/112.0/37.3
241-TX-118a	NE	DNA	DNA	NE	NE	DNA
241-TY-101	2.29 E+04	4.06 E+05	1.35 E+05	1.51 E+05	0.04	1.0/17.7/5.9
241-TY-103	2.80 E+04	4.81 E+05	1.60 E+05	1.79 E+05	0.04	1.0/17.2/5.7
241-TY-104	1.20 E+04	2.02 E+05	6.72 E+04	7.50 E+04	0.04	1.00/16.8/5.6

[a]DNA: Does not apply. Tank did not receive significant amounts of scavenged solids during or after the scavenging campaign; therefore, this relationship has no meaning.

[b]Tank is not on the ferrocyanide watch list, but was investigated to determine if it should be added.

[c]Tank 241-T-101 was sluiced in 1956; after it received ferrocyanide solids, it was assumed emptied and thus no longer contains ferrocyanide.

NOTE: Nitrates/nitrites counted in this inventory are only those intimately mixed with the ferrocyanide in the interstitial liquid space. Nitrite amount assumed to be one-third nitrate amount. Values differ slightly from Borsheim and Simpson (1991) because of rounding.

NE = not evaluated--Records show tank did not receive ferrocyanide solids.

This page intentionally left blank.

Table 4-23. Ferrocyanide Tank Historical Data Summary.

Tank	Waste processing source	Ferrocyanide content 1,000 mol	^{137}Cs decayed to January 1991 (Ci)		^{90}Sr decayed to January 1991 (Ci)		Stabilization status			Solids volume/height kgal/ft			Supernate above solids	Liquid levels (ft)		Maximum temperature as of July 1991 (°F)
										Total	Ferrocyanide sludge					
		(1)	(2)	(1)	(2)	(1)	Interim Stab.	Salt well jet pumped (end date)	Contains LOW	(3)	(4)	(1)	(3)	DT/MT ZC/FIC	LOW n/γ	
241-BX-102	U Plant	<1	2.6 E+5	--	1.7 E+5	--	Yes	No	No	96/3.5	NM	0	No	2.5	--	64
241-BX-106	U Plant	<1	6.1 E+6	--	1.7 E+6	--	No	No	No	31/1.6	NM	0	Yes	1.0	--	64
241-BX-110	U Plant	<1	4.4 E+5	--	2.6 E+5	--	Yes	No	No	198/6.6	NM	0	Yes	5.6	--	66
241-BX-111	U Plant	<1	4.4 E+5	--	2.6 E+5	--	No	No	Yes	211/7.0	NM	0	Yes	6.6	7.5/7.4	67
241-BY-101	U Plant	<1	5.2 E+5	--	3.5 E+5	--	Yes	Yes (1/84)	Yes	387/12.3	NM	0	No	2.6	4.9/5.6	74
241-BY-103	U Plant	66	2.6 E+4	1.6 E+5	6.9 E+5	2.3 E+5	No	P	Yes	400/12.7	NM	212/7.0	No	10.0	11.9/11.3	88 (LOW)
241-BY-104	U Plant	83	5.2 E+5	2.0 E+5	2.6 E+5	3.0 E+5	Yes	Yes (11/84)	Yes	406/12.9	244/8.0	260/8.5	No	4.0	7.0/6.7	130
241-BY-105	U Plant	36	4.4 E+5	8.8 E+4	2.6 E+5	1.3 E+5	No	No	Yes	503/15.9	213/7.1	96/3.5	No	--	13.6/14.8	112
241-BY-106	U Plant	70	5.2 E+5	2.2 E+5	3.5 E+5	3.3 E+5	No	No	Yes	642/20.1	111/4.0	228/7.5	No	--	18.5/18.6	130
241-BY-107	U Plant	42	1.7 E+5	1.3 E-5	1.7 E+5	2.2 E+5	Yes	Yes (7/79)	Yes	266/8.7	172/5.8	158/5.4	No	--	5.1/5.6	80
241-BY-108	U Plant	58	2.6 E+5	2.1 E+5	5.2 E+4	2.6 E+5	Yes	Yes (12/84)	No	228/7.5	201/6.7	208/6.9	No	4.8	--	97
241-BY-110	U Plant	71	5.2 E+5	1.9 E+5	3.5 E+5	3.2 E+5	Yes	Yes (12/84)	Yes	398/12.7	211/7.0	225/7.4	No	5.0	6.2/5.9	120
241-BY-111	U Plant	6	5.2 E+5	1.1 E+4	3.5 E+5	1.9 E+4	Yes	Yes (11/84)	Yes	459/14.5	26/1.4	14/1.1	No	2.3	6.8/4.0	84 (LOW)
241-BY-112	U Plant	2	7.8 E+4	5.1 E+3	7.8 E+4	8.1 E+3	Yes	Yes (5/84)	Yes	291/9.4	NM	7/0.7	No	1.6	2.8/3.1	81 LOW)
241-C-108	In-Farm	25	4.0 E+0	6.5 E+4	2.6 E+4	5.9 E+2	Yes	No	No	66/2.6	79/3.0	77/3.0	No	1.6	--	75
241-C-109	In-Farm	30	5.2 E+3	1.1 E+5	7.0 E+1	3.6 E+3	Yes	No	No	62/2.5	90/3.3	109/3.9	Yes	1.6	--	77
241-C-111	In-Farm	33	4.3 E+3	1.4 E+4	8.6 E+4	8.1 E+2	Yes	No	No	57/2.3	95/3.5	98/3.6	No	1.3	--	80
241-C-112	In-Farm	31	3.5 E+3	1.3 E+5	4.3 E+4	1.3 E+3	Yes	No	No	104/3.8	46/2.0	84/3.2	No	--	--	80
241-T-101	U Plant	<1	2.6 E+4	--	1.7 E+3	--	No	No	No	103/3.7	NM	0	Yes	3.7	--	67
241-T-107	U Plant	5	0	7.8 E-3	3.5 E+4	1.8 E+4	No	No	No	171/5.8	201/6.7	212/7.0	Yes	5.1	--	68
241-TX-118	U/T	<1	9.0 E+5	--	1.0 E+6	--	Yes	Yes (2/83)	Yes	347/11.1	6/0.6	--	No	3.3	4.4/4.8	71
241-TY-101	T Plant	23	7.0 E+3	4.2 E+4	1.7 E+4	3.7 E+4	Yes	Yes (2/83)	No	118/4.2	183/6.2	151/5.2	No	1.4	--	68
241-TY-103	T Plant	28	1.7 E+5	5.2 E+4	8.7 E+4	4.5 E+4	Yes	Yes (12/82)	Yes	162/5.5	188/6.3	179/6.0	No	4.7	4.9/4.1	65 (LOW)
241-TY-104	T Plant	12	1.7 E+3	2.1 E+4	7.0 E+3	1.9 E+4	Yes	No	No	43/1.9	74/2.9	75/2.9	Yes	2.0	--	68

Sources: (1) Borsheim and Simpson (1991), (2) TRAC - Jungfleisch (1984), (3) Hanlon (1991), (4) Anderson (1990).
DT = Dip Tubes
LOW = TC in Liquid Observation Well
P = Partially
ZC = Zip cord
FIC = Food Inst. Corp. Auto Tape
MT = Manual Tape
NM = Not measured

THIS PAGE INTENTIONALLY
LEFT BLANK

of ferrocyanide solids precipitated varied by batch; the volume of ferrocyanide sludge was accepted to be a constant 4.25 vol% of the waste processed, and the batch ferrocyanide concentration varied from 0.0025 *M* to 0.0075 *M*. This calculated concentration includes the effect of sludge transfers and the total amount of interstitial liquid contained in the settled waste matrix. Because the neutralized feeds to the In-Farm scavenging process were settled in upstream tanks prior to scavenging, many of the alkaline insoluble salts (iron, aluminum, hydroxide, sulfate, and phosphate) may not be present in the ferrocyanide sludge deposited in C Farm tanks. Therefore, on a water-free basis, these sludges are likely to have much higher overall ferrocyanide concentrations.

The model results for bulk ferrocyanide inventory compare favorably with the recent TY Farm core sample results for total CN^- (Section 4.2.2). In addition, recent simulant analysis corroborates model values for ferrocyanide location and U Plant sludge settling properties (Sections 4.3.1 and 4.5.5). Gamma scans performed to determine the inventory of ^{137}Cs may also aid in determining ferrocyanide location, because ferrocyanide will be preferentially associated with ^{137}Cs. The scans show generally higher ^{137}Cs activity in the lower sludge layers of the tanks identified as ferrocyanide-settling tanks (Section 4.5.2).

4.10.2 Nitrate/Nitrite Concentrations

Because nitrate and nitrite salts are very water soluble, the bulk of the components in the ferrocyanide sludge matrix were there as dissolved salts in the interstitial liquid. Table 4-22 lists the calculated molar ratio of ferrocyanide to nitrate and nitrite ion. These results were calculated using a 71 vol% liquid fraction for the sludge and are considered representative of the waste matrix [based on moisture analysis from core samples of the salt-well pumped tank 241-TY-101 (Weiss 1986)]. The nitrate ion concentration was estimated from the data contained in the applicable scavenging flowsheets (T Plant, U Plant, or In-Farm). The primary source of nitrite is the radiolysis of nitrate; thus, a nitrite concentration of one-third the nitrate concentration was assumed from radiolytic degradation of nitrate. The nitrate concentration is conservative because the production of nitrite was not subtracted. According to all calculations, nitrate is likely to be present in vast excess of the stoichiometric ratios required for reaction with ferrocyanide in the U Plant sludges. In-Farm sludges, however, may lack the solid diluents associated with the U Plant material, rendering it much more concentrated. Further simulant analysis and core sample data are needed to determine the physical properties, chemical composition, and exothermic reaction properties of In-Farm process sludge.

4.10.3 Organic Carbon Content/Concentrations

The inventory of TOC is of interest concerning the ferrocyanide tanks for two reasons. The first reason is that organic complexants may significantly decrease the temperature necessary to initiate an oxidation reaction between the ferrocyanide and the nitrate. The second reason is that the organic constituents themselves present a safety concern because they can also serve as fuel in a reaction.

Organic complexants were used in large quantities in the fission product recovery operations conducted in B Plant. Citrates, EDTA, N-(hydroxyethyl)-ethylenediaminetriacetic acid (HEDTA), and hydroxyacetic acid sodium salts were introduced into the Hanford Site SSTs. All of these compounds contain acetate or modified acetate groups or fragments and could be expected to provide fuel values in deflagrations much as acetates do (Borsheim and Kirch 1991). Sucrose was used in the denitration operations at PUREX and is also expected to provide fuel in an organic/nitrate oxidation reaction. The potential for exothermic reactions resulting from nitrate oxidation of these soluble organics during waste processing and storage was recognized, and studies on waste stability were conducted before the chemicals were used (Phillips 1967).

All of the organic agents used in chemical processing at the Hanford Site are very water soluble, and organic carbon is detectable by standard analytical methods. The surface solids in the BY Farm tanks are salt cake; i.e., primarily sodium nitrate/nitrite. Sodium nitrate/nitrite is a strong oxidant that is also very water soluble. Because of their similar solubility properties, if the organic complexants are not found in the supernatant or mixed with the salt cake, they are not likely to be found in the tank (Farley and Grigsby 1991). However, because of conflicting indications from the available data, the status of TOC concerning the waste's fuel contribution and reactivity is not well known at this time.

Examinations of the estimated and available data for waste compositions in the Hanford Site SSTs indicate that, of 149 SSTs, 7 appear as likely candidates to contain solids and/or liquids capable of forming explosive mixtures of acetate-like substances with sodium nitrate/nitrite. These tanks are listed in Table 4-24 (Borsheim and Kirch 1991). Of these tanks, only one appears on the list of ferrocyanide tanks (241-TX-118), and its ferrocyanide inventory cannot be confirmed from other available records. Indeed, the records show that tank 241-TX-118 was never used as a process settling tank and likely only received supernates from other ferrocyanide tanks. The remaining available data, listed in Table 4-25, indicate that any organic materials in the ferrocyanide tanks make up a relatively small part of their inventory. However, there are 12 tanks for which no analytical sample data are available. The contribution of TOC to the fuel content of the ferrocyanide tanks can only be verified by core sample data.

Table 4-24. Tanks Containing Significant Amounts of Organic Salts.

Tank	Ferrocyanide (from TRAC) (mol)	Sodium acetate equivalent (wt%)	$NaNO_3$ and $NaNO_2$ (wt%)	Data source
241-B-103	200	11.2	60.5	Jungfleisch 1984
241-S-102	20	21.0	41.0	Schultz 1980
241-SX-106	600	14.6	80.9	Jungfleisch 1984
241-TX-105	0	12.8	52.7	Jungfleisch 1984
241-TX-118	3,000	20.2	50.4	Schultz 1980
241-U-106	0	46.6	52.4	Schultz 1980
241-U-107	0	14.7	75.4	Jungfleisch 1984

NOTE: Data table condensed from WHC-EP-0347 Rev. 0 (Borsheim and Kirch 1991).

Table 4-25. Organic Content of Ferrocyanide Tanks.

Tank	Liquid volume (kgal)	Solid volume (kgal)	Total waste volume (kgal)	Solid TOC concentration (g TOC/L)	Liquid TOC concentration (g TOC/L)	TOC inventory (kg)	Waste mass[a] (mg)	TOC (wt%[b])
241-BX-106	15	31	46	NA	4.4	249	279	0.1
241-BX-110	21	198	199	1.0	5.6	1,192	1,205	0.1
241-BX-111	19	211	230	NA	5.7	409	1,393	<0.1
241-BY-103	108	400	400	NA	3.8	1,551	2,422	<0.1
241-BY-105	194	503	503	NA	2.9	2,126	3,046	<0.1
241-BY-106	235	642	642	NA	3.2	2,842	3,888	<0.1
241-BY-107	25	266	266	NA	4.0	378	1,611	<0.1
241-T-101	35	103	133	NA	0.6	79	805	<0.1
241-T-107	22	171	180	NA	0.9	75	1,090	<0.1
241-TY-101	0	118	118	1.1	NA	490	715	<0.1
241-TY-103	5	162	162	2.5	1.9	1,567	981	0.16
241-TY-104	15	43	46	6.0	2.1	1,094	279	0.4

NOTE: Data table developed from WHC-EP-0182-40 (Hanlon 1991) and WHC-EP-0424 Rev. 0 (Klem 1991).

[a]Assumes an average density of 1.6 g/cm^3 for the waste matrices.

[b]Total organic carbon weight-percent calculations done on wet basis; therefore, they differ from Klem (1991) because those values were calculated on a dry basis.

NA = not available.

TOC = total organic carbon.

An inspection of the process history of the ferrocyanide tanks also indicates that the inventory of organics in the sludges of those tanks could be expected to be very small. For a reaction to take place, there must be sufficient fuel to support combustion. The only significant sources of fuel expected to be in the tanks are ferrocyanide compounds and organic complexants.

In the BY Tank Farm, degradation of the complexants from radiolysis and from the heat supplied from atmospheric pressure evaporation that occurred during the In-Tank solidification program could be expected to reduce the amount of organic compounds remaining in the tanks. In addition to radiolytic degradation, waste disposal records indicate that the C and TY tanks did not receive much waste that contained organics, either directly from the process source or in intertank transfers (Anderson 1990). Table 4-26 contrasts the organic inventory information contained in TRAC and the available information from laboratory analysis of waste samples. Because the BY ferrocyanide tanks all had similar process histories, the values stated in the table are considered representative of all the BY tanks. Also, because the ferrocyanide compounds are quite insoluble in water and predate the addition of the complexants by many years, and because no mechanism for mixing the waste existed in the tanks, ferrocyanide is not expected to be in intimate contact with the organic compounds.

Interstitial convective mixing of the waste driven by the temperature difference provided from the decay heat is not considered likely for three reasons. First, several years passed from the time of the ferrocyanide campaign before organic materials were introduced into the tanks. This allowed the sludge to almost completely settle. During the time between the scavenging program and the addition of organics, the tanks received other waste inputs that contributed to the solids inventories of most of the tanks (Anderson 1990). These additional solids would have formed a layer of solids above the ferrocyanide sludge and prevented any significant mixing, although localized mixing at the site of the waste input would have occurred.

Second, the physical properties of the waste material would have reduced the possibility of interstitial convective mixing by increasing the amount of time and energy necessary for mixing. The small-particle diameter provides long, tortuous paths for the liquid to flow through, increasing the necessary residence time of the waste containing organics. In addition, the hydrophilic nature of the waste matrix effectively bound much of the interstitial liquid, not allowing it to move, thus preventing any mixing of the organic complexants with the sludge.

Third, the residence times of many of the transfers containing organics were relatively short, especially transfers during the ITS-2 program (Anderson 1990). The short residence times of these supernates would also prevent any thorough mixing from occurring. Although waste transfer into the tanks could also provide a mechanism for mixing, this is considered to be a localized effect and not significant enough to disturb the entire waste matrix. In addition, waste additions generally contained diluent solids that would further dilute the ferrocyanide (or organics) in the waste, thus

Table 4-26. Comparison of Measured and Predicted Organic Content.

Tank	TRAC TOC wt%	Estimated TOC wt% from analytical data*
241-BX-106	1.4	0.1
241-BX-110	9.6	0.1
241-BX-111	4.2	<0.1
241-BY-103	<0.1	<0.1
241-BY-105	0.2	<0.1
241-BY-106	1.6	<0.1
241-BY-107	0.8	<0.1
241-T-101	2.0	<0.1
241-T-107	0	<0.1
241-TY-101	0	<0.1
241-TY-103	1.5	0.16
241-TY-104	0	0.4

Data condensed from WHC-EP-0424 Rev. 0 (Klem 1991).
*Calculated on a wet basis.
TOC = total organic carbon.

decreasing their exothermic reaction potential. Thus, based on a logical assessment of the available information, the organic complexants are not expected to be a significant component of the ferrocyanide sludge and should not contribute to their reactivity.

4.10.4 Water Content

Water has high heat capacity and high heat of vaporization when compared to many other possible materials in the sludge. Moisture in the sludge is an important heat sink, and Section 5.1.3 discusses the importance of the inert materials, including water, in absorbing heat from possible ferrocyanide reactions.

It is expected that water can be retained by the ferrocyanide sludge in several ways. It is convenient to discuss the following mechanisms:

- Chemical water--water of hydration
- Gel water

- Capillary water--held between the precipitated grains in the sludge and will not drain

- Free water--water that fills the interparticle voids when submerged but can drain by gravity.

4.10.4.1 Chemical Water. The major precipitated ferrocyanide solid in the sludge is $Na_2NiFe(CN)_6$. Other insoluble ferrocyanide compounds could be $K_2NiFe(CN)_6$, $Cs_2NiFe(CN)_6$, and $Ni_2Fe(CN)_6$. Each of these compounds will retain chemically bound waters of hydration at the tank conditions. Waters of hydration reported by Loos-Neskovic (Loos-Neskovic et al. 1984, Loos Neskovic and Fedoroff 1989) are given in Table 4-27.

Table 4-27. Water of Hydration on Ferrocyanide Compounds.

Nominal compound	Water hydration
$Na_2NiFe(CN)_6$	2.7*
$K_2NiFe(CN)_6$	3 H_2O
$Cs_2NiFe(CN)_6$	4.3 H_2O
$Ni_2Fe(CN)_6$	5 H_2O

*Loos-Neskovic and Fedoroff (1989).

Recent work by PNL with $Na_2NiFe(CN)_6$ using TGA techniques shows $Na_2NiFe(CN)_6$ (produced using process flowsheets) to lose water equal to 2 H_2O at 220 °C, 3 H_2O at 250 °C, and 4 H_2O at 280 °C (Johnson 1991). Thus, considering the most probable insoluble ferrocyanide compounds in the sludge, three waters of hydration seem reasonable. This is equivalent to 6.1 wt% water in a stoichiometric hydrated mix of ferrocyanide and nitrate or 14.6 wt% of the pure hydrated $Na_2NiFe(CN)_6 \cdot 3\ H_2O$.

4.10.4.2 Gel Water. The insoluble ferrocyanide that was formed to remove the cesium is a flocculent precipitate that slowly settles to form a layer with a volume much larger than expected considering the density of the expected solids. As an example, recent laboratory studies of material formed using the Sloat flowsheet (Sloat 1954) as described in Section 4.3.1 measured the settled volume after time equivalent to 30 gravity-yr. This stable, compacted sludge was 4.2 vol% of the starting solution volume (the volume of the dried solids would be 0.1% of the original solution volume) and contained 66.1 wt% water. The exact mechanism of the water retention was not determined from the tests, but the chemical water would be about 1/2 wt% of the total waste mass. A typical granular solid will have interstitial water equal to about 30 wt% of the total waste mass; thus, more than twice that much water has been retained in the compacted sludge.

Other compounds in addition to the ferrocyanide may contain water of hydration. Many of the scavenging runs included dissolved iron, which will precipitate at the high pH conditions in the sludge as $Fe_2O_3 \cdot H_2O$, goethite, or hydrous iron oxide. High water content in this flocculent gel material is possible, and some authorities suggest up to six waters; however, the actual number of waters of hydration is not clearly defined. The single water of hydration shown for $Fe_2O_3 \cdot H_2O$ above amounts to 10.1 wt%; 86% of this bound water is released below 250 °C (Naono 1981).

This simple experiment assumes time as being proportional to the applied relative centrifugal force and is thought to be conservative in that if the floc has low strength, the high centrifuge forces would compact the floc more than would normal gravity. Conversely, the viscous effects of water motion past the small floc particles are ignored, and this may be nonconservative. Also, the floc or gel may change with time, but many flocs are observed to become more rigid with time.

However, it is concluded that the ferrocyanide sludges do not readily compact, and the settled sludges can contain significant amounts of water even after long storage times. The high water content in the sludge is supported by the core sample data reported in Appendix A, Tables A2 through A9, and summarized in Table 4-28 where the average water content is 52 wt%.

4.10.4.3 Capillary Water. The interstitial liquid in a fine-particle sludge will be held in place against gravity forces by capillary forces. Important parameters that control this water retention are particle size, liquid density, surface tension, and the void volume in the sludge.

Data on the particle size of the waste tank sludges are given by Weiss (1986) and in Table 4-7 for mass median particle sizes. For retention of capillary water, the surface median particle size is needed (see equation 4-6). The surface median size will be smaller than the mass median size and can be calculated from the particle size data by assuming that the sizes are log-normal distributions. The results of those calculations are summarized in Table 4-29 and show the average sludge particle surface median diameter to be 14 μm.

Based on an average sludge particle diameter, the height of the saturated zone can be calculated using equation 4-6 given by Atherton (1974):

$$Z_d = 3.368 \frac{(1-e)\,\delta}{D_p\,\rho_\ell\,e^{3/2}} \qquad (4\text{-}6)$$

where

Z_d = height of undrainable liquid (ft)

δ = liquid surface tension (lb/ft)

ρ_ℓ = liquid density (lb/ft^3)

Table 4-28. Water Content of Sludge Samples.

Tank and sample number	Water (wt%)[a]	Bulk density (g/cm^3)	Water (vol%)[b]
241-BY-104[c]	28.3[d]	1.61	46
241-TY-101-51XC	43.5	1.64	71
241-TY-103-3	53[b]	1.74	92
241-TY-103-4	60[b]	1.67	100
241-TY-103-COMP	53[b]	1.50	80
241-TY-103-31XC	51.2	1.70	87
241-TY-103-32XC	52.5	1.70	89
241-TY-104-232S	50.7	1.85	94
241-TY-104-241S	59	1.77	104
241-TY-104-251S	62.7	1.66	104
241-TY-104-261S	55.5	1.48	82
Average ± 1σ	51.8 ± 9.4	1.67 ± 0.11	86 ± 17

[a]Based on weight loss, 20 to 400 °C.
[b]Calculated.
[c]Tank 241-BY-104 sample is probably salt cake and not ferrocyanide sludge, as stated in Section 4.2.1.
[d]Drying temperature not stated.
Data condensed from Weiss (1986) and Horton (1976).

Table 4-29. Sludge Particle Size Parameters.

Tank	Count mean dia. (μm)	Mass median dia. (μm)	Geo. std. dev. (σ_g)[a]	Surface median dia. (μm)[b]
241-A-104[c,d]	--	22	1.6	18
241-BY-104[d]	--	21	1.4	19
241-C-106[c,d]	--	15	1.8	11
241-TY-101[d]	8.2	12.5	1.5	11
241-TY-103[d]	12.2	30.1	1.8	21
241-TY-104[d]	8.3	12.2	1.5	10
241-TY-104[d]	7.7	28.2	2.0	17
241-TY-104[d]	8.1	11.4	1.4	10
241-TY-104[d]	8.2	11.6	1.4	10
241-TY-104[d]	8.1	29.7	2.0	18
Average ± Std. Dev.		19 ± 8		14 ± 4

[a]Geometric standard deviation calculated assuming log-normal size distribution; MMD = CMD $\exp(2.5\ \ln^2 \sigma_g)$.
[b]Surface median diameter calculated as (MMD)/$\exp(\ln^2 \sigma_g)$.
[c]Not ferrocyanide tanks.
[d]Weiss (1986).

e = particle bed void space (fraction)

D_p = particle characteristic dimension, diameter of sphere with equal surface-to-volume ratio (ft).

Assuming a 6 *M* sodium nitrate solution in the interstitial space for which ρ_l = 80.5 lb/ft^3 and δ = 0.0055 lb/ft (Atherton 1974), the hold-up height can be calculated for a range of bed porosity and particle sizes, as shown in Table 4-30. The capillary hold-up height shown represents the vertical distance over which liquid will be retained in the sludge against the force of gravity.

Table 4-30. Capillary Holdup in Porous Beds.

Particle size (μm)	Capillary hold-up height (ft) bed porosity*		
	e = 0.1	e = 0.3	e = 0.5
10	200	30	10
20	100	15	5
30	67	10	3.3

*This is connected porosity, which may be less than the total liquid content of the sludge.

These heights represent the zone that would be expected to be fully saturated and indicate the strong water retention by capillary effects. It is expected, therefore, that sludge beds will retain interstitial water to significant heights even if pumped. Ferrocyanide tank data of measured liquid level verses sludge heights can be compared by reviewing Table 4-23. In general, the data indicate tanks that have been salt-well jet pumped still have liquid levels (as measured by gamma and neutron scans) within 1 ft of the sludge height. Given the accuracy of both measurements, these results appear to be consistent with the belief that the sludges retain significant moisture due to capillary effects.

The question of what porosity to use for the ferrocyanide sludges must be considered. Metz (1976) reports the void volume of synthetic sludges (composition not specified) to be 0.08 cm^3/g or, assuming a density of ρ = 2 g/cm^3, 16 vol%. He reports other sludges to have 30 to 40 vol% interstitial liquids. Current Tank Farm practice is to assume 12.5% for the drainable liquid in sludges. Data obtained by pumping three sludges give porosity of 0%, 6%, and 9%. Considering the importance of capillary holdup in sludges, the actual porosity must be higher than the pumpable, or drainable, porosity. A bed of randomly packed uniform-size spheres will have a porosity of about 38%. The porosity of beds of mixed-size particles will generally be less, as the smaller grains can fit into the spaces between larger particles, but nonspherical particles can increase the porosity.

The 66 wt% water reported previously for a centrifuged U Plant flowsheet synthetic ferrocyanide sludge with a stated bulk density of 1.4 g/cm^3 leads to 92 vol% water. Additional data on water content and density in tank sludges are reported in Table 4-5 and Appendix A, Tables A3 through A9, and summarized in Table 4-28.

This calculation of the volume percent H_2O assumes the water is at a density of 1 g/cm^3. For the salt-saturated interstitial liquid, this water density of 1 g/cm^3 is too low (saturated salt solutions of $NaNO_3$ are typically 1.32 g/cm^3) (Weast 1976). As the samples were heated to 400 °C, bound water will also be removed; and for bound water, the effective density can be greater than 1 g/cm^3. In addition, all the samples include significant amounts of $NaNO_3$ and $NaNO_2$, which will start to decompose (slowly) at 380 °C and 320 °C, respectively, by loss of NO_x. Thus, the weight loss for these samples will not all be water, and both reported weight percent and volume percent calculated may be high. Tests at PNL (Hallen 1991) measured the weight loss of a nitrate/nitrite mixture upon heating to 500 °C to be 2.4%. As the tank sludge samples typically contained about 16% nitrates, the moisture will be overestimated by less than 1/2 wt%. The volume percent of water calculated in this manner in Table 4-28 leads to porosity values higher than the experimental values of 16% to 40% noted previously.

The porosity estimated by using the water content in this manner will be in error for the reasons given and will overestimate the porosity. This is because the total water will include gel water trapped in the flocculent precipitate. This water is not free to move. Considering the range of water content given above, a conservative estimate of the total porosity of the wet sludge (for evaluating capillary effects) would be approximately 50 vol%. Table 4-29 shows, for the measured particle sizes of less than 15 μm, the sludge will be undrainable for the sludge heights observed in any of the tanks. Larger particle sizes or higher porosity could lead to partial draining of upper zones.

Assuming that some of the reported sludge moisture may be high because of possible weight loss by decomposition of $NaNO_3$ and $NaNO_2$ in the samples, a conservative total sludge water content would be 40% by weight.

4.10.4.4 Free Water. The previous discussion concluded that for the probable sludge characteristics, the interstitial water would be held by capillary forces to considerable heights. For beds of a thickness less than that height, there is no free water that would drain from the bed. Water could be lost from the sludge by evaporation. Considering that such loss would be by diffusion through any overlaying salt cake to the air space in the tank, the rate of loss would be very slow. Also, the compounds in the crusts such as $NaNO_3$ and Na_2CO_3 will reduce the water vapor pressure, which would further retard any loss by evaporation. An estimation of these losses is given in Section 6.2.

4.10.4.5 Salt Cake. The previous discussion focused on water in the sludges. Water could be retained in the salt cake layers by similar mechanisms. The salt cake is mainly composed of sodium nitrate crystals in a saturated mother liquor. The salt cakes are often coarse material and will have lower capillary forces than the sludges. Present plant practice is to use 1 ft for the capillary hold-up height. The salt cakes also are more permeable than the

sludge, and interstitial liquid will drain relatively fast; thus, the upper zone above the liquid levels can be expected to have reduced water contents.

The salt cake zone above the liquid level, however, will retain a small fraction of the original liquid by capillary forces. Dombrowski and Brownell (1954) report a nearly constant residual capillary liquid content of 7.5% of the bed void volume for beds with a capillary number of less than 10^{-3}. The capillary number for a salt cake with saturated $NaNO_3$ solution having a permeability of 20 darcies (Metz 1976) and a 1-ft capillary rise is 3.4×10^{-6}; thus, the 7.5% liquid content can be estimated. Salt cake porosity values range from 30% to 35% (Metz 1976) to 40% to 48% determined by pumping (Kirk 1980).

The 35 vol% pumpable porosity value and the 7.5 vol% residual liquid volume give a total porosity of 37.8%, and therefore 2.8 vol% liquid will be held in the salt cake by capillary forces. If this liquid is a saturated $NaNO_3$ solution at 20 °C (ρ=1.38 g/cm^3, 47 wt% $NaNO_3$), the residual capillary water in the drained salt cake will be 2.0 vol%.

Additional water will be held in salt cake as water of hydration. Tank 241-SY-101 crust, which is thought to be similar to the ferrocyanide tank cake, has been analyzed and found to contain 7 to 19 wt% Na_2CO_3. The Na_2CO_3 forms several crystals that have water of hydration: $Na_2CO_3 \cdot 10\ H_2O$ (63% H_2O) and $Na_2CO_3 \cdot 7H_2O$ (54% H_2O) which are both stable in high humidity, below 32 °C, and $Na_2CO_3 \cdot H_2O$ (15 wt% H_2O), which is stable in relative humidity over 82% up to 100 °C. The other major salts in the cake, $NaNO_3$ 19 to 26 wt%, $NaNO_2$ 13 to 25 wt%, and $NaAlO_2$ 3 to 13 wt%, do not form hydrated crystals.

A salt cake containing 10 wt% Na_2CO_3 could have bound water content from 1.5 wt% at 100 °C to 6 wt% below 32 °C.

Thus, mechanisms exist that can cause water retention in the salt cakes even after removing the pumpable liquid.

Moisture content of tank 241-SY-101 crust samples has been measured as 10 wt% in the three samples from dry regions and 26% in a sample from a wet region. As these crusts are thought to be similar to the ferrocyanide tank crusts, the 10 wt% measured value is suggested as the lowest crust water content to be expected.

4.10.4.6 Water Measurement by Neutron Scans. Neutron scans of tanks containing LOWs are routinely used to assist in determining liquid levels in the tanks (see Section 4.4). Such scans have potential value in quantifying the amounts of moisture in the tank sludges and salt cakes. The neutron scans for tanks with LOWs are given in Appendix B, Figures B-1 through B-24. These figures show the detector response to scattered neutrons, which is related to the hydrogen content of the zone being traversed. Although the scans show the presence of water, they cannot be quantified until additional calculations and calibration of the system response have been completed.

4.10.4.7 Water Content Summary. The preceding discussion showed that water will be retained in sludges and salt cake by several mechanisms. The amount of water will depend on both the physical and chemical characteristics of the waste layers. Examination of available data from tank samples and laboratory

simulants shows that significant amounts of water, in most cases more than the predicted water content, can be expected. When applicable data are not available, based on the data previously discussed, conservative estimates of the water in the tank solids are given in Table 4-31.

Table 4-31. Lowest Suggested Water Content.

Waste type	Waste condition (wt%)	
	Saturated	Drained
Ferrocyanide sludge	40	40
Salt cake	20	10

4.10.5 Diluent Types and Concentrations

Diluents associated with the ferrocyanide sludge include liquid solution filling void spaces in the sludge, solids slurried with the scavenging solution feed, coprecipitating solids during scavenging, and solids introduced through mixing with other waste types. The concentrations of solid diluents depended on the feed type, flowsheet used, and mixing occurring after storage.

4.10.5.1 Feed Types. There were in general three scavenging feed types processed at the Hanford Site: (1) uranium recovery waste (U Plant), (2) tank farm supernatant (In-Farm), and (3) bismuth phosphate waste solution (T Plant). The concentrations of diluents in the sludges produced from these feed solutions, as determined from flowsheets along with available analytical results determined from waste sludge samples, are presented below in Tables 4-32 and 4-33.

Additional In-Farm flowsheet sludge for waste treated to 0.0075 *M* $Na_4Fe(Cn)_6$, 0.010 *M* $NiSO_4$, 0.03 *M* Na_2S, and no $Ca(NO_3)_2$ is being produced in the chemical engineering laboratory.

This synthetic In-Farm sludge is expected to have the least amount of diluents and has been produced in the chemical engineering laboratory for characterization and reactivity testing. The settled sludge will be evaluated to identify any ferrocyanide concentration as a result of layer settling. The sulfide may also provide an additional source of fuel. Although the sulfide's contribution to the available fuel in the waste is small compared to the ferrocyanide, further studies of In-Farm sludge simulants are being done to evaluate the effect, if any, of sulfide on the reaction properties in the waste materials.

4.10.5.2 Expected Reactivity of Various Sludges. Initial results of flowsheet evaluations and tank sample analyses of composited ferrocyanide sludge indicate that the ferrocyanide is at concentrations that cannot propagate and that the diluents are great enough to prevent a propagation

Table 4-32. Synthetic U Plant Flowsheet Sludge.

Diluents	Flowsheet (wt frac)[a]
Disodium mononickel $Fe(CN)_6$	0.078
Iron hydroxide	--
Sodium sulfate	0.018
Strontium phosphate	0.025
Sodium nitrate	0.25
Water	0.50[b]
Total	0.871

NOTE: U Plant for 0.0025 *M* $Fe(CN)_6^{-4}$ and 0.004 *M* $Sr(NO_3)_2$.

[a]Analytical content of most concentrated layer of synthetic centrifuged U Plant sludge.

[b]Water content conservatively estimated based on composite analysis value (0.565 weight fraction) of all layers. Iron hydroxide analysis is not completed yet, but it is expected to make up most of the difference in mass between the 0.87 and 1.00 weight fraction.

Table 4-33. T Plant Sludge Analysis.

Diluents	Tank samples* (wt frac)
Mononickel $Fe(CN)_6$	0.0060
Bismuth	0.024
Iron	0.022
Sulfates	0.008
Nitrate	0.135
Nitrite	0.007
Carbonate	0.005
Uranium	0.016
Silicon	0.002
Sodium	0.115
Phosphate (assumed P all PO_4)	0.089
Water	0.512
Total	0.942

*Analysis of tanks 241-TY-101 and -103 (Winters 1988) (min diluents, max cyanide; note that total max organic was 0.002).

reaction for the sludge produced by scavenging the U Plant and T Plant wastes. Further evaluations should be made on the more concentrated layers of synthetic flowsheet material produced to support this conclusion. In-Farm flowsheet material and C Farm samples should be characterized to identify the ferrocyanide and diluent concentrations present in the In-Farm produced sludge. The lack of solid diluents in the In-Farm material indicates that the ferrocyanide solids in C Farm may be reactive. Sludge samples should be obtained from the BY and C Farm tanks to verify the ferrocyanide and diluent concentrations.

4.10.6 Decay Heat Load and Its Distribution

The rate of heat generation from radioactive decay in each tank and its distribution within the tank are required as input to calculations of tank temperatures and dry-out rates. Decay heat generation is predominantly from ^{137}Cs and ^{90}Sr and their daughters, because the wastes are well aged. The total heat generation in each tank will be discussed first, then its distribution.

The total decay heat loads in each tank may be calculated from the inventories of ^{137}Cs and ^{90}Sr. Such calculations are summarized in Table 4-34 for each of the following three data sources:

- Inventories from TRAC records
- Inventories from the Borsheim-Simpson (Borsheim and Simpson 1991) model (Section 4.1.5). These values do not account for nuclides added or removed after 1958 and may be low
- Inventories estimated from ^{137}Cs gamma scans (Section 4.5.2) and Borsheim-Simpson values for ^{90}Sr. These values are available only for the tanks in which gamma scans can be made.

Table 4-34 also includes the "published" heat loads (Hanlon 1991). These estimates were calculated from the measured tank temperatures and from the rate of moisture loss from those tanks with active exhausters at that time. These values may be high in that they have not been corrected for recent decay or removal of liquid. Table 4-34 also lists the maximum temperature measured in each tank and the total depth of solids, which are relevant to the estimation of its heat load.

Two more detailed analyses have been made recently to provide a better estimate of the heat load in tank 241-BY-104. In the first analysis, the "published" heat load (Hanlon 1991) was reduced from 17,000 Btu/h (5.0 kW) to approximately 10,500 Btu/h (3.1 kW) by correcting for liquid removal and decay to 1990. Utilizing the 1976 core sample results for tank 241-BY-104 (Horton 1976) and estimated solids volumes (Anderson 1990 for sludge or Hanlon 1991 for total solids) results in a range of 7,300 Btu/h (2.1 kW) to 12,200 Btu/h (3.6 kW) in the solids in 1990. A thermal analysis by McLaren (1991) based on measured temperatures and an estimate of tank breathing yielded a head load of 8,000 Btu/h (2.3 kW) (see Section 4.9.2). Similar detailed calculations have not been made yet for other tanks.

Table 4-34. Estimated Decay Heat Generation in Ferrocyanide Tanks.

Tank[e]	Heat generation rate (kW)				Maximum temperature (°C)[c]	Depth of solids (m)[c]
	TRAC[a]	Borsheim Simpson[a]	Gamma scans[b]	Hanlon[f]		
241-BY-103	4.7	2.3	2.2	2.5	31	3.9
241-BY-104[d]	4.1	2.9	3.0	5.0	54	3.9
241-BY-105	3.8	1.3	1.8	11.0	44	4.8
241-BY-106	4.7	3.2	4.4	3.6	54	6.1
241-BY-107	1.9	2.1	2.3	4.2	27	2.7
241-BY-108	1.6	2.7	N/A	6.7	36	2.3
241-BY-110	4.7	2.9	3.3	7.4	49	3.9
241-BY-111	4.7	0.2	0.6	10.0	29	4.4
241-BY-112	0.9	0.1	0.4	<3	27	2.9
241-C-108	0.2	0.3	N/A	<3	24	0.8
241-C-109	0.02	0.6	N/A	<3	25	0.8
241-C-111	0.6	0.1	N/A	<3	27	0.7
241-C-112	0.3	0.6	N/A	<3	27	1.2
241-T-101	0.1	--	N/A	<3	19	1.1
241-T-107	0.2	0.1	N/A	<3	20	1.8
241-TX-118	11	--	N/A	1.4	22	3.4
241-TY-101	0.1	0.4	N/A	<3	20	1.3
241-TY-103	1.4	0.6	0.5	<3	18	1.7
241-TY-104	0.1	0.2	N/A	<3	20	0.6

N/A = not available (no gamma scans).

[a]Calculated from data of Table 4-22. Decayed to January 1991. 0.00478 W/Ci for ^{137}Cs, 0.00671 W/Ci for ^{90}Sr.

[b]From Table 4-17.

[c]From Table 4-23.

[d]Heat load of tank 241-BY-104 calculated as 2.3 kW by thermal analysis and as 2.1 to 3.6 kW by reanalysis of historical data.

[e]Tanks 241-BX-102, -106, -110, -111, and 241-BY-101 are not presented here because investigation of the historical records indicates that these tanks never received ferrocyanide solids.

[f]From Hanlon (1991).

The distribution of the decay heat generation within each tank will be the distribution of the radionuclides that produce it. The distribution of ^{137}Cs in the vertical direction is given by the spectral gamma scans, as described in Section 4.5.2. These generally show only modest non-uniformities. The ratio of peak-to-average concentrations in the region of the ferrocyanide sludge are 1.2 to 3.1 (see Table 4-18). A considerable amount of ^{90}Sr is also expected to reside in the ferrocyanide sludge because it was associated with the scavenged wastes and was precipitated with the cesium ferrocyanide. The spectral gamma scans show ^{154}Eu to be concentrated more strongly at the bottom of the tank than ^{137}Cs; similar concentration of ^{90}Sr would be possible because the batch concentrations of ^{90}Sr were not reported initially and may have been much higher than in later batches.

The gamma scan data of Table 4-17 are probably representative of other tanks for which such scans cannot be made, at least for those using the U Plant flowsheet. As the ^{137}Cs and ^{90}Sr were precipitated during the ferroycanide scavenging operation, they are likely to be spread throughout the sludge. It is therefore unlikely that the decay heat load is all concentrated in a thin layer at the bottom of the tanks containing U Plant sludge.

The distribution of heat generation in the horizontal direction is also of interest. No direct measurements of the heat generation distribution are available. However, there are no mechanisms that could produce significant lateral concentration of the heat-generating species because any disturbances from waste inputs would be localized and because additional solids added to the tank probably would be uniformly distributed in the incoming slurry. These suspended solids would settle uniformly from the slurry. Therefore, it is reasonable to assume that significant lateral concentration does not exist.

The correlation between heat generation rate and tank temperature is not good. However, the ambient temperature in the tank is affected by several variables such as the thermal conductivities of the various waste matrices, the heat transfer area of the sludge, and the ventilation characteristics of the tank, which are not well known at this time. Further simulant and core sample analyses and thermal modeling studies are needed to better define these variables and their effect on ambient tank temperatures.

More accurate values of the decay heat load and distribution will be obtained by core samples. The above estimates should be considered as tentative until core sample data are available.

4.10.7 Reaction Initiation and Ignition Temperature

4.10.7.1 Ferrocyanide Sludge Reaction Initiation Temperature. Currently available thermal analysis data of synthetic ferrocyanide-nitrate/nitrite U Plant flowsheet mixtures indicate that no significant exothermic chemical activity occurs until approximately 200 °C.

4.10.7.2 Ignition Temperature. The ignition temperature is used to define the minimum temperature at which a ferrocyanide/oxidant mixture flashes or reacts vigorously. This is taken as the temperature at which there is a significant increase in reaction rates. The reaction changes from an Arrhenius-type reaction to a propagating reaction, potentially heading to a

thermal runaway condition. It should not be considered a material property because the value is dependent on the testing device or method. The results presented here are from three different procedures and are shown in Table 4-35.

Table 4-35. Ignition Temperature $Cs_2NiFe(CN)_6$ Stoichiometric Mix.

Testing method	Laboratory	Temperature (°C)
Adiabatic calorimeter	Fauske & Associates, Inc.	275-280
Henkin test	Los Alamos National Laboratory	367
Modified Henkin test	Pacific Northwest Laboratory	330-335

The reference material is a stoichiometric mix of cesium nickel ferrocyanide and oxidant with the oxidant being a 50%-50% molar mix of sodium nitrate and sodium nitrite. It is possible to obtain temperature values 50 to 60 °C lower when large quantities (greater than 5 wt%) of additives such as HEDTA or various activators are included. Results should be available for materials more representative of those in the tank by the conclusion of the testing program. For the present work, the accepted ignition temperature is 275 °C.

4.10.8 Waste Thermal Properties (Thermal Conductivity, Heat Capacity, Density)

Some knowledge of the thermal properties of the waste tank contents is needed to estimate the heat transfer characteristics of the system. Thermal conductivity values for both the ferrocyanide sludge and the salt cake are used for studying the steady-state temperature distributions expected from postulated "hot spots." For transient analysis of heating or cooling of the tank contents with respect to potential thermal runaway, the thermal diffusivity of the materials is the crucial parameter. Thermal diffusivity is a measure of the speed at which heat propagates through a material and is related to other material properties by the relation:

$$\alpha = \frac{k}{\rho c_p} \tag{4-7}$$

where

α = thermal diffusivity (m^2/s)
k = thermal conductivity ($J/m \cdot s \cdot °C$)
ρ = density (kg/m^3)
c_p = specific heat ($J/kg\ °C$).

4.10.8.1 Measurements from Core Samples. Data from physical measurements of the thermal properties of the ferrocyanide sludges and salt cakes are scant. Reports of analysis of core samples of sludge from tank 241-BY-104 and from three TY Farm tanks are included in Section 4.2. These include density values for the sludges. The range of measured bulk densities for the TY tanks is 1,480 to 1,850 kg/m^3. The value for the tank 241-BY-104 waste is reported to be 2,090 kg/m^3, which may have been from the salt cake layer in this tank.

A density range for dry sludge was calculated using the density and water content values for the core samples. The following equation was used:

$$\rho_{wet} = x \times 1000 \frac{kg}{m^3} + (1 - x) \times \rho_{dry} \qquad (4\text{-}8)$$

where

x = weight fraction water in sample
ρ_{dry} = calculated dry density
ρ_{wet} = measured density of wet sludge.

Core sample	Weight fraction water	Wet density (kg/m^3)	Dry density calculated (kg/m^3)
241-TY-101	0.435	1,640	2,130
241-TY-103	0.488	1,700	2,370
241-TY-104	0.555	1,480	1,860

Weiss (1986).

Some thermal conductivity measurements on samples from tanks in the S, SX, and U Farms were reported by Bouse (1975). None of these tanks is a ferrocyanide tank. However, the lowest value measured at tank temperatures for those wet sludges might be considered a lower-bound estimate for the ferrocyanide sludges until better data become available. This value was 0.43 W/m °C (0.25 Btu/h ft °F).

4.10.8.2 Conductivity Values from Thermal Modeling. McLaren (1991) derived estimates for the thermal conductivities of the ferrocyanide sludge layer and the salt cake in tank 241-BY-104 by fitting a thermal model of the tank and its surroundings to the measured temperature profile in the tank. The method of analysis is discussed in Section 4.9.2.1. The conductivity estimates given are 0.28 W/m °C (0.16 Btu/h ft °F) for the salt cake and 0.47 W/m °C (0.27 Btu/h ft °F) for the sludge. In addition, a value for the interface layer between the sludge and the salt cake is given as 0.36 W/m °C (0.21 Btu/h ft °F).

4.10.8.3 Specific Heat. Specific heats for solids may be approximated by using Kopp's Law (Marks 1951). It states that the specific heat of a solid

compound at room temperature is equal to the sum of the specific heats of the atoms forming the compound. Specific heats for the salt cake and ferrocyanide sludge were estimated using this method. Values for the specific heats of the elements were taken from Weast (1976).

For purposes of this calculation, it was assumed that the ferrocyanide sludge consisted of $Na_2NiFe(CN)_6 \cdot 2.7H_2O$ with 65% by weight of gel and capillary water (see Section 4.10.3). The specific heat of the ferrocyanide salt is calculated as follows:

Element	Specific heat (cal/g mol/°C)	Atomic mass (g/g mol)
2 Na	2 x 6.7 = 13.4	2 x 23 = 46
Ni	6.2	59
Fe	5.9	56
6 C	6 x 2.0 = 12.0	6 x 12 = 72
6 N	6 x 3.5 = 21.0	6 x 14 = 84
5.4 H	5.4 x 3.5 = 18.9	5.4 x 1 = 5.4
2.7 O	2.7 x 3.5 = 9.4	2.7 x 16 = 43.2
Totals	86.8	365.6

$$c_{(Na_2NiFe(CN)_6 \cdot 2.7H_2O)} = \frac{86.8 \frac{cal}{g\ mol \cdot {}^\circ C}}{365.6 \frac{g}{g\ mol}} = 0.24 \frac{cal}{g\ {}^\circ C}. \qquad (4\text{-}9)$$

For the wet material:

$$c_{(sludge)} = .35 \times .24 \frac{cal}{g \cdot {}^\circ C} + .65 \times 1.0 \frac{cal}{g \cdot {}^\circ C} = 0.73 \frac{cal}{g \cdot {}^\circ C}. \qquad (4\text{-}10)$$

Similarly calculated, the specific heat of the salt cake is taken to be that of dry sodium nitrate, 0.24 cal/g·°C.

4.10.8.4 Thermal Diffusivity. Substituting values for thermal conductivity, density, and specific heat into equation 4-10, the thermal diffusivities of the salt cake and sludge can be derived. Table 4-36 summarizes all the values.

Table 4-36. Thermal Diffusivity.

	Density (kg/m^3)	Thermal conductivity ($W/m \cdot °C$)	Specific heat ($J/kg \cdot °C$)	Thermal diffusivity (m^2/s)
Salt cake	2,000 ($NaNO_3$ dry crystal)	0.28[a]	1,000 (Calculated)	1.3×10^{-7}
Dry sludge	1,860 - 2,370 (core samples)	0.17[a]	1,000 (Calculated)	7.2×10^{-8} to 9.1×10^{-8}
Wet sludge	1,480 - 2,090 (core samples)	0.47[a] 0.43[b]	3,000 (Calculated)	6.8×10^{-8} to 1.0×10^{-7}

[a]From McLaren (1991).
[b]From Bouse (1975).

Fauske (Section 5.2.1.2) assumed a thermal diffusivity value of 1.5×10^{-7} m^2/s for estimating the characteristic cooling time of the tank contents. This value is consistent with those calculated above.

5.0 POTENTIAL FOR ENERGETIC FERROCYANIDE REACTIONS

5.1 EVALUATION OF REACTIVITY

Section 3.3 identified the potential of tank contents to support propagating energetic reactions as one of the hazards to be considered. In this section chemical thermodynamics are used to assess the reactivity of various combinations of fuel/oxidant mixture, water, and other inert substances. The expected compositions of ferrocyanide sludges are then examined to determine whether they fall within the range of concern.

5.1.1 Basis of Calculation

If the composition of the material in the waste tanks includes a sufficient quantity of water, excess $NaNO_3$, or other diluents, the material cannot sustain an exothermic reaction. The propagation of a reaction requires that a gram of fresh fuel be heated to the ignition temperature for each gram of fuel consumed. If the total heat capacity is too great to reach the ignition temperature, propagation cannot occur. Therefore, it is possible by thermodynamic calculation to define compositions for which a sustained chemical reaction is impossible. Such a composition will be referred to as "noncombustible."

This assessment addresses the possibility of a reaction that propagates fast enough to do significant damage and to generate radioactive aerosols and exceed the capacity of the vent filtration. "Propagation" or "combustible" as used here is defined as referring to such a reaction, not to slow reactions possible at lower temperature.

5.1.2 Assumptions

The contents of the tank are considered for the sake of simplification as consisting of the following three components.

1. A stoichiometric mixture of ferrocyanide and oxidant taken as:

$$Na_2NiFe(CN)_6 + 6\ NaNO_3.$$

   It is assumed that there is sufficient $NaNO_3$ to react with all ferrocyanide present, because excess $NaNO_3$ is present in the waste tanks. $NaNO_2$ is also present as a possible oxidant but in lower concentrations than $NaNO_3$ (see Table 4-4).

2. Inert materials, taken as excess $NaNO_3$. The $NaNO_3$ is the most abundant material present in the waste tanks. Other diluents may be considered as represented by an amount of $NaNO_3$ having the same product of heat capacity and mass.

3. Water, including water of hydration as well as interstitial water.

The following two modes of ferrocyanide burning are considered:

1. A confined burn in which the combustion products are contained at high pressure within a cavity surrounded by the tank contents. This mode is characteristic of a rapid reaction and of the initial stages of a slower burn before the reaction cavity has expanded enough to vent the reaction gases and reduce the pressure. The ignition of a small quantity of fuel (e.g., from a local hot spot or externally applied heat source) will generate very high pressures as gas is generated from solids in a confined region. These high pressures will persist until the volume available is greatly increased by expansion against the inertia of the overburden. This mode is treated as a constant volume process at constant internal energy. A high final pressure is assumed (1,000 atm) typical of a constant volume reaction. Under these conditions water is not vaporized.

2. A vented burn at atmospheric pressure. This mode is characteristic of a slower reaction after the combustion products have vented to the tank head space or to the atmosphere. The vented burn also applies to possible ignition mechanisms at the surface of the tank contents. This mode is treated as a constant pressure process at constant enthalpy. The water is vaporized and its heat of vaporization must be supplied.

Calculating the range of composition for which sustained combustion is not possible requires the input of the following four parameters:

- Energy released by the chemical reaction
- Initial temperature
- Temperature to which material must be heated to ignite
- Heat capacity of reactive and inert materials.

The available data on the heat release by a ferrocyanide reaction are discussed in Section 4.7.1. A value of 3,025 kJ/mol of ferrocyanide was selected as a reference value for these calculations. This value corresponds approximately to the complete reaction going to the carbonate using the most abundant oxidant ($NaNO_3$). This value is conservative in that an incomplete reaction, which is characteristic of explosions, would release less energy. Other values are included in a parametric analysis. The heat capacities of the reactants and products are nearly equal. Therefore, the above heat of reaction may be applied at any temperature in the range of interest with only minor error.

A reference initial temperature of 55 °C was assumed, which is the maximum temperature measured in any ferrocyanide tank. Other temperatures were included in a parametric analysis. The lowest temperature of interest is about 25 °C, which is about the surface temperature in tank 241-BY-104. This temperature is applicable to possible reactions on the top surface of the salt cake. Temperatures higher than 55 °C might be expected in local hot spots. A temperature of approximately 130 °C is the boiling point of a saturated solution of $NaNO_3$ at the pressure existing at the bottom of tank 241-BY-104 and is thus the highest temperature at which unbound water could be present. Higher local temperatures, as high as the ignition temperature, could exist if sufficiently high local heating were postulated. Therefore, dry material is

also considered at initial temperatures between 130 and 275 °C. However, mechanisms to produce such elevated temperatures in the waste tanks are considered highly unlikely, as discussed in Section 5.2.

The temperature to which the fuel must be heated to cause combustion may be estimated from adiabatic calorimeter measurements of synthetic material (see Section 4.7.2). Although these measurements showed measurable exothermic reaction at temperatures as low as 200 °C, these rates were very slow. The Arrhenius-type reaction changes to a propagation reaction at 275 to 280 °C, where the self-heating rate abruptly increases with temperature from approximately 10 °C/min to rates orders-of-magnitude greater (see Section 4.10.7 and Figures 4-27 and 4-30). Therefore, for anything more than a very slow smoldering reaction, the fresh fuel must be heated to at least 275 °C, and this temperature is used as the ignition temperature in these calculations.

There is some evidence for higher ignition temperatures. The minimum explosion temperature from the modified Henkin test is approximately 330 °C (see Section 4.10.7). The ignition temperatures measured to date have been for stoichiometric or near-stoichiometric mixtures. The ignition temperature may be higher for highly diluted compositions. On the other hand, it is possible that some materials present in the tank, such as EDTA, may reduce the ignition temperature, because they have been found to reduce the minimum reaction temperature in a modified Henkin test (Scheele et al. 1991).

The following heat capacities were used. The heat capacity of solid $NaNO_3$ is (Perry and Chilton 1973):

$$C_p = 4.56 + 0.0580T \qquad (5\text{-}1)$$

where C_p is heat capacity (cal/mol °C) and T is temperature (K).

The heat capacity of $Na_2NiFe(CN)_6$ was estimated by Kopp's rule as 73 cal/mol °C. The enthalpy and specific volume of water were taken from the American Society of Mechanical Engineers Steam Tables (ASME 1976), and the internal energy was calculated from them.

The differences in the enthalpy and internal energy between the initial and ignition temperatures are listed in Table 5-1.

The melting point of $NaNO_3$ (307 °C) is above the range of ignition temperatures considered here. However, the mixture of $NaNO_3$ and other salts present in the waste tanks will melt at a lower temperature, probably below the probable ignition temperature of 275 °C. Fusion of the oxidant may be required for good contact with the ferrocyanide to give a vigorous reaction. Such fusion would be an additional heat sink for which credit is not taken in this analysis.

Table 5-1. Differences in Internal Energy and Enthalpy.

Temperature (°C)		FeCN and oxidant (J/g)	$NaNO_3$ (J/g)	Water (J/g)	
Initial	Ignition	$\Delta U = \Delta H$	$\Delta U = \Delta H$	Confined ΔU	Vented ΔH
55	200	176	199	566	2,645
55	225	210	239	666	2,694
55	250	245	281	769	2,744
55	275	281	325	872	2,794
55	300	318	371	977	2,845
25	275	313	359	1,000	2,922
85	275	248	289	746	2,668
130	275	195	230	556	2,478

The division between noncombustible and possibly combustible compositions occurs when the heat of reaction is just equal to the heat absorbed by the fuel, oxidant, excess $NaNO_3$, and water. Thus, for the vented burn

$$X_F(-\Delta H_R) = X_F \Delta H_F + X_i \Delta H_i + X_W \Delta H_W \qquad (5\text{-}2)$$

where

$-\Delta H_R$ = heat released by reaction
ΔH_F = enthalpy rise for fuel plus oxidant (J/g; see Table 5-1)
ΔH_i = enthalpy rise for inerts (J/g; see Table 5-1)
ΔH_W = enthalpy rise for water (J/g; see Table 5-1)
X_F = mass fraction of fuel plus stoichiometric oxidant
X_i = mass fraction of inerts
X_W = mass fraction of water.

For the confined burn, ΔH is replaced by ΔU, the change of internal energy.

5.1.3 Results of Calculations

The combustion limits calculated as described above are presented in this section. Their application to the ferrocyanide tanks is discussed in Section 5.1.4.

The combustion limits are plotted in Figure 5-1 for the reference values of the heat of reaction, initial temperature, and ignition temperature, as discussed above. The limits for a confined burn (solid line) and a vented burn (broken line) are shown separately. The composition is expressed as

Figure 5-1. Combustibility Limits of Ferrocyanide Mixtures Reference Case.

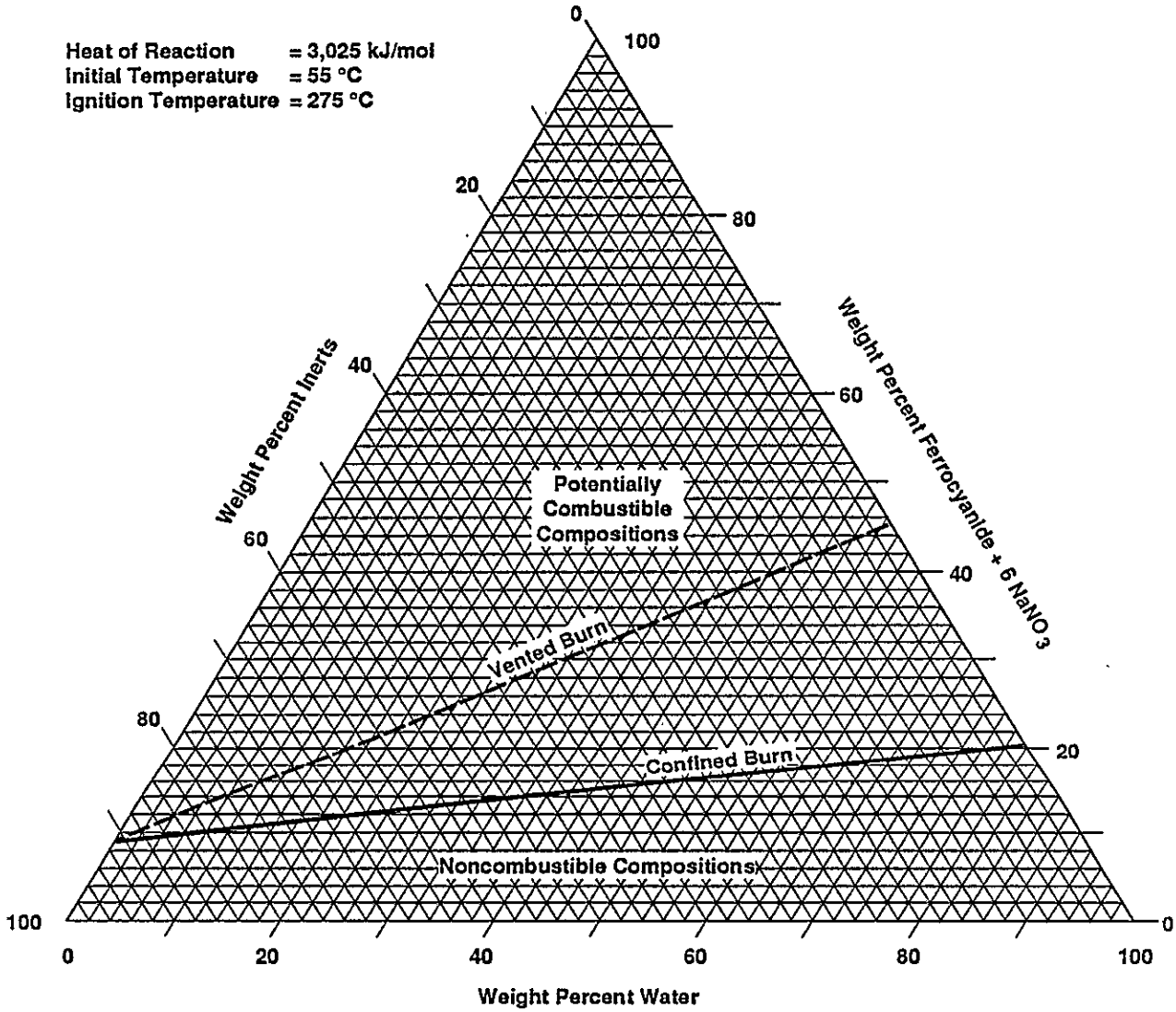

H9111028.17b

weight percent of water, of fuel plus stoichiometric oxidant ($Na_2NiFe(CN)_6$ + $6NaNO_3$), and of inerts. Because the sum of these three values must equal 100%, there are only two independent parameters, and all compositions may be represented in two dimensions on a triangular diagram. The region below the curve represents compositions that are too dilute in fuel to be able to support sustained combustion. For regions above the curve, combustion is energetically possible. For the confined burn (constant volume, no vaporization of water), the limiting concentration of fuel plus oxidant increases from 9% with no water present (91% inerts) to 20% with no inerts present (80% water). The range is greater for the vented burn (atmospheric pressure) because of the heat absorbed in vaporizing the water; the region extends up to 45% of fuel plus oxidant at high water content.

Figures 5-2 through 5-4 show the sensitivity of the combustion limits to the assumed values of initial temperatures, ignition temperature, and heat of reaction. Initial temperatures of 25, 55, and 130 °C are compared in Figure 5-2. There is only moderate sensitivity to the initial temperature. The noncombustible concentrations of ferrocyanide vary by a factor of approximately 1.6 over the range of initial temperature of 25 to 130 °C for a confined burn, less for a vented burn.

Figure 5-3 compares the effect of ignition temperatures of 200 and 275 °C. There is also only moderate sensitivity to the ignition temperature. The resulting variation in the noncombustible concentration of ferrocyanide is within a factor of approximately 1.5 for a confined burn but much less than this for a vented burn. Note that the noncombustible range of ferrocyanide concentration increases for increased ignition temperatures and for decreased initial temperature, because both of these require more heat to be added to fresh fuel. Note also for the vented burn with high moisture content that the heat required is dominated by the heat of vaporization of water and is therefore not strongly dependent on the initial and final temperatures.

The effect of the heat of reaction is shown in Figure 5-4. Curves are shown for 60%, 80%, 100%, and 120% of the reference value of 3,025 kJ/mol. The heat of reaction has a greater effect on the combustion limits than the initial or the ignition temperature. The reactivity limits would be increased significantly by using the heat of reaction measured by PNL (2,150 and 2,470 kJ/mol) or by LANL (1,180 and 1,330 kJ/mol) (see Section 4.7.1). However, the products and the extent of the chemical reaction may depend on the conditions of the test, and therefore test data are not necessarily applicable to a reaction in a waste tank. Additional measurements of the heat of reaction or of the reaction products would be desirable to justify using a lower heat of reaction.

The combustibility limits of hot, dry material may also be of interest. If some location in the tank could somehow become heated to the ignition temperature by a combination of radioactive decay and slow chemical reaction, the ignition point would be surrounded by a dry region ranging in temperature from the boiling point (about 130 °C for a saturated $NaNO_3$ solution) to the ignition temperature (assumed to be 275 °C). The combustion limits for dry material in this temperature range are shown in Figure 5-5. The maximum

Figure 5-2. Combustibility Limits of Ferrocyanide Mixtures Effect of Initial Temperature.

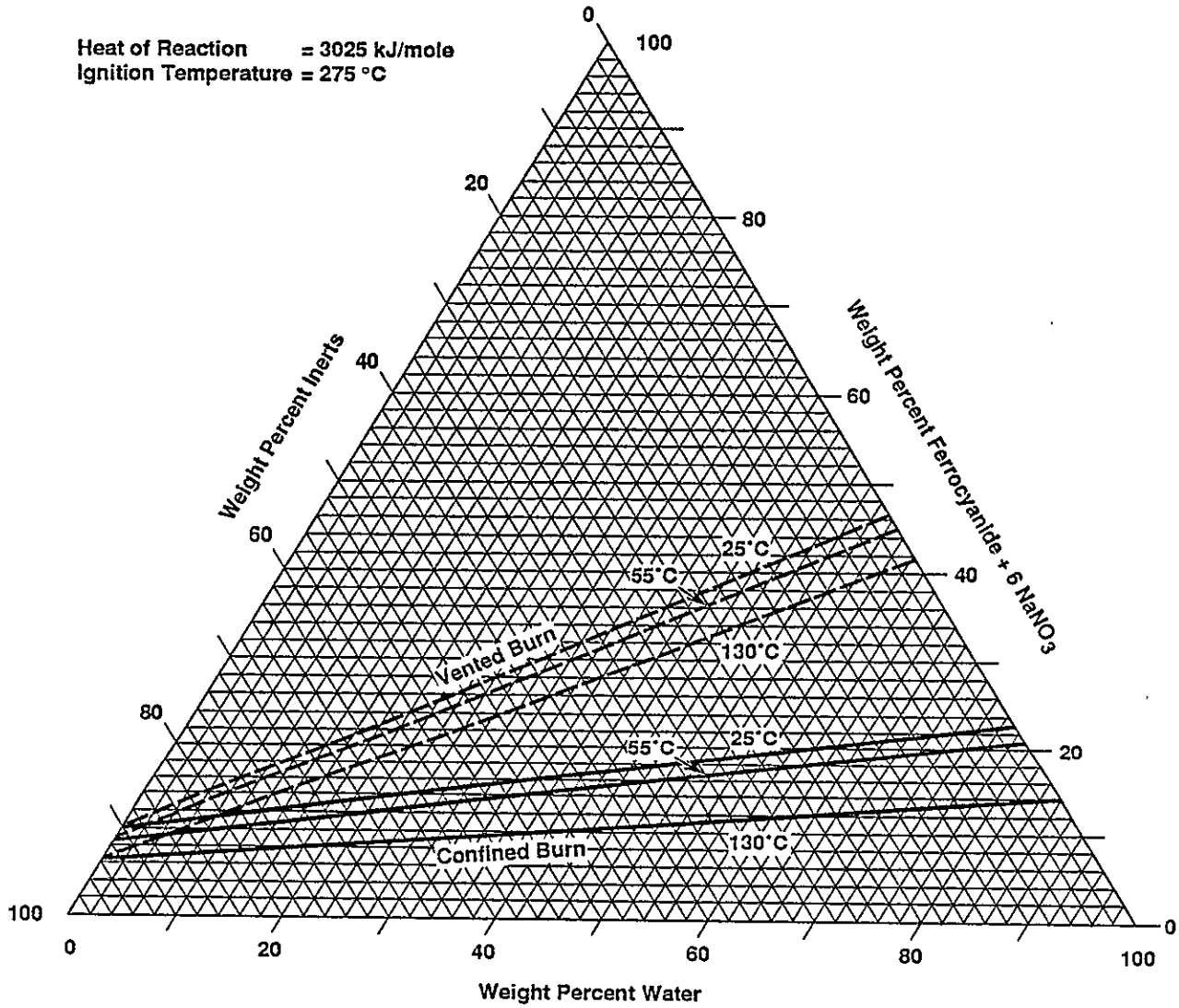

H9111028.17c

Figure 5-3. Combustibility Limits of Ferrocyanide Mixtures Effect of Ignition Temperature.

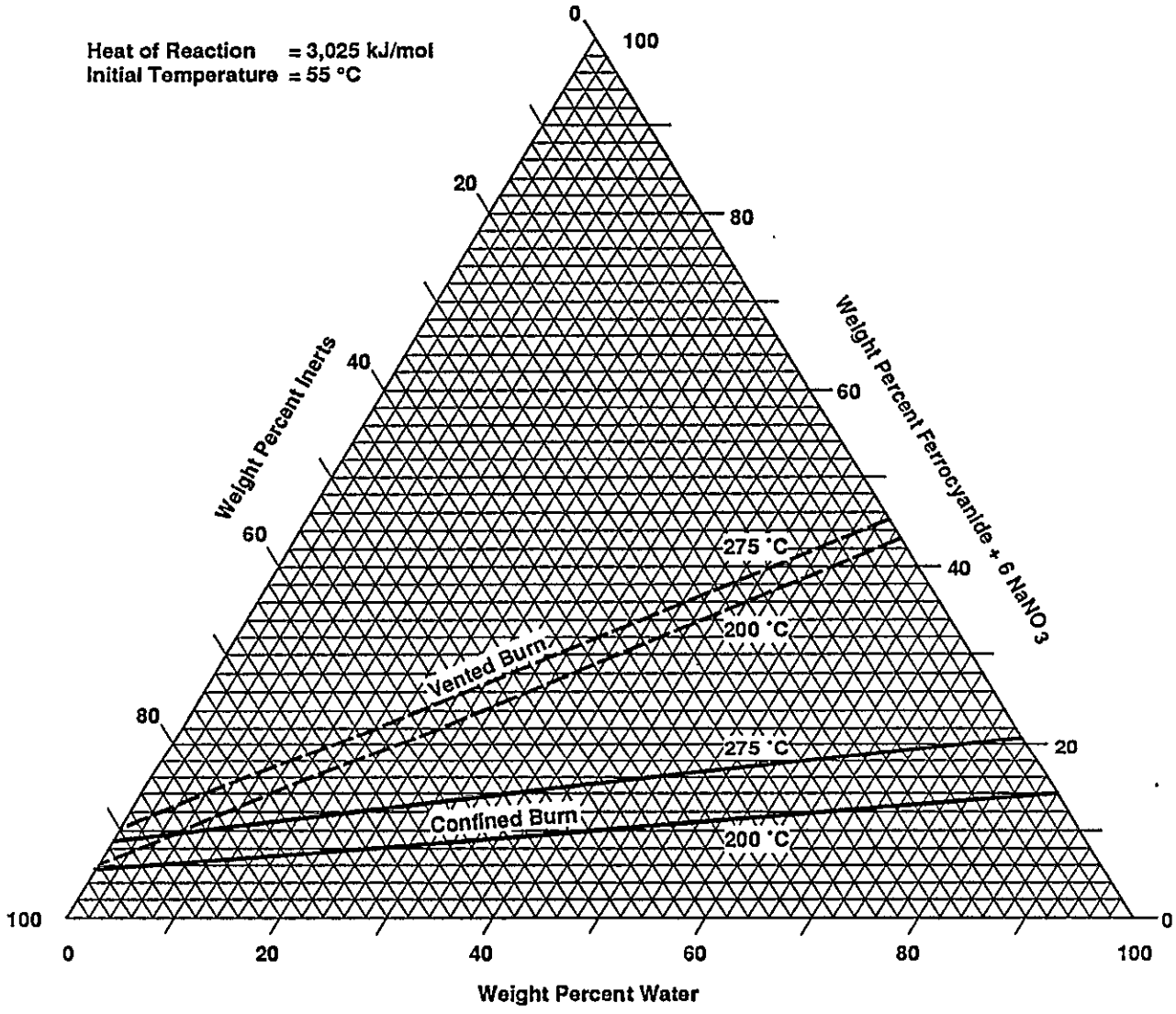

H9111028.17d

Figure 5-4. Combustibility Limits of Ferrocyanide Mixtures Effect of Heat of Reaction.

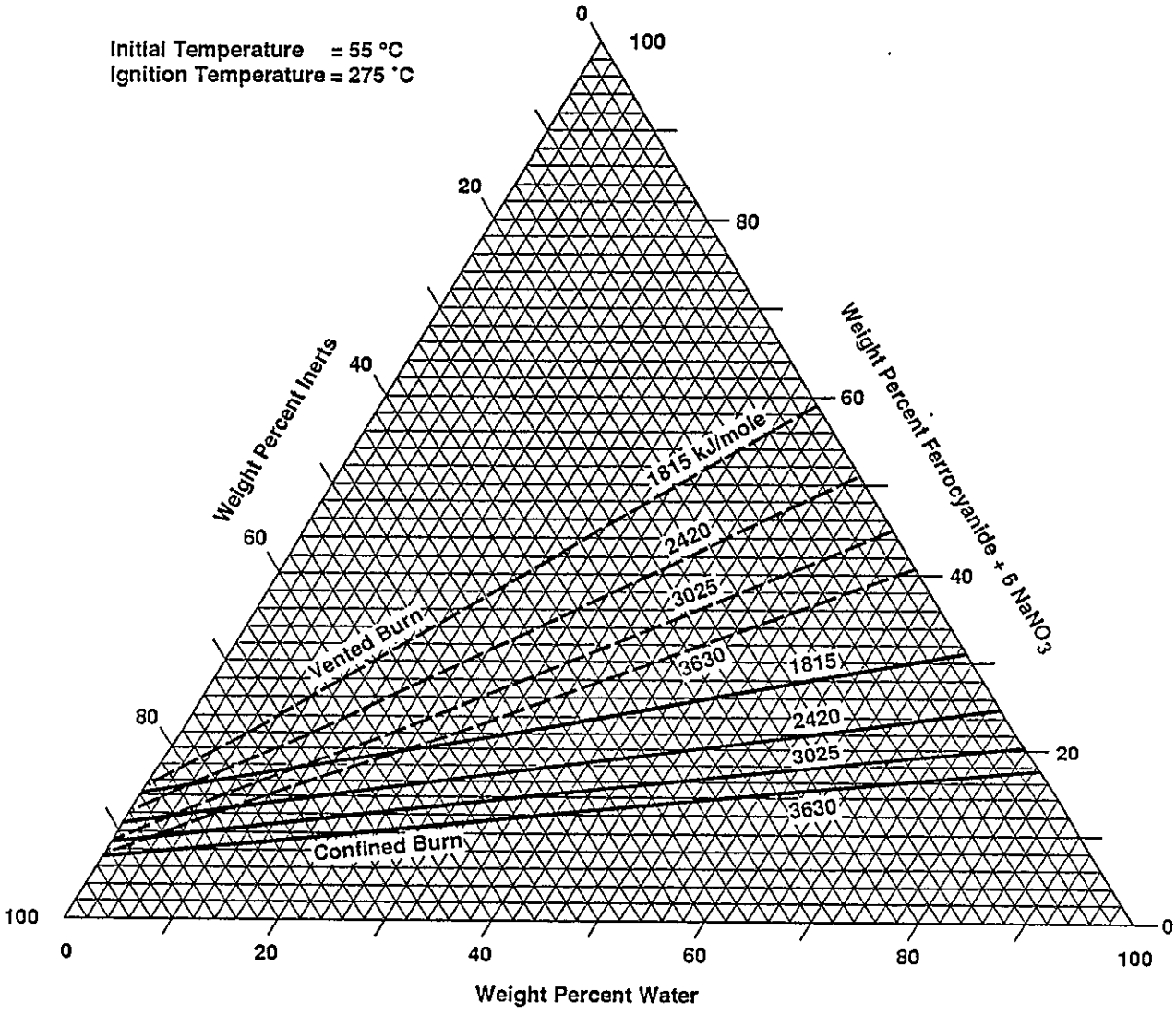

H9111028.17e

Figure 5-5. Combustibility Limits of Dry Ferrocyanide Mixtures at High Temperatures.

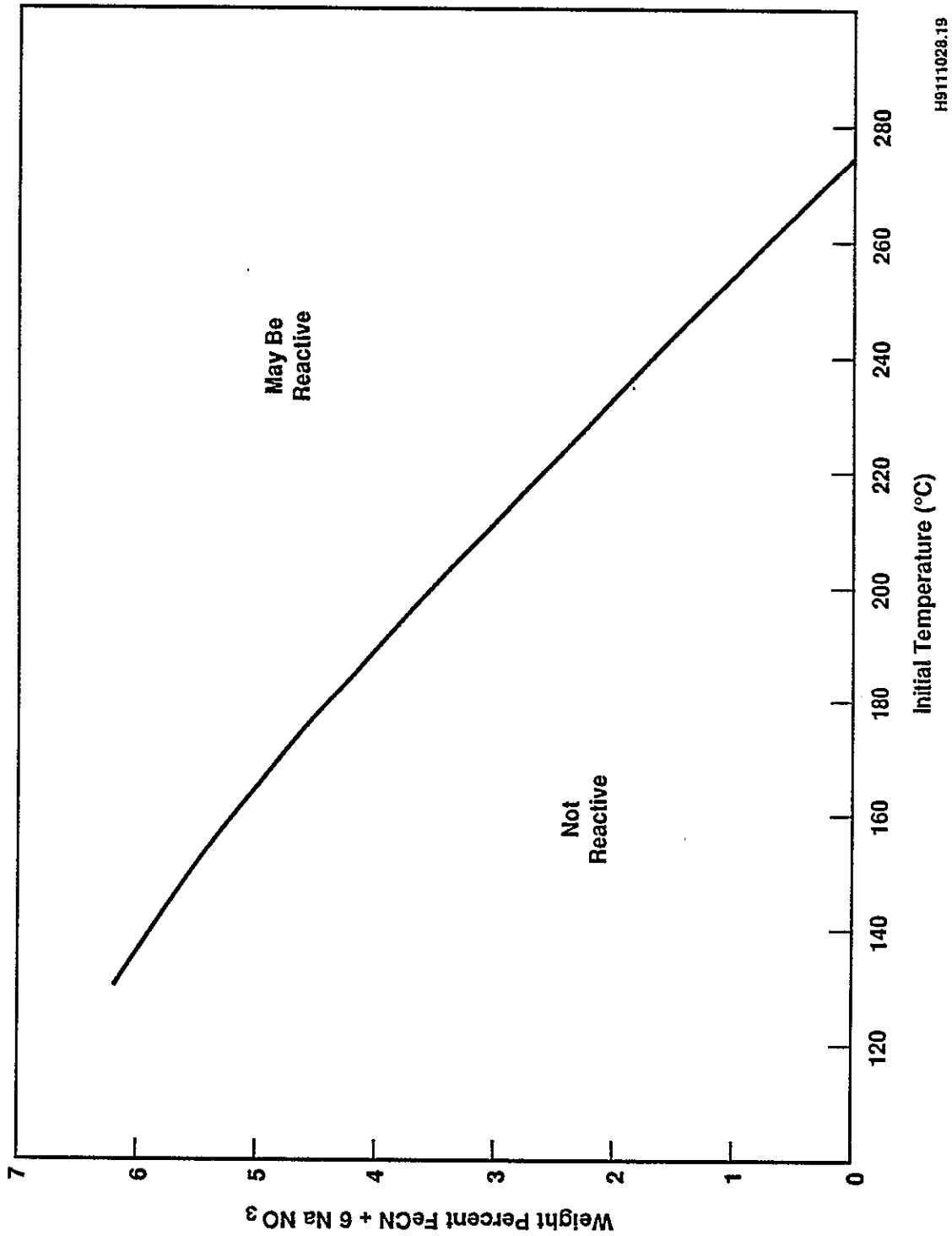

noncombustible fuel concentration decreases from 6.2% [of $Na_2NiFe(CN)_6$ + 6 $NaNO_3$] at 130 °C and approaches zero at 275 °C. It should be noted, however, that these dilute mixtures may require a temperature well above 275 °C to ignite, and higher concentrations may be noncombustible.

The present calculations assume that all of the heat generated is used to heat fresh fuel. For the confined burn surrounded by fresh fuel, this is a reasonable assumption because the heat cannot otherwise escape. For the vented burn, however, part of the heat may escape with the combustion gases and entrained solids and not be available to heat fresh fuel. Evaporation of water from moist fuel (on heating it to the ignition temperature) may create a steam barrier that separates and insulates fresh fuel from the burning material. Vaporization of even 1% moisture at atmospheric pressure would produce 35 cm^3 of steam for each cubic centimeter of solids heated. Thus, material may be less reactive in a vented burn than calculated.

It should be kept in mind that the thermodynamic possibility of combustion reaction does not mean that combustion will actually occur or, if it does occur, that it will be an explosion. Thermodynamics do not predict the speed of the reaction, which may be rather slow, particularly for compositions near the limits of reactivity. Testing may show that ferrocyanide is noncombustible at concentrations higher than calculated here. As an example, the calculated combustibility limits may be compared to the composition found by Fauske to be noncombustible. As discussed in Section 4.3.1, dried flowsheet material was found to be unreactive when heated in the RSST calorimeter to temperatures up to 380 °C. The composition of this material when dried was 12.5% of $Na_2NiFe(CN)_6$ + $6NaNO_3$ and 87.5% inerts, primarily excess $NaNO_3$. This ferrocyanide concentration lies somewhat above the calculated combustion limit. This illustrates that the calculated combustion limits are conservative, and higher ferrocyanide concentrations may in fact be noncombustible.

The preceding discussion considers only whether combustion could propagate at all, however weakly, when all the energy released is used to heat fresh fuel. It is also pertinent to consider the requirements for a reaction vigorous enough to generate appreciable radioactive aerosols. Aerosols of ^{137}Cs will be produced by vaporization of volatile cesium compounds and subsequent condensation as the gas cools. At 275 °C the vapor pressure of CsOH is only 5×10^{-8} atm (Cummings et al. 1982). If all of the cesium typically present with the ferrocyanide were to be vaporized, its partial pressure would be 2×10^{-4} atm.* Thus, only 0.03% of the cesium could be vaporized if the final temperature were only 275 °C. To vaporize all the cesium would require a temperature of about 500 °C. Other possible cesium compounds (oxide and carbonate) are even less volatile at these temperatures. Thus, the potential for combustion does not necessarily imply the potential to produce radioactive aerosols.

---

*Basis of calculation: a ratio of 3 Ci = 2.5×10^{-4} mol ^{137}Cs per mole of ferrocyanide is typical of the data in Table 4-4. After decay from 1950 to 1991 there will be 14.98 mol total cesium per 2.28 mol ^{137}Cs (Etherington 1958). Each mole of ferrocyanide produces 8 mol of gas. Total pressure = 1 atm.

5.1.4 Application to Ferrocyanide Tanks

The tank compositions estimated in Chapter 4.0 may be compared to the combustion limits previously calculated. The estimated average concentration of ferrocyanide in the waste tank sludge ranges from near-zero values up to a maximum of 0.10 mol/L (see Table 4-4). If the density of the sludge is taken as 1.4 g/cm^3 (measured for centrifuged flowsheet sludge; see Section 4.3.1), the maximum concentration is 7.1 x 10^{-5} mol/g or 5.9% by weight of fuel/oxidant mix ($Na_2NiFe(CN)_6$ + 6 $NaNO_3$). A conservative estimate of the minimum water concentration in the sludge is 40% by weight (see Section 4.10.4); a maximum may be taken as 70%. This composition range is compared to the combustion limits in Figure 5-6, in which the limit lines of Figure 5-1 are redrawn. All ferrocyanide concentrations are in the noncombustible region for both confined and vented burns. At 40% water, a composition with at least 15% fuel/oxidant mixture is required for a confined reaction, 36% for a vented reaction. The waste tank composition is also noncombustible for any of the parametric cases considered in Figures 5-2 through 5-4. The 5.9% concentration of ferrocyanide plus oxidant is noncombustible at any water content. Thus, the estimated average sludge compositions of all tanks are noncombustible and safe.

The combustion limits may also be compared to the upper-bound estimates of the peak ferrocyanide concentrations derived from the ^{137}Cs gamma scans, as given in Table 4-18. These range from 0.10 to 0.25 *M* or from 6% to 15% of fuel plus oxidant. The upper end of this range, possibly representative of the bottom of tank 241-BY-106, is just at the combustion limit at 40% water for a confined reaction but still well below it for a vented reaction. For all other tanks listed in Table 4-18, the peak concentration falls below the combustion limit.

The water content of the salt cake may go as low as 10% if the tank is drained (see Section 4.10.4). However, the gamma scan data and analyses of salt cake added on top of the ferrocyanide sludge suggest that ferrocyanide concentrations in the salt cake are much lower than in the sludge. Thus, the salt cake is also well within the noncombustible region.

Because peak concentrations of ferrocyanide are not known, particularly for the tanks for which no ^{137}Cs gamma scans have been made, it is of interest to note how far the average concentration of each tank is from the combustion limit. A margin of safety may be defined as the ratio of the maximum noncombustible ferrocyanide concentration to the average ferrocyanide concentration in the sludge. The margin of safety is thus the concentration of ferrocyanide (ratio of peak-to-average concentration) that would have to exist to get a possibly combustible composition. The margin of safety for each tank is given in Table 5-2, along with the corresponding average ferrocyanide concentration for each tank. Concentrations are based on the estimated original volume of the settled ferrocyanide sludge, as shown in Table 4-4. For a confined burn, the margin of safety ranges between 2.5 and 3.6 for the 13 highest concentration tanks, all of which are in the BY and C tank farms. These factors are only slightly higher than the upper-bound peak-to-average concentration ratios of 1.2 to 3.1 estimated in Section 4.5.4 from the gamma scans. Thus, the possibility of local combustible

Figure 5-6. Comparison of Combustibility Limits with Waste Tank Composition.

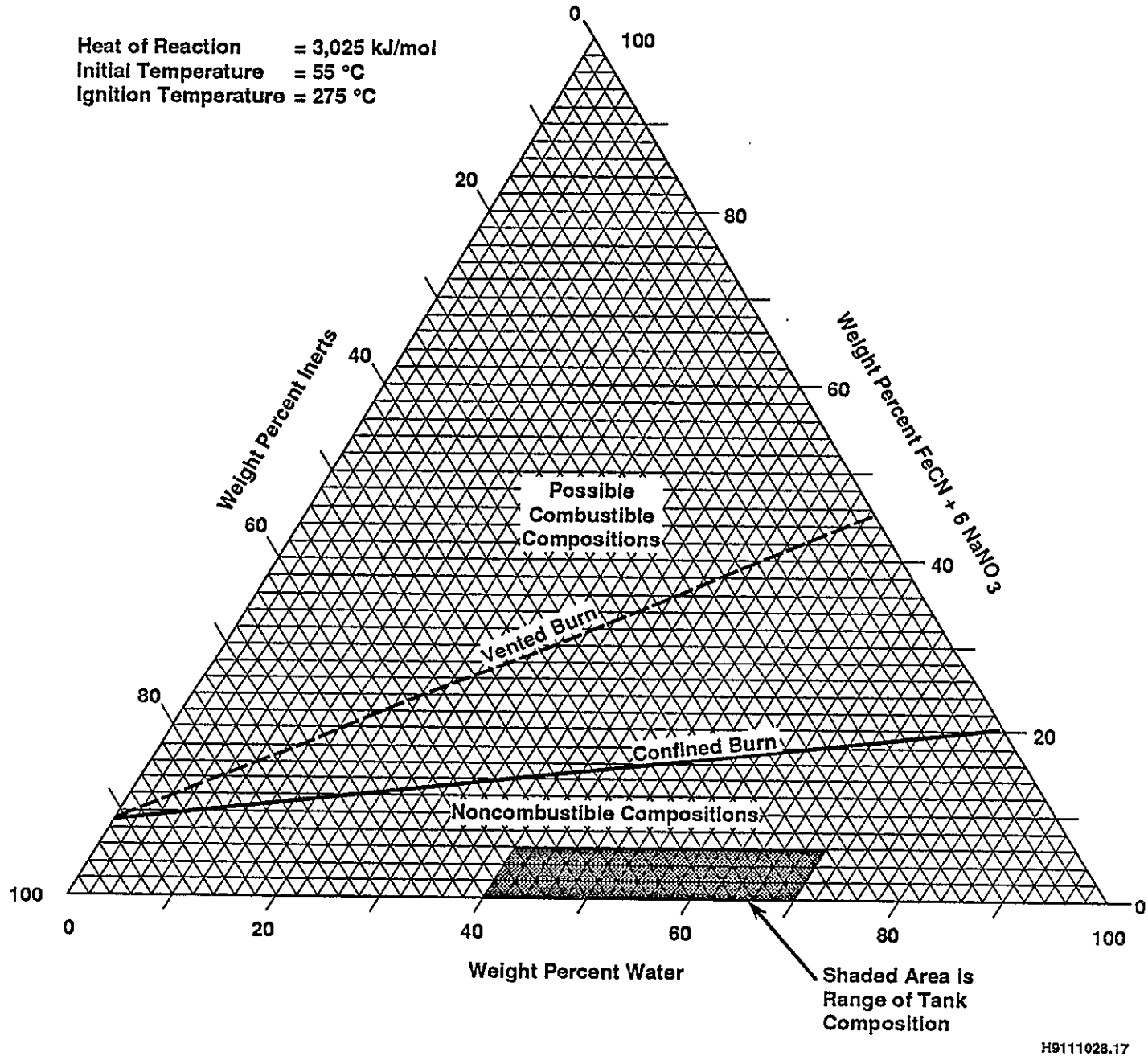

Table 5-2. Margin of Safety Between Ferrocyanide Combustibility Limits and Average Concentration in Sludge.

Tank	Average concentration[a] (*M* FeCN/L)	Margin of safety[b]	
		Confined burn[c]	Vented burn[d]
241-BY-103	0.082	3.0	7.4
241-BY-104	0.084	3.0	7.2
241-BY-105	0.099	2.5	6.1
241-BY-106	0.081	3.1	7.5
241-BY-107	0.070	3.5	8.6
241-BY-108	0.070	3.6	8.7
241-BY-110	0.080	3.1	7.6
241-BY-111	0.094	2.6	6.4
241-BY-112	0.076	3.3	8.0
241-C-108	0.086	2.9	7.1
241-C-109	0.073	3.4	8.3
241-C-111	0.089	2.8	6.8
241-C-112	0.098	2.6	6.2
241-T-107	0.006	40	98
241-TY-101	0.042	5.9	14
241-TY-103	0.041	6.0	15
241-TY-104	0.042	5.9	14

[a]From Table 4-4.

[b]Margin of safety is the ratio of the maximum allowable ferrocyanide concentration for a noncombustible composition (from Figure 5-1 at 40% water) to the average concentration present in the sludge. It is thus the ratio of peak-to-average ferrocyanide concentration in the sludge required for the existence of any combustible material.

[c]Maximum noncombustible concentration = 14.7% or 0.249 *M* ferrocyanide, at an assumed density of 1.4 g/cm^3.

[d]Maximum noncombustible concentration = 35.8% or 0.606 *M* ferrocyanide.

concentrations cannot be ruled out by the thermodynamic calculation presented here. For a vented burn, the factor of safety in these 13 tanks is between 6 and 9. Local concentration peaks of this magnitude appear to have a low probability, and a vented burn of such a concentration peak is very unlikely.

The effect of a possible local hot spot needs to be considered. For local temperatures below 130 °C, the tank contents are estimated to be noncombustible. At 130 °C and 40% water, Figure 5-2 shows a limit of 10% fuel plus oxidant for a confined burn, 31% for a vented burn. However, if the temperature is increased above 130 °C, water will be driven off from a saturated solution of $NaNO_3$, and the material will become dried out. If all the water is removed by vaporization, a composition with 5.9% fuel mixture and 70% water is changed to 20% fuel mixture. This composition is potentially combustible. Therefore, hot spots up to about 130 °C will be noncombustible, but a local combustible region could exist if local heat generation were great

enough to produce sustained temperatures above 130 °C. However, the concentration of heat required to produce a 130 °C hot spot appears to be highly unlikely, as discussed in Section 5.2.

The composition of the synthetic flowsheet materials described in Section 4.3 may also be compared to the combustibility limits. The estimated average composition of U Plant sludge (Table 4-11) is 4.7% of $Na_2NiFe(CN)_6$ plus $6NaNO_3$, 66.1% water, and 29.2% inerts. This composition lies within the shaded area of Figure 5-6 representing the range of tank compositions and is noncombustible. If dried by internal heating, the composition would become 14% fuel mixture and 86% inerts. This dry composition lies above the limit lines of Figure 5-6 and must therefore be regarded as possibly combustible. However, in view of the conservatism in the thermodynamic combustibility limits, it may be possible to show by propagation tests that this dry material is also noncombustible.

As noted in Section 4.3.2, the In-Farm flowsheet may have produced a material with a lower concentration of diluents than the U Plant sludge. This would render the sludge in the C Farm tanks, which used the In-Farm process, more likely to be combustible than other waste if it becomes dry.

The consequences of a confined burn would be limited in a material that cannot sustain a vented burn. The pressure in a confined pocket of combustion gases will be very high initially but will decrease rapidly as the cavity expands and becomes vented to the head space. When the pressure falls below the vapor pressure of water at the prevailing temperature, the water present will evaporate and produce strong cooling. If a vented burn is not thermodynamically sustainable, the combustion will stop. The extent of the reaction up to this point will depend on the propagation velocities of the reaction and on the inertia (height and density) of the overburden. Further data on propagation velocities as a function of pressure, and further analyses of the expansion transient are needed to estimate how much can react. However, preliminary measurements of the reaction propagation velocity being made by FAI suggest low velocities on the order of 1 cm/s. Calculations based on these data suggest that the extent of a reaction before venting would be much less than that required to rupture the storage tank.

Because an explosion typically releases only about 80% of the theoretical energy (Scheele et al. 1991), a heat of reaction of 2,420 kJ/mol is more realistic than the 3,025 kJ/mol (100% of theoretical), which was conservatively assumed above. For 2,420 kJ/mol, a mixture with 40% water would be noncombustible up to 18.3% fuel mixture [0.31 *M* $Fe(CN)_6^{-4}$] for a confined reaction and 44.2% [0.75 *M* $Fe(CN)_6^{-4}$] for a vented reaction.

5.1.5 Conclusions on Possible Combustibility of Tank Waste

The comparison of combustion limits and possible tank composition in Section 5.1.4 leads to the following conclusions.

- The average concentration of the ferrocyanide sludge in all tanks is noncombustible. Sustained combustion involving the entire tank is therefore not possible.

- A local region that is combustible in a confined burn may exist if the ferrocyanide could become concentrated to about three times its average value. Such a confined burn could exist only a brief time, until a path is created to vent the high-pressure product gases to the head space. After this pressure reduction, the combustion would be stopped by flashing of water.

- A local region capable of combustion at pressures low enough to vaporize the water present would require concentration of ferrocyanide by a factor of 6 to 9 above its average value in the sludge. This amount of concentration is considered unlikely based on the discussion in Sections 4.5.4 and 4.5.5.

- If the ferrocyanide sludge could dry out (if sufficient high-heat generation existed), the dry spot could be combustible. The extent of such a combustible region would be limited to the extent of the dry spot.

- The foregoing conclusions apply to U and T Plant waste material. Information on In-Farm wastes is insufficient for reaching comparable conclusions at this time.

5.1.6 Need for Experimental Measurements

Experimental measurements are needed to support the calculations presented here to better define the range of combustible compositions. Such measurements would remove the conservatism now applied by assuming that 100% of theoretical energy is released and by neglecting convective heat flow away from the fresh fuel. Measurements of synthetic flowsheet materials believed to be conservatively representative of the tank contents will be particularly useful. Confirmatory measurements may be made on actual tank waste after core samples are taken.

Measurements of propagation velocity are currently in progress at FAI. Some of the compositions to be tested are not expected to react at all, and these tests will identify noncombustible compositions.

5.2 POTENTIAL FOR ENERGETIC CHEMICAL RUNAWAY

The preceding section showed that, judging from currently available data, the overall compositions of the ferrocyanide sludges are unlikely to sustain a propagating reaction. However, if there were regions within the waste where both the radionuclides and the ferrocyanide were significantly concentrated, conditions for runaway might exist. Section 4.5 presented a discussion of the physical mechanisms that could have produced concentrated regions in the waste. The conclusion drawn was that uneven distributions in the tanks are likely to be in the form of layers homogeneous over the cross-sectional area of the tank. The potential for maldistribution across the tank was shown to be unlikely. In this section, concentrated regions are examined for their likelihood to sustain runaway reactions.

The thermal analyses in this section used 200 °C as the temperature for the onset of exothermic chemical activity. The results of thermal testing, reported in Section 4.7, indicate that significant exothermic behavior does not occur below about 275 °C. Therefore, the use of the lower temperature contributes to the conservatism of these analyses. In addition, thermal conductivities used are lower than those reported in Section 4.10, also as a conservatism.

5.2.1 Reactants and Heat Source Concentrated in a Layer

It has been previously shown from physical considerations that unevenly distributed waste in the tanks would have to be in the form of layers. Accordingly, efforts were made to examine the potential for a highly concentrated layer to achieve a condition of thermal runaway.

Slab geometry analyses were performed by J. M. McClaren using the HEATING7 computer code (Childs 1991). The model representing tank 241-BY-104 used in this calculation was described in Section 4.9. A very low thermal conductivity, 0.00173 W/cm-°C (0.10 Btu/h-ft-°F), for the entire tank contents was assumed for conservatism. The decay energy was concentrated in layers of various thicknesses as shown in Table 5-3. The layers were centered at tank elevation 41 ft or approximately 1 ft from the bottom of the tank. This location is where the highest temperatures are observed in tank measurements.

Table 5-3. Maximum Temperature Versus Slab Thickness.

Layer thickness (ft)	Volumetric heat rate (Btu/h/ft^3)	Maximum temperature	
		(°C)	(°F)
2.0	0.9	88	(189)
1.0	1.81	89	(191)
0.5	3.62	89	(192)
0.33	5.4	90	(193)
0.25	7.24	90	(194)

This calculation was based on a total decay heat generation rate of 8,000 Btu/h for the entire tank or 0.245 Btu/h/ft^3. This is the highest heat load for tank 241-BY-104 as estimated by thermal analyses using tank measured temperatures (see Section 4.9.2). When the total decay energy is concentrated by a factor of approximately 30 (7.24/0.245), the peak temperature is less than 100 °C.

These calculations indicate that concentrating all of the heat-generating fission products in a layer with a volume equal to the volume of the entire ferrocyanide inventory of the tank (combined with stoichiometric oxidant) could not lead to a propagating reaction by a margin in excess of 100 °C (90 °C versus 200 °C).

As another evaluation of slab geometry, upper-bound estimates were made of the heat rate required for the bottom of the tank to reach 200 °C. A one-dimensional model was used with all energy input concentrated in the bottom 7% to 10% of the tank contents. The bottom of the tank was taken as an adiabatic surface. The values used in these calculations are shown in Table 5-4.

Table 5-4. Input Values for Upper-Bound Heat Rate Estimates.

Initial temperature = 80 °F = 27 °C
Outer or upper surface temperature = 80 °F = 27 °C
Boiling point = 266 °F = 130 °C (for saturated $NaNO_3$)
Thermal conductivity (wet) = 0.27 Btu/h ft °F (.47 W/m °C)
Thermal conductivity (dry) = 0.1 Btu/h/ft°F (.17 W/m °C)
Volumetric heat capacity (wet) = 70 Btu/ft^3 °F (4.7 x 10^6 J/m^3 °C)
Volumetric heat capacity (dry) = 10 Btu/ft^3 °F (6.7 x 10^5 J/m^3 °C)
Heat of vaporization = 53,500 Btu/ft^3 (2 x 10^9 J/m^3)

The heating rate required for the maximum temperature in the tank to reach 200 °C is given in Table 5-5, compared to the available heating rate for the tanks containing in excess of 1,000 mol of ferrocyanide. It is noted that the available heat rate is always less than that required, even with this extremely conservative model.

5.2.2 Reactants and Heat Source Concentrated in a Sphere

Even though concentrated regions other than layers are deemed implausible from physical considerations, they were examined for the potential to produce runaway conditions. A spherical shape was chosen as the extreme worst case, having the lowest surface-to-volume ratio.

Hans K. Fauske of FAI presented an assessment of spherical hot spots based on calculation of (1) the minimum concentration of heat generation capability and (2) the maximum time required to reach the temperature (200 °C) necessary for energetic runaway to occur. The concentrated region was modeled as a sphere with a diameter equal to the height of the sludge in the tank (Figure 5-7).

These calculations considered an extremely improbable configuration of heat source concentration in the waste. It must be noted that, in addition to concentration of the heat source, this analysis also requires that the ferrocyanide concentration in the hot spot be significantly increased in order to support the reaction. No mechanism for ferrocyanide accumulation can be identified. This compounds the improbability of this scenario.

Table 5-5. Comparison of Upper-Bound Estimates of Heating Rates Required for Thermal Runaway Versus Available Heating Rates for a Layer Concentration.

Tank	Depth of solid waste[a] (ft)	Heating rate required (W)	Available heating rate (W)[b]
241-BY-103	12.7	7.3 E3	2.4 E3
241-BY-104	12.9	7.3 E3	3.5 E3
241-BY-105	15.9	6.1 E3	2.5 E3
241-BY-106	20.1	5.3 E3	3.5 E3
241-BY-107	8.7	1.0 E4	2.0 E3
241-BY-108	7.5	1.1 E4	2.2 E3
241-BY-110	12.7	7.3 E3	3.8 E3
241-BY-111	14.5	6.4 E3	2.5 E3
241-BY-112	9.4	9.4 E3	4.7 E2
241-C-108	2.6	3.2 E4	2.4 E2
241-C-109	2.5	3.2 E4	5.3 E2
241-C-111	2.3	3.5 E4	5.9 E2
241-C-112	3.8	2.1 E4	4.7 E2
241-T-107	5.8	1.5 E4	1.8 E2
241-TY-101	4.2	2.0 E4	2.9 E2
241-TY-103	5.5	1.5 E4	9.7 E2
241-TY-104	1.9	4.4 E4	1.2 E2

[a]From Table 4-23.
[b]From Table 4-34--Average of representative values.

Figure 5-7. Illustration of the Hot Spot Model in Tank 241-C-112.

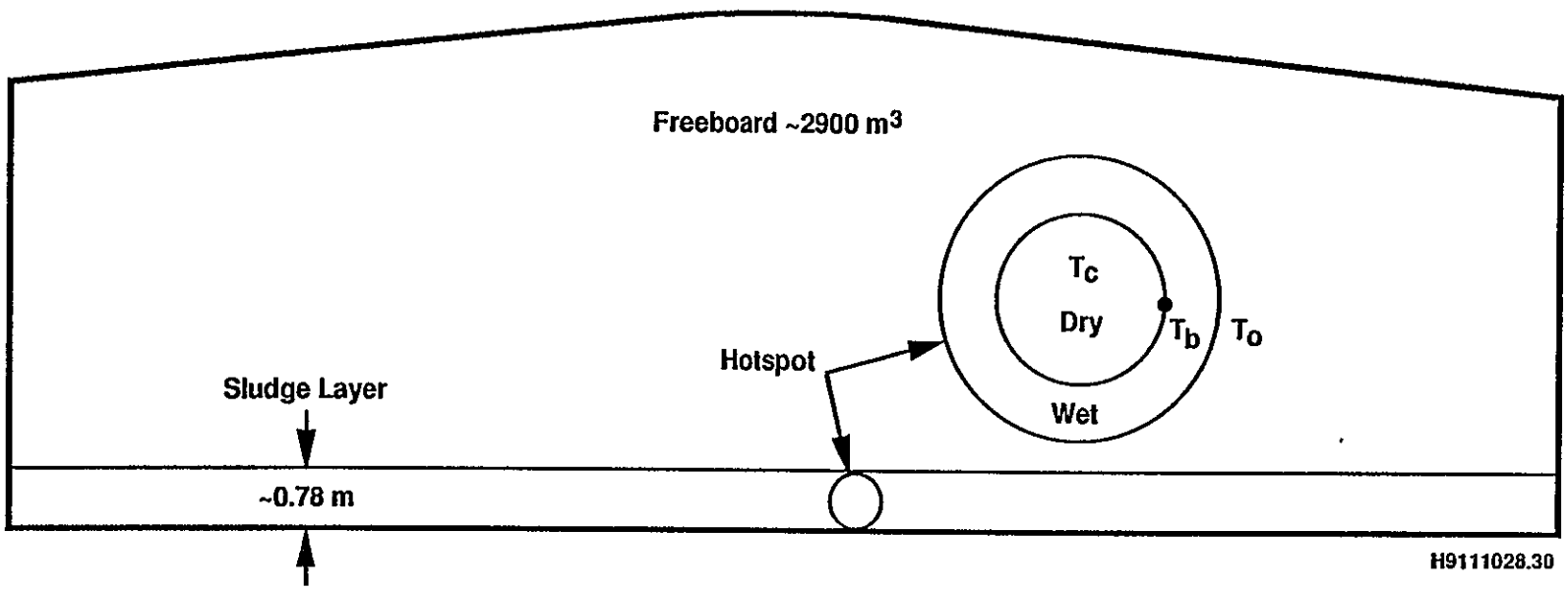

Note: T_c ~200°C, T_b ~130°C and T_o ~60°C.
The thermal conductivities for the dry and wet zones are set equal to 0.17 and 0.45 W $m^{-1}K^{-1}$, respectively.

The necessary volumetric heat generation rate, Q (W m^{-3}), can be obtained from the solution of the steady-state heat conduction equation for a solid sphere with internal heat generation.

$$Q = \frac{6\ k_D\ (T_c - T_b)}{R_D^2} \tag{5-3}$$

where

k_D (W m^{-1} K^{-1}) = thermal conductivity of the dried-out material in the hot spot, taken to be equal to 0.17 W m^{-1} K^{-1}

T_c (K) = temperature for onset of exothermic activity; set equal to 473K (200 °C)

T_b (K) = the boiling temperature; set equal to 403K (130 °C) based on a saturated solution of sodium nitrate

R_D (m) = radius of the dried-out region of the hot spot, given by

$$\frac{R_D}{R} = \sqrt{\frac{T_c - T_b}{T_c - T_o + (k_w/k_D - 1)\ (T_b - T_o)}} \tag{5-4}$$

where

T_o (K) = the temperature outside the hot spot; set equal to 333K (60 °C)

k_w (W m^{-1} K^{-1}) = the thermal conductivity of the wet waste material in the hot spot; set equal to 0.45 W m^{-1} K^{-1}

R (m) = radius of the hot spot.

Considering tank 241-BY-104 (R = 1.2 m) it was estimated that more than 50% of the total decay heat generation rate must be concentrated in the hot spot to reach the onset temperature. This represents only 0.7% of the total waste volume. Corresponding information for the other two tanks considered in this exercise is summarized in Table 5-6.

Table 5-6. Illustration of Required Hot Spot Characteristics with Hot Spot Diameter Equal to Nonconvective Sludge Height.

Tank	Average volumetric heating rate (W/m^{-3})	Minimum volumetric heating rate to produce hot spot (W/m^{-3})	Percent of total heating rate in hot spot	Percent of total waste volume in hot spot
241-BY-104	2.4	181	55	0.7
241-C-109	<5.7	2,893	~24	0.05
241-C-112	<4.7	2,009	~28	0.07

These results show that the radioactive heat load in these tanks would have to be concentrated by large factors to produce a spherical hot spot with its center at 200 °C. Decay heat concentration factors are calculated by taking the heat rate required to produce the hot spot divided by the average heat rate. The concentration factors are 75, 510, and 430, respectively, for tanks 241-BY-104, 241-C-109, and -112. There is no known mechanism for concentrating fission products in the tanks by these large factors.

The likelihood of hot spot formation is very low based on fission product maldistribution as outlined above. If hot spots are still postulated in spite of this low probability, one must ask whether the time required to form the hot spot exceeds the time since the last event that could have induced it. The formation time was estimated (Appendix C). The method is outlined as follows. The time to reach the onset temperature would not be exceeded by

$$t = \frac{R^2}{\alpha} + \frac{\rho\, y\, \lambda}{Q} \qquad (5\text{-}5)$$

where

ρ ($kg\ m^{-3}$) = density of the sludge, taken to be 1,600 $kg\ m^{-3}$

y = weight fraction of liquid (water) in the sludge, set equal to 0.6

λ ($J\ kg^{-1}$) = latent heat of vaporization; taken to be $2.2 \times 10^6\ J\ kg^{-1}$.

The first term in equation 5-5 reflects the time to satisfy the sensible heat buildup in the hot spot. The second term represents the time to vaporize all the liquid in the dried-out portion of the hot spot.

Estimated times to form critical hot spots with diameters set equal to the nonconvective sludge heights (giving rise to the longest times) are given in Table 5-7. Considering that these time estimates are small relative to the storage exposure times since last stabilization of the waste tanks leads to the conclusion that any concerns related to hot spots and runaway reactions would have appeared shortly after the last liquid pump-out operations.

Table 5-7. Hot Spot Characteristics.

Tank	Time since last pumping operation	Time to form a critical hot spot (Equation 5)
241-BY-104	~7 yr	<250 days
241-C-109	~8 yr	<16 days
241-C-112	~1 yr	<20 days

The above considerations suggest that passive safety is ensured as long as the existing conditions are not significantly changed. Because the relatively small amount of heat generated in the tanks is easily removed to the atmosphere by passive means (conduction and free convection) at temperatures well below the boiling point of water, the sludge layer will remain invariant in terms of liquid content.

5.2.3 An Approach to Runaway Based on Tank Cooling Response Time

A supplemental approach to the assessment of thermal runaway has been applied by Hans K. Fauske of FAI (Appendix C). This approach is based on thermal runaway criteria used in the chemical process industry to assess safe storage. The usual requirement employed in that industry to ensure passive safety is

$$t_a \gg t_c \tag{5-6}$$

where t_a is the characteristic time of adiabatic runaway and t_c is the characteristic passive cooling response time of the system. In case of the waste tanks, t_c can be estimated from

$$t_c \approx \frac{L^2}{\alpha} \tag{5-7}$$

where

L (m) = characteristic dimension, conservatively set equal to the total nonconvective waste height in the tank

α (m^2 s^{-1}) = thermal diffusivity, which is taken to be 1.5 x 10^{-7} m^2 s^{-1}. This is representative of many materials including the Hanford Site waste.

Fauske chose three tanks for application of the foregoing approach. The tanks chosen were tanks 241-BY-104 (maximum total ferrocyanide inventory), 241-C-109 (maximum concentration), and 241-C-112 (most recently stabilized tank). Information on this set of tanks is given in Table 5-8. Using sludge heights (nonconvective waste heights) from Table 5-8, cooling response time t_c is shown in Table 5-9 and compared with the time that has already elapsed without runaway having occurred. These data suggest that the inequality ($t_c \ll t_a$) is satisfied for the ferrocyanide waste tanks at the present time. It is noted that this conclusion can be made without requiring a knowledge of t_a or the actual chemical composition and water content.

Table 5-8. Enveloping Ferrocyanide Tank Characteristics.

Tank	Total waste (1,000 gal)	Ferrocyanide inventory (1,000 mol)	Ferrocyanide concentration (g/L)	Pumpable liquid remain (1,000 gal)
241-BY-104	406	100-200	41	0
241-C-109	66	30-50	67	0
241-C-112	104	50-70	56	26
	Nonconvective waste height (m)	Heat rate (W)	Maximum measured temperature (°C)	Stabilized date
241-BY-104	3.7	2,400	54	1/85
241-C-109	0.6	<1,400	24	11/83
241-C-112	0.72	<1,400	27	9/90

Table 5-9. Tank Characteristic Times.

Tank	Storage time since last stabilization (yr)	Cooling response time, eq. (2)
241-BY-104	~7	~2.9 years
241-C-109	~8	~28 days
241-C-112	~1	~40 days

6.0 POTENTIAL FOR CHANGES IN TANK CONDITIONS

The hazard assessments presented in Chapter 5.0 concluded that, with information currently available, the contents of the ferrocyanide tanks would appear to be noncombustible and propagating reactions are unlikely. The next question would be, "Can the conditions in the tanks change significantly in the future to invalidate these conclusions?"

Postulated changes that might occur are grouped into changes in fuel or heat load concentrations, loss of moisture, and chemical changes in the ferrocyanide compounds that might make them more reactive than assumed in this report.

6.1 POTENTIAL FOR CONCENTRATION OF FERROCYANIDE DURING WASTE STORAGE

Historical and present evidence indicates that the precipitated ferrocyanide and all of the hydroxides settled, in a few weeks, into a sludge. There seems to be no mechanism that would significantly change that initial state over time.

There may have been some compaction that would decrease the amount of water but not change the relative ratios of ferrocyanide to insoluble diluents. Evidence indicates a large amount (greater than 40%) of liquid remains in the sludge even after draining.

The compacted sludge will consist of particles and tortuous paths of interstitial capillary water. Tests on compacted synthetic sludges show high viscosities, greater than 10,000 cP (Section 4.3.1), and a low permeability, in the millidarcy range or lower (Metz 1976). As a result, the compacted sludge state inhibits molecular diffusion and effectively stops convection movement. The absence of strong driving forces and the resistance to mass transport prevent relative concentration changes by mechanical differentiation, recrystallization, condensation, etc. In short, the absence of mechanisms leads to no change from the initial settled state.

To illustrate the limits of molecular diffusion, a calculation was made of the time necessary to accomplish a change in concentration under steady-state conditions (Foust 1960, p. 131). Diffusitivities of 2.6×10^{-5} cm^2/s for HNO_3 in water and 1.35×10^{-5} for NaCl were used. Because these are for solutes in dilute solutions, the actual tank diffusivities are likely to be much less.

The assumptions were a 2-m layer of sludge at initially 2 *M* $NaNO_3$ with an overlayer of a 6 *M* $NaNO_3$ solution with no barrier to mass transport between the two phases. Starting 37 yr or 1.17×10^9 s ago, and using the diffusivity listed above, the bottom concentration would now be between 4 and 5.2 *M*. Given the actual diffusivities, it appears that the tank bottom concentration would approach 6 *M* $NaNO_3$ sometime late in the 21st century. Thus, significant changes by diffusion will be very slow.

6.2 POTENTIAL FOR LOSS OF MOISTURE

The tank moisture is an important diluent and can change under some conditions. Moisture can be removed from the tank by leakage, radiolysis, evaporation, and pumping. Water loss from pumping a tank can be administratively controlled and will not be discussed.

6.2.1 Leakage

Loss of free water in the stored waste by drainage through new or existing leaks is possible when the liquid level above the leak exceeds the capillary holdup height of the tank content. Chemically bound water and gel water are not subject to loss through leaks.

The two major solid wastes, ferrocyanide sludge and salt cake, have different chemical and physical properties that affect the ability to retain moisture (see Section 4.10.4). Waste tank sludge has been shown to strongly retain interstitial water by capillary forces (see Table 4-30) to heights of 10 to 15 ft. Tank 241-BY-104 has the thickest sludge layer at 8.5 ft (see Table 4-23). Because the capillary hold-up height exceeds the sludge thickness, water will not drain from the sludge even if a leak were to develop.

Capillary water retention by the salt cake is less than sludge water retention because the expected larger particle size will reduce the capillary height. A leak in the wet salt cake region of the tank would be expected to drain the free water to a height of about 1 ft above the leak. Chemical water and some capillary water will remain in the drained salt cake, as discussed in Section 4.10.4.5. Some of the ferrocyanide-containing tanks have been jet pumped, which drains liquid down to a flow rate of 0.05 gal/min, or less, into the pump well. Because, in general, a leak will be less optimally located than the salt well, any new leak in these tanks would be at rates less than 0.05 gal/min.

6.2.2 Evaporation

Evaporation of water from the upper surface of the tank waste into the air in the dome space will depend on the amount of tank breathing or ventilation, the temperature, and the crust composition. The loss can be conservatively estimated by assuming what the maximum water transport would be if any air flow into the tank becomes saturated with water at the tank waste surface temperature.

6.2.2.1 Tank Breathing Losses. Tank breathing is caused by atmospheric pressure changes and can result in moisture loss by humidification of the air exchanged. Klem (1991, pp. 3-11) examined Hanford Weather Station data for two typical years (1973 and 1990) and determined the average daily barometric pressure change to be 4.57 mm mercury (0.18 in. mercury) or 0.0060 atm. The ferrocyanide tank with the most vapor space is tank 241-TY-104, a nominal 750,000-gal tank that contains 43,000 gal of waste (Hanlon 1991, pp. B11 and 12). Allowing for the tank dome volume, the vapor space will be

approximately 3,400 m^3 (120,000 ft^3), and thus in 1 yr the air breathing volume that could be saturated is

$$(0.0060)\ (120{,}000)\ (365) = 264{,}000\ ft^3. \qquad (6\text{-}1)$$

Review of tank temperature data for September 1991 shows no tank thermocouple with a waste surface or vapor space reading above 31 °C (88 °F). Assuming the inlet air is at an average dewpoint of 1 °C (34 °F) (Stone et al. 1983, p. VIII-2) and that the outlet air is saturated at the maximum 31.1 °C (88 °F), annual moisture breathing losses for the worst-case tank can be calculated using psychometric tables (Perry and Chilton 1973, p. 15-9) to be

$$\frac{(264{,}000\ ft^3)}{yr}\left(0.029 - 0.004\frac{lb\ H_2O}{lb\ Air}\right)\left(\frac{lb\ Air}{14.5\ ft^3}\right) = 450\frac{lb\ H_2O}{yr} \qquad (6\text{-}2)$$

or 54 gal/yr water loss. This would amount to a liquid level change of 2.5 cm (1 in.) in 50 yr. It was concluded that moisture loss resulting from tank breathing would be small.

6.2.2.2 Tank Ventilation Losses. For ventilated tanks, moisture loss can be larger depending on the flow; such ventilation can be forced by use of blowers or can be driven by convection through inadvertent air leaks in the tank head space. No ferrocyanide tanks are currently on forced ventilation. However, Section 4.9 shows that tank 241-BY-104 may have a convective ventilation flow of 21 ft^3/min. The water pickup by such an airflow, with a 1 °C average annual dewpoint temperature and using a saturated 28 °C (82 °F) (as determined for tank 241-BY-104 surface T.C., September 22, 1991) outlet temperature, is calculated to be

$$\left(0.0239 - 0.0041\frac{lb\ H_2O}{lb\ air}\right)\left(\frac{1\ lb\ air}{14.2\ ft^3}\right)\left(\frac{21\ ft^3}{min}\right)\left(\frac{1{,}440\ min}{day}\right)\left(\frac{365\ day}{yr}\right) \qquad (6\text{-}3)$$

$$= 15{,}400\ lb\ H_2O/yr$$

or 1,850 gal/yr water loss. This water loss is for saturated air at the tank surface temperature. The water will, in fact, be evaporating from a saturated $NaNO_3$ salt solution. The humidity over this surface at 28 °C is about 75% relative humidity (Washburn 1926, Vol. 1, p. 67); hence, the rate would be 1,390 gal/yr. This rate of water loss would amount to a liquid level change of 0.5 in./yr, which could be significant over an extended period of time. The actual loss is probably lower, however, for several reasons. The assumption of equilibrium of the exit air with the liquid surface is

conservative, and the humidity will be reduced by poor mixing in the dome space. The evaporation rate will slow as water removal from the salt cake surface will result in thicker layers through which the moisture must diffuse. Actual moisture loss from actively ventilated tanks can be readily evaluated by suitable flow and psychometric measurement. Also, water loss by convective ventilation can be reduced, if needed, by locating and repairing major air leaks.

6.2.3 Moisture Loss Due to Radiolysis

Decomposition of water by hydrolysis in the highly radioactive waste has been evaluated by Klem (1991, p. A-7). Tank 241-BY-105 was the upper-bounding tank with a calculated hydrogen generation of 11.4 ft^3/d, which is equal to the decomposition of 25 gal H_2O/yr. This would result in a liquid level change of 1.1 cm (0.5 in.) in 50 yr.

Radiolysis is not an important mechanism for water loss from the ferrocyanide-containing waste tanks.

6.2.4 Moisture Loss--Summary

Of the mechanisms discussed previously, the most significant source of moisture loss from the waste would be a leak in an unpumped salt cake zone or possibly evaporation to air leakage flow caused by convective forces. Losses caused by atmospheric pressure changes and by radiolysis are both very small. Water levels in the tanks are monitored. Liquid level data (Section 4.4.2) do not show any decrease, suggesting that no significant moisture loss has occurred.

6.3 POTENTIAL FOR CHANGES IN FERROCYANIDE REACTIVITY (CHEMICAL CHANGES/DEGRADATION)

The potential for significant changes in reactivity towards the oxidants in tank waste is real, based on several plausible processes. The $Cs_2NiFe(CN)_6$ and $Na_{4-2x}Ni_xFe(CN)_6$ ($0 < x < 2$) sludges laid down in the 1950's have had over three decades to degrade, wetted by an aqueous solution high in sodium nitrate, and possibly sodium nitrite, and at alkaline pH ranges from mild (pH 8) to caustic (pH > 13). The solution probably contains other anions, such as sulfate. Precipitates of phosphates and aluminates are also present in variable amounts, as are hydroxide sludges of transition metals, noble metals, and rare earths. During this time, the ferrocyanides have been exposed to ionizing radiation and the radiolytic products of water.

Core samples of tanks 241-TY-101 and -103 taken in 1985 (Weiss 1986) have been composited and analyzed for total cyanide (Winters 1988). The findings were that the total cyanide in both cases was greater than 93% water insoluble and that the ^{137}Cs was greater than 99.9% water insoluble at composite pHs varying from 8 to 12.2. This suggests that the solid cesium nickel ferrocyanide is still largely intact. The small fraction of soluble cyanide may have come from an excess of ferrocyanide reagent used in the scavenging or possibly from a slow degradation of the precipitated solids.

Very preliminary work (Burger et al. 1991) suggests that solid ferrocyanides are stable towards radiolysis, although new experiments are planned to more fully characterize this stability.

It is maintained by chemists experienced in ferrocyanide chemistry that nickel ferrocyanides will exhibit significant solubility in aqueous solutions at pHs of 12 or higher, liberating free ferrocyanide and precipitating nickel hydroxide. It makes good chemical sense that a large excess of hydroxide ion can penetrate the coordination spheres of nickel and iron and thus break up the mixed metal ferrocyanide structure. Once the ferrocyanide is in alkaline solution, it can undergo very slow alkaline hydrolysis to ammonia, the alkali formate, and hydrous iron oxide. Alternatively, it could be attacked by silver salts (silver is a possible waste constituent at trace levels), leading to silver cyanide (American Cyanide Co. 1953). Free ferrocyanide is also oxidizable by radiolytic products of water to ferrocyanide, whose cyanide ligands are much more labile and susceptible to displacement by hydroxide ion. This path can also lead to complete degradation of ferrocyanide and liberation of cyanide ion.

The knowledge of the hydrolysis of free cyanide is much more detailed. For example, sufficient kinetic information is available on hydrolysis of aqueous cyanide through formamide to ammonia and formate, as a function of pH and temperature, to predict the half life of aqueous cyanide at 30 °C and pH 8 to be 50 yr. The half life is similarly predicted to be 3.7 yr at 30 °C and pH 10 or higher.

Taken together, these considerations give one plausible explanation for the appearance of soluble total cyanide in ferrocyanide tank waste and suggest the possibility that further, slow degradation of cyanide to products of lesser energy content (formate) and/or greater volatility (ammonia) is occurring:

$$\underline{Na_{4-2x}Ni_xFe(CN)_6} \downarrow + 2xNaOH \rightarrow Na_4Fe(CN)_6 + \underline{xNi(OH)_2}\downarrow$$

$$Na_4Fe(CN)_6 + NaOH \rightarrow Na_4Fe(CN)_5OH + NaCN \qquad (6\text{-}4)$$

$$NaCN + H_2O \rightarrow NaHCONH$$

$$NaHCOHN + H_2O \rightarrow NaHCO_2 + NH_3.$$

These products are significant because their existence may appreciably change the onset temperature of exothermic sludge reactions for better or worse and will almost certainly lessen the ultimate releasable energy if the onset temperature is reached. Note that volatile products will be driven away from the oxidants before onset temperatures are reached. The gaps in knowledge that prevent us from predicting the extent to which this degradation has happened include the true temperature and pH of the tank sludge contents, the kinetics of radiolytic attack on the sludge, and the kinetics of sludge dissolution/hydrolysis. The quantitative contribution of each of the degradation products to changes in onset temperature is also not determinable except by direct experiment.

This page intentionally left blank.

7.0 REFERENCES

Abrams, R. B., 1956, *History: Metal Recovery Waste Scavenging Program*, HW-43066, General Electric-Hanford Atomic Products Operation, Richland, Washington.

American Cyanide Co., 1953, *The Chemistry of the Ferrocyanides*, American Cyanide Co., New York, New York.

Anderson, J. D., 1990, *A History of the 200 Areas Tank Farms*, WHC-MR-0132, Westinghouse Hanford Company, Richland, Washington.

ASME, 1976, *Steam Charts*, American Society of Mechanical Engineers, New York, New York.

Atherton, J. A., 1974, *Prediction of Liquor Retention in Salt Cakes and Sludges*, ARH-CD-230, Atlantic Richfield Hanford Company, Richland, Washington.

Baker, W. E., 1983, *Explosion Hazards and Evaluation*, Elsevier Science Pub., New York, New York.

Borsheim, G. L. and N. W. Kirch, 1991, *Summary of Single-Shell Tank Waste Stability*, WHC-EP-0347, Westinghouse Hanford Company, Richland, Washington.

Borsheim, G. L. and B. C. Simpson, 1991, *An Assessment of the Inventories of the Ferrocyanide Watchlist Tanks*, WHC-SD-WM-ER-133, Rev. 0, Westinghouse Hanford Company, Richland, Washington.

Bouse, D. G., 1975, *Thermal Conductivity of Hanford Waste Tank Solids and SX and Tank Farm Soil Samples*, ARH-CD-378, Atlantic Richfield Hanford Company, Richland, Washington.

Brown, G. G., 1959, *Unit Operations*, p. 24, John Wiley and Sons, New York, New York.

Brown, E. and R. B. Firestone, 1986, *Table of Radioactive Isotopes*, John Wiley and Sons, New York, New York.

Burger, L. L., D. M. Stachan, D. A Reynolds, and W. W. Schultz, 1991, *A Summary of Available Information on Ferrocyanide Tank Wastes*, PNL-7822, Pacific Northwest Laboratory, Richland, Washington.

Burger, L. L. and R. D. Scheele, 1991, *The Reactivity of Cesium Nickel Ferrocyanide Towards Nitrate and Nitrite Salts, A Status Report*, PNL-7550, Pacific Northwest Laboratory, Richland, Washington.

Burger, L. L. and R. D. Scheele, 1992, *Interim Report Cyanide Safety Studies*, PNL-7175, Pacific Northwest Laboratory, Richland, Washington.

Carpenter, G. K., 1954, *TBP Waste Scavenging*, HW-30995, General Electric Company, Richland, Washington.

Cash, R. J., 1991, *Implementation Plan for the Defense Nuclear Facilities Safety Board Recommendation 90-7*, WHC-EP-0415, Westinghouse Hanford Company, Richland, Washington.

Cash, R. J. and G. B. Mellinger, 1991, *Program Plan for Stabilization of Hanford Tanks Containing Ferrocyanide Waste*, WHC-EP-0399, Predecisional Draft, Westinghouse Hanford Company, Richland, Washington.

Childs, K. W., 1991, *HEATING 7.1 User Manual*, Oak Ridge National Laboratory, Oak Ridge, Tennessee.

Clukey, H. V., 1955, *Sampling of Scavenged Waste*, HW-37-478, General Electric Company, Richland, Washington.

Creed, M. J. and H. K. Fauske, 1990, "An Easy Inexpensive Approach to the DIERS Procedure," *Chemical Engr. Progress*, pp. 45-49.

Cummings, J. C., R. M. Elrich, and R. A. Sallach, 1982, *Status Report on the Fission-Product Research Program*, Sandia Report 80-2662 (NUREG/EC-1820), Sandia National Laboratory, Livermore, California.

Deaton, D. E., 1990, *Occurrence Report, WHC-90-B003-R1, Update, 10-22-90 - Unreviewed Safety Question Regarding Tanks Containing Ferrocyanide*, Westinghouse Hanford Company, Richland, Washington.

DOE, 1987, *Final Environmental Impact Statement, Disposal of Hanford High-Level, Transuranic, and Tank Waste*, DOE/EIS-0113, 5 Vol., U.S. Department of Energy, Washington, D.C.

Dombrowski, H. S. and L. E. Brownell, 1954, "Residual Equilibrium Saturation of Porous Media," *Industrial and Engineering Chemistry*, Vol. 46, pp. 1207-1219.

Etherington, H., (ed), 1958, *Nuclear Engineering Handbook*, pp. 11-30, McGraw-Hill Book Company, New York, New York.

Farley, W. G. and J. M. Grigsby, 1991, *Safety Assessment for Gas Sampling System to be Utilized in BY Farm Ferrocyanide Tanks*, WHC-SD-WM-SAD-009, Rev. 0, Westinghouse Hanford Company, Richland, Washington.

Foust, A. S., 1960, *Principles of Unit Operations*, John Wiley and Sons, New York, New York.

Gasper, K. A. and I. E. Reep, 1991, *Waste Tank Safety Programs Overview Plan*, WHC-EP-0426, Rev. 1, Westinghouse Hanford Company, Richland, Washington.

Hallen, R. T., 1991, "Ferrocyanide Safety Project - August 1991 Monthly Report," Letter to R. J. Cash, September 26, 1991.

Hanlon, B. M., 1991, *Tank Farm Surveillance and Waste Status Report*, WHC-EP-0182-39, Westinghouse Hanford Company, Richland, Washington.

Henkin, H. and R. McGill, 1952, *Ind. Eng. Chem.*, 44:1391-1395.

Horton, J. E., 1976, "Characterization and Analysis of 104-BY Tank Sludge," (Internal Memo to W. R. Christensen, March 16, 1976), Atlantic Richfield Hanford Company, Richland, Washington.

Johnson, B. M., 1991, *External Advisory Panel Presentation*, Pacific Northwest Laboratory, Richland, Washington.

Jungfleisch, F. M., 1984, *Preliminary Estimation of the Waste Inventories in Hanford Tanks Through 1980*, SD-WM-TI-057, Rockwell Hanford Operations, Richland, Washington.

Kirk, J. J., 1980, *Permeability, Porosity and Capillarity of Hanford Waste Materials and Its Limits of Pumpability*, RHO-CD-925 REV 2, Rockwell Hanford Operations, Richland, Washington.

Klem, M. J., 1991, *Vapor Space Sampling Criteria for Single-Shell Tanks Containing Ferrocyanide Waste*, WHC-EP-0424, Westinghouse Hanford Company, Richland, Washington.

Knudsen, J. D. and D. L. Katz, 1958, *Fluid Dynamics and Heat Transfer*, pp. 136-138, McGraw-Hill Book Company, New York, New York.

Leggett, W. D., 1990, *Safety Improvement Plan - Hydrogen in Waste Tanks*, WHC-EP-0377, Rev. 1, Westinghouse Hanford Company, Richland, Washington.

Loos-Neskovic, C., M. Fedoroff, E. Garnier, and P. Gravereau, 1984, "Zinc and Nickel Ferrocyanides: Preparation, Composition, and Structure," *Talanta* Vol. 31, No. 12, pp. 1133-1147.

Loos-Neskovic, C. and M. Fedoroff, 1989, "Fixation Mechanisms of Cesium on Nickel and Zinc Ferrocyanides," *Solvent Extraction and Ion Exchange*, Vol. 7, No. 1, pp. 131-158.

Marks, L. S., 1951, *Mechanical Engineers' Handbook*, Fifth Edition, McGraw-Hill Book Company, New York, New York.

McLaren, J. M., 1991, *Single-Shell Tank 104-BY Thermal Hydraulic Analysis*, WHC-EP-0521, Westinghouse Hanford Company, Richland, Washington.

Metz, W. P., 1976, *A Topical Report on Interstitial Liquid Removal from Hanford Salt Cake*, ARH-CD-545, Atlantic Richfield Hanford Company, Richland, Washington.

Naono, H., K. Nakai, T. Sueyoshi, and H. Yagi, 1987, *Journal of Colloid and Interface Science*, Vol. 120, No. 2, pp. 439-450.

Nguyen, D. M., 1989, "Data Analysis of Conditions in Single-Shell Tanks Suspected of Containing Ferrocyanide," (Internal Memo 13314-89-025 to N. W. Kirch, March 2, 1989), Westinghouse Hanford Company, Richland, Washington.

Perry, R. H. and C. H. Chilton, 1973, *Chemical Engineers' Handbook*, Fifth Edition, McGraw-Hill Book Company, New York, New York.

Phillips, J. F., Jr., 1967, *A Survey of B-Plant Waste for Explosion Hazards*, BNWL-CC-1070, Pacific Northwest Laboratory, Richland, Washington.

Pickett, K. S., 1984, "Hexacyanoferrate (II) in Waste Tanks as a Result of Scavenging Operations," (External letter R84-0846 to L. L. Burger, March 23, 1984), Rockwell Hanford Operations, Richland, Washington.

Reynolds, D. A., 1990, "HEATING5 Modeling of 241-BY-104," Internal Memorandum 13314-90-001, Westinghouse Hanford Company, Richland, Washington.

Scheele, R. D., L. L. Burger, J. M. Tingey, S. A. Bryan, G. L. Borsheim, B. C. Simpson, R. J. Cash, and H. H. Cady, 1991, *Ferrocyanide-Containing Waste Tanks: Ferrocyanide Chemistry and Reactivity*, PNL-SA-19924, Pacific Northwest Laboratory, Richland, Washington.

Scheele, R. D. and H. H. Cady, 1992, *Preliminary Safe-Handling Experiments on a Mixture of Cesium Nickel Ferrocyanide and Equimolar Sodium Nitrate/ Nitrate*, PNL-7928, Pacific Northwest Laboratory, Richland, Washington.

Schmidt, W. C. and M. J. Stedwell, 1954, *Production Test 221-T-18 Scavenging of First Cycle Waste*, HW-33252, General Electric-Hanford Atomic Products Operation, Richland, Washington.

Schulz, W. W., 1980, *Removal of Radionuclides from Hanford Defense Waste Solutions*, RHO-SA-51, Rockwell Hanford Operations, Richland, Washington.

Sloat, R. J., 1954, *TBP Plant Nickel Ferrocyanide Scavenging Flow Sheet*, HW 30399, General Electric Company, Richland, Washington.

Sloat, R. J., 1955, *In-Farm Scavenging Operating Procedures and Control Data*, HW-38955, General Electric Company, Richland, Washington.

Smith, D. A., 1986, *Single-Shell Tank Isolation Safety Analysis Report*, SD-WM-SAR-006, Rev. 2, Rockwell Hanford Operations, Richland, Washington.

Stedwell, M. J., 1957, *Waste Scavenging Costs*, HW-47832, General Electric Company, Richland, Washington.

Stone, W. A., J. M. Thorp, O. P. Gifford, and D. J. Hoitink, 1983, *Climatological Summary for the Hanford Area*, PNL-4622, Pacific Northwest Laboratory, Richland, Washington.

Stong, F. S., 1986, *Dry Well Van In-Tank Liquid Observation Well Surveillance Data Interpretation*, RHO-SD-WM-TI-237, Rockwell Hanford Operations, Richland, Washington.

Subrahmanyam, V. B., G. L. Troyer, B. D. Keele, R. S. Addleman, and C. S. McClellan, 1991, *Application of a CdTe Gamma-Ray Spectrometer to Remote Characterization of High-Level Radioactive Waste Tanks*, WHC-SA-1196-FP, Westinghouse Hanford Company, Richland, Washington.

Sullivan, L. H., 1991, "Ferrocyanide Reanalysis Method," Presentation to High-Level Radioactive Waste Tank Task Force and Waste Tank Advisory Panel, Albuquerque, New Mexico, February 20-21, 1991.

Washburn, E. W. (ed), 1926, *International Critical Tables of Numerical Data, Physics, Chemistry and Technology*, McGraw-Hill Book Company, New York, New York.

Weast, R. C., 1976, *Handbook of Chemistry and Physics*, 57th Edition, CRC Press, The Chemical Rubber Company, Cleveland, Ohio.

Weiss, R. L., 1986, *TY Tank Farm Waste Characterization Data*, RHO-WM-TI-1P, Rockwell Hanford Operations, Richland, Washington.

Winters, W. I., 1988, "Analysis of Archive Samples from Tanks 241-TY-101 and 241-TY-103 for Total Cyanide," memo 12715-ASL88-067 to D. M. Nguyen, December 29, 1988.

Winters, W. I., L. Jensen, L. M. Sasaki, R. L. Weiss, J. S. Keller, A. J. Schmidt, and M. G. Woodruff, 1990, *Waste Characterization Plan for the Hanford Site Single-Shell Tanks*, WHC-EP-0210, Rev. 0, Westinghouse Hanford Company, Richland, Washington.

Winters, W. I., L. Jensen, L. M. Sasaki, R. L. Weiss, J. S. Keller, A. J. Schmidt, and M. G. Woodruff, 1991, *Waste Characterization Plan*, Appendix I, "Test Plan for Sampling and Analysis of Ten Single-Shell Tanks," WHC-EP-0210, Rev. 2 and 3, Westinghouse Hanford Company, Richland, Washington.

This page intentionally left blank.

APPENDIX A

FERROCYANIDE TANKS LABORATORY RESULTS

Appendix A presents analytical laboratory results for core samples taken from the TY Farm ferrocyanide tanks (241-TY-101, -103, and -104).

Tank 241-TY-103 was core sampled in 1979. The results of laboratory analysis for this sample were reported in Mitchell (1980) and are shown in Table A-1.

The six TY Farm tanks were core sampled in 1985 as part of the effort to develop reliable techniques for full depth-of-waste core sampling. One core was taken from tank 241-TY-101, two cores were taken from tank 241-TY-103, and four core samples were taken from tank 241-TY-104. These core samples were composited (homogenized) and analyzed. The results of laboratory analysis were reported in Weiss (1986) and are shown in Tables A-2 through A-9. Table A-2 presents a summary of the physical analysis results for the seven cores. Table A-3 presents the analytical chemistry results for the core taken from tank 241-TY-101. Tables A-4 and A-5 present the results for the two cores taken from tank 241-TY-103, and Tables A-6 through A-9 present the results for the four cores taken from tank 241-TY-104.

This page intentionally left blank.

Table A-1. Tank 241-TY-103--1979 Core Sample Chemical Characteristics. (sheet 1 of 2)

Ion	H_2O soluble wt%	H_2O insoluble wt%
Al^{3+}	NR	BDL
Bi^{3+}	0.03	5.48
Cd^{2+}	NR	BDL
Cl^-	1.78	NR
CO_3^{2-}	BDL	NR
Cr^{3+}	0.04	0.18
Fe^{3+}	NR	2.82
F^-	0.09	0.003
Hg^{2+}	NR	BDL
La^{3+}	NR	0.51
Mn^{2+}	NR	BDL
Na^+	9.58	1.11
Ni^{2+}	0.01	0.26
NO_3^-	21.37	BDL
OH^-	BDL	NR
Pb^{2+}	BDL	NR
PO_4^{3-}	3.04	2.63
Si^{4+}	0.09	1.47
SO_4^{2-}	BDL	BDL
Zr^{4+}	NR	BDL
TOC	0.004	BDL
% Soluble 36.03		% Insoluble 14.46
^{137}Cs	0.65 μCi/g	20.99 μCi/g
Pu	3.56×10^{-4} g/g	8.04×10^{-6} g/g
$^{89,90}Sr$	0.08 μCi/g	18.89 μCi/g
U	5.42×10^{-6} g/g	1.66×10^{-3} g/g

Table A-1. Tank 241-TY-103--1979 Core Sample Chemical Characteristics. (sheet 2 of 2)

Physical characteristics					
Segment number	1	2	3	4	Composite
% H_2O	--	--	53	60	53
Bulk density	--	--	1.74 g/cm^3	1.67 g/cm^3	1.50 g/cm^3
Particle density	--	--	2.37 g/cm^3	3.09 g/cm^3	2.18 g/cm^3
Thermal analysis	--	--	--	--	Exotherm 340-380 °C 34 cal/g

NOTE: As reported in Mitchell (1980).

Table A-2. Summary of 1985 TY Farm Core Sample Physical Analysis Results.

Analysis	TY-101	TY-103		TY-104			
	51XC*	31XC*	32XC*	232S*	241S*	251S*	261S*
Specific heat, J/g- °C	0.600	0.291	0.337	NT	NT	NT	NT
Softening point, °C	276	287	287	>1,000	>1,000	>1,000	>1,000
Bulk density, g/mL	1.64	1.70	1.70	1.85	1.77	1.66	1.48
Particle density, g/mL	0.92	0.69	0.75	1.12	0.87	0.93	1.19
Mean particle size, µm	8.2	12.2	8.3	7.7	8.1	8.2	8.1
Mass loss:							
Room to 400 °C, µg/g	4.35 E+05	5.12 E+05	5.25 E+05	5.07 E+05	5.90 E+05	6.27 E+05	5.55 E+05
400 to 1,000 °C, µg/g	1.60 E+05	1.48 E+05	1.53 E+05	7.31 E+04	9.40 E+04	8.41 E+04	1.17 E+05
% moisture	43.5	51.2	52.5	50.7	59.0	62.7	55.5
Viscosity, CP	>1.0 E+04	>1.0 E+04	>1.0 E+04	>1.0 E+04	>1.0 E+04	>1.0 E+04	>1.0 E+04

NOTE: As reported in Weiss (1986).
*Represent core composite sample IDs.
NT = no transition.

Table A-3. TY-101--1985 Core Composite 51XC Results. (sheet 1 of 2)

Component	Report unit	Report value (direct)	Report value (water)	Report value (acid)	Report value (fusion)	Report total	Maximum total
Aluminum	µg/g		3.90 E+01	1.34 E+04	1.56 E+04	2.91 E+04	2.91 E+04
Barium	µg/g		<3.92 E-01	1.67 E+01	1.91 E+03	1.92 E+03	1.92 E+03
Bismuth	µg/g		<8.63 E+00	2.65 E+04	7.17 E+02	2.72 E+04	2.72 E+04
Cadmium	µg/g		<1.96 E+00	3.14 E+00	3.52 E+00	8.66 E+00	1.06 E+01
Chromium	µg/g		4.24 E+02	5.00 E+02	7.48 E+03	8.40 E+03	8.40 E+03
Iron	µg/g		5.31 E+01	1.30 E+04	2.71 E+04	4.02 E+04	4.02 E+04
Lead	µg/g		<6.36 E+00	1.57 E+02	6.08 E+01	2.18 E+02	2.24 E+02
Manganese	µg/g		<1.57 E+01	3.83 E+01	5.04 E+02	5.42 E+02	5.58 E+02
Nickel	µg/g		7.67 E+01	8.95 E+02	4.12 E+03	5.10 E+03	5.10 E+03
Phosphorous	µg/g		5.39 E+03	1.91 E+04	7.56 E+02	2.53 E+04	2.53 E+04
Silicon	µg/g		3.22 E+02	6.57 E+02	3.77 E+04	3.87 E+04	3.87 E+04
Silver	µg/g		<7.85 E-01	<9.81 E-01	<2.08 E+00	0.00 E+00	3.85 E+00
Sodium	µg/g		7.50 E+04	3.33 E+04	1.30 E+04	1.21 E+05	1.21 E+05
Zirconium	µg/g		<3.61 E+00	<4.51 E+00	3.77 E+02	3.77 E+02	3.85 E+02
Uranium	µg/g		1.12 E+01	2.29 E+03	3.75 E+01	2.33 E+03	2.33 E+03
Chloride	µg/g		7.57 E+02			7.57 E+02	7.57 E+02
Fluoride	µg/g		3.37 E+03	0.00 E+00		3.37 E+03	3.37 E+03
Nitrate	µg/g		1.45 E+05	0.00 E+00		1.45 E+05	1.45 E+05
Sulfate	µg/g		<5.49 E+03	0.00 E+00	0.00 E+00	0.00 E+00	5.49 E+03
Nitrite	µg/g						
Carbonate	µg/g						
Total organic carbon	µg/g		2.53 E+02	4.10 E+02		6.63 E+02	6.63 E+02
Free hydroxide	µg/g		2.12 E-01			2.12 E-01	2.12 E-01
pH	log(1/M)	10.00	8.20 E+00			8.20 E+00	8.20 E+00

Table A-3. TY-101--1985 Core Composite 51XC Results. (sheet 2 of 2)

Component	Report unit	Report value (direct)	Report value (water)	Report value (acid)	Report value (fusion)	Report total	Maximum total
Mass loss							
Room to 400 °C	µg/g	4.35 E+05				4.35 E+05	4.35 E+05
400 to 1,000 °C	µg/g	1.60 E+05				1.60 E+05	1.60 E+05
$^{239,240}Pu$	uCi/g		<5.73 E-04	1.19 E-01	7.17 E-02	1.91 E-01	1.91 E-01
Total alpha	uCi/g						
^{14}C	uCi/g		<3.98 E-04	<4.85 E-04		0.00 E+00	8.72 E-04
^{90}Sr	uCi/g		<1.93 E-04	1.22 E+01	2.79 E-01	1.24 E+01	1.24 E+01
^{99}Tc	uCi/g		4.35 E-03	3.01 E-03	0.00 E+00	7.36 E-03	7.36 E-03
Total beta	uCi/g						
^{241}Am	uCi/g		<3.65 E-04	<2.21 E-03	<1.05 E-02	0.00 E+00	1.30 E-02
^{60}Co	uCi/g		<1.11 E-04	<5.09 E-03	<4.77 E-03	0.00 E+00	9.97 E-03
^{137}Cs	uCi/g		2.63 E-04	1.63 E-01	1.21 E-01	2.84 E-01	2.84 E-01
^{129}I	uCi/g	<4.70 E-05				0.00 E+00	4.70 E-05
Total gamma	uCi/g		2.63 E-04	1.63 E-01	1.21 E-01	2.84 E-01	2.84 E-01
Mass (total)	g	3.65 E+01				3.65 E+01	3.65 E+01
Radiation	mR/h	1.00 E+01	1.00 E+00	4.00 E+00	<7.20 E+01		
Specific heat	J/g °C	6.00 E-01				6.00 E-01	6.00 E-01
Softening point	°C	2.76 E+02				2.76 E+02	2.76 E+02
Bulk density	g/mL	1.64 E+00				1.64 E+00	1.64 E+00
Particle density	g/mL	9.24 E-01				9.24 E-01	9.24 E-01
Viscosity							
25 °C	cP	>1.00 E+04				>1.00 E+04	
40 °C	cP	>1.00 E+04				>1.00 E+04	
70 °C	cP	>1.00 E+04				>1.00 E+04	

Table A-4. TY-103--1985 Core Composite 31XC Results. (sheet 1 of 2)

Component	Report unit	Report value (direct)	Report value (water)	Report value (acid)	Report value (fusion)	Report total	Maximum total
Aluminum	µg/g		1.38 E+01	1.43 E+01	1.46 E+03	1.48 E+03	1.48 E+03
Barium	µg/g		3.19 E-01	5.54 E+01	5.23 E+02	5.79 E+02	5.79 E+02
Bismuth	µg/g		<6.88 E+00	2.41 E+04	2.28 E+01	2.42 E+04	2.42 E+04
Cadmium	µg/g		<1.56 E+00	3.04 E+00	<1.12 E+00	3.04 E+00	5.72 E+00
Chromium	µg/g		3.53 E+02	4.80 E+02	3.80 E+01	8.71 E+02	8.71 E+02
Iron	µg/g		7.07 E+01	2.14 E+04	6.93 E+02	2.22 E+04	2.22 E+04
Lead	µg/g		<5.07 E+00	5.14 E+02	7.15 E+00	5.21 E+02	5.26 E+02
Manganese	µg/g		<1.25 E+01	1.40 E+02	<8.94 E+00	1.40 E+02	1.62 E+02
Nickel	µg/g		4.34 E+01	1.39 E+03	5.32 E+02	1.97 E+03	1.97 E+03
Phosphorous	µg/g		9.88 E+03	1.89 E+04	2.97 E+02	2.91 E+04	2.91 E+04
Silicon	µg/g		7.01 E+01	3.34 E+02	1.05 E+03	1.50 E+03	1.50 E+03
Silver	µg/g		<6.26 E-01	1.25 E+00	1.70 E+00	2.95 E+00	3.57 E+00
Sodium	µg/g		7.82 E+04	3.30 E+04	3.98 E+03	1.15 E+05	1.15 E+05
Zirconium	µg/g		<2.88 E+00	<4.11 E+00	4.16 E+02	4.16 E+02	4.23 E+02
Uranium	µg/g		5.82 E+01	1.92 E+04	2.18 E+01	1.93 E+04	1.93 E+04
Chloride	µg/g		1.04 E+03			1.04 E+03	1.04 E+03
Fluoride	µg/g		1.91 E+03	0.00 E+00		1.91 E+03	1.91 E+03
Nitrate	µg/g		1.29 E+05	6.04 E+03		1.35 E+05	1.35 E+05
Sulfate	µg/g		7.81 E+03	<4.57 E+02	0.00 E+00	7.81 E+03	8.27 E+03
Nitrite	µg/g		7.51 E+03			7.51 E+03	7.51 E+03
Carbonate	µg/g		7.32 E+03			7.32 E+03	7.32 E+03
Total organic carbon	µg/g		4.96 E+02	2.19 E+02		7.15 E+02	7.15 E+02
Free hydroxide	µg/g		1.68 E+02			1.68 E+02	1.68 E+02
pH	log (1/M)	10.5	1.12 E+01			1.12 E+01	1.12 E+01

Table A-4. TY-103--1985 Core Composite 31XC Results. (sheet 2 of 2)

Component	Report unit	Report value (direct)	Report value (water)	Report value (acid)	Report value (fusion)	Report total	Maximum total
Mass loss							
Room to 400 °C	µg/g	5.12 E+05				5.12 E+05	5.12 E+05
400 to 1,000 °C	µg/g	1.48 E+05				1.48 E+05	1.48 E+05
$^{239,240}Pu$	uCi/g		<1.77 E-04	1.84 E-01	5.59 E-03	1.90 E-01	1.90 E-01
Total alpha	uCi/g		<1.56 E-03	0.00 E+00	0.00 E+00	0.00 E+00	1.56 E-03
^{14}C	uCi/g		<7.57 E-04	0.00 E+00		0.00 E+00	7.57 E-04
^{90}Sr	uCi/g		1.31 E-02	1.15 E+02	6.17 E-02	1.15 E+02	1.15 E+02
^{99}Tc	uCi/g		1.01 E-02	5.00 E-03	0.00 E+00	1.51 E-02	1.51 E-02
Total beta	uCi/g		0.00 E+00	4.83 E+02	1.71 E+01	5.00 E+02	5.00 E+02
^{241}Am	uCi/g		<1.28 E-03	<3.71 E-02	<9.34 E-04	0.00 E+00	3.75 E-02
^{60}Co	uCi/g		1.19 E-03	1.35 E-03	<1.15 E-03	1.19 E-03	3.69 E-03
^{137}Cs	uCi/g		1.13 E-03	9.03 E-01	9.87 E+00	1.08 E+01	1.08 E+01
^{129}I	uCi/g	<4.90 E-02				0.00 E+00	4.90 E-02
Total gamma	uCi/g		2.31 E-03	1.13 E+00	9.87 E+00	1.10 E+01	1.10 E+01
Mass (total)	g	3.86 E+01				3.86 E+01	3.86 E+01
Radiation	mR/h	5.00 E+01	3.50 E+00	5.00 E+01	7.20 E+01		
Specific heat	J/g °C	2.91 E-01				2.91 E-01	2.91 E-01
Softening point	°C	2.87 E+02				2.87 E+02	2.87 E+02
Bulk density	g/mL	1.70 E+00				1.70 E+00	1.70 E+00
Particle density	g/mL	6.89 E-01				6.89 E-01	6.89 E-01
Viscosity							
25 °C	cP	>1.00 E+04				>1.00 E+04	
40 °C	cP	>1.00 E+04				>1.00 E+04	
70 °C	cP	>1.00 E+04				>1.00 E+04	

Table A-5. TY-103--1985 Core Composite 32XC Results. (sheet 1 of 2)

Component	Report unit	Report value (direct)	Report value (water)	Report value (acid)	Report value (fusion)	Report total	Maximum total
Aluminum	µg/g		4.24 E+00	3.78 E+03	4.28 E+02	4.22 E+03	4.22 E+03
Barium	µg/g		7.07 E+00	4.13 E+01	4.52 E+02	5.01 E+02	5.01 E+02
Bismuth	µg/g		<7.07 E+00	2.74 E+04	5.51 E+00	2.74 E+04	2.74 E+04
Cadmium	µg/g		<1.61 E+00	4.87 E+00	<1.15 E+00	4.87 E+00	7.62 E+00
Chromium	µg/g		4.06 E+02	5.88 E+02	8.73 E+00	1.00 E+03	1.00 E+03
Iron	µg/g		1.56 E+02	2.26 E+04	1.05 E+03	2.38 E+04	2.38 E+04
Lead	µg/g		<5.21 E+00	4.41 E+02	<2.23 E+01	4.41 E+02	4.68 E+02
Manganese	µg/g		<1.29 E+01	1.38 E+02	<9.18 E+00	1.38 E+02	1.60 E+02
Nickel	µg/g		6.36 E+01	1.35 E+03	1.12 E+03	2.53 E+03	2.53 E+03
Phosphorous	µg/g		6.31 E+03	1.46 E+04	5.28 E+01	2.10 E+04	2.10 E+04
Silicon	µg/g		7.26 E+01	5.14 E+02	8.82 E+03	9.40 E+03	9.40 E+03
Silver	µg/g		<6.43 E-01	7.44 E+00	<9.18 E-01	7.44 E+00	9.00 E+00
Sodium	µg/g		7.39 E+04	2.86 E+04	3.42 E+03	1.06 E+05	1.06 E+05
Zirconium	µg/g		<2.96 E+00	<4.22 E+00	4.45 E+01	4.45 E+01	5.16 E+01
Uranium	µg/g		4.14 E+01	1.62 E+04	6.06 E+00	1.62 E+04	1.62 E+04
Chloride	µg/g		1.20 E+03			1.20 E+03	1.20 E+03
Fluoride	µg/g		<8.60 E+02	0.00 E+00		0.00 E+00	8.60 E+02
Nitrate	µg/g		1.49 E+05	6.95 E+03		1.56 E+05	1.56 E+05
Sulfate	µg/g		9.26 E+03	5.33 E+02	0.00 E+00	9.80 E+03	9.80 E+03
Nitrite	µg/g		8.10 E+03			8.10 E+03	8.10 E+03
Carbonate	µg/g		4.78 E+03			4.78 E+03	4.78 E+03
Total organic carbon	µg/g		9.90 E+02	5.01 E+02		1.49 E+03	1.49 E+03
Free hydroxide	µg/g		8.68 E+01			8.68 E+01	8.68 E+01
pH	log (1/M)	10.5	1.09 E+01			1.09 E+01	1.09 E+01

Table A-5. TY-103--1985 Core Composite 32XC Results. (sheet 2 of 2)

Component	Report unit	Report value (direct)	Report value (water)	Report value (acid)	Report value (fusion)	Report total	Maximum total
Mass loss							
Room to 400 °C	µg/g	5.25 E+05				5.25 E+05	5.25 E+05
400 to 1,000 °C	µg/g	1.53 E+05				1.53 E+05	1.53 E+05
$^{239,240}Pu$	uCi/g		<1.72 E-04	1.75 E-01	1.35 E-03	1.77 E-01	1.77 E-01
Total alpha	uCi/g		<1.60 E-03	0.00 E+00	0.00 E+00	0.00 E+00	1.60 E-03
^{14}C	uCi/g		<7.78 E-04	<4.55 E-04		0.00 E+00	1.23 E-03
^{90}Sr	uCi/g		8.94 E-03	1.05 E+02	2.38 E-02	1.05 E+02	1.05 E+02
^{99}Tc	uCi/g		1.13 E-02	5.07 E-03	0.00 E+00	1.64 E-02	1.64 E-02
Total beta	uCi/g		<4.91 E-02	4.44 E+02	3.84 E+01	4.82 E+02	4.82 E+02
^{241}Am	uCi/g		<9.64 E-04	<2.48 E-02	<1.02 E-03	0.00 E+00	2.68 E-02
^{60}Co	uCi/g		9.00 E-04	<2.76 E-03	<1.01 E-03	9.00 E-04	4.67 E-03
^{137}Cs	uCi/g		<5.14 E-04	2.00 E+00	2.27 E+01	2.47 E+01	2.47 E+01
^{129}I	uCi/g	<2.70 E-03				0.00 E+00	2.70 E-03
Total gamma	uCi/g		1.41 E-03	1.91 E+00	2.27 E+01	2.46 E+01	2.46 E+01
Mass (total)	g	4.58 E+01				4.58 E+01	4.58 E+01
Radiation	mR/h	1.00 E+02	3.00 E+00	4.50 E+01	7.20 E+01		
Specific heat	J/g °C	3.37 E-01					
Softening point	°C	2.87 E+02				2.87 E+02	2.87 E+02
Bulk density	g/mL	1.70 E+00				1.70 E+00	1.70 E+00
Particle density	g/mL	7.45 E-01				7.54 E-01	7.54 E-01
Viscosity							
25 °C	cP	>1.00 E+04				>1.00 E+04	
40 °C	cP	>1.00 E+04				>1.00 E+04	
70 °C	cP	>1.00 E+04				>1.00 E+04	

Table A-6. TY-104--1985 Core Composite 232S Results. (sheet 1 of 2)

Component	Report unit	Report value (direct)	Report value (water)	Report value (acid)	Report value (fusion)	Report total	Maximum total
Aluminum	µg/g		2.78 E+02	6.55 E+03	3.23 E+03	1.00 E+04	1.00 E+04
Barium	µg/g		7.45 E-01	4.24 E+01	2.78 E+02	3.21 E+02	3.21 E+02
Bismuth	µg/g		<1.02 E+01	9.10 E+03	5.75 E+01	9.15 E+03	9.16 E+03
Cadmium	µg/g		<2.33 E+00	8.57 E+00	<1.40 E+00	8.57 E+00	1.23 E+01
Chromium	µg/g		6.24 E+02	2.99 E+02	4.80 E+00	9.28 E+02	9.28 E+02
Iron	µg/g		6.86 E+01	2.20 E+04	3.98 E+02	2.25 E+04	2.25 E+04
Lead	µg/g		<7.45 E+00	4.15 E+02	1.06 E+01	4.26 E+02	4.33 E+02
Manganese	µg/g		<1.86 E+01	2.66 E+03	<1.12 E+01	2.66 E+03	2.69 E+03
Nickel	µg/g		1.12 E+01	8.10 E+02	2.86 E+01	8.50 E+02	8.50 E+02
Phosphorous	µg/g		3.50 E+04	3.82 E+03	5.14 E+01	3.89 E+04	3.89 E+04
Silicon	µg/g		7.26 E+01	2.14 E+02	2.29 E+03	2.58 E+03	2.58 E+03
Silver	µg/g		2.61 E+00	6.52 E+00	3.35 E-01	9.46 E+00	9.46 E+00
Sodium	µg/g		1.23 E+05	1.22 E+04	1.94 E+03	1.37 E+05	1.37 E+05
Zirconium	µg/g		<4.28 E+00	<4.28 E+00	1.31 E+02	1.31 E+02	1.39 E+02
Uranium	µg/g		9.16 E+01	1.22 E+04	7.32 E-01	1.23 E+04	1.23 E+04
Chloride	µg/g		<8.48 E+02			0.00 E+00	8.48 E+02
Fluoride	µg/g		1.02 E+04	0.00 E+00		1.02 E+04	1.02 E+04
Nitrate	µg/g		3.31 E+04	1.92 E+03		3.50 E+04	3.50 E+04
Sulfate	µg/g		<7.03 E+03	<1.17 E+03	0.00 E+00	0.00 E+00	8.20 E+03
Nitrite	µg/g		9.30 E+03			9.30 E+03	9.30 E+03
Carbonate	µg/g		1.46 E+04			1.46 E+04	1.46 E+04
Total organic carbon	µg/g		1.81 E+03	2.96 E+02		2.10 E+03	2.10 E+03
Free hydroxide	µg/g		1.58 E+03			1.58 E+03	1.58 E+03
pH	log (1/M)		1.20 E+01			1.20 E+01	1.20 E+01

Table A-6. TY-104--1985 Core Composite 232S Results. (sheet 2 of 2)

Component	Report unit	Report value (direct)	Report value (water)	Report value (acid)	Report value (fusion)	Report total	Maximum total
Mass loss							
Room to 400 °C	µg/g	5.07 E+05				5.07 E+05	5.07 E+05
400 to 1,000 °C	µg/g	7.31 E+04				7.31 E+04	7.31 E+04
$^{239,240}Pu$	uCi/g		<7.11 E-04	1.34 E-01	1.44 E-03	1.36 E-01	1.36 E-01
Total alpha	uCi/g		<2.84 E-03	5.74 E-01	<7.71 E-04	5.74 E-01	5.77 E-01
^{14}C	uCi/g		9.78 E-04	2.29 E-03		3.27 E-03	3.27 E-03
^{90}Sr	uCi/g		4.98 E-02	2.94 E+01	7.71 E-03	2.95 E+01	2.95 E+01
^{99}Tc	uCi/g		2.04 E-02	3.14 E-03	0.00 E+00	2.35 E-02	2.35 E-02
Total beta	uCi/g		1.24 E+01	8.94 E+02	5.87 E-01	9.07 E+02	9.07 E+02
^{241}Am	uCi/g		<1.74 E-03	1.83 E-02	<1.88 E-03	1.83 E-02	2.22 E-02
^{60}Co	uCi/g		<1.69 E-03	<1.22 E-02	<1.53 E-03	0.00 E+00	1.55 E-02
^{137}Cs	uCi/g		7.05 E+00	7.78 E+00	2.68 E-01	1.51 E+01	1.51 E+01
^{129}I	uCi/g	<4.70 E-02				0.00 E+00	4.70 E-02
Total gamma	uCi/g		7.05 E+00	1.17 E+01	2.68 E-01	1.90 E+01	1.90 E+01
Mass (total)	g						
Radiation	mR/h	2.00 E+02	1.30 E+01	5.00 E+02	7.20 E+01		
Specific heat	J/g °C	No transition				No transition	No transition
Softening point	°C	>1.00 E+03				1.00 E+03	1.00 E+03
Bulk density	g/mL	1.85 E+00				1.85 E+00	1.85 E+00
Particle density	g/mL	1.12 E+00				1.12 E+00	1.12 E+00
Viscosity							
25 °C	cP	>1.00 E+04					>1.00 E+04
40 °C	cP	>1.00 E+04					>1.00 E+04
70 °C	cP	>1.00 E+04					>1.00 E+04

Table A-7. TY-104--1985 Core Composite 241S Results. (sheet 1 of 2)

Component	Report unit	Report value (direct)	Report value (water)	Report value (acid)	Report value (fusion)	Report total	Maximum total
Aluminum	µg/g		3.21 E+02	7.47 E+03	1.54 E+03	9.33 E+03	9.33 E+03
Barium	µg/g		8.46 E-01	4.66 E+01	4.57 E+02	5.05 E+02	5.05 E+02
Bismuth	µg/g		<1.03 E+01	1.67 E+04	2.76 E+01	1.68 E+04	1.68 E+04
Cadmium	µg/g		<2.35 E+00	1.98 E+01	<1.41 E+00	1.88 E+01	2.26 E+01
Chromium	µg/g		6.64 E+02	1.22 E+03	1.37 E+01	1.90 E+03	1.90 E+03
Iron	µg/g		7.52 E+01	5.52 E+04	3.51 E+03	5.88 E+04	5.88 E+04
Lead	µg/g		<7.61 E+00	5.83 E+02	1.04 E+01	5.93 E+02	6.01 E+02
Manganese	µg/g		<1.88 E+01	2.31 E+03	2.43 E+01	2.34 E+03	2.36 E+03
Nickel	µg/g		1.20 E+01	1.70 E+03	4.09 E+01	1.75 E+03	1.75 E+03
Phosphorous	µg/g		1.87 E+04	1.09 E+04	8.23 E+01	2.97 E+04	2.97 E+04
Silicon	µg/g		8.36 E+01	1.50 E+02	9.25 E+03	9.48 E+03	9.48 E+03
Silver	µg/g		2.82 E+00	9.40 E+00	7.89 E-01	1.30 E+01	1.30 E+01
Sodium	µg/g		8.16 E+04	3.40 E+04	3.46 E+03	1.19 E+05	1.19 E+05
Zirconium	µg/g		<4.32 E+00	<4.32 E+00	1.73 E+02	1.73 E+02	1.82 E+02
Uranium	µg/g		2.61 E+01	2.12 E+04	4.39 E+00	2.13 E+04	2.13 E+04
Chloride	µg/g		4.63 E+02			4.63 E+02	4.63 E+02
Fluoride	µg/g		5.54 E+03	0.00 E+00		5.54 E+03	5.54 E+03
Nitrate	µg/g		3.47 E+04	1.22 E+03		3.59 E+04	3.59 E+04
Sulfate	µg/g		<2.71 E+03	<1.18 E+03	0.00 E+00	0.00 E+00	3.89 E+03
Nitrite	µg/g		9.77 E+03			9.77 E+03	9.77 E+03
Carbonate	µg/g		1.64 E+04			1.64 E+04	1.64 E+04
Total organic carbon	µg/g		2.27 E+03	5.17 E+02		2.78 E+03	2.78 E+03
Free hydroxide	µg/g		1.24 E+03			1.24 E+03	1.24 E+03
pH	log (1/M)		1.19 E+01			1.19 E+01	1.19 E+01

Table A-7. TY-104--1985 Core Composite 241S Results. (sheet 2 of 2)

Component	Report unit	Report value (direct)	Report value (water)	Report value (acid)	Report value (fusion)	Report total	Maximum total
Mass loss							
Room to 400 °C	µg/g	5.90 E+05				5.90 E+05	5.90 E+05
400 to 1,000 °C	µg/g	9.40 E+04				9.40 E+04	9.40 E+04
$^{239,240}Pu$	uCi/g		<7.55 E-04	1.84 E-01	8.68 E-03	1.93 E-01	1.94 E-01
Total alpha	uCi/g		<2.87 E-03	2.70 E-01	8.63 E-03	2.78 E-01	2.81 E-01
^{14}C	uCi/g		4.10 E-03	6.90 E-04		4.79 E-03	4.79 E-03
^{90}Sr	uCi/g		2.73 E-02	2.15 E+02	2.09 E-02	2.15 E+02	2.15 E+02
^{99}Tc	uCi/g		1.75 E-02	1.32 E-02	0.00 E+00	3.06 E-02	3.06 E-02
Total beta	uCi/g		1.06 E+01	4.73 E+02	1.63 E+01	5.00 E+02	5.00 E+02
^{241}Am	uCi/g		<1.95 E-03	<2.79 E-02	<1.92 E-03	0.00 E+00	3.17 E-02
^{60}Co	uCi/g		<2.09 E-03	2.30 E-02	9.92 E-04	0.00 E+00	2.61 E-02
^{137}Cs	uCi/g		7.97 E+00	9.96 E+00	8.18 E+00	2.61 E+01	2.61 E+01
^{129}I	uCi/g	3.35 E-05				3.35 E-05	3.35 E-05
Total gamma	uCi/g		7.97 E+00	1.10 E+01	8.18 E+00	2.71 E+01	2.71 E+01
Mass (total)	g	3.13 E+01				3.13 E+01	3.13 E+01
Radiation	mR/h	2.50 E+02	1.30 E+01	7.50 E+02	7.20 E+01		
Specific heat	J/g °C	No transition				No transition	No transition
Softening point	°C	>1.00 E+03				1.00 E+03	1.00 E+03
Bulk density	g/mL	1.77 E+00				1.77 E+00	1.77 E+00
Particle density	g/mL	8.67 E-01				8.67 E-01	8.67 E-01
Viscosity							
25 °C	cP	>1.00 E+04				>1.00 E+04	
40 °C	cP	>1.00 E+04				>1.00 E+04	
70 °C	cP	>1.00 E+04				>1.00 E+04	

Table A-8. TY-104--1985 Core Composite 251S Results. (sheet 1 of 2)

Component	Report unit	Report value (direct)	Report value (water)	Report value (acid)	Report value (fusion)	Report total	Maximum total
Aluminum	µg/g		7.05 E+02	7.17 E+03	8.94 E+02	8.77 E+03	8.77 E+03
Barium	µg/g		<9.12 E-01	5.93 E+01	5.55 E+02	6.15 E+02	6.15 E+02
Bismuth	µg/g		<9.12 E+00	2.57 E+04	4.93 E+00	2.57 E+04	2.57 E+04
Cadmium	µg/g		<5.47 E+00	1.64 E+01	<1.14 E+00	1.64 E+01	2.30 E+01
Chromium	µg/g		1.18 E+03	3.07 E+02	1.25 E+00	1.48 E+03	1.48 E+03
Iron	µg/g		1.67 E+02	2.55 E+04	1.30 E+02	2.59 E+04	2.58 E+04
Lead	µg/g		<1.82 E+01	6.29 E+02	4.27 E+00	6.33 E+02	6.51 E+02
Manganese	µg/g		3.47 E+00	1.36 E+03	9.22 E+00	1.37 E+03	1.37 E+03
Nickel	µg/g		1.28 E+01	1.61 E+03	9.44 E+00	1.63 E+03	1.63 E+03
Phosphorous	µg/g		5.01 E+03	3.18 E+03	1.21 E+02	8.31 E+03	8.31 E+03
Silicon	µg/g		2.74 E+01	3.01 E+02	9.30 E+03	9.63 E+03	9.68 E+03
Silver	µg/g		4.56 E+00	1.82 E+01	7.76 E-01	2.36 E+01	2.36 E+01
Sodium	µg/g		6.66 E+04	1.35 E+04	4.05 E+03	8.42 E+04	8.42 E+04
Zirconium	µg/g		<6.39 E+00	7.21 E+00	1.98 E+02	2.06 E+02	2.12 E+02
Uranium	µg/g		1.93 E+01	1.57 E+04	2.72 E+00	1.57 E+04	1.57 E+04
Chloride	µg/g		8.09 E+02			8.09 E+02	8.09 E+02
Fluoride	µg/g		1.06 E+03	0.00 E+00		1.06 E+03	1.06 E+03
Nitrate	µg/g		6.05 E+04	1.79 E+03		6.23 E+04	6.23 E+04
Sulfate	µg/g		3.68 E+03	<1.15 E+03	0.00 E+00	3.68 E+03	4.83 E+03
Nitrite	µg/g		1.69 E+04			1.69 E+04	1.69 E+04
Carbonate	µg/g		2.39 E+04			2.39 E+04	2.39 E+04
Total organic carbon	µg/g		1.73 E+03	2.19 E+02		1.95 E+03	1.95 E+03
Free hydroxide	µg/g		7.78 E+02			7.78 E+02	7.78 E+02
pH	log (1/M)		1.17 E+01			1.17 E+01	1.17 E+01
Mass loss							
Room to 400 °C	µg/g	6.27 E+05				6.27 E+05	6.27 E+05
400 to 1,000 °C	µg/g	8.41 E+04				8.41 E+04	8.41 E+04

Table A-8. TY-104--1985 Core Composite 251S Results. (sheet 2 of 2)

Component	Report unit	Report value (direct)	Report value (water)	Report value (acid)	Report value (fusion)	Report total	Maximum total
$^{239,240}Pu$	uCi/g		<7.58 E-04	1.87 E-01	2.81 E-03	1.90 E-01	1.91 E-01
Total alpha	uCi/g		<1.52 E-02	1.81 E-01	<2.02 E-03	1.81 E-01	1.98 E-01
^{14}C	uCi/g		2.03 E-03	<4.52 E-04		2.03 E-03	2.49 E-03
^{90}Sr	uCi/g		5.21 E-02	4.56 E+01	1.37 E-01	4.58 E+01	4.58 E+01
^{99}Tc	uCi/g		3.10 E-02	3.52 E-03	0.00 E+00	3.45 E-02	3.45 E-02
Total beta	uCi/g		1.13 E+01	5.41 E+02	1.09 E+02	6.61 E+02	6.61 E+02
^{241}Am	uCi/g		<1.82 E-03	3.47 E-02	<6.43 E-03	3.47 E-02	4.29 E-02
^{60}Co	uCi/g		<3.08 E-03	<3.72 E-02	<2.90 E-03	0.00 E+00	4.32 E-02
^{137}Cs	uCi/g		1.15 E+01	1.61 E+01	6.57 E+01	9.32 E+01	9.32 E+01
^{129}I	uCi/g	<9.00 E-02				0.00 E+00	9.00 E-02
Total gamma	uCi/g		1.15 E+01	1.69 E+01	6.71 E+01	9.54 E+01	9.54 E+01
Mass (total)	g	1.83 E+02				1.83 E+02	1.83 E+02
Radiation	mR/h	4.50 E+02	1.30 E+01	6.00 E+02	7.20 E+01	4.50 E+02	4.50 E+02
Specific heat	J/g °C	No transition				No transition	No transition
Softening point	°C	>1.00 E+03				1.00 E+03	1.00 E+03
Bulk density	g/mL	1.66 E+00				1.66 E+00	1.66 E+00
Particle density	g/mL	9.28 E-01				9.28 E-01	9.28 E-01
Viscosity							
25 °C	cP	>1.00 E+04				>1.00 E+04	
40 °C	cP	>1.00 E+04				>1.00 E+04	
70 °C	cP	>1.00 E+04				>1.00 E+04	

Table A-9. TY-104--1985 Core Composite 261S Results. (sheet 1 of 2)

Component	Report unit	Report value (direct)	Report value (water)	Report value (acid)	Report value (fusion)	Report total	Maximum total
Aluminum	µg/g		3.54 E+02	6.64 E+03	1.21 E+03	8.21 E+03	8.21 E+03
Barium	µg/g		1.29 E+00	6.35 E+01	2.66 E+02	3.30 E+02	3.30 E+02
Bismuth	µg/g		<1.06 E+01	1.91 E+04	2.81 E+02	1.94 E+04	1.94 E+04
Cadmium	µg/g		<2.41 E+00	6.74 E+00	<1.20 E+00	6.74 E+00	1.03 E+01
Chromium	µg/g		1.12 E+03	2.11 E+02	1.15 E+01	1.35 E+03	1.35 E+03
Iron	µg/g		3.23 E+01	2.26 E+04	6.01 E+02	2.32 E+04	2.32 E+04
Lead	µg/g		<7.79 E+00	5.99 E+02	2.60 E+01	6.25 E+02	6.32 E+02
Manganese	µg/g		<1.92 E+01	4.77 E+02	9.86 E+00	4.87 E+02	5.06 E+02
Nickel	µg/g		3.06 E+01	1.64 E+03	6.25 E+01	1.73 E+03	1.73 E+03
Phosphorous	µg/g		1.24 E+04	1.52 E+04	3.09 E+02	2.79 E+04	2.79 E+04
Silicon	µg/g		4.67 E+02	2.54 E+02	9.96 E+03	1.07 E+04	1.07 E+04
Silver	µg/g		1.15 E+00	<9.62 E-01	1.25 E+00	2.41 E+00	3.37 E+00
Sodium	µg/g		7.34 E+04	3.64 E+04	2.40 E+03	1.12 E+05	1.12 E+05
Zirconium	µg/g		<3.85 E+00	5.39 E+00	1.84 E+02	1.90 E+02	1.94 E+02
Uranium	µg/g		1.48 E+01	2.81 E+04	4.91 E+02	2.86 E+04	2.86 E+04
Chloride	µg/g		6.72 E+02			6.72 E+02	6.72 E+02
Fluoride	µg/g		4.61 E+03	0.00 E+00		4.61 E+03	4.61 E+03
Nitrate	µg/g		5.04 E+04	2.78 E+03		5.32 E+04	5.32 E+04
Sulfate	µg/g		<2.77 E+03	<1.21 E+03	0.00 E+00	0.00 E+00	3.98 E+03
Nitrite	µg/g		1.29 E+04			1.29 E+04	1.29 E+04
Carbonate	µg/g		1.99 E+04			1.99 E+04	1.99 E+04
Total organic carbon	µg/g		7.41 E+02	1.66 E+02		9.07 E+02	9.07 E+02
Free hydroxide	µg/g		1.56 E+03			1.56 E+03	1.56 E+03
pH	log (1/M)	11.5	1.20 E+01			1.20 E+01	1.20 E+01

Table A-9. TY-104--1985 Core Composite 261S Results. (sheet 2 of 2)

Component	Report unit	Report value (direct)	Report value (water)	Report value (acid)	Report value (fusion)	Report total	Maximum total
Mass loss							
Room to 400 °C	µg/g	5.55 E+05				5.55 E+05	5.55 E+05
400 to 1,000 °C	µg/g	1.17 E+05				1.17 E+05	1.17 E+05
$^{239,240}Pu$	uCi/g		3.49 E-04	1.87 E-01	1.47 E-02	2.02 E-01	2.02 E-01
Total alpha	uCi/g		<2.01 E-03	2.07 E-01	8.76 E-03	2.16 E-01	2.18 E-01
^{14}C	uCi/g		<1.08 E-03	<1.08 E-03		0.00 E+00	2.16 E-03
^{90}Sr	uCi/g		2.78 E-02	2.35 E+02	1.28 E+00	2.36 E+02	2.36 E+02
^{99}Tc	uCi/g		2.71 E-02	7.28 E-03	0.00 E+00	3.44 E-02	3.44 E-02
Total beta	uCi/g		7.50 E+01	7.62 E+02	5.24 E+00	8.42 E+02	8.42 E+02
^{241}Am	uCi/g		<2.21 E-03	<3.31 E-02	<1.57 E-03	0.00 E+00	3.69 E-02
^{60}Co	uCi/g		<4.27 E-03	<1.16 E-03	<2.89 E-04	0.00 E+00	5.73 E-03
^{137}Cs	uCi/g		3.93 E+01	6.94 E+00	7.60 E-01	4.70 E+01	4.70 E+01
^{129}I	uCi/g	<5.90 E-02				0.00 E+00	5.90 E-02
Total gamma	uCi/g		3.93 E+01	7.03 E+00	7.60 E-01	4.71 E+01	4.71 E+01
Mass (total)	g	2.08 E+02				2.08 E+02	2.08 E+02
Radiation	mR/h	2.50 E+03	1.50 E+01	2.20 E+02	7.20 E+01		
Specific heat	J/g °C	No transition				No transition	No transition
Softening point	°C	1.00 E+03				1.00 E+03	1.00 E+03
Bulk density	g/mL	1.48 E+00				1.48 E+00	1.48 E+00
Particle density	g/mL	1.19 E+00				1.19 E+00	1.19 E+00
Viscosity							
25 °C	cP	>1.00 E+4				>1.00 E+04	
40 °C	cP	>1.00 E+4				>1.00 E+04	
70 °C	cP	>1.00 E+$				>1.00 E-04	

REFERENCES

Mitchell, M. E., 1980, "Physical and Chemical Characteristics of Tanks 105-TY, and 102-TY" (Internal Memo 65124-80-077 to P. J. Fiesher, February 1, 1980) Rockwell Hanford Operations, Richland, Washington.

Weiss, R. L., 1986, *TY Tank Farm Waste Characterization Data*, RHO-WM-TI-IP, Rockwell Hanford Operations, Richland, Washington.

APPENDIX B

FERROCYANIDE TANK GAMMA AND NEUTRON SCANS

Figures B-1 through B-24 provide gross gamma and neutron scans for the ferrocyanide tanks that contain liquid observation wells. These scans are performed on a routine basis for tanks that have a liquid observation well. These scans are used primarily to monitor liquid levels in the tanks. Baseline gamma scans are provided generally from 1985 along with scans performed in 1991 for comparison.

Figures B-25 through B-36 provide collimated cadium telluride gamma scan traces for the same tanks. The collimated cadium telluride gamma scans were performed in September 1991.

This page intentionally left blank.

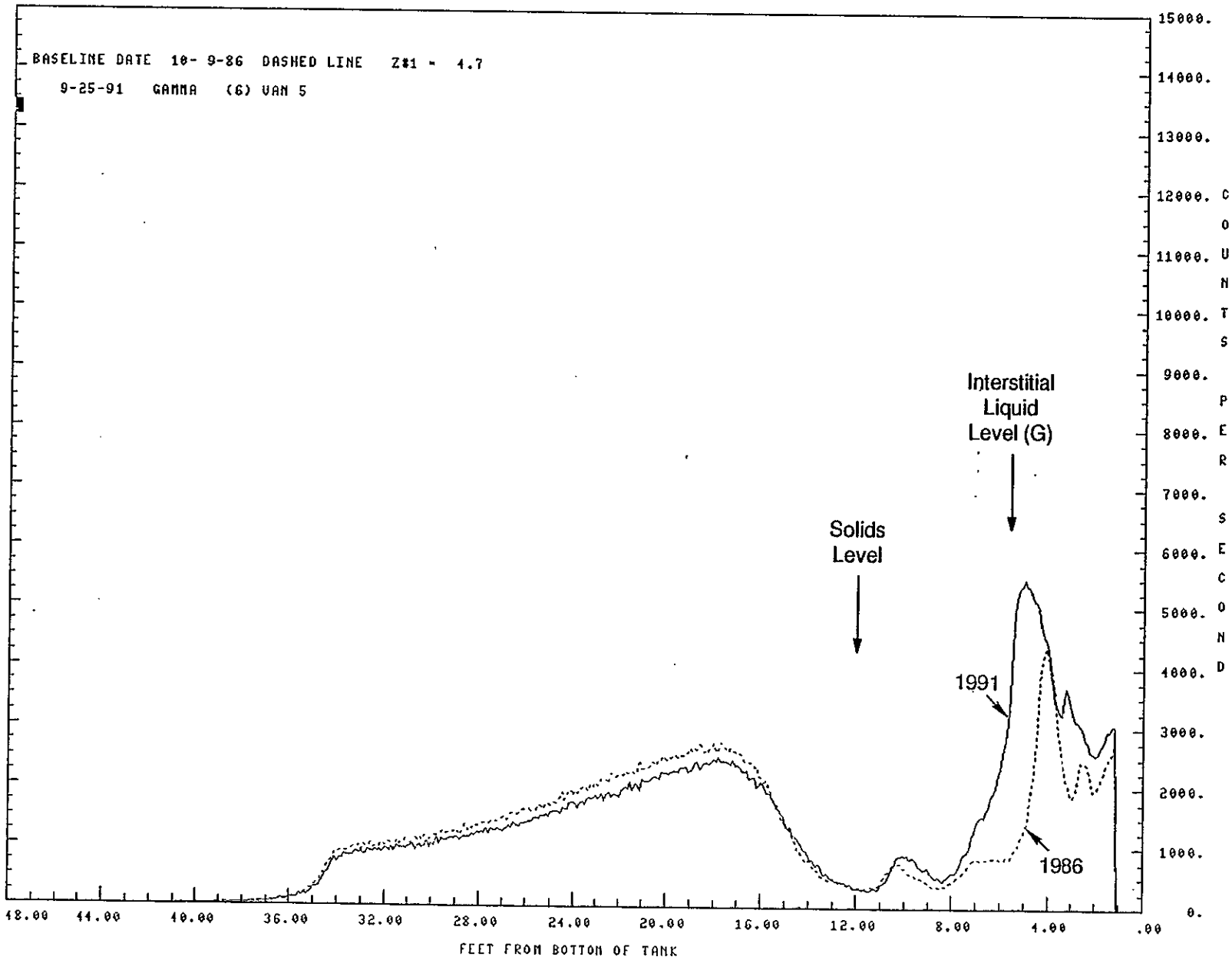

Figure B-1. Gamma Scans of Tank 241-BY-101 (Baseline vs. 1991).

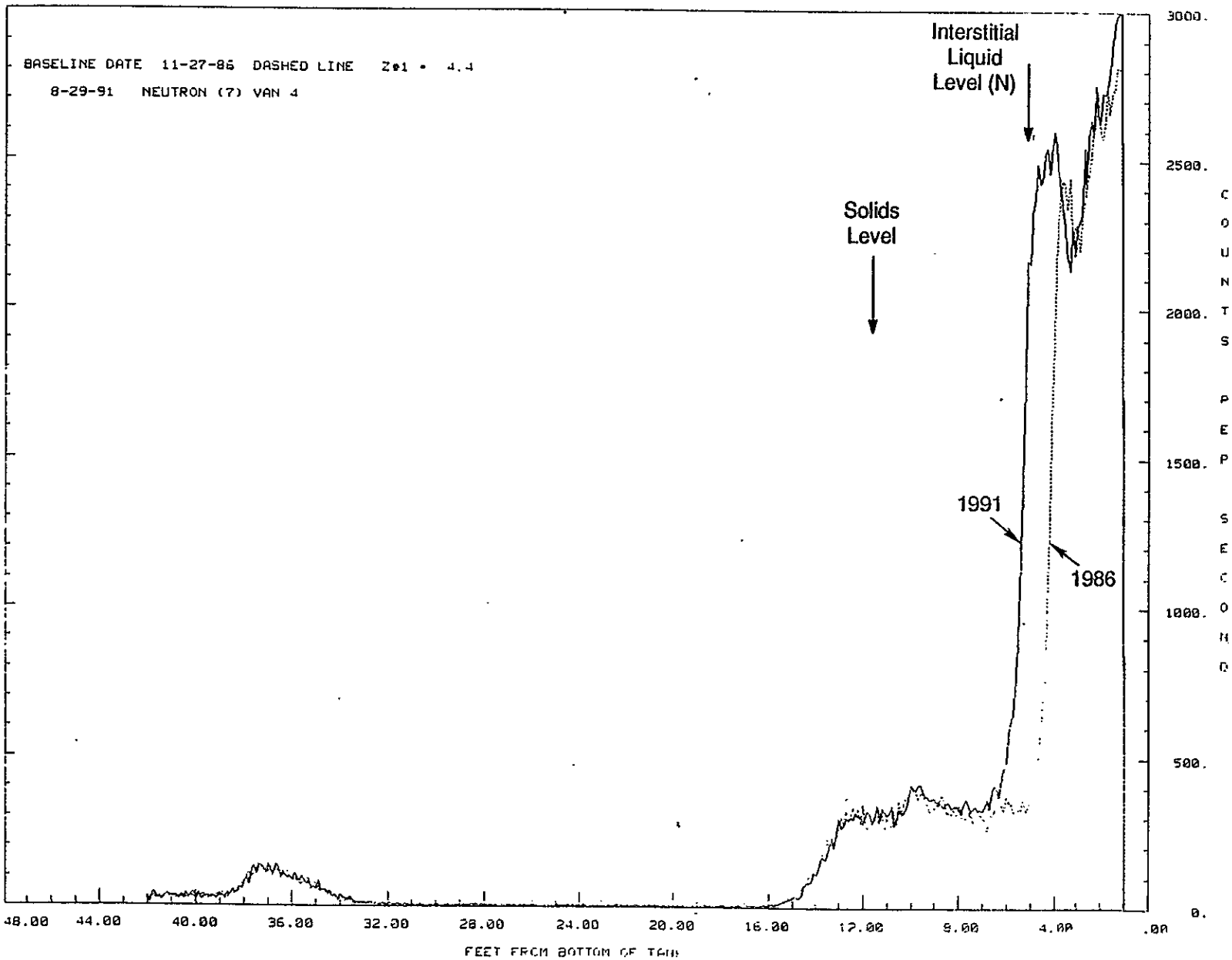

Figure B-2. Neutron Scans of Tank 241-BY-101 (Baseline vs. 1991).

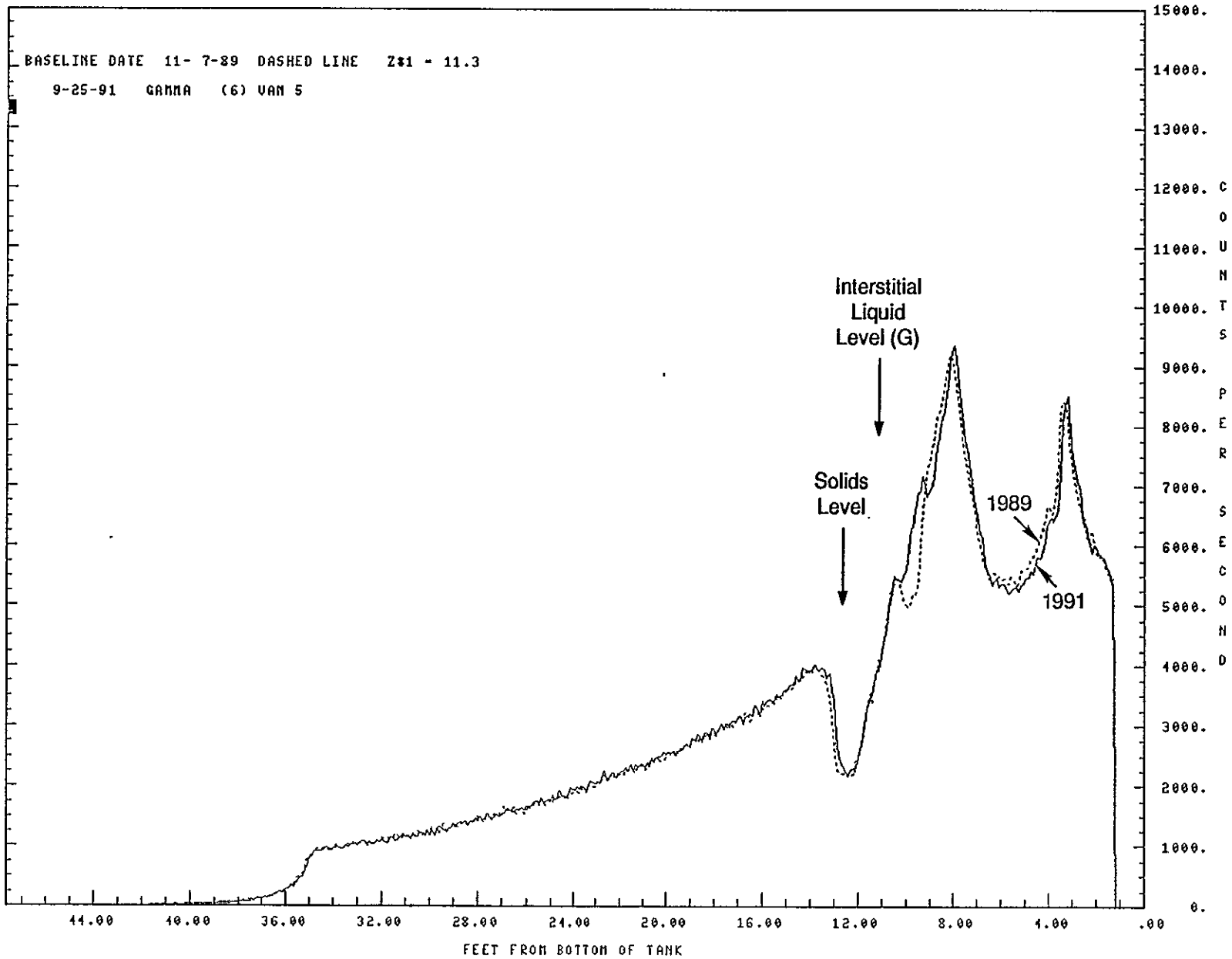

Figure B-3. Gamma Scans of Tank 241-BY-103 (Baseline vs. 1991).

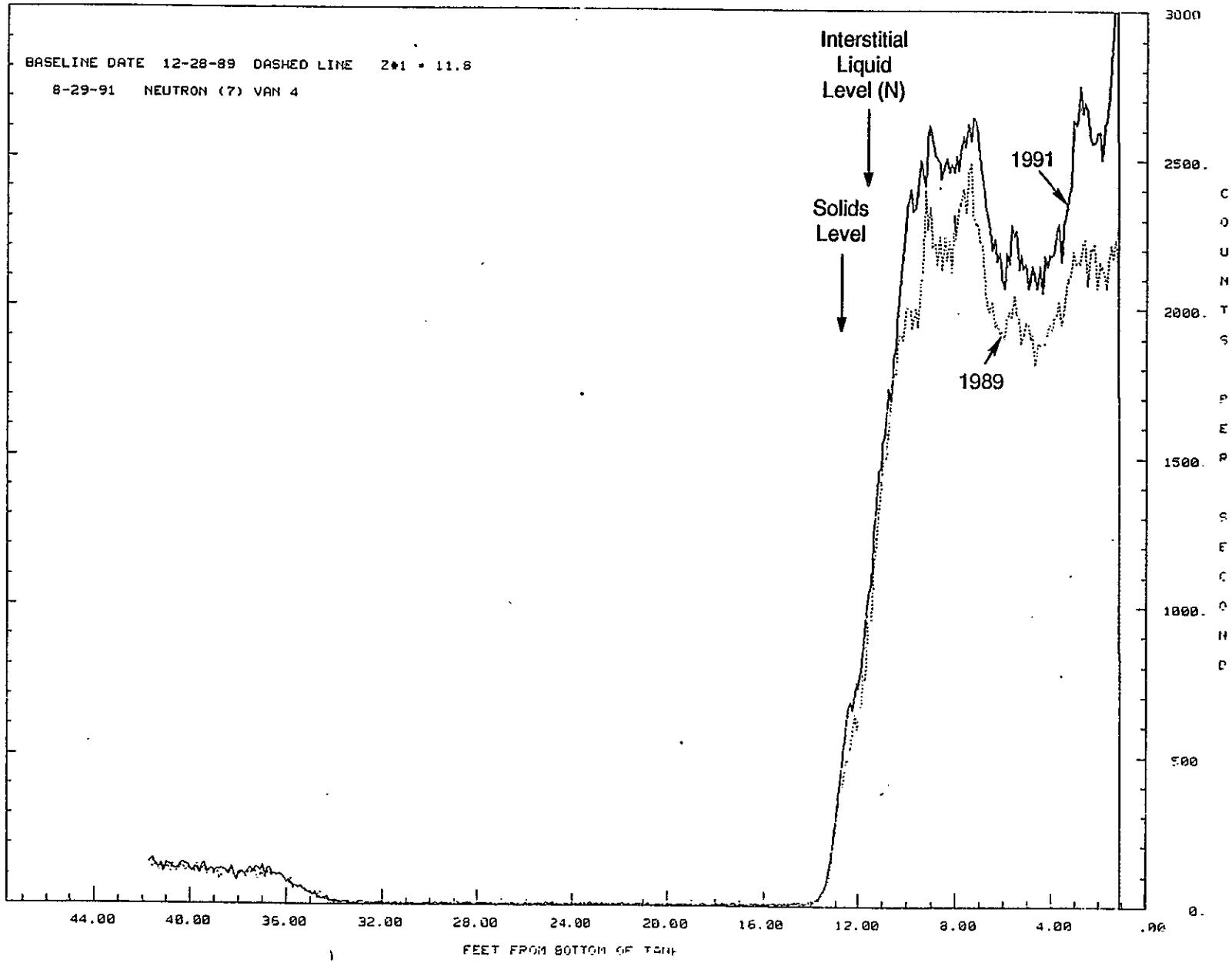

Figure B-4. Neutron Scans of Tank 241-BY-103 (Baseline vs. 1991).

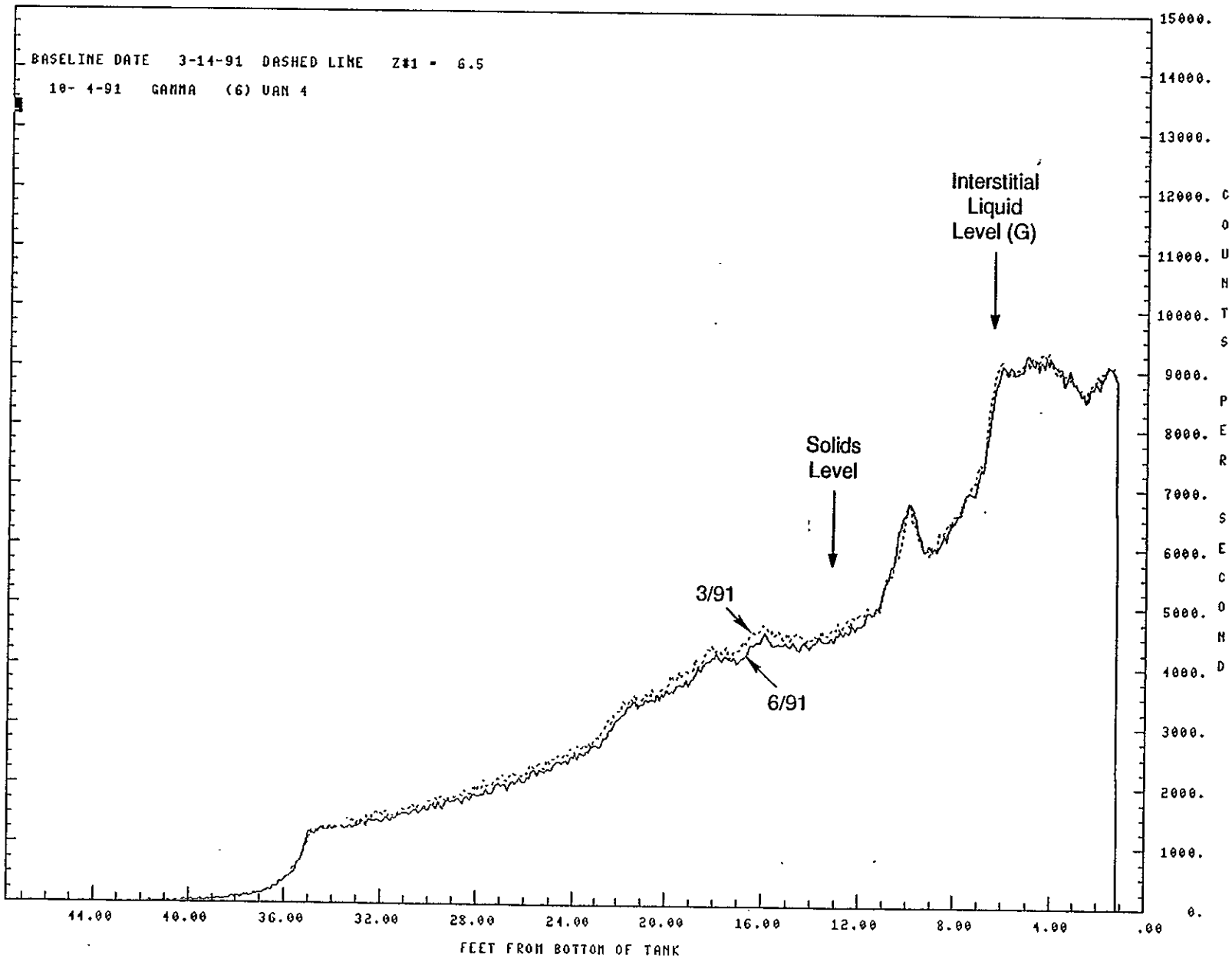

Figure B-5. Gamma Scans of Tank 241-BY-104 (Baseline vs. 1991).

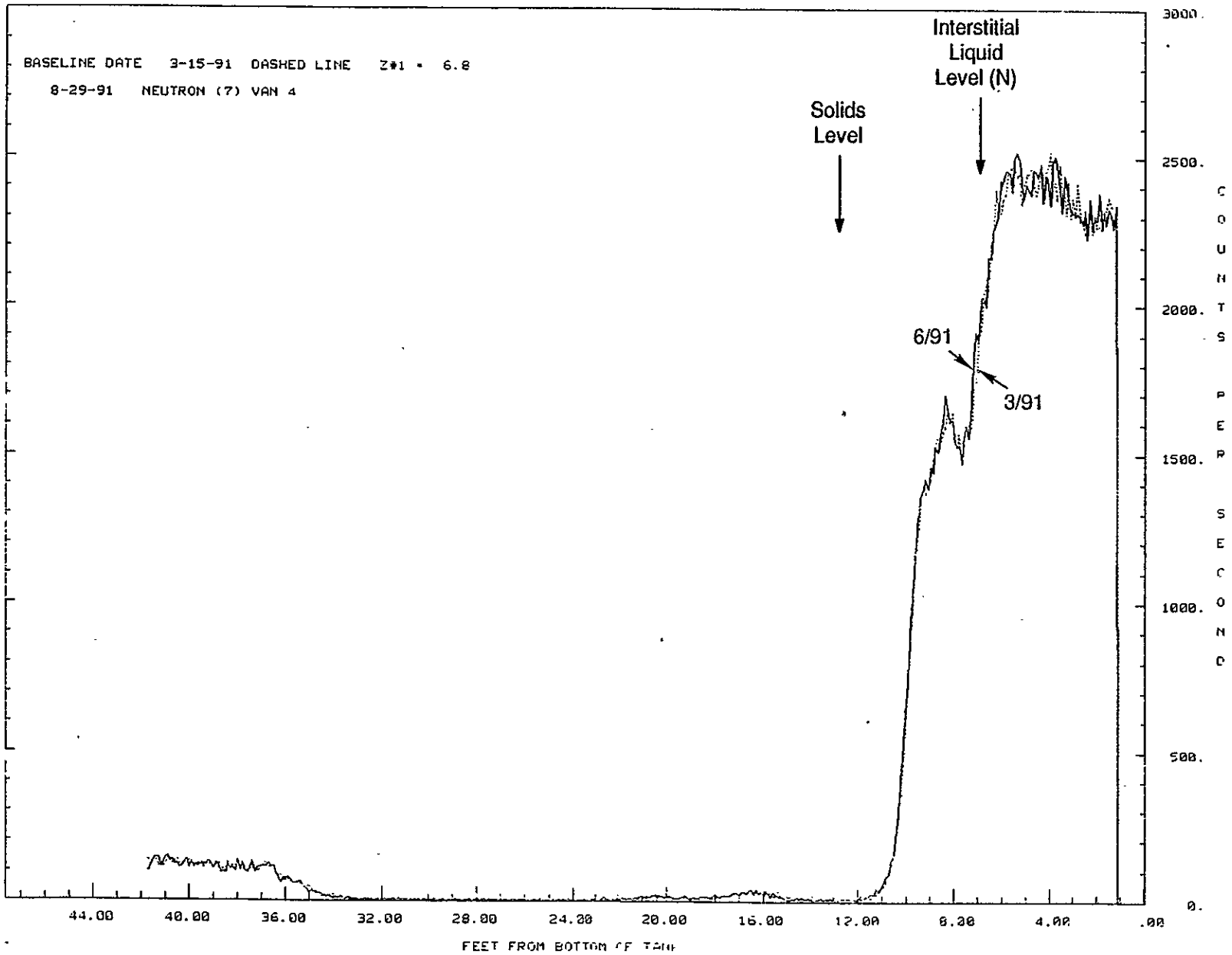

Figure B-6. Neutron Scans of Tank 241-BY-104 (Baseline vs. 1991).

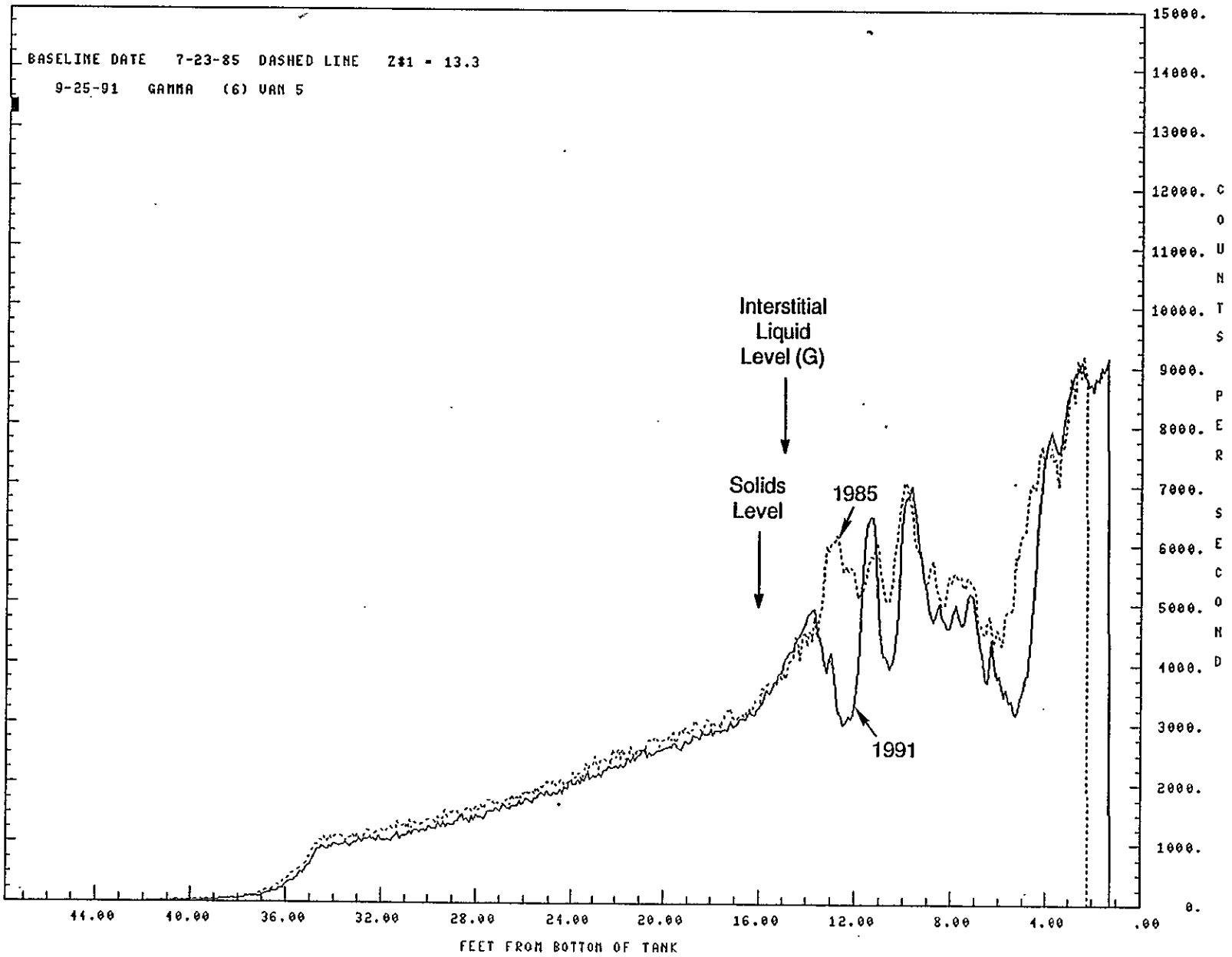

Figure B-7. Gamma Scans of Tank 241-BY-105 (Baseline vs. 1991).

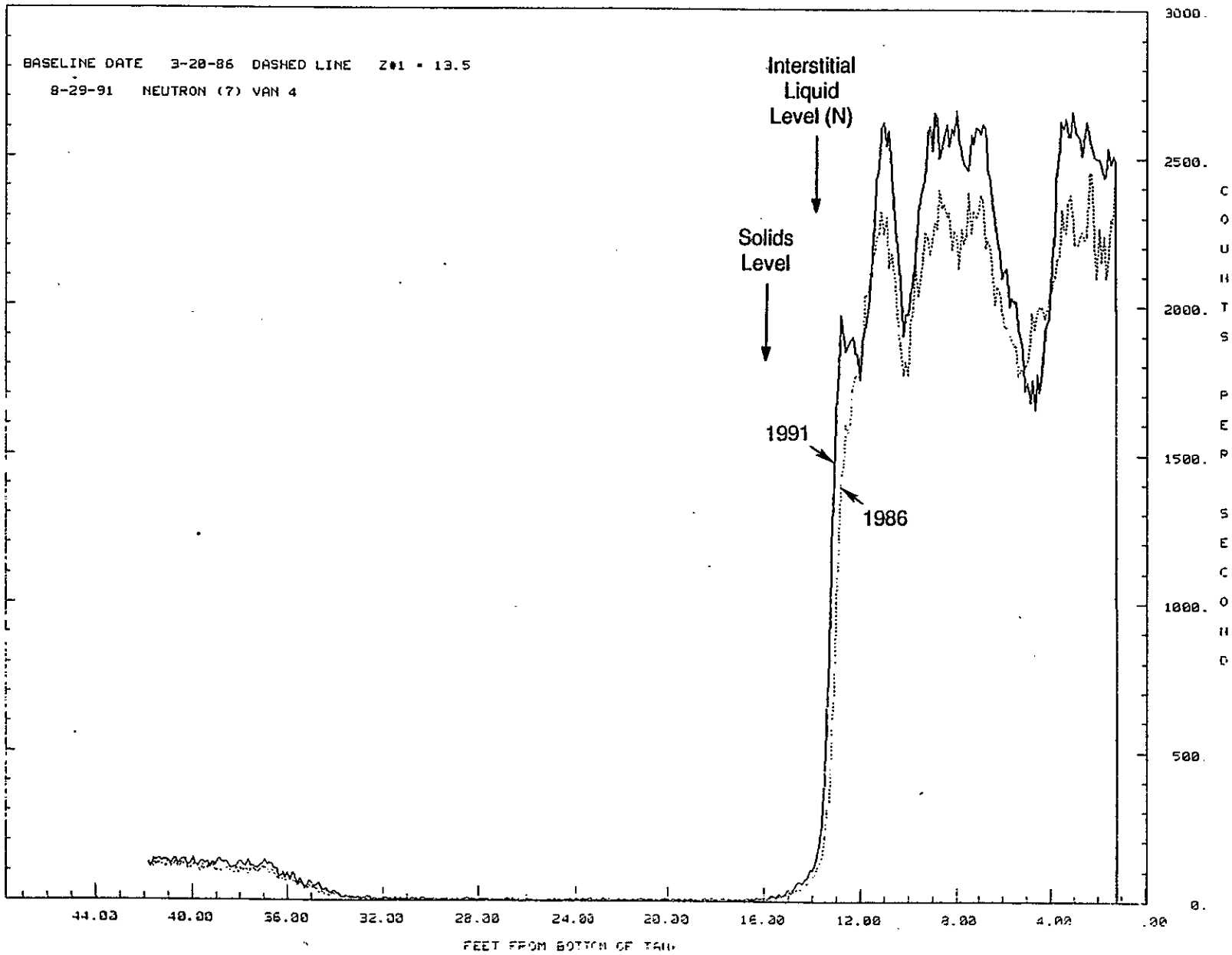

Figure B-8. Neutron Scans of Tank 241-BY-105 (Baseline vs. 1991).

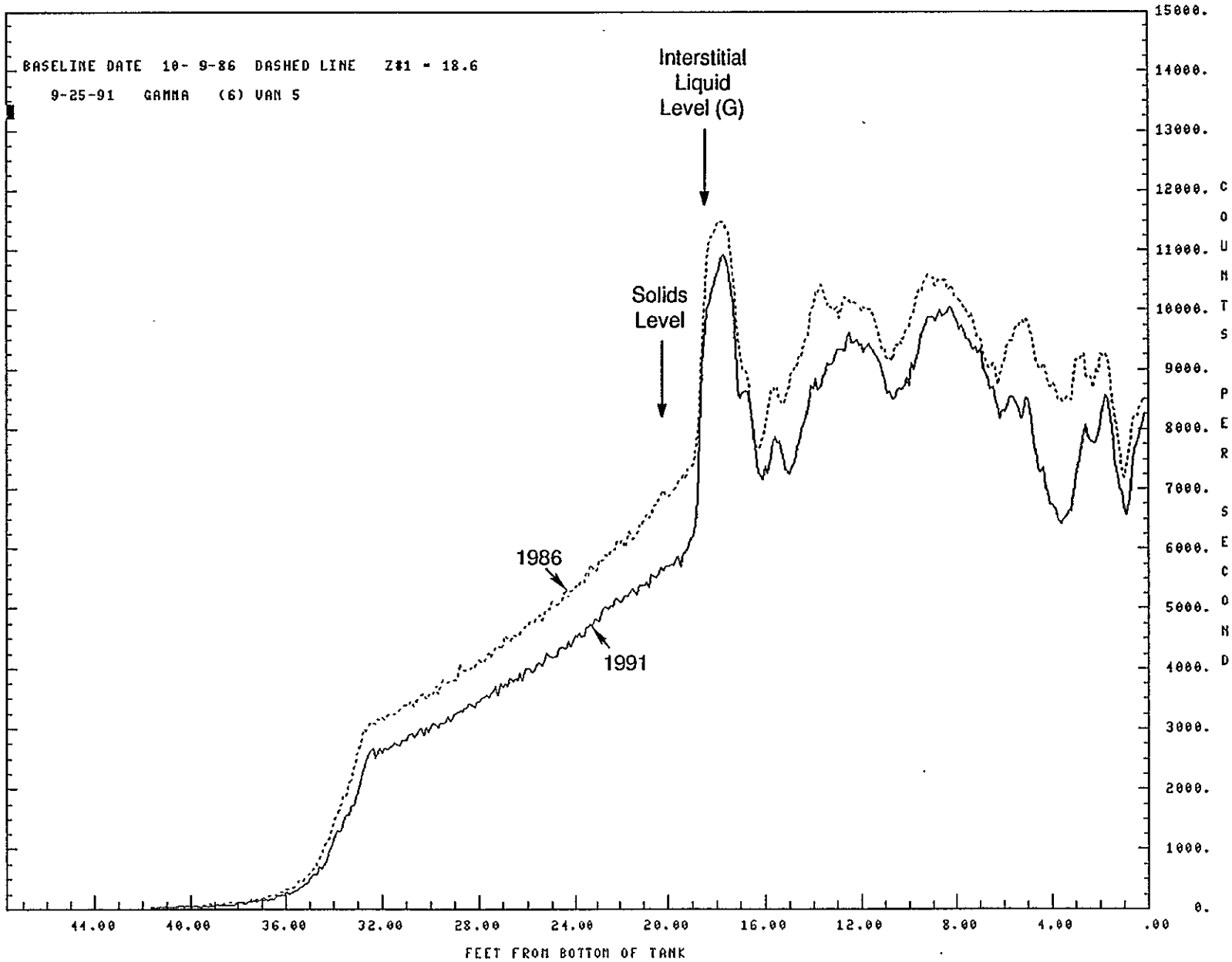

Figure B-9. Gamma Scans of Tank 241-BY-106 (Baseline vs. 1991).

Figure B-10. Neutron Scans of Tank 241-BY-106 (Baseline vs. 1991).

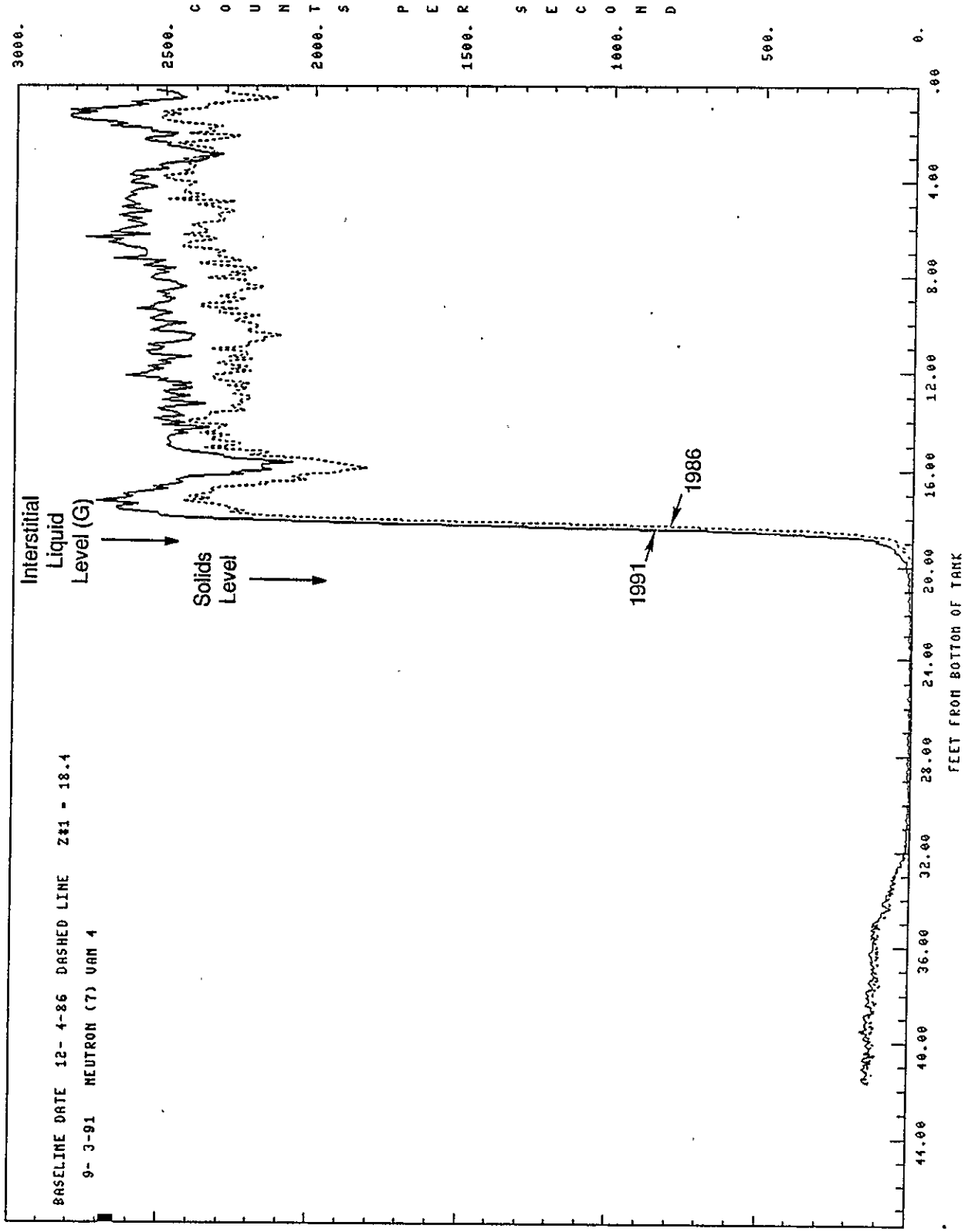

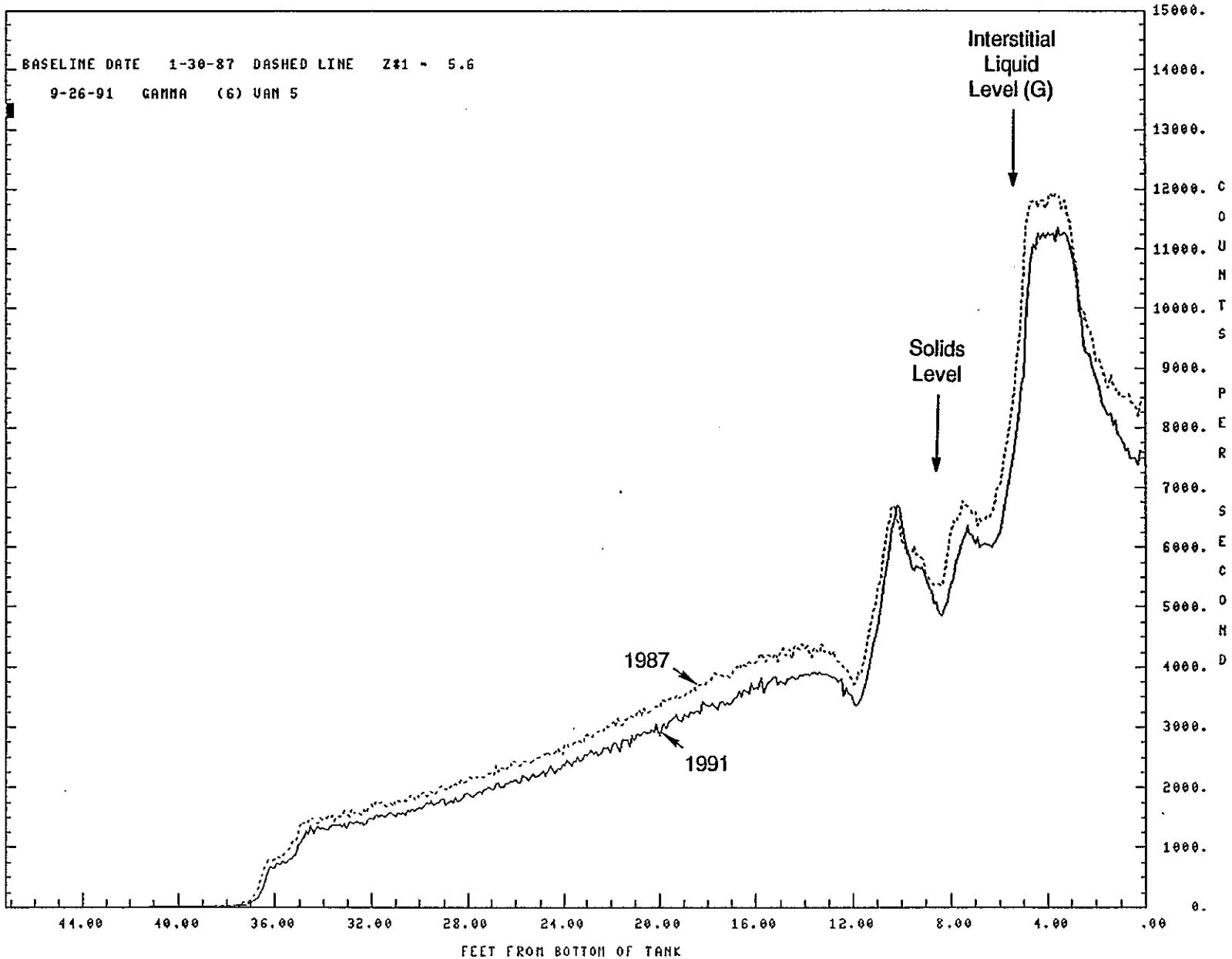

Figure B-11. Gamma Scans of Tank 241-BY-107 (Baseline vs. 1991).

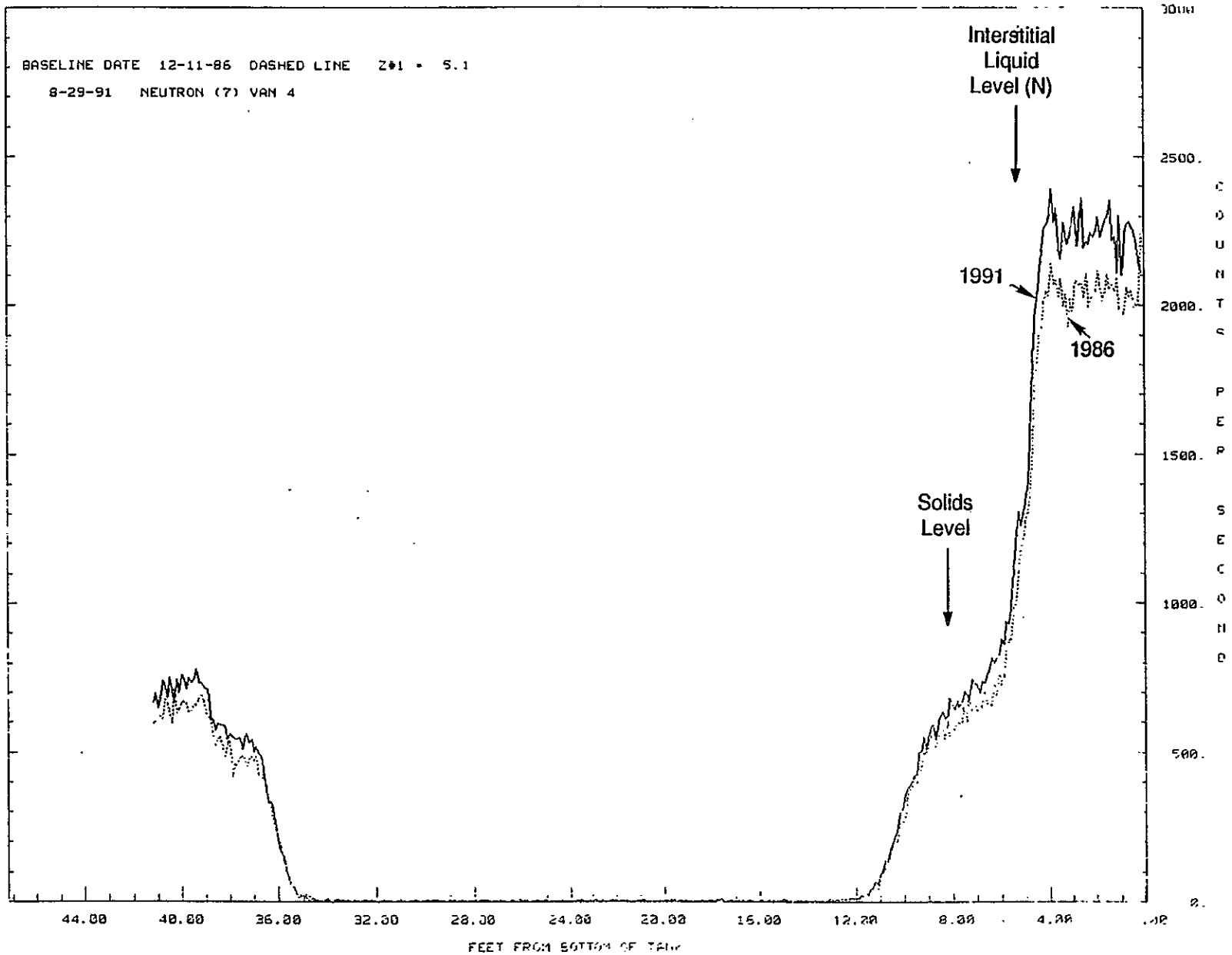

Figure B-12. Neutron Scans of Tank 241-BY-107 (Baseline vs. 1991).

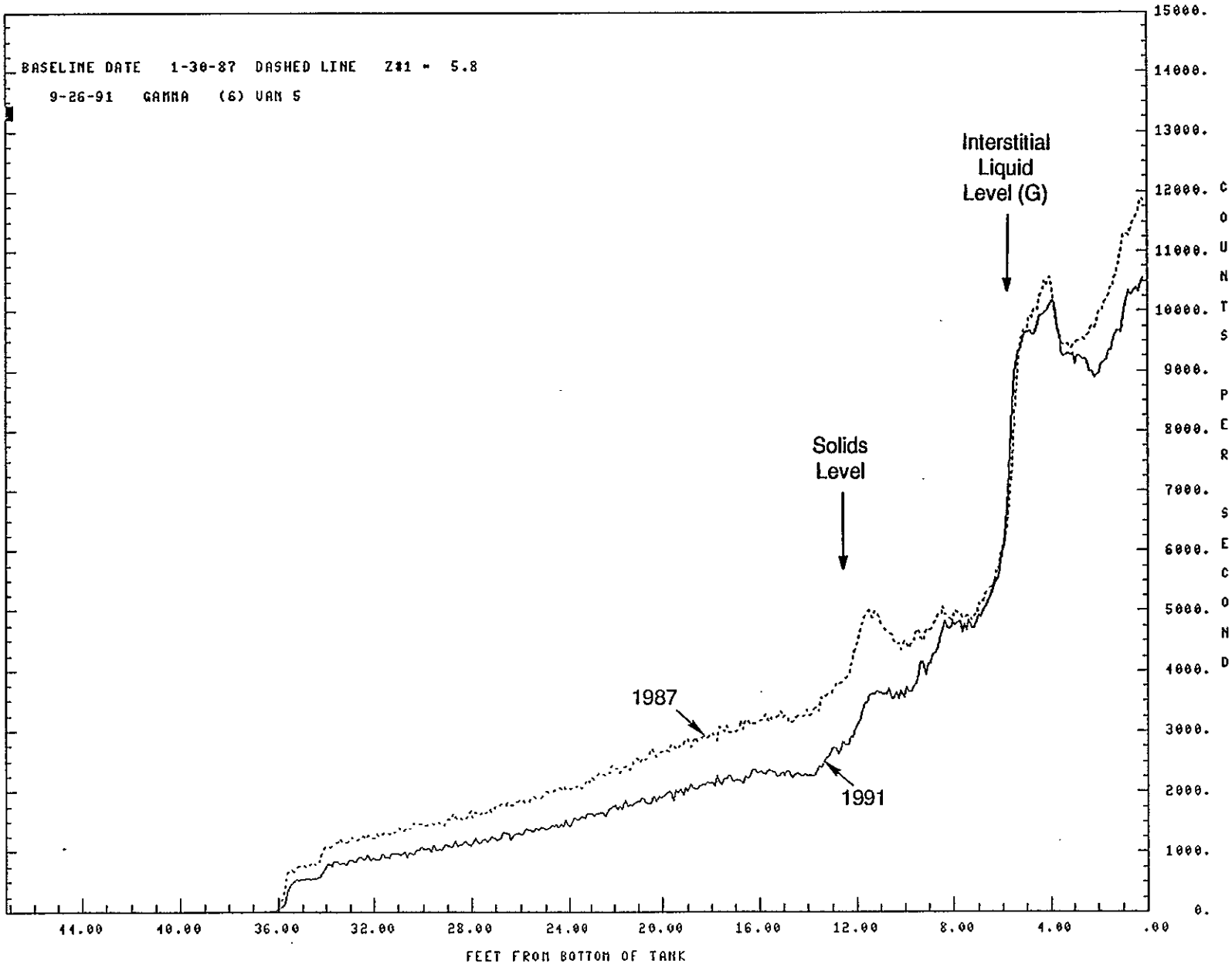

Figure B-13. Gamma Scans of Tank 241-BY-110 (Baseline vs. 1991)

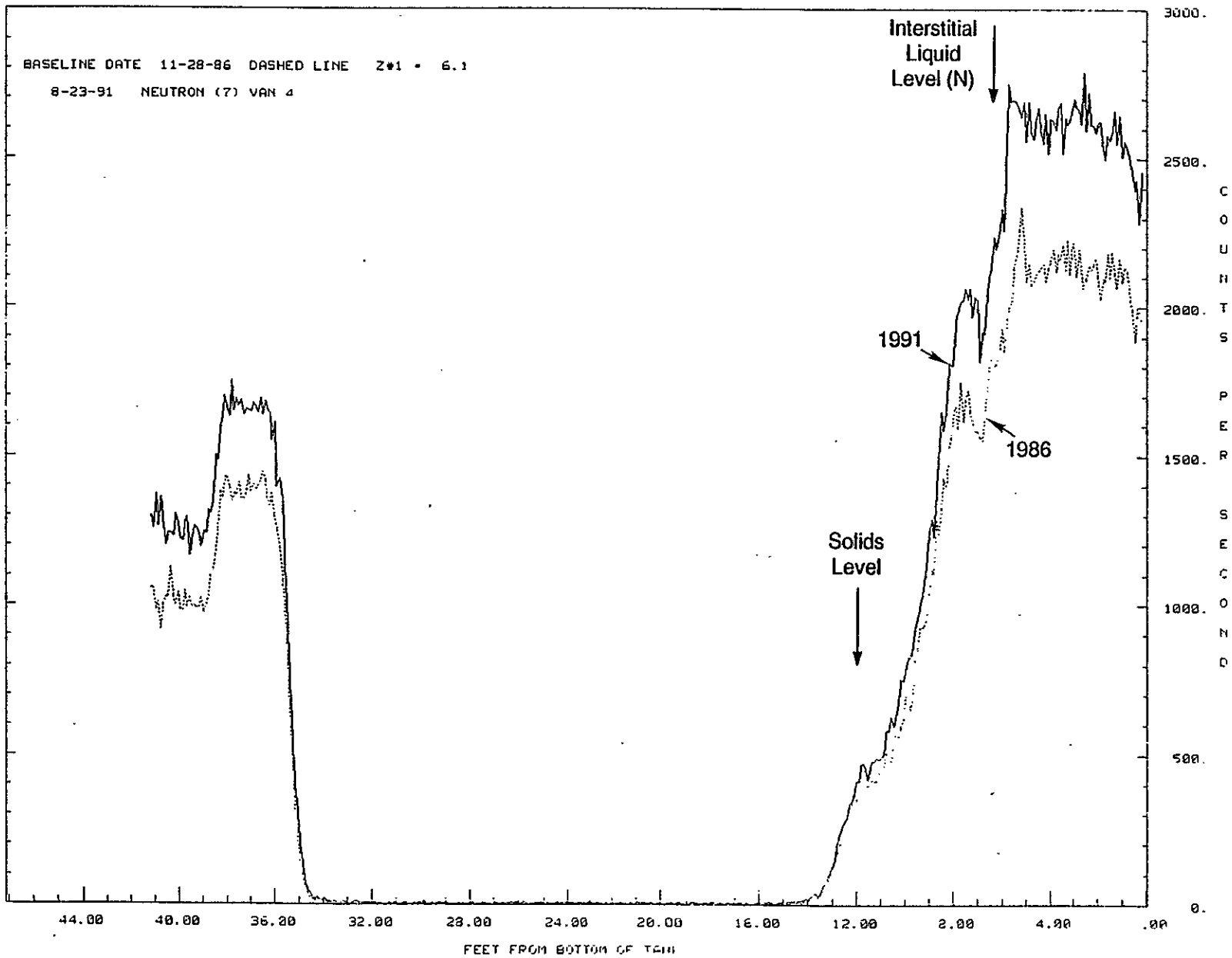

Figure B-14. Neutron Scans of Tank 241-BY-110 (Baseline vs. 1991)

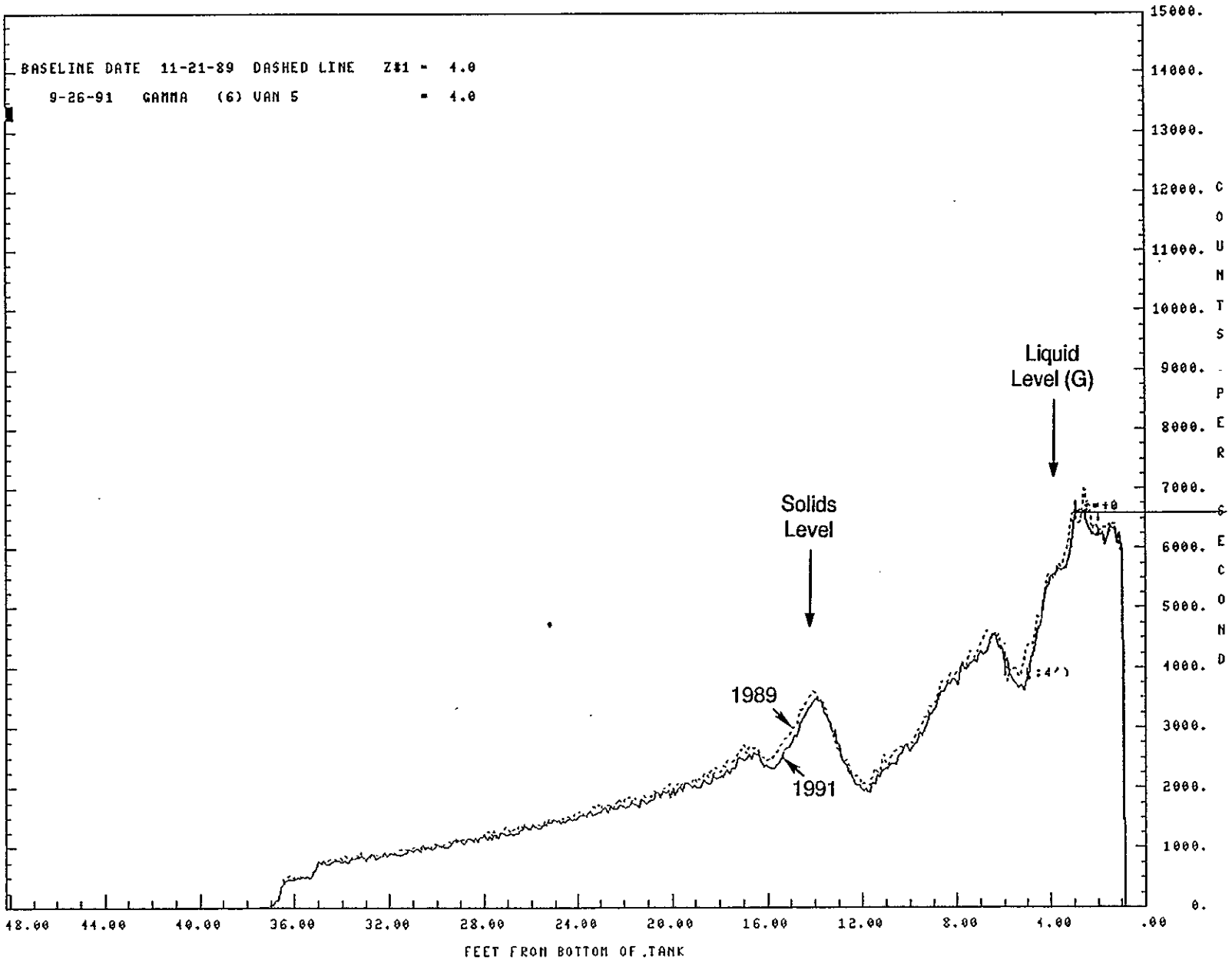

Figure B-15. Gamma Scans of Tank 241-BY-111 (Baseline vs. 1991)

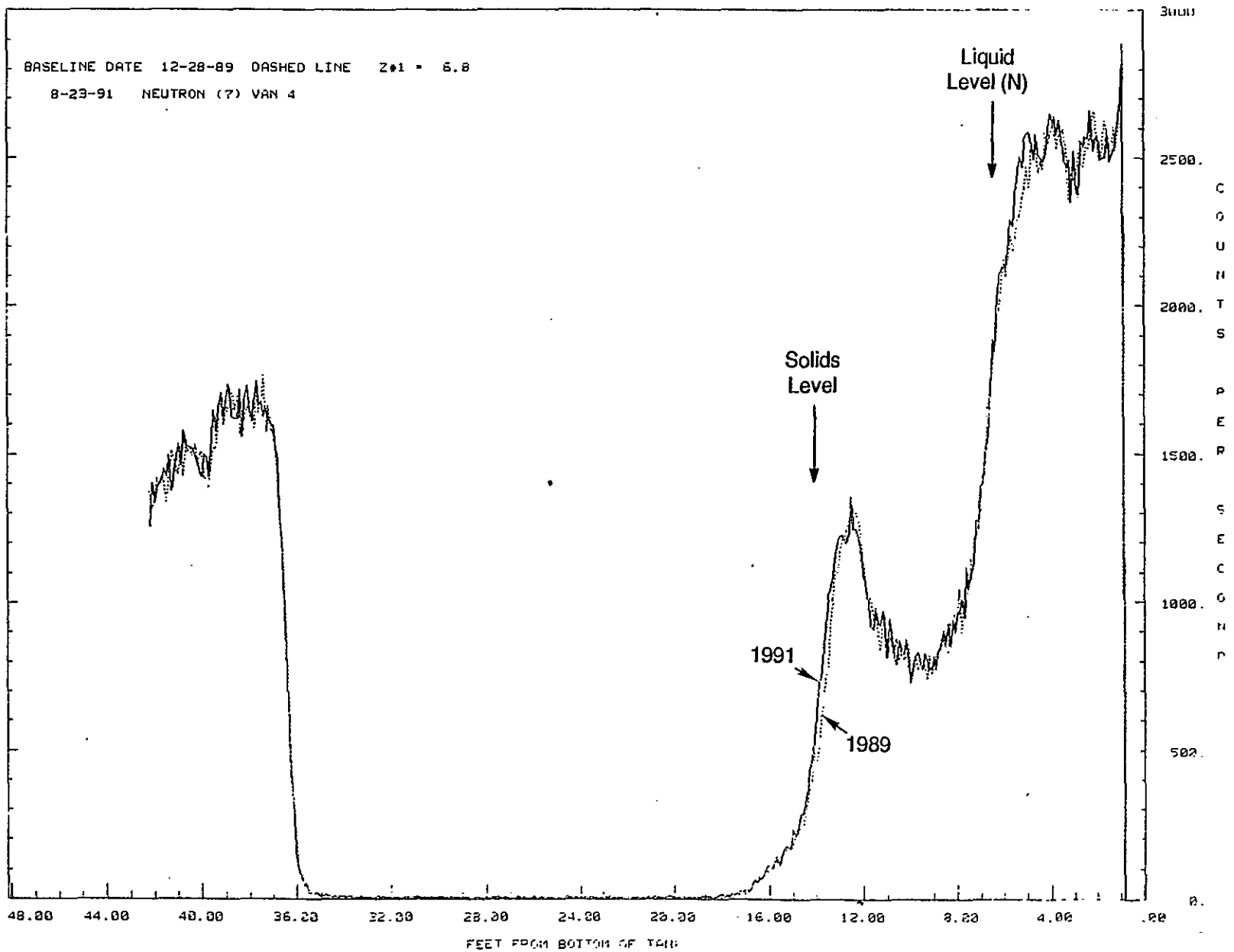

Figure B-16. Neutron Scans of Tank 241-BY-111 (Baseline vs. 1991)

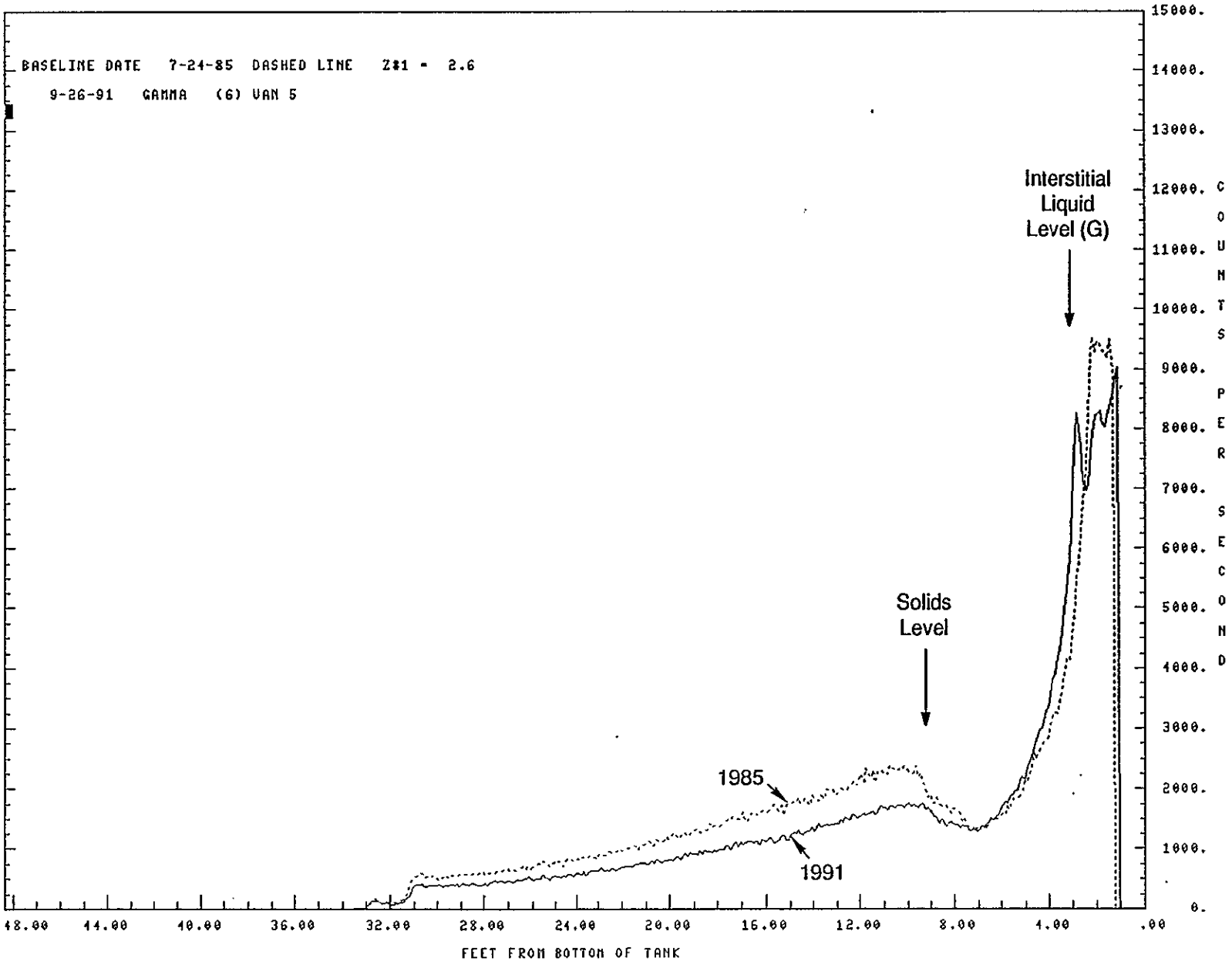

Figure B-17. Gamma Scans of Tank 241-BY-112 (Baseline vs. 1991)

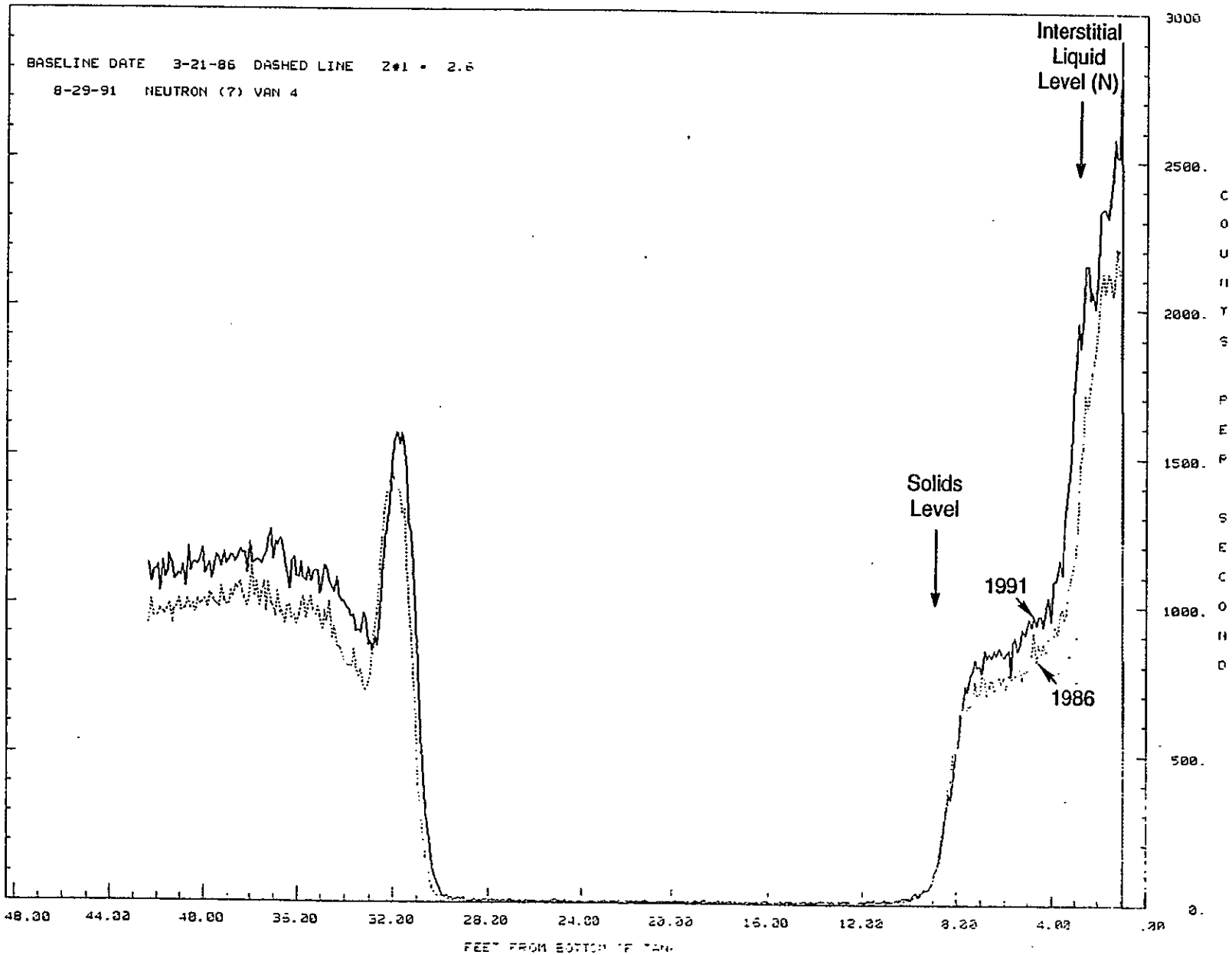

Figure B-18. Neutron Scans of Tank 241-BY-112 (Baseline vs. 1991)

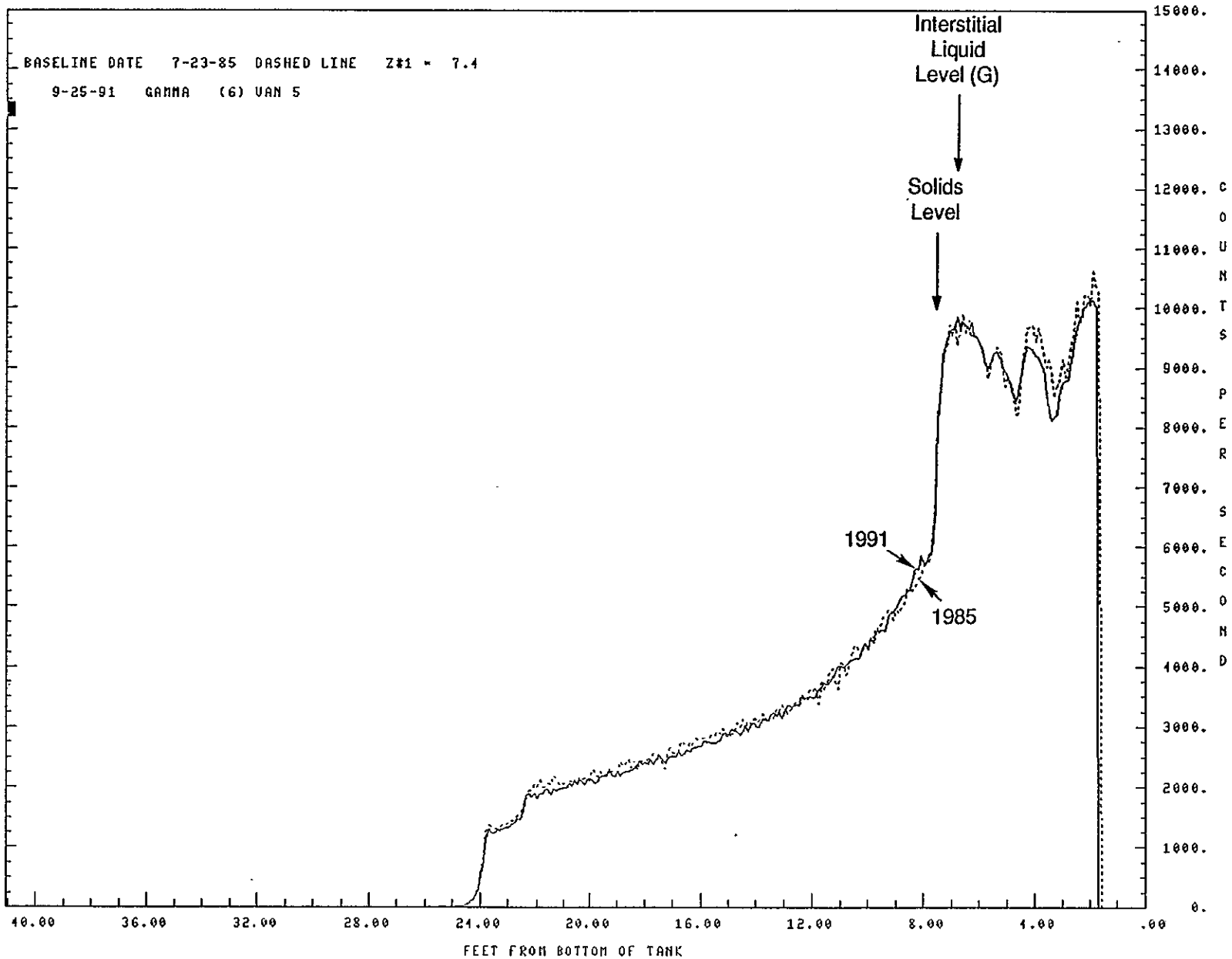

Figure B-19. Gamma Scans of Tank 241-BX-111 (Baseline vs. 1991)

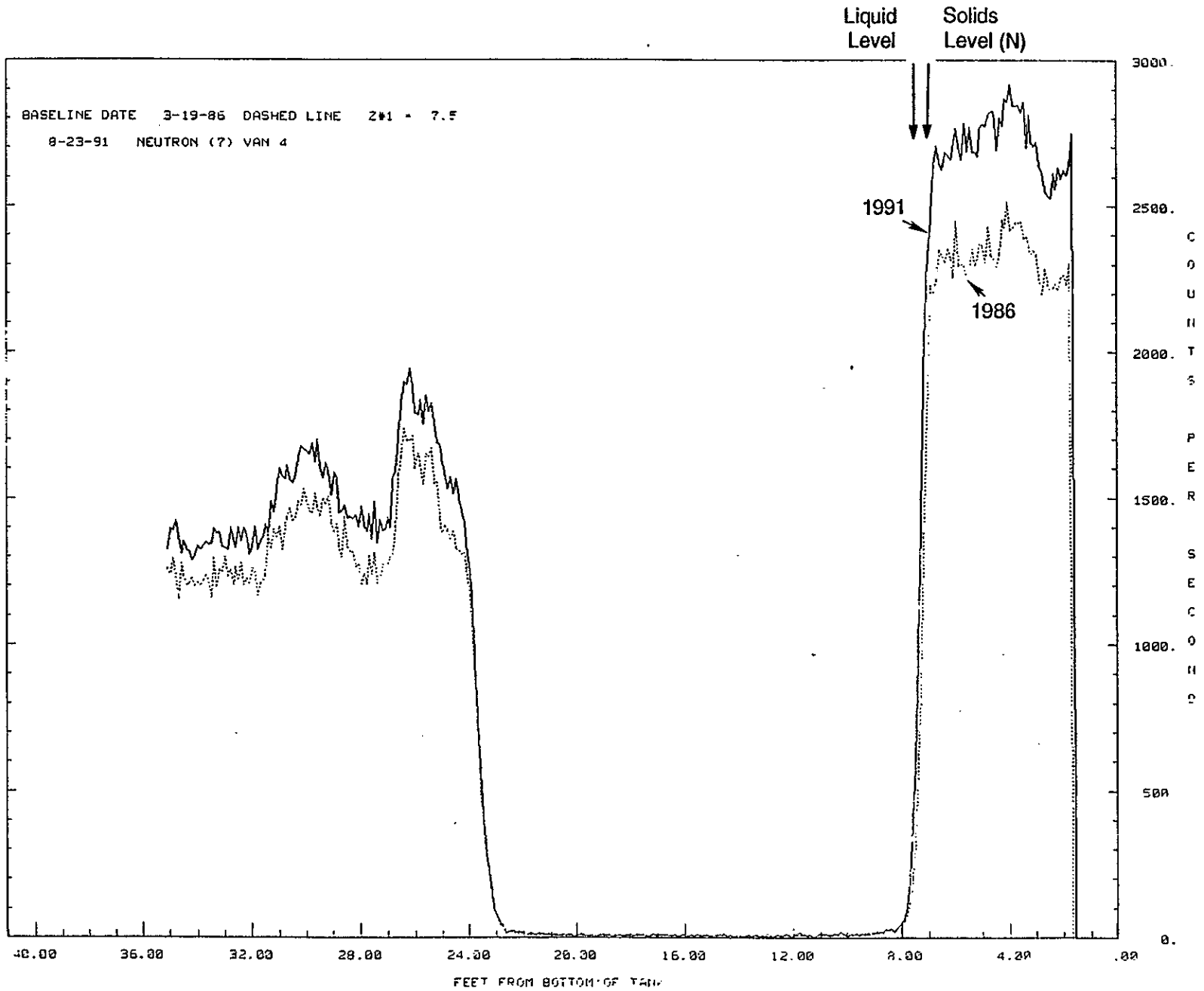

Figure B-20. Neutron Scans of Tank 241-BX-111 (Baseline vs. 1991)

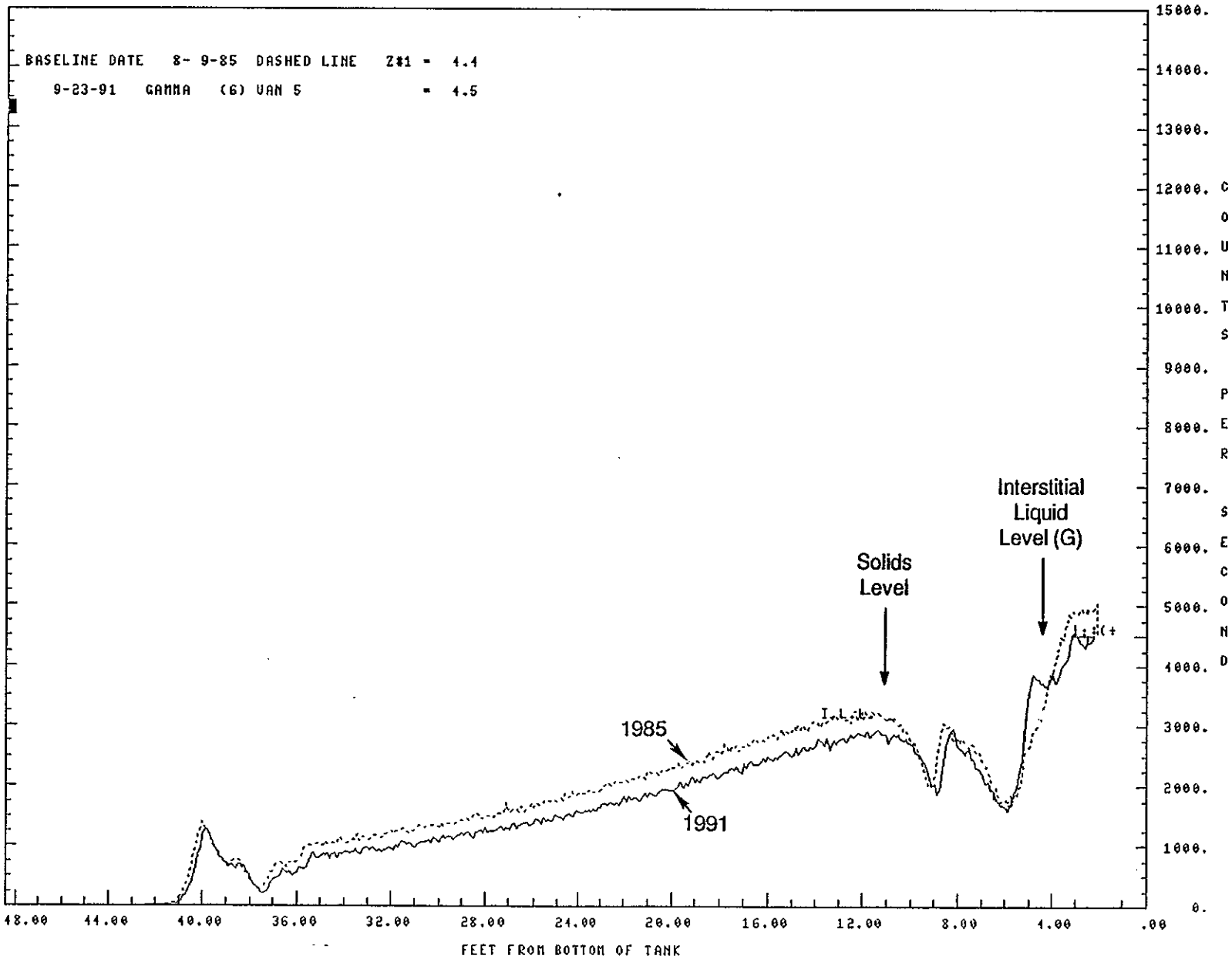

Figure B-21. Gamma Scans of Tank 241-TX-118 (Baseline vs. 1991)

Figure B-22. Neutron Scans of Tank 241-TX-118 (Baseline vs. 1991)

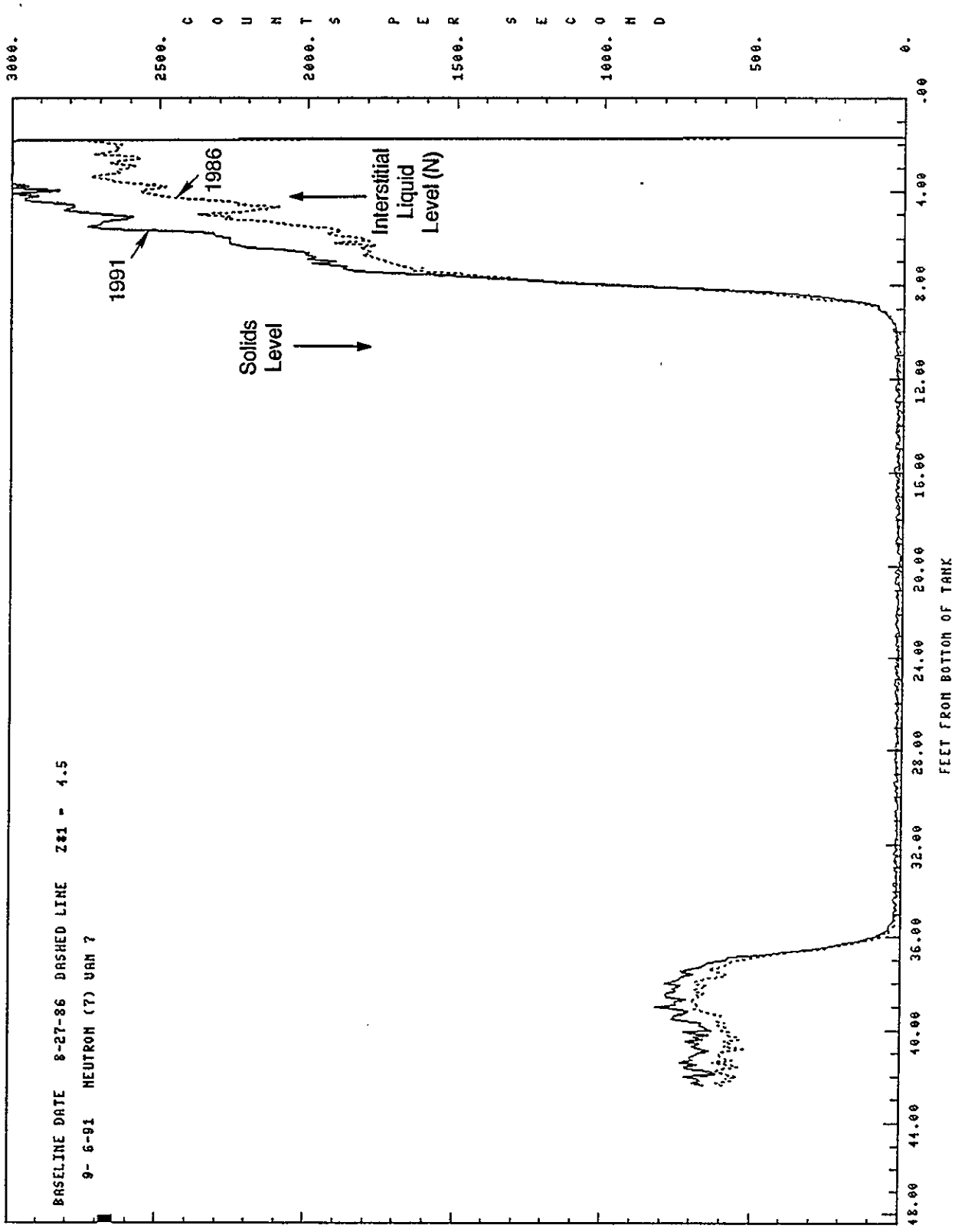

Figure B-23. Gamma Scans of Tank 241-TY-103 (Baseline vs. 1991)

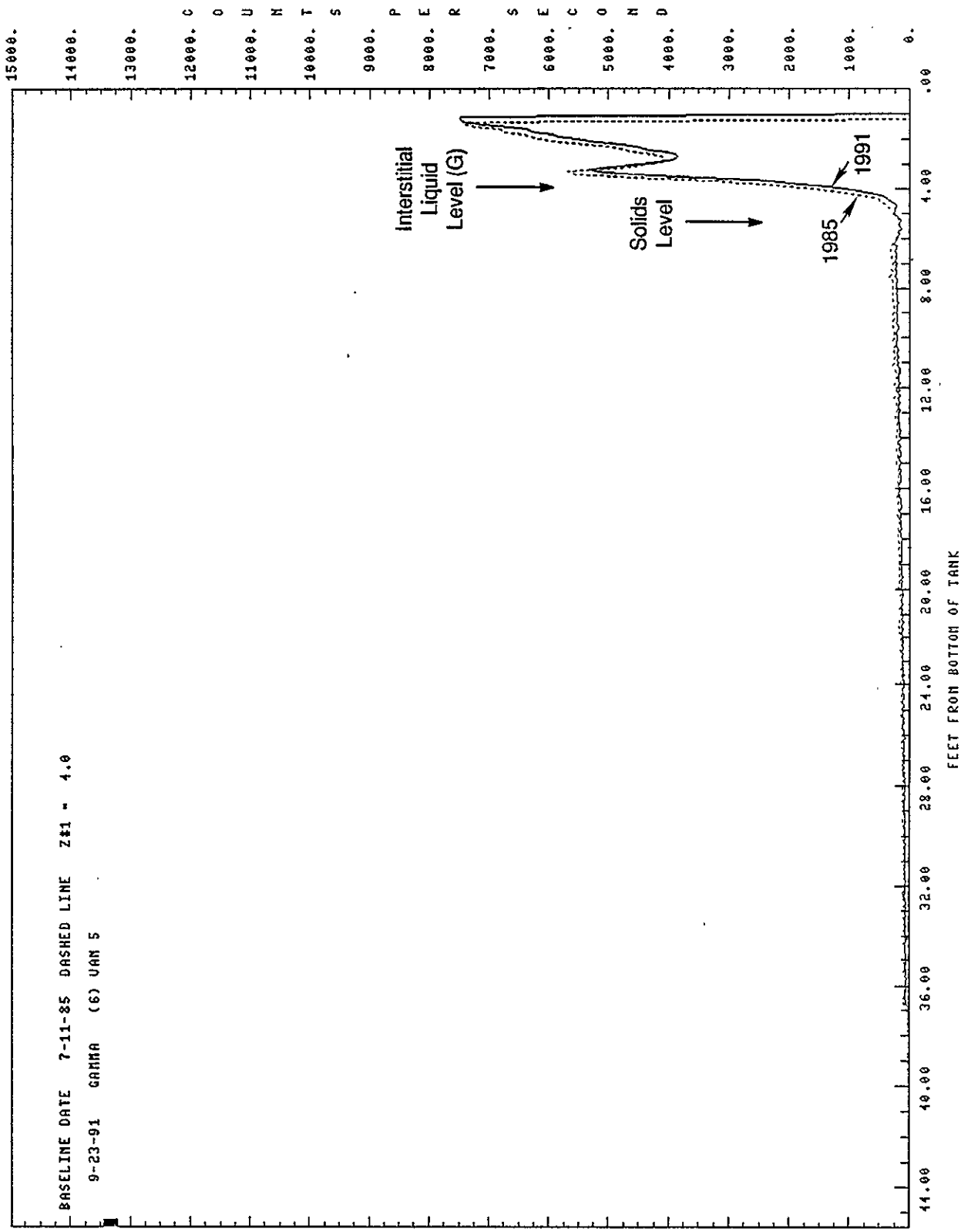

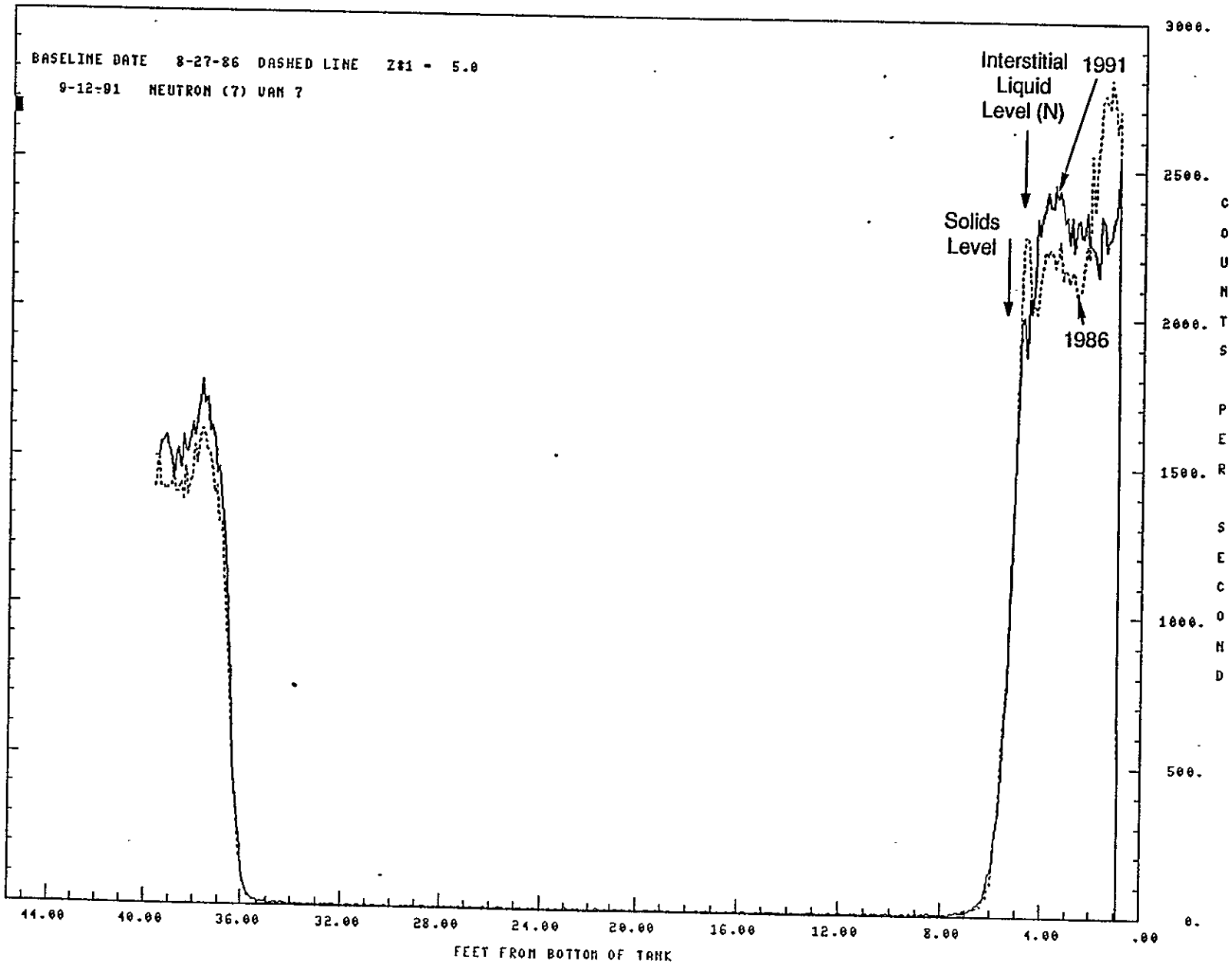

Figure B-24. Neutron Scans of Tank 241-TY-103 (Baseline vs. 1991)

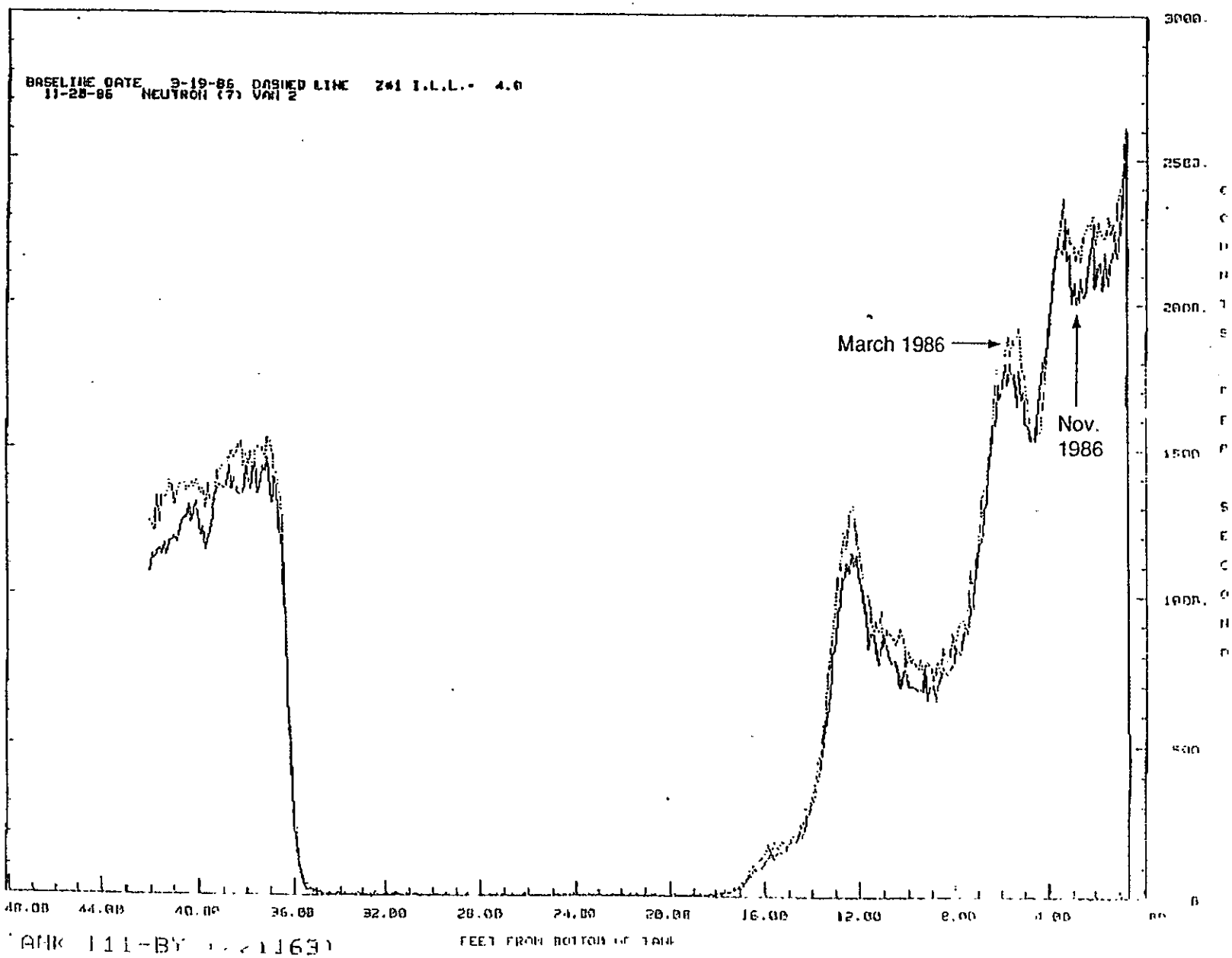

Figure B-25. Neutron Scan of Tank 241-BY-111 (Baseline vs. 1986)

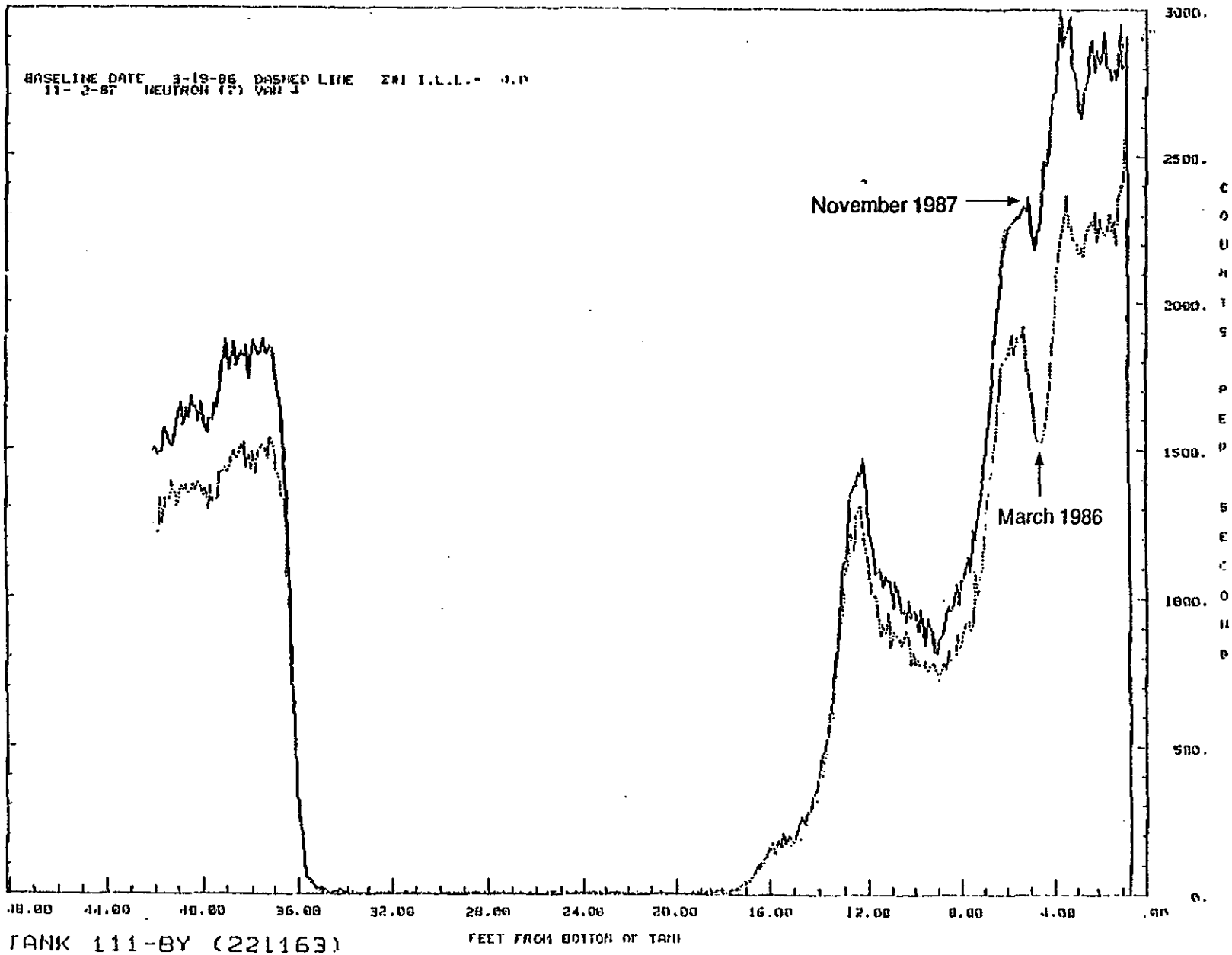

Figure B-26. Neutron Scan of Tank 241-BY-111 (Baseline vs. Dec. 1989)

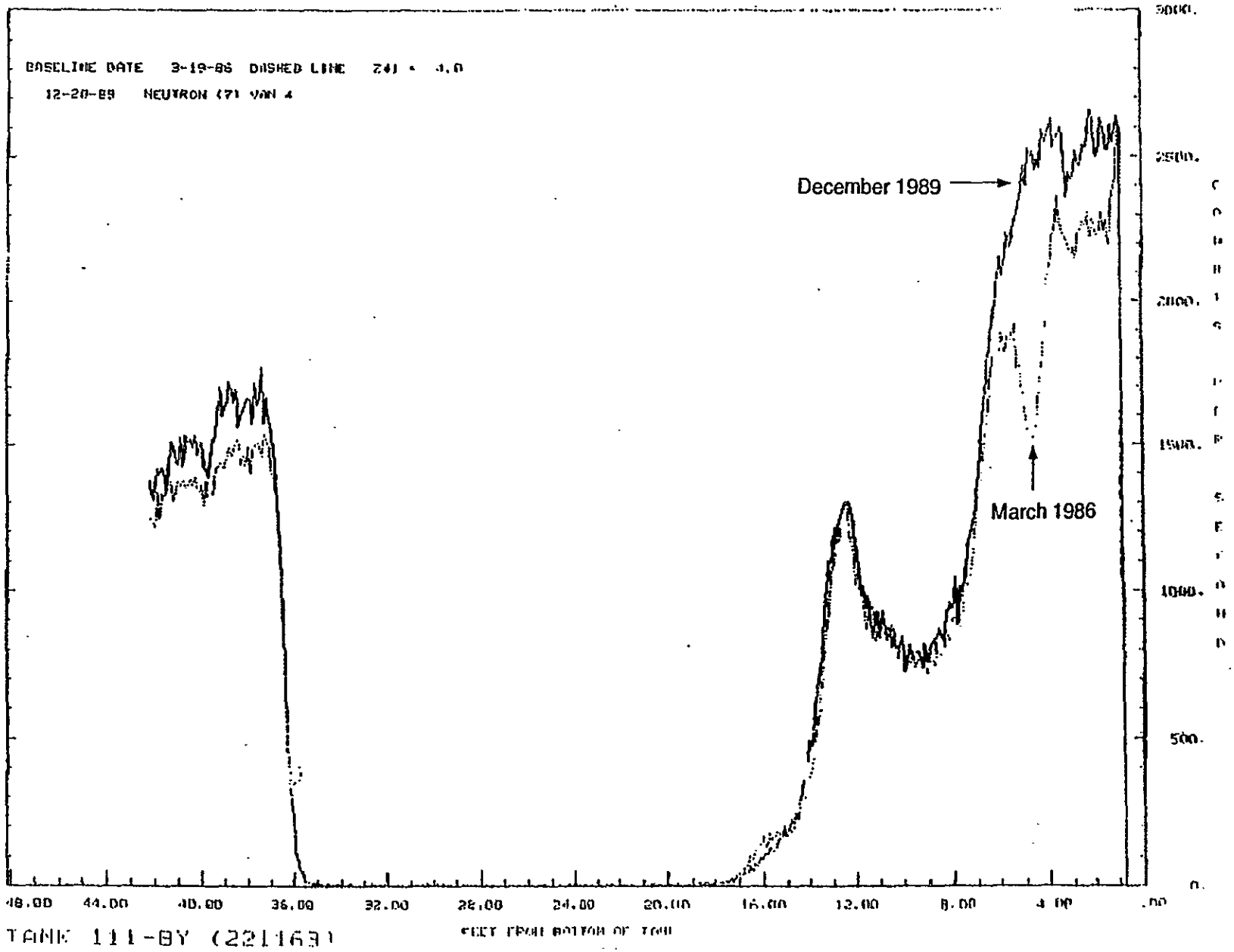

Figure B-27. Neutron Scan of Tank 241-BY-111 (Baseline vs. Nov. 1987)

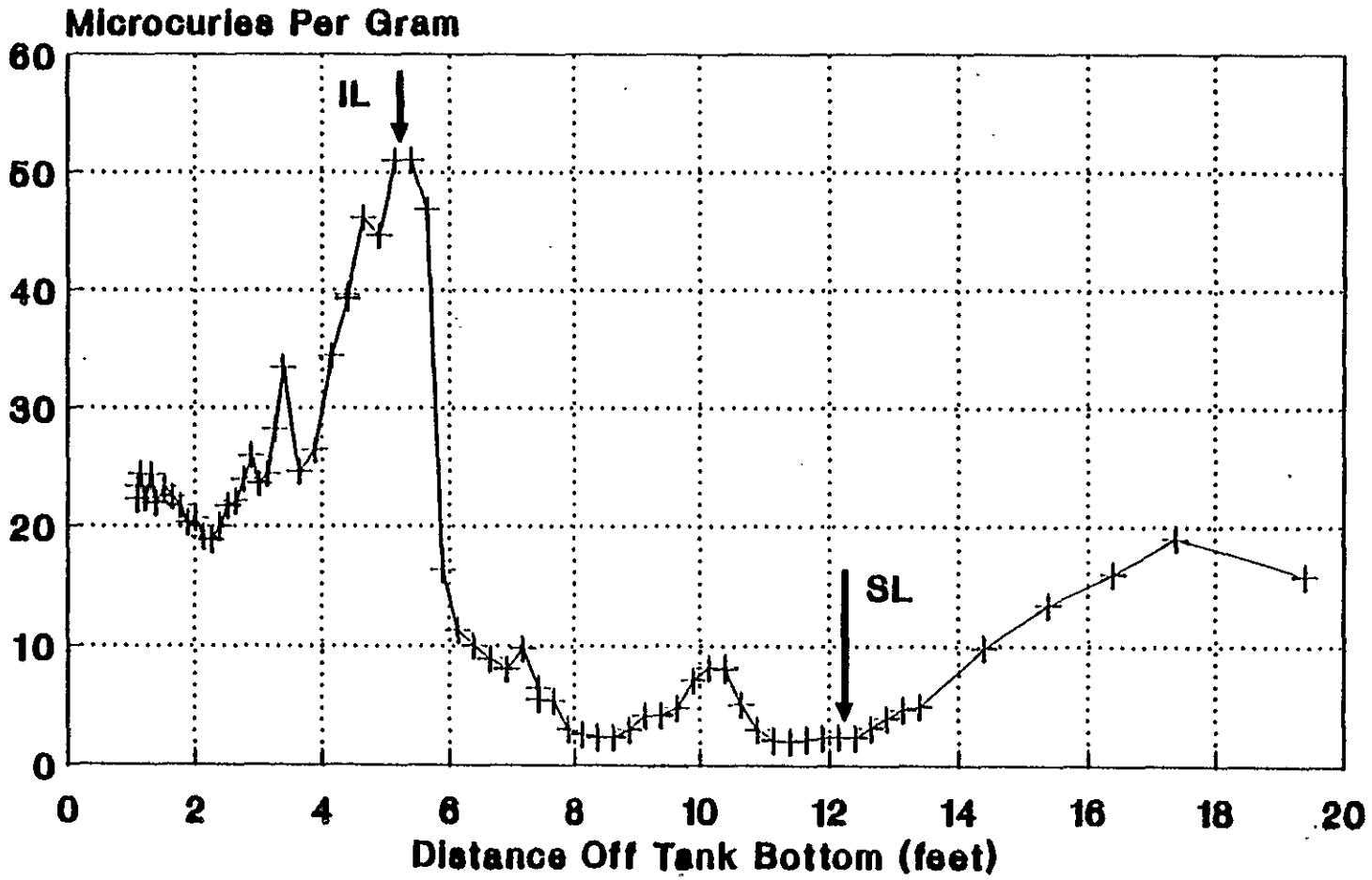

IL: Interstitial Liquid Level
SL: Solids Level

Figure B-28. Tank 241-BY-101 ^{137}Cs Activity.

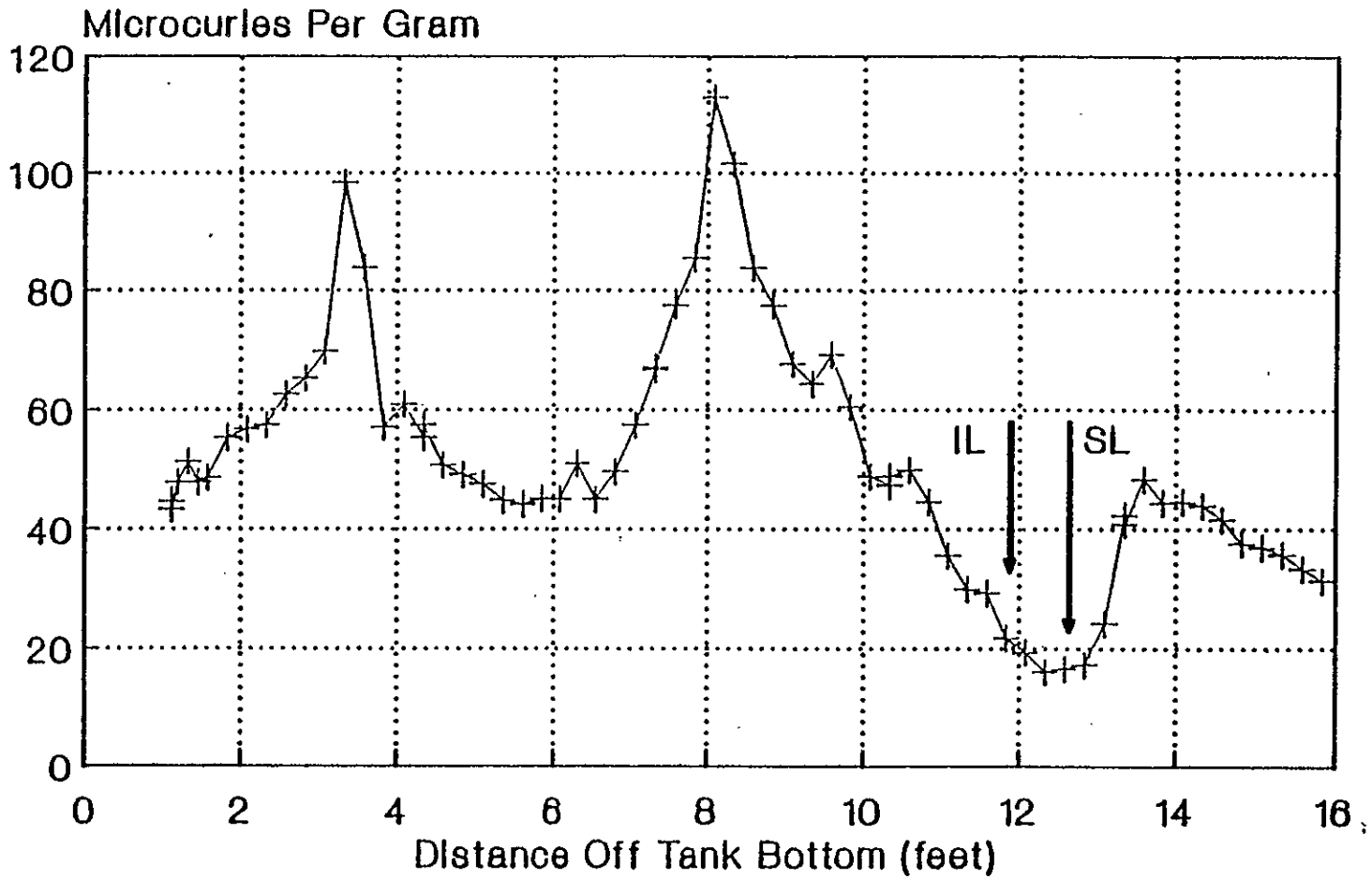

Figure B-29. Tank 241-BY-103 ^{137}Cs Activity.

IL: Interstitial Liquid Level
SL: Solids Level

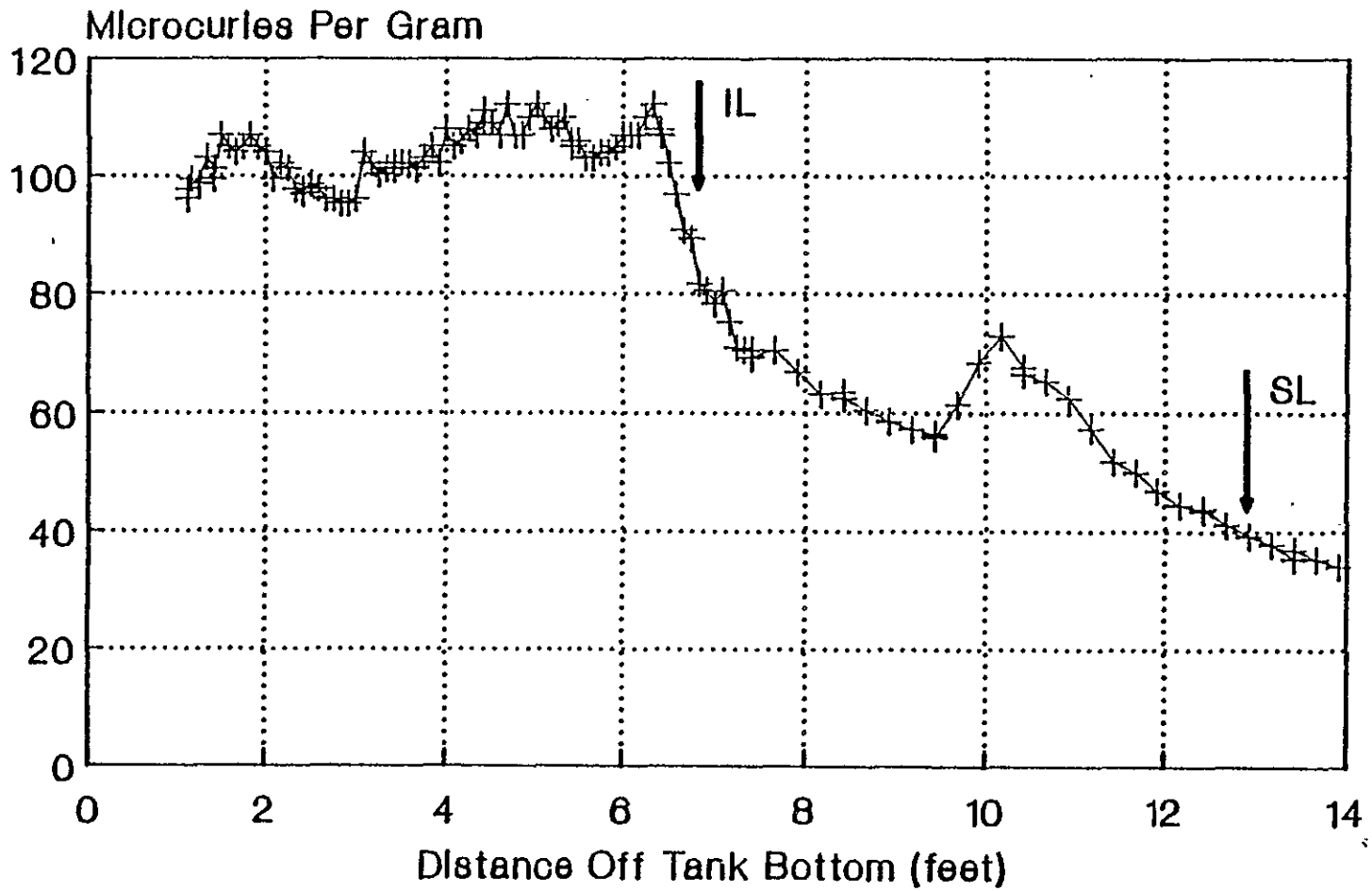

IL: Interstitial Liquid Level
SL: Solids Level

Figure B-30. Tank 241-BY-104 ^{137}Cs Activity.

Figure B-31. Tank 241-BY-105 ^{137}Cs Activity.

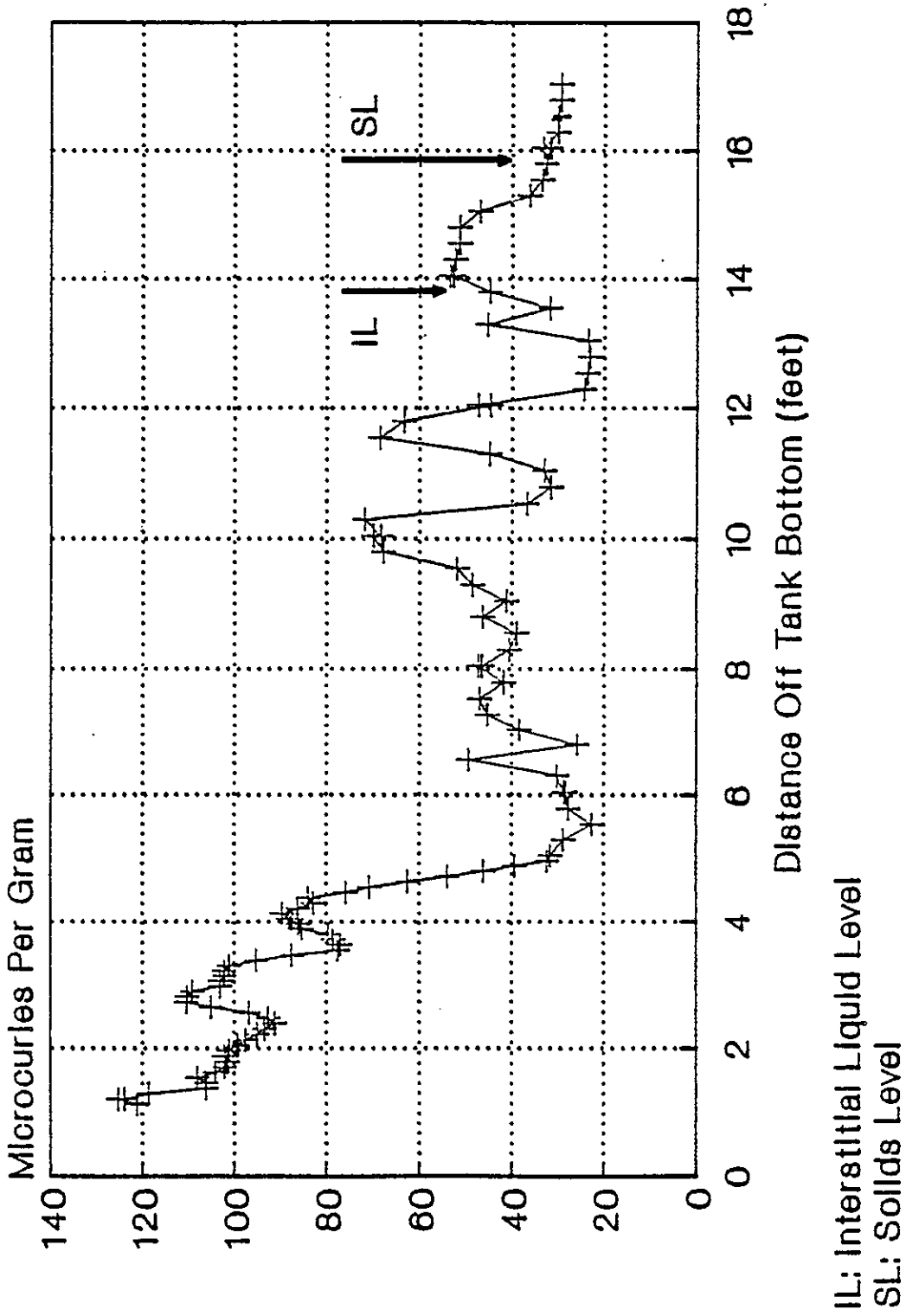

Figure B-32. Tank 241-BY-106 ^{137}Cs Activity.

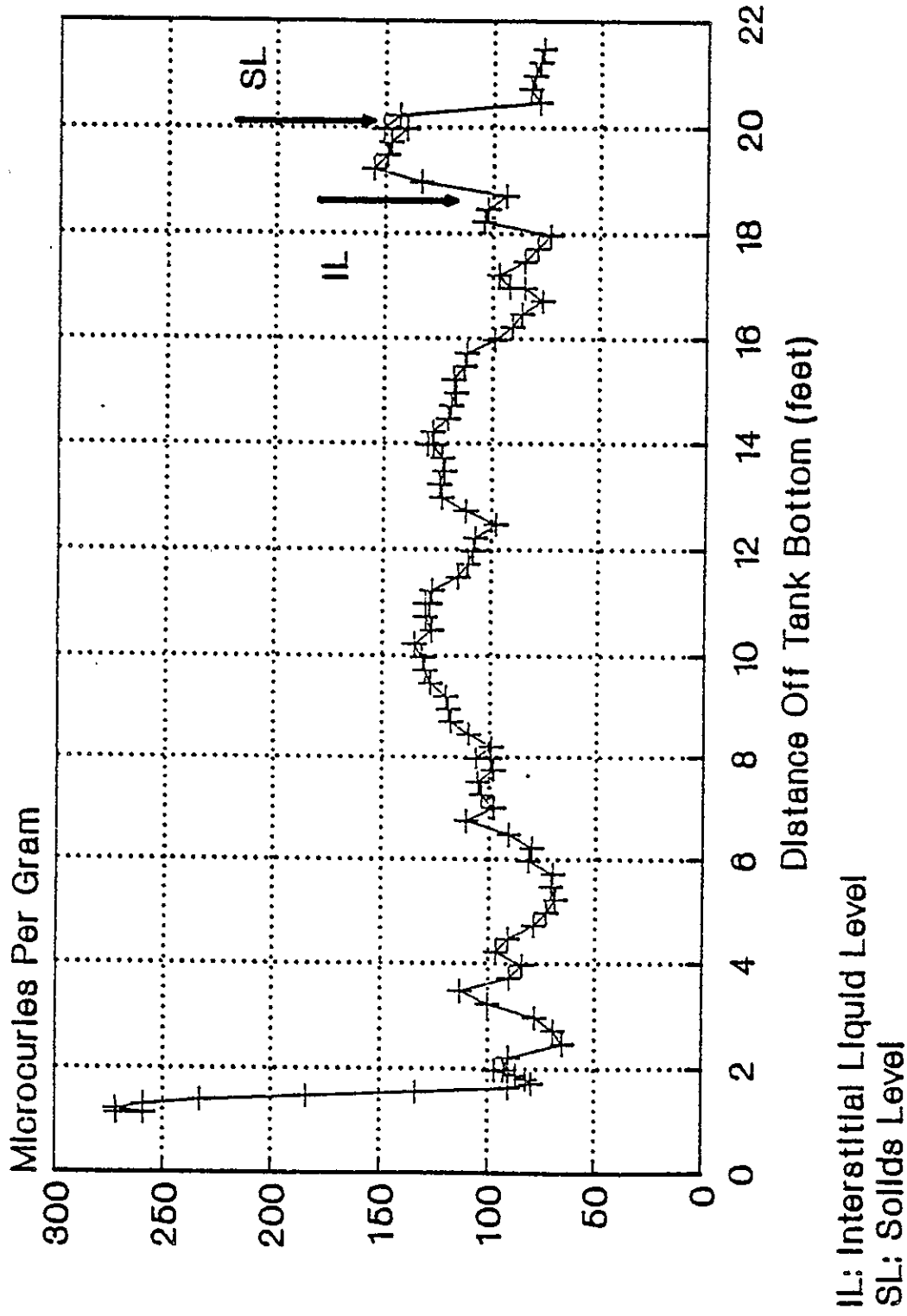

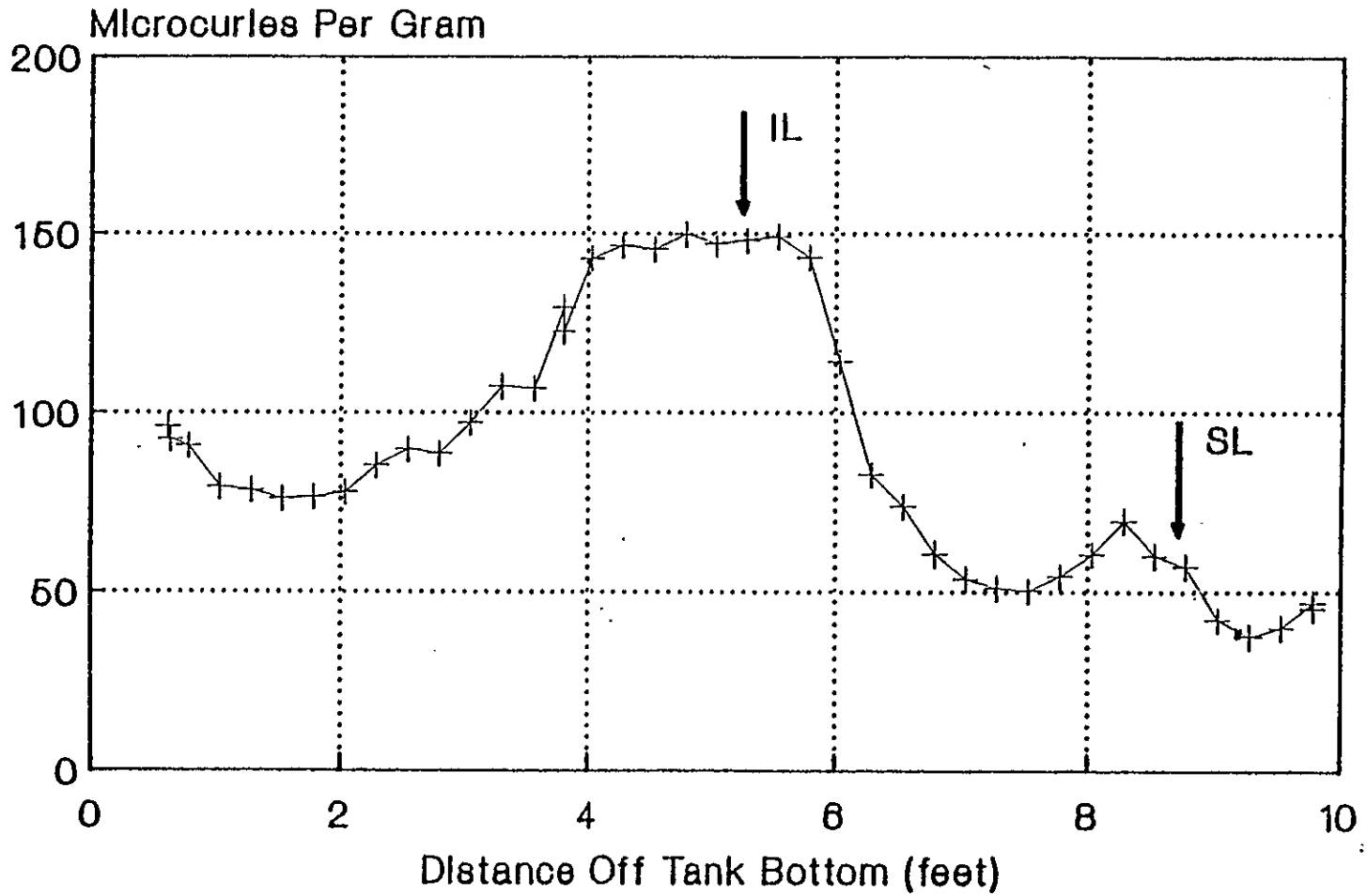

IL: Interstitial Liquid Level
S: Solide Level

Figure B-33. Tank 241-BY-107 ^{137}Cs Activity.

Figure B-34. Tank 241-BY-110 ^{137}Cs Activity.

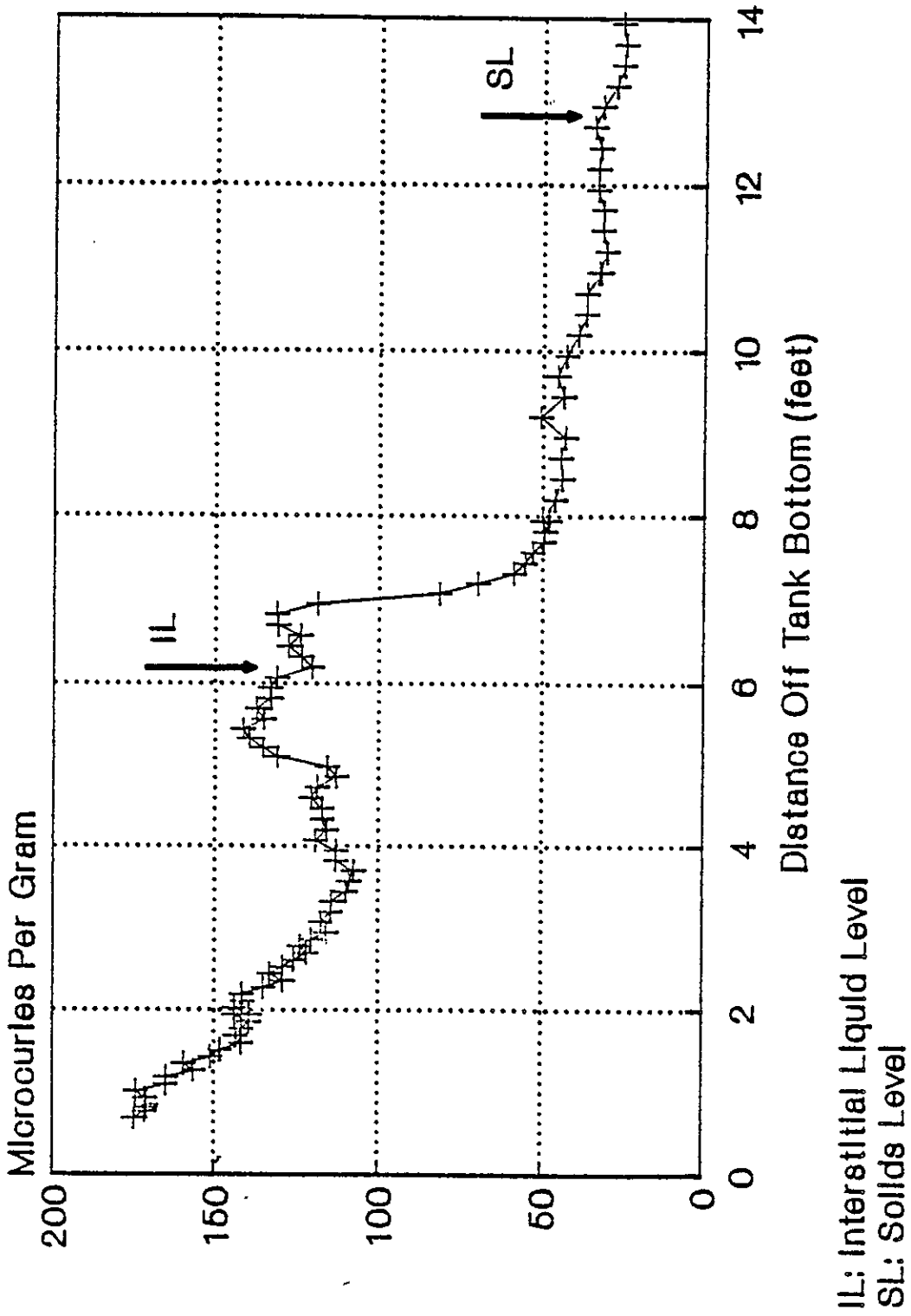

Figure B-35. Tank 241-BY-111 ^{137}Cs Activity.

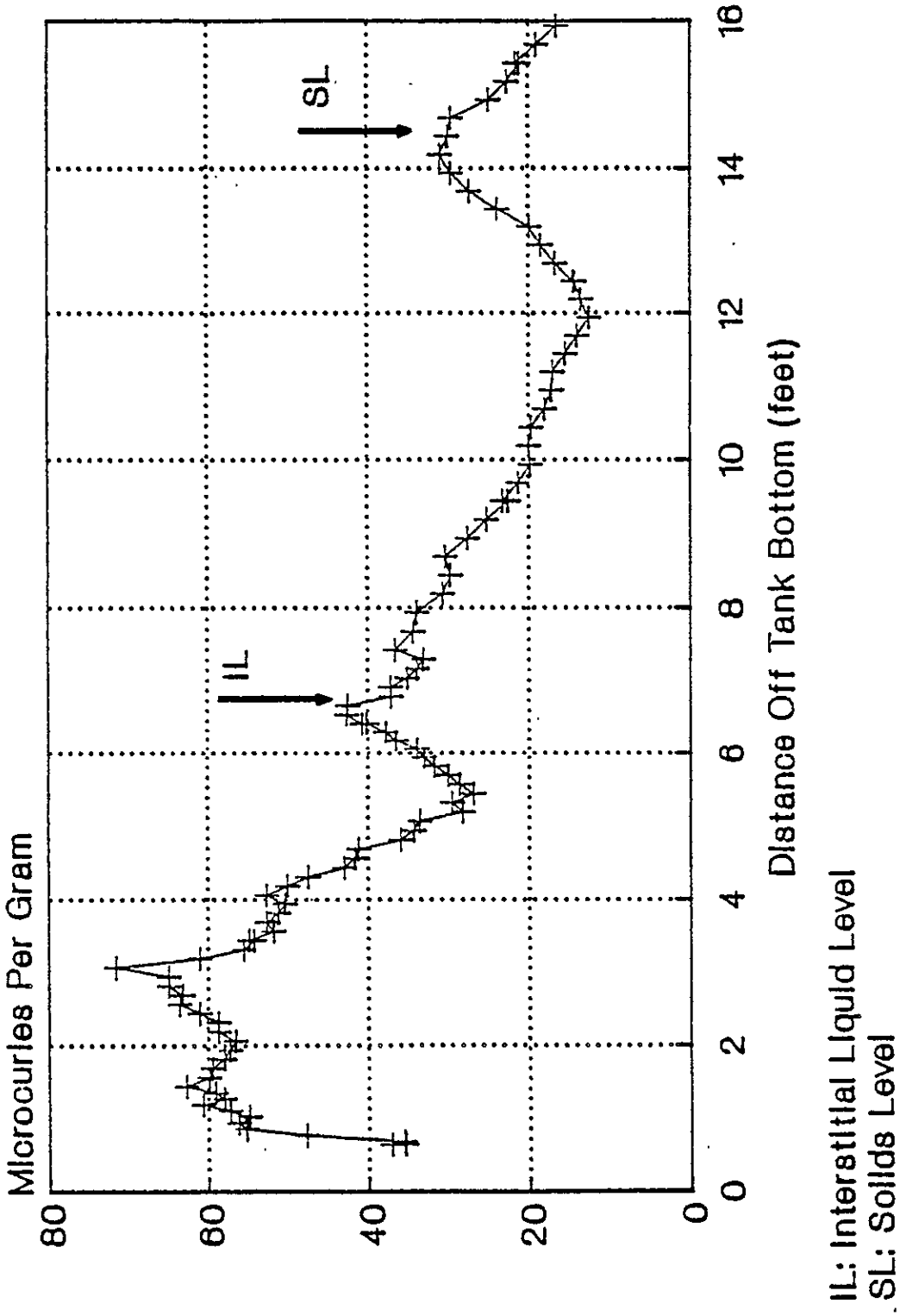

Figure B-36. Tank 241-BY-112 ^{137}Cs Activity.

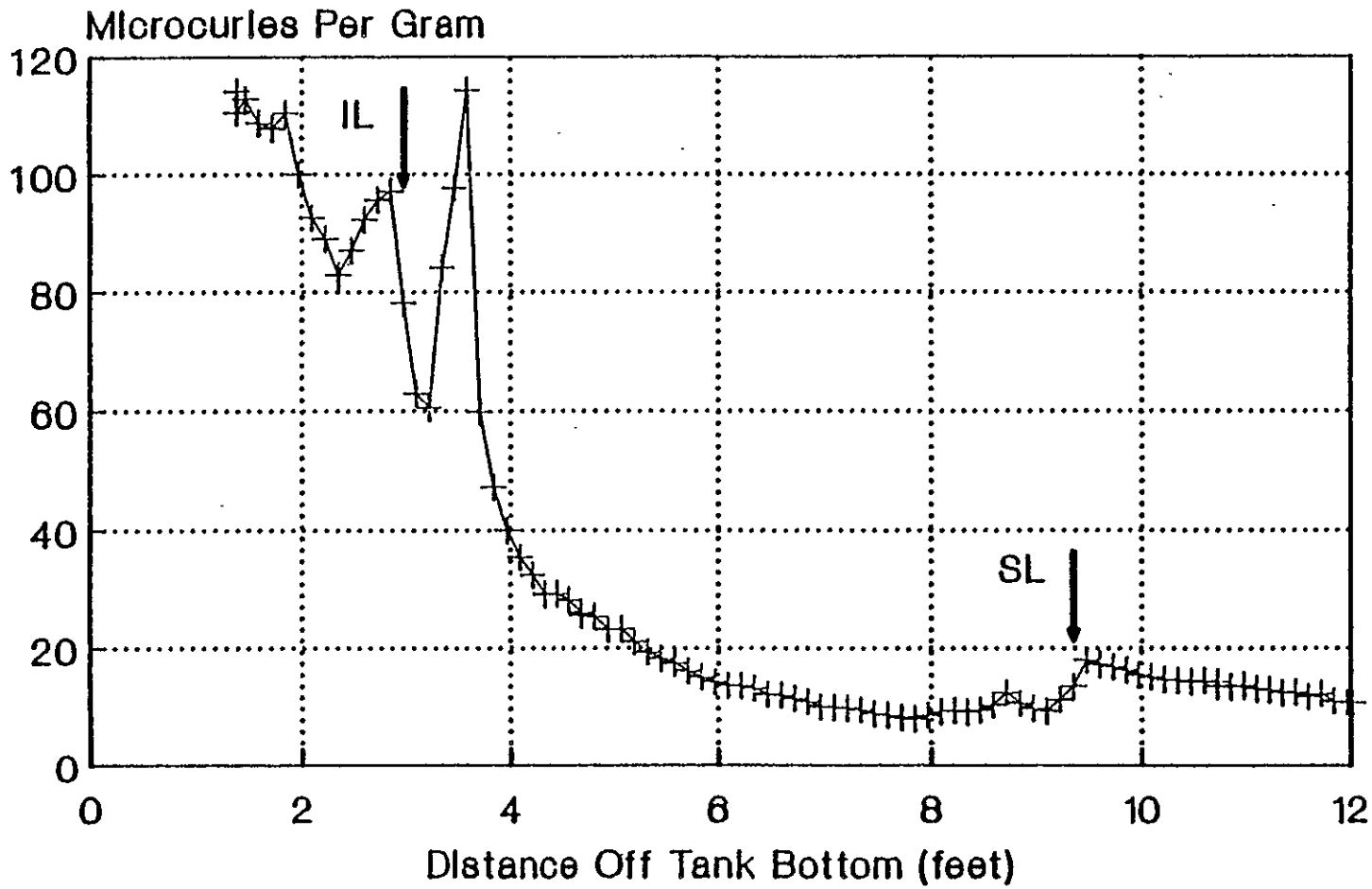

IL: Interstial Liquid Level
SL: Solids Level

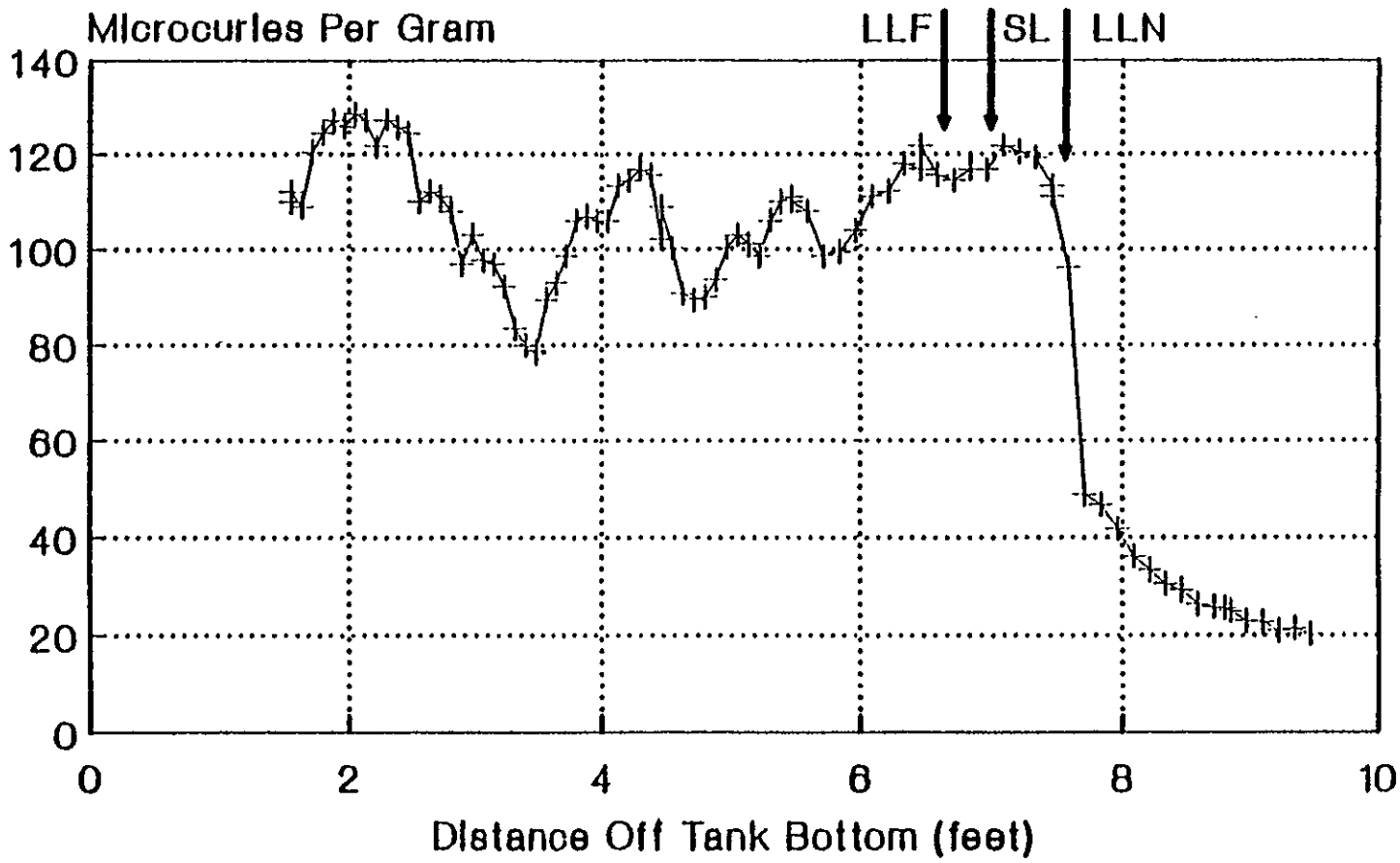

LLF: Liquid Level (FIC)
LLN: Liquid Level (neutron probe)
SL: Solids Level

Figure B-37. Tank 241-BX-111 ^{137}Cs Activity.

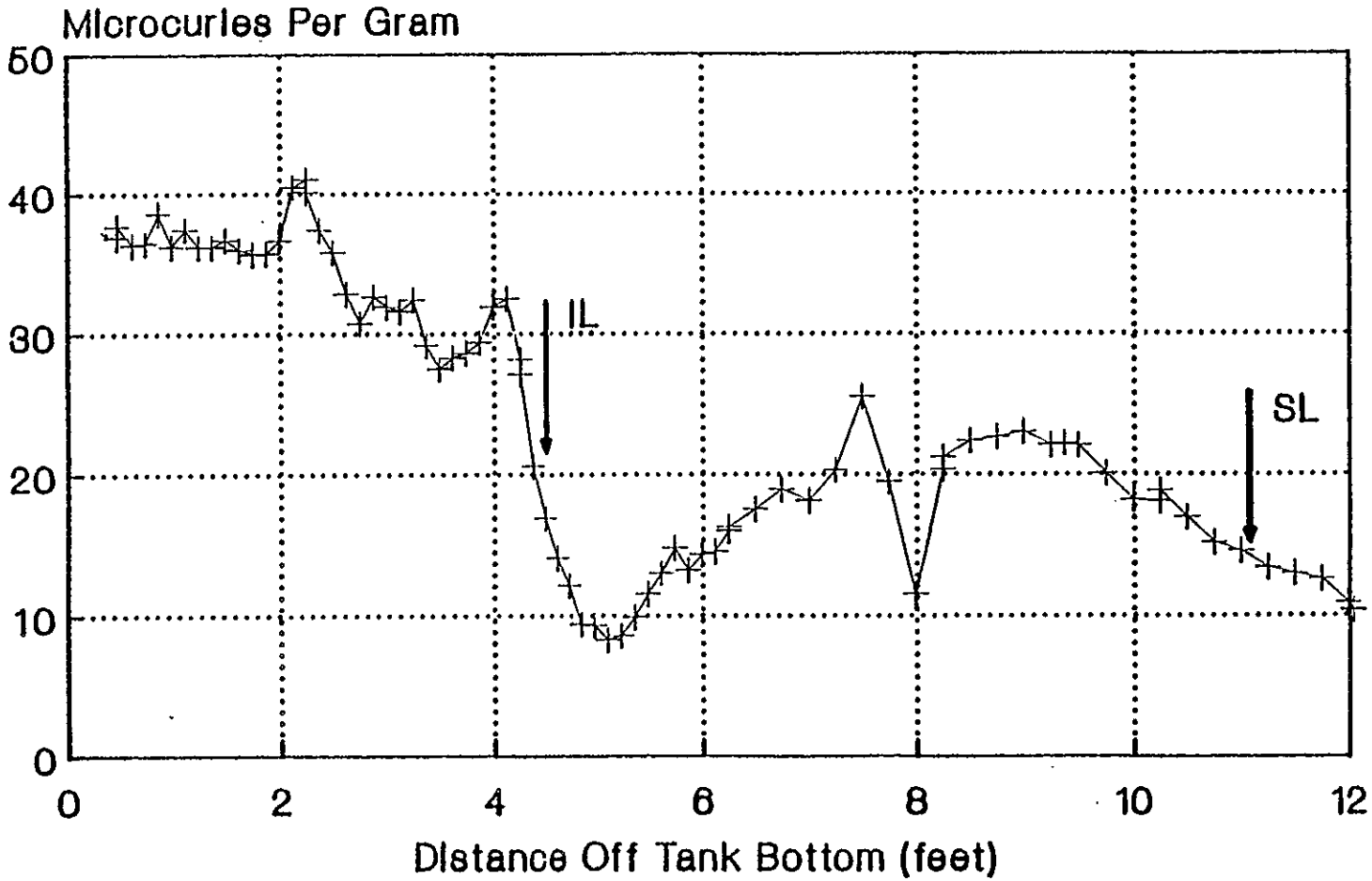

IL: Interstial Liquid Level
SL: Solids Level

Figure B-38. Tank 241-TX-118 ^{137}Cs Activity.

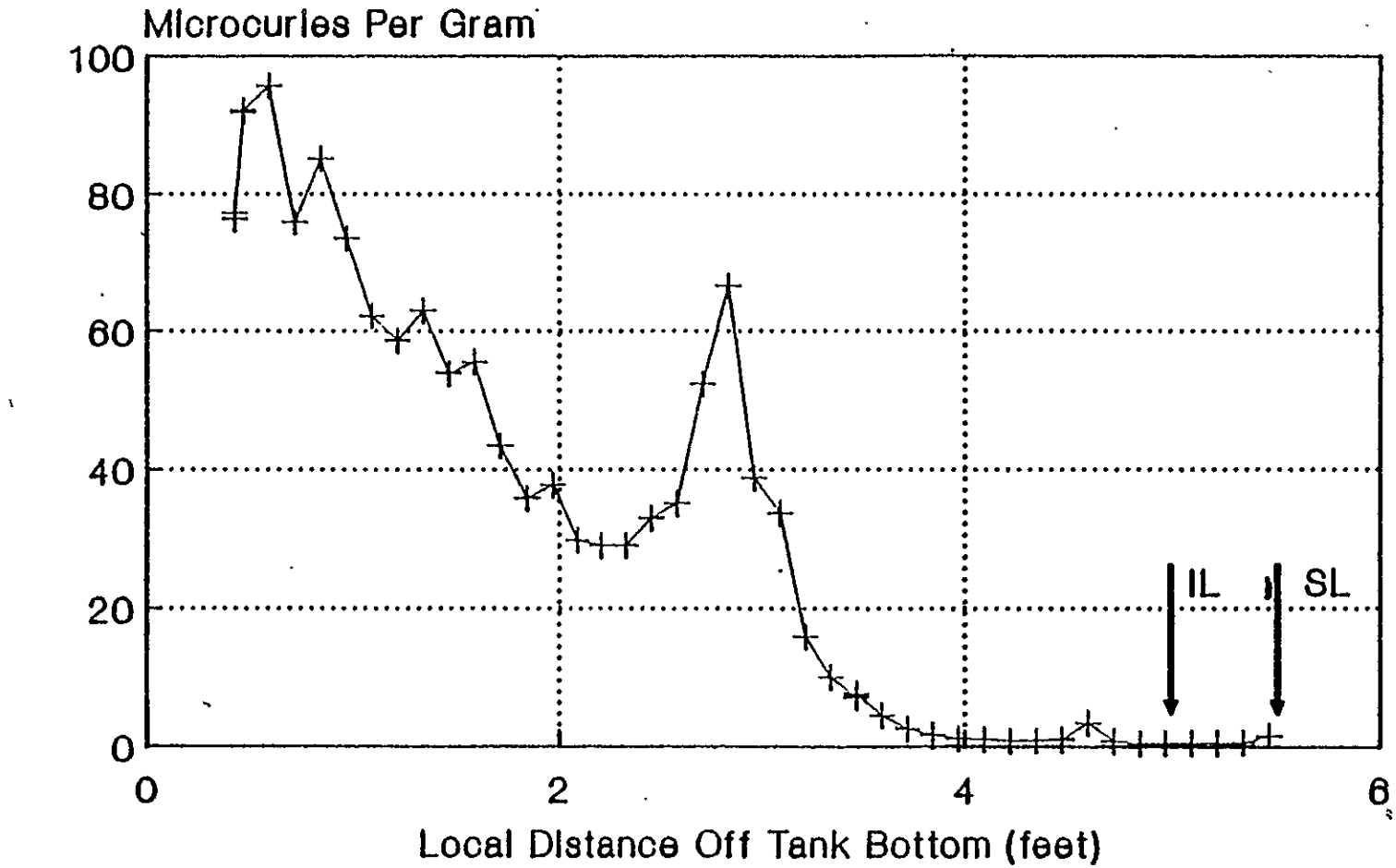

Figure B-39. Tank 241-TY-103 ^{137}Cs Activity.

IL: Interstitial Liquid Level
SL: Solids Level

This page intentionally left blank.

APPENDIX C

SUPPORTING DOCUMENTATION

This page intentionally left blank.

Fauske & Associates, Inc.

RECEIVED
JUL 30 1991
D.D. STEPNEWSKI

8-2-91

DATE: July 25, 1991

TO: Dan Stepnewski, WHC

FROM: Hans K. Fauske, FAI

SUBJECT: **The Potential for Runaway Ferrocyanide Reactions in Hanford Waste Tanks**

The attached material represents a slightly revised version of the earlier paper covering the subject material. Any comments would be appreciated.

The same material has also been sent to Professor Kazimi. He will be using this material in a panel report he is currently preparing. As such, I believe it is important to distribute as well as promote the subject assessment to the Hanford management team.

HKF:jab
Attachment

16W070 West 83rd Street • Burr Ridge, Illinois 60521 • (708) 323-8750
Telefax (708) 986-5481

THE POTENTIAL FOR RUNAWAY FERROCYANIDE REACTIONS IN HANFORD WASTE TANKS

Hans K. Fauske
Fauske & Associates, Inc.
16W070 West 83rd Street
Burr Ridge, Illinois 60521

July, 1991

THE POTENTIAL FOR RUNAWAY FERROCYANIDE REACTIONS IN HANFORD WASTE TANKS

Introduction

A number of single-shell tanks in the Hanford Waste Tank Farms are believed to contain large quantities of ferrocyanide and sodium nitrate with as much as 30 metric tons of ferrocyanide in one tank (104-BY).* Tank 104-BY had its excess supernate water pumped out in January, 1985, leaving behind a 1.5 m crust layer on top of a 2.2 m non-convective sludge layer with a total heat generation rate of about 3000 w (see Figure 1).** The passively ventilated and cooled tank and has remained stable and has not experienced an increase in its temperature since this operation (~ 6 years).

Since certain combinations of ferrocyanides and nitrates are known to be explosive, the possibility of a ferrocyanide runaway reaction and explosion has been used as the basis for the dose calculations shown in the Environmental Impact Statement (EIS). However, recent independent reviews have calculated that the off-site dose from a postulated ferrocyanide explosion would be about two orders of magnitude higher than shown in the EIS [1].

Since ferrocyanides can react with nitrates to release large amounts of heats the above discrepancies in the dose calculations may be difficult to resolve. An alternative would be to examine if the potential exists for a runaway reaction in the single-shell tanks in the first place. If the ferrocyanides are distributed throughout the sludge layer, the high ratio of

*Ferrocyanides (sodium and potassium) were used to precipitate ^{137}Cs out of solution to reduce storage volumes. Sodium nitrate is a major waste component as a result of the neutralization by sodium hydroxide of the nitric acid used in the fuel processing.

**In contrast to the 101-SY tank where the crust and non-convective slurry layer is separated by a convective liquid layer, the "roll-over" phenomenon is of no concern in Tank 104-BY.

Tank 104-BY

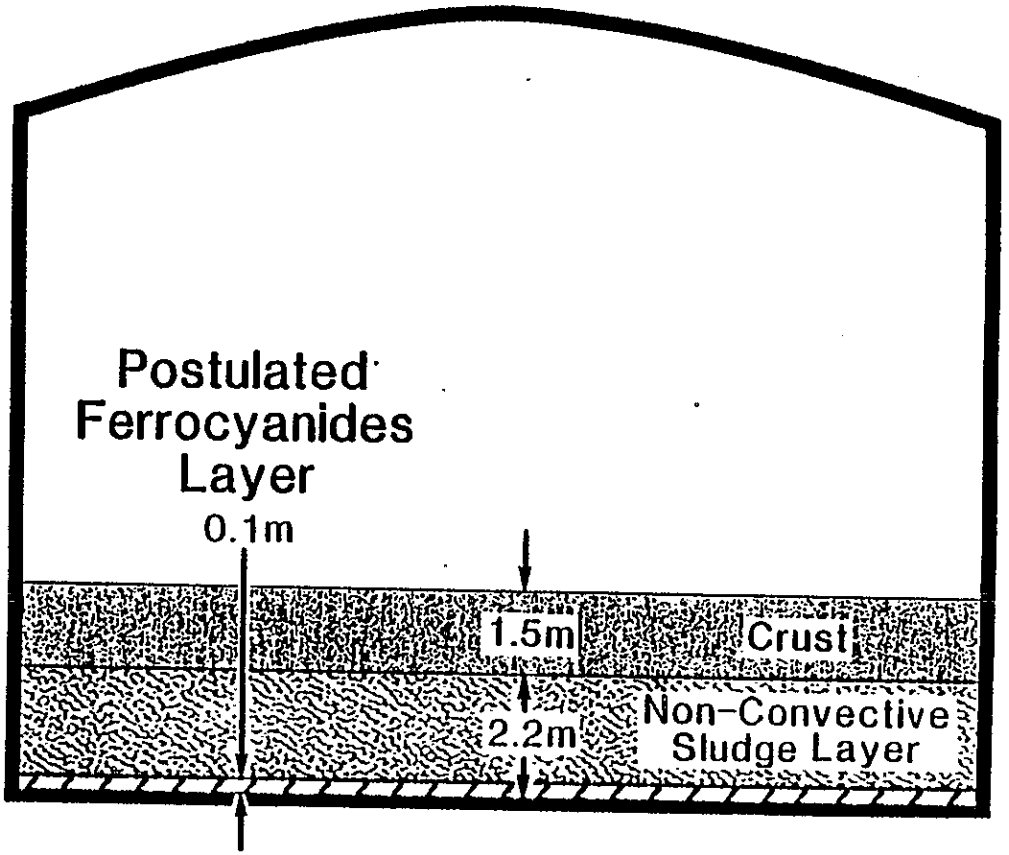

Figure 1 Illustration of waste content in Tank 104-BY including a postulated thin layer of ferrocyanides in the bottom of the tank.

inerts including interstitial water would render an explosion impossible. On the other hand, if the ferrocyanides are assumed to be concentrated in a ~ 0.1 m thin layer (see Figure 1) at the bottom of the tank (the postulated accident scenario) an explosive condition would be possible if the conditions for a runaway reaction are satisfied. Fortunately, based on observations summarized below, we conclude that a runaway reaction in Tank 104-BY can be ruled out.

Assessment of Runaway Potential

Large Scale Experience - Safe operating conditions of Tank 104-BY containing a postulated thin layer of ferrocyanides can be assessed by comparing adiabatic runaway and characteristic cooling response times to the storage or exposure time.

The characteristic time of adiabatic runaway can be estimated from [2]

$$t_a = \frac{R\,T_o^2}{\dot{T}\,E_a} \qquad (1)$$

where R = gas constant,

E_a = activation energy,

T_o = storage temperature, and

$\dot{T}$ = self-heating rate at T_o.

If the following inequality is satisfied

$$t_a \gg t_s \qquad (2)$$

where t_s is the storage time, the situation can immediately be judged to be safe, i.e., a runaway ferrocyanide reaction cannot take place. Unfortunately, since the value of t_a is not known for the materials in the Hanford waste tanks and furthermore, t_s is very large (many years), Inequality (2) is of little use. The possibility that

$$t_a \ll t_s \tag{3}$$

cannot be ruled out which raises the potential for a runaway condition. If

$$t_a \ll t_c \tag{4}$$

where t_c is the characteristic cooling response time given by

$$t_c = \frac{L^2}{\alpha} \tag{5}$$

where L = characteristic dimension of the postulated ferrocyanide layer, and

α = thermal diffusivity,

the potential for a runaway condition clearly exists.

Fortunately, it can be shown that*

$$t_c \ll t_s \tag{6}$$

and the fact that no runaway conditions have been experienced to date, we can conclude that

$$t_a \gg t_c \tag{7}$$

without requiring a knowledge of t_a. <u>Inequality (7), is the usual requirement employed in the chemical process industry to assure safe operation</u>.

<u>Adiabatic Calorimetry Experience</u> - It is of interest to note that interpretation of recent adiabatic calorimetry tests [3] with synthetic

*Setting $\alpha = 1.5 \cdot 10^{-7}$ m^2 s^{-1}, and considering a value of L of 0.1 m (corresponding to the postulated ferrocyanide layer), Equation (5) leads to a cooling response time of about one day, which is well below the current exposure time (about six years since the last pumping operation).

ferrocyanide mixtures collaborates Inequality (7). Arrhenius type behavior consistent with Equation (1) was generally observed prior to the onset of an energetic propagating reaction. For a stoichiometric mixture of ferrocyanide and nitrate the data suggest a value of the activation energy of about $E_a \approx 20$ kcal mol^{-1} and an extrapolated value of the self-heat rate of about $\dot{T} = 10^{-4}$°C min^{-1} at a tank storage temperature of about 60°C (see Figure 2). Substituting the above values into Equation (1) results in a conservative estimate of the adiabatic runaway time of about 100 days, clearly well in excess of the cooling response time of about one day for the postulated ferrocyanide layer.

Concluding Remarks

We conclude from the above considerations that a runaway ferrocyanide reaction in Tank 104-BY can be ruled out as long as the existing conditions are not significantly changed. Since the relatively small amount of heat (~ 3000 w) generated in the tank is easily removed to the atmosphere by passive means (conduction and free convection)* at temperatures well below the boiling point of water, the sludge layer will remain invariant in terms of liquid content. It is estimated that about 4 gallons of water per day is removed from the tank in connection with passive venting [4]. This translates to only about 2% drop (or 3 inches) in the tank content level over a period of about six years. Concerns raised relative to hot spot formation (or dry spots), if real, should have appeared less than a year after the last liquid pump-out operation, considering the necessary large local concentration of the heat sources as compared to the average value in order to reach critical runaway conditions.**

*The surface heat flux at the top of the crust material is less than 7 w m^{-2} requiring a negligible temperature drop in tank dome space in order to transfer the heat load by free convection.

**At ten times the average heating value (~ 33 w m^{-3}) and 20% interstitial water, local dryout conditions would be reached in about 200 days.

Adiabatic Calorimetry Data

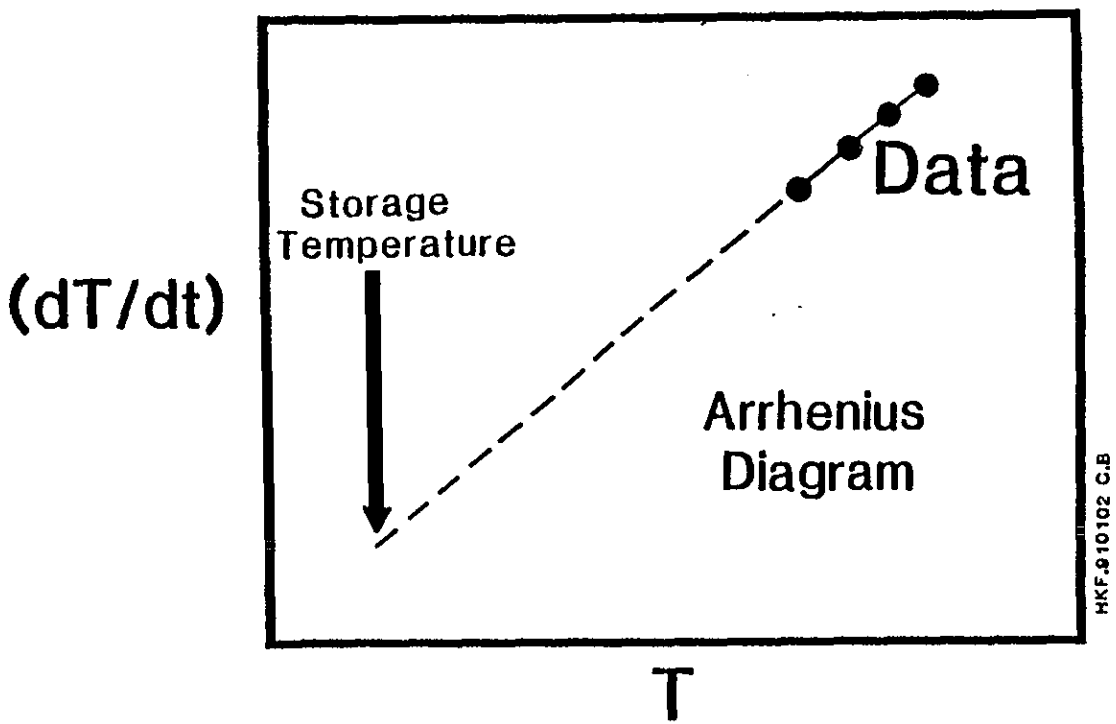

Figure 2 Extrapolation of adiabatic calorimetry data - provides an estimate of the self-heat rate at the storage temperature.

Based upon the above considerations including the six year stable storage experience we conclude that such concerns are no longer real. As such, in terms of interim storage, there is no need to consider explosive interactions involving ferrocyanide as part of the EIS. Efforts should instead focus on long term permanent storage considerations with emphasis on improved understanding of the actual composition of the materials in the waste tanks and the energetics potential for relatively dry conditions that may have to be considered in terms of safe permanent storage.

References

1. Hinman, George W., "The Ferrocyanide Issue", Draft Report, (August 24, 1990).

2. Townsend, H. P. and Tou, J. C., Thermochim. Acta, 37, pp. 1-30, (1980).

3. Fauske, H. K., "An Update of RSST Scoping Tests With Synthetic Ferrocyanide Mixtures", FAI Memo to D. D. Stepnewski, (November 15, 1990).

4. McLaren, J., Personal Communication, June 12, 1991.

Fauske & Associates, Inc.

RECEIVED
JAN 15 91
D.D. STEPNEWSKI

XC
L5-01 E Fox
H0-32 A Padilla
T6-58 D. Bechtold
L5-03 G. Johnson
B1-35 M Shannon
B3-68 R. Cash
1-15-91

DATE: January 4, 1991

TO: D. D. Stepnewski Westinghouse Hanford Company

FROM: H. K. Fauske JB for HKF Fauske & Associates, Inc.

SUBJECT: **RSST Scoping Tests With Synthetic Ferrocyanide Mixtures Without EDTA**

Reference [1] provided an update of RSST scoping tests with synthetic ferrocyanide mixtures including EDTA as prescribed in Reference [2]. Reference [3] also requested an adiabatic calorimetry test on an equal weigh mixture of Cs_2 Ni Fe $(CN)_6$ and 55.2% $NaNO_3$/44.8% $NaNO_2$ by Wt. without EDTA. The test data are summarized below. A comparison test with a weight ratio of oxidant to ferrocyanide of 2.2 without EDTA is also summarized.

Fuel/Oxidant Ratio of 1 (Weight Basis)

The sample (9.92 gm) was heated from room temperature at an imposed rate of between 1 and 2°C/min. Similar to previous adiabatic tests with ferrocyanide mixtures (including EDTA), an Arrhenius type reaction changed to an energetic propagation reaction (see Figures 1 through 3). The onset of a propagating reaction occurs around 280°C resulting in a temperature in excess of 1350°C and a RSST containment vessel pressure of about 330 psig. After cooldown the pressure was about 111 psig. These results are quite similar to the previous test including EDTA (representing a fuel/oxidant ratio of 1) with one exception. The incipient propagation temperature without EDTA was about 280°C as compared to 220°C with EDTA.

Oxidant/Fuel Ratio of 2.2 (Weight Basis)

The sample (9.98 gm) was heated from room temperature at an imposed rate of about 1°C/min. Pertinent data are provided in Figures 4 through 6. The trends are quite similar to the test with an oxidant/fuel ratio of 1 (noticeable Arrhenius behavior at about 185°C with a change to a propagation reaction at around 275°C), with the exception of considerable lower peak temperature (~ 870°C) and pressure (~ 75 psig). After cooldown the measured containment pressure was 32 psig. The lower values are consistent with the increased percentage of inert material relative to the oxidant/fuel ratio test of 1.

16W070 West 83rd Street • Burr Ridge, Illinois 60521 • (708) 323-8750
Telefax (708) 986-5481

References

1. Fauske, H. K., "An Update of RSST Scoping Tests With Synthetic Ferrocyanide Mixtures", FAI Memo to D. D. Stepnewski, (November 15, 1990).

2. Bechtold, D. B., "Adiabatic Calorimetry Tests on Synthetic Ferrocyanide Mixtures", Memo to H. K. Fauske, (October 17, 1990).

3. Bechtold, D. B., "Adiabatic Calorimetry Test on Synthetic Ferrocyanide Mixture", Memo to H. K. Fauske, (December 27, 1990).

HKF:jab

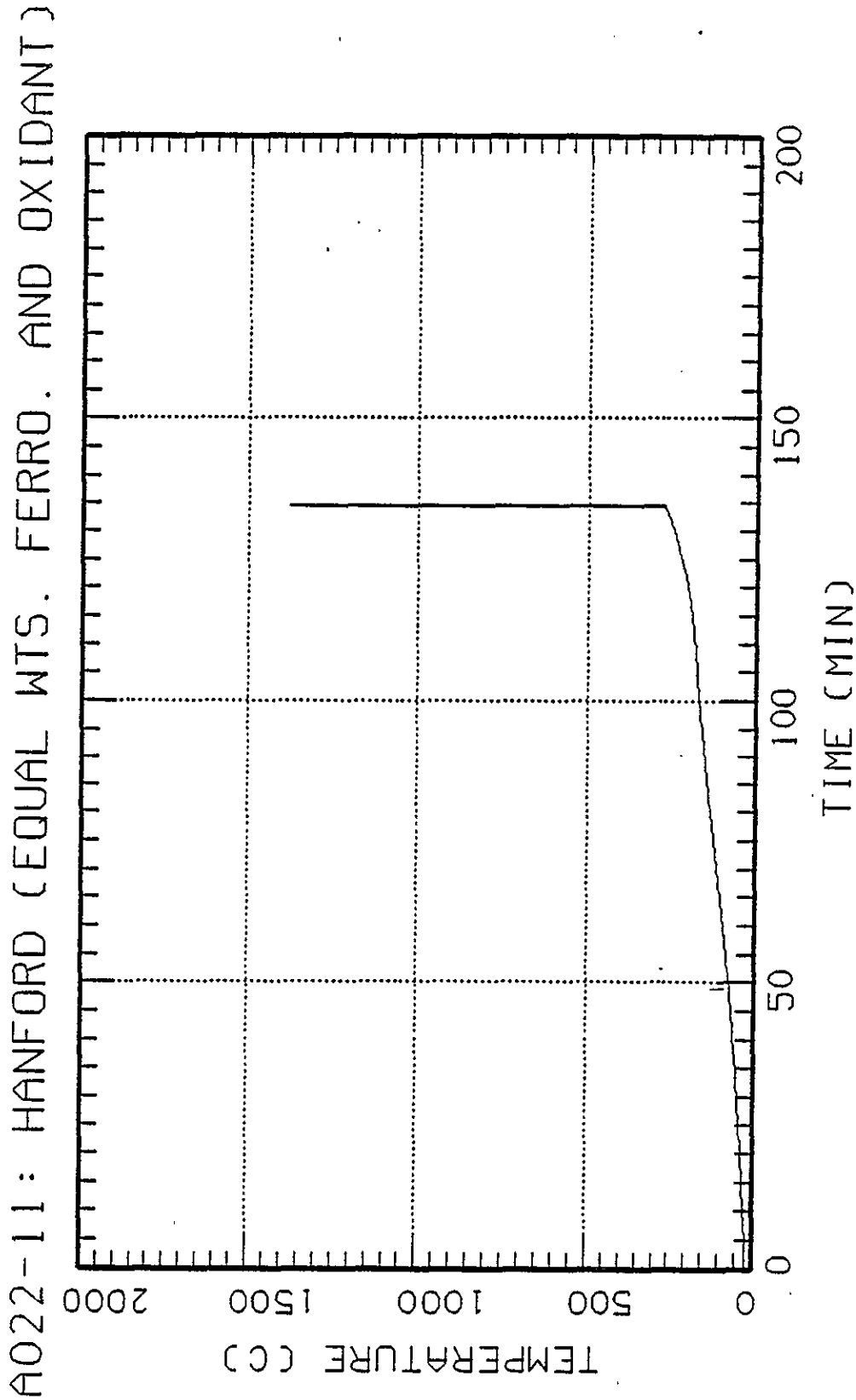

FIGURE 1 TEMPERATURE DATA FROM A022-11

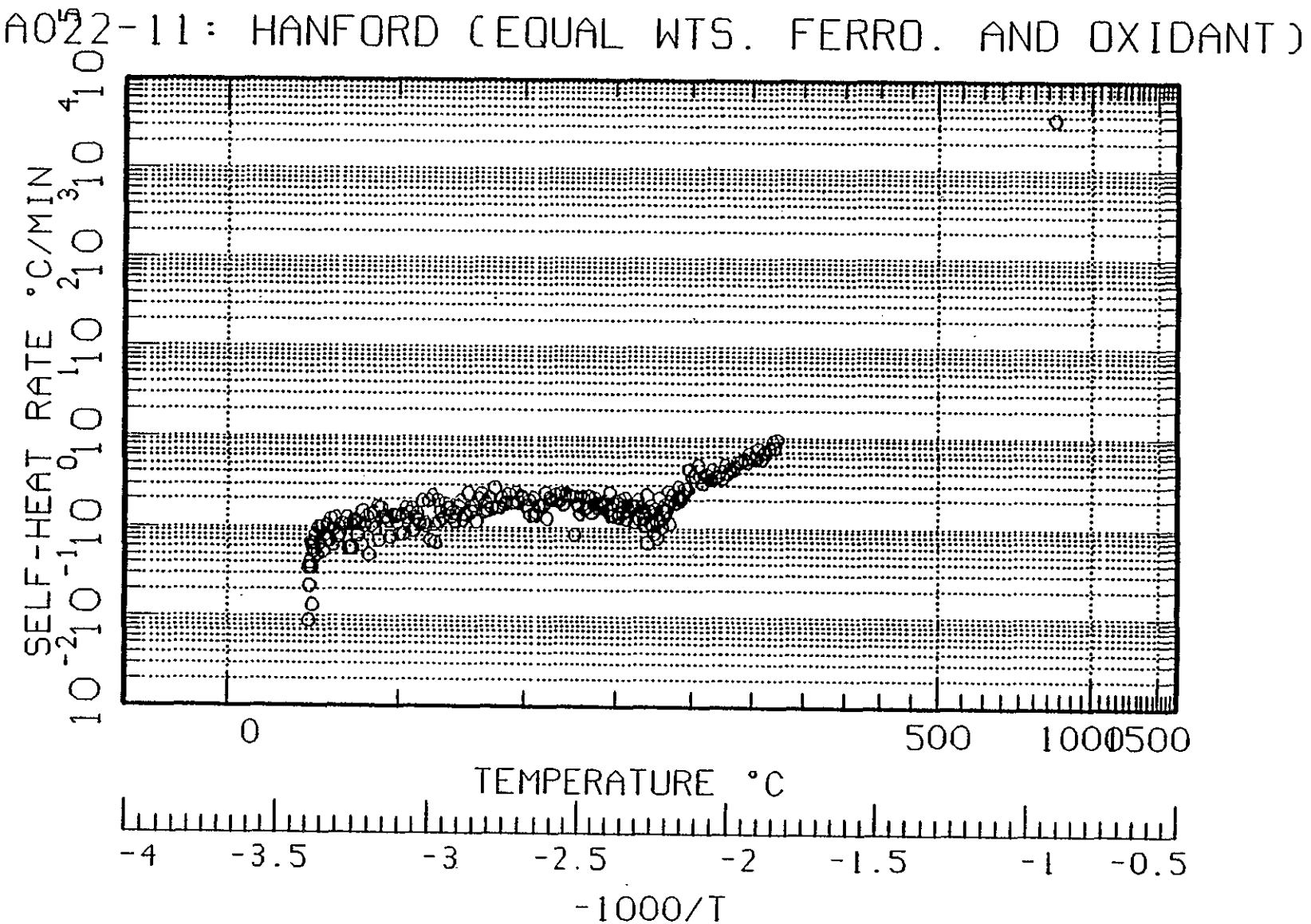

FIGURE 2 SELF-HEAT RATE DATA FROM A022-11

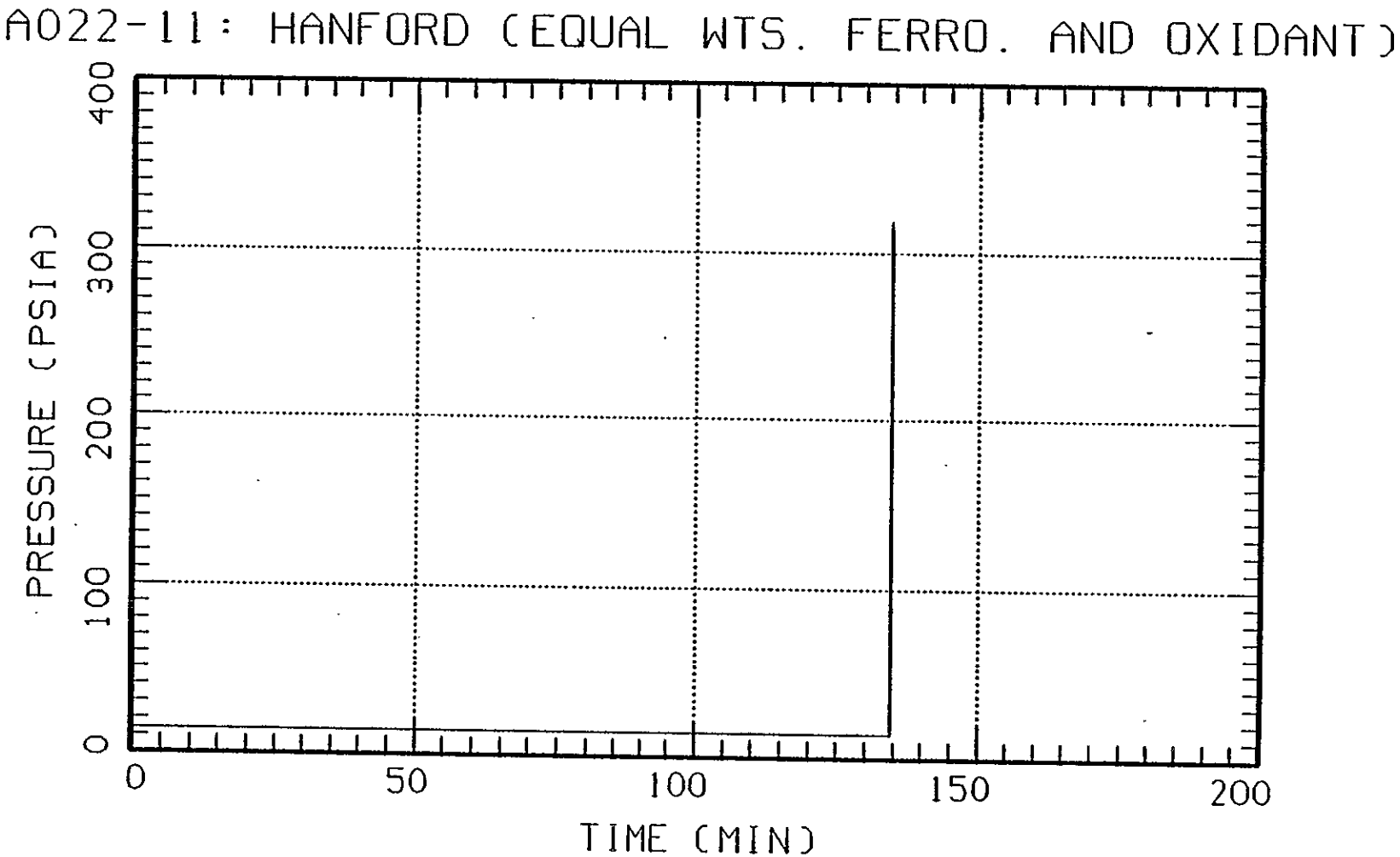

FIGURE 3 PRESSURE DATA FROM A022-11

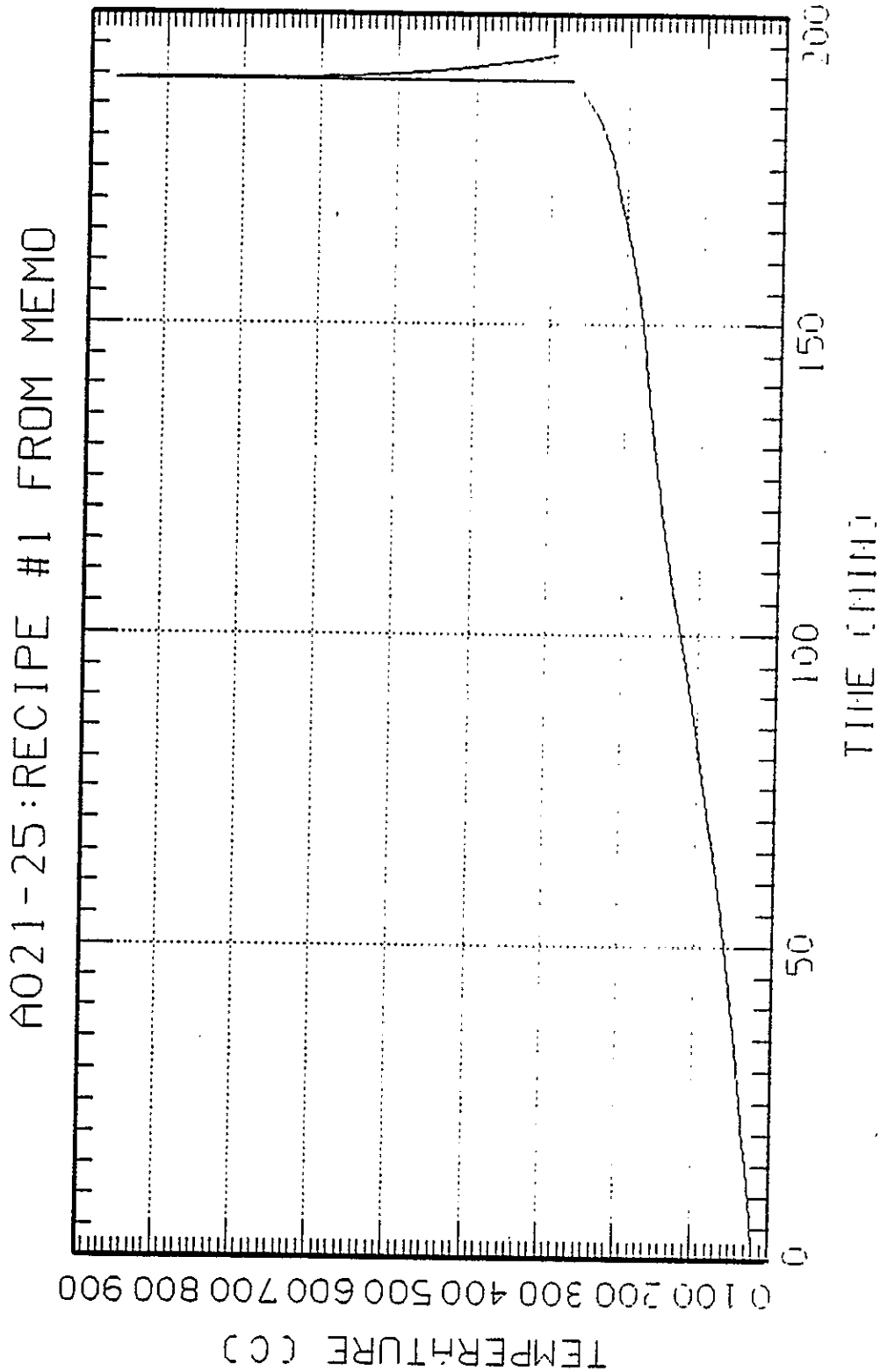

FIGURE 4 TEMPERATURE DATA FROM A021-25

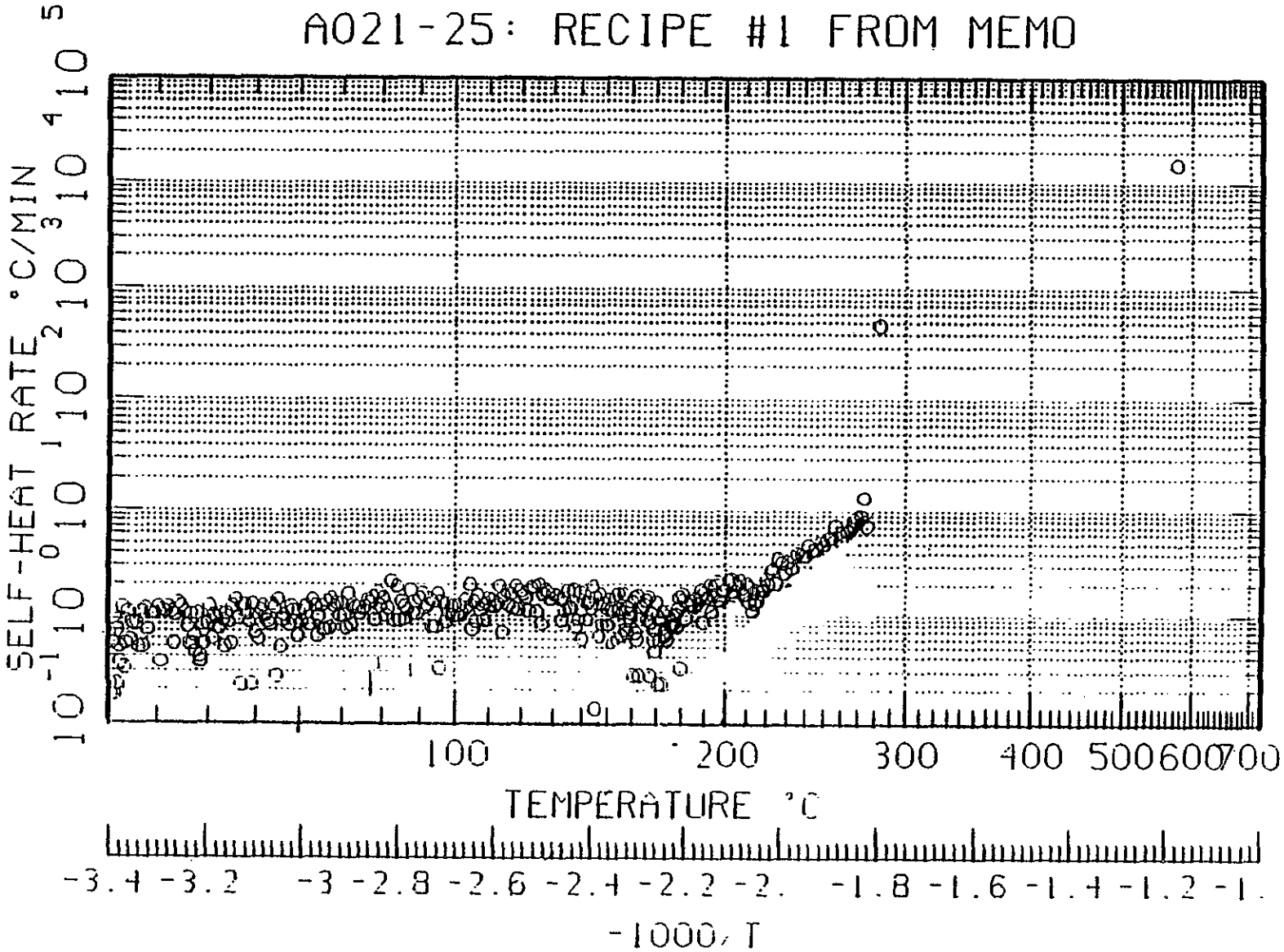

FIGURE 5 SELF-HEAT RATE DATA FROM A021-25

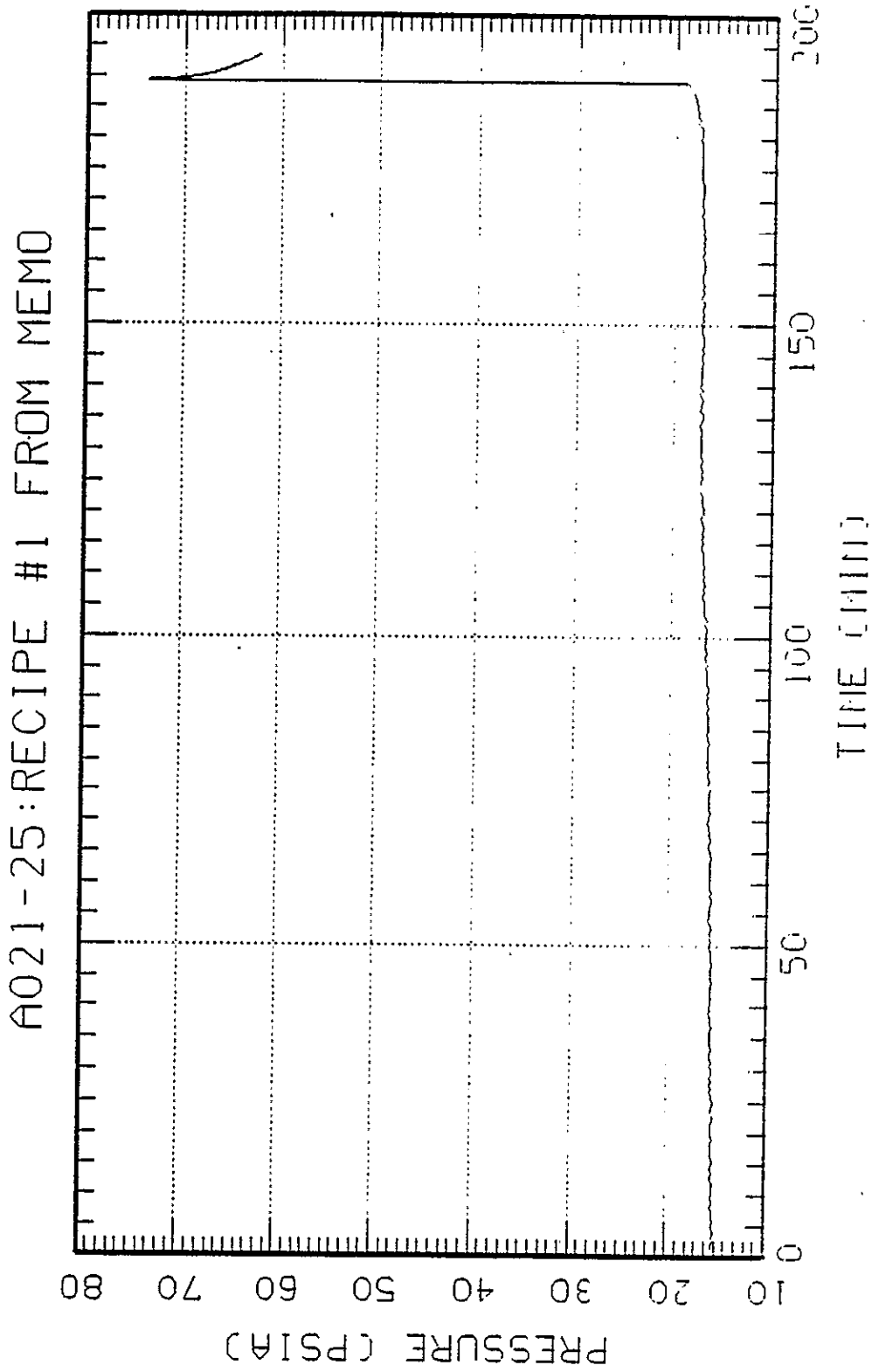

FIGURE 6 PRESSURE DATA FROM A021-25

This page intentionally left blank.

Date Received: ~~5/29/92~~ ~~11/9/92~~	~~Ret.~~	INFORMATION RELEASE REQUEST	Reference: WHC-CM-3-4

Complete for all Types of Release

Purpose

- [] Speech or Presentation
  - [] Full Paper (Check only one suffix)
  - [] Summary
  - [] Abstract
  - [] Visual Aid
- [] Speakers Bureau
- [] Poster Session
- [] Videotape
- [] Reference
- [X] Technical Report
- [] Thesis or Dissertation
- [] Manual
- [] Brochure/Flier
- [] Software/Database
- [] Controlled Document
- [] Other

ID Number (include revision, volume, etc.): WHC-SD-WM-RPT-032 Rev 1

List attachments.

Date Release Required: 6/1/92

Title: Ferrocyanide Waste Tank Hazard Assessment Interim Report

Unclassified Category: UC-

Impact Level: 259

New or novel (patentable) subject matter? [X] No [] Yes
If "Yes", has disclosure been submitted by WHC or other company?
[] No [] Yes Disclosure No(s).

Information received from others in confidence, such as proprietary data, trade secrets, and/or inventions?
[X] No [] Yes (Identify)

Copyrights? [X] No [] Yes
If "Yes", has written permission been granted?
[X] No [] Yes (Attach Permission)

Trademarks?
[X] No [] Yes (Identify)

Complete for Speech or Presentation

Title of Conference or Meeting

Group or Society Sponsoring

Date(s) of Conference or Meeting

City/State

Will proceedings be published? [] Yes [] No
Will material be handed out? [] Yes [] No

Title of Journal

CHECKLIST FOR SIGNATORIES

Review Required per WHC-CM-3-4	Yes	No	Reviewer - Signature Indicates Approval: Name (printed)	Signature	Date
Classification/Unclassified Controlled Nuclear Information	[]	[X]			
Patent - General Counsel	[X]	[]	B. D. Williamson	[signature]	6/1/92
Legal - General Counsel	[X]	[]	B. D. Williamson	[signature]	6/1/92
Applied Technology/Export Controlled Information or International Program	[]	[X]			
WHC Program/Project	[X]	[]	R. J. Cash	[signature]	6-1-92
Communications	[X]	[]	E. J. Campbell	[signature]	6/22/92
RL Program/Project	[X]	[]	R. F. Christensen WFH	[signature]	7/24/92
Publication Services	[X]	[]	L. A. Brown	L.A. Brown	7/24/92
Other Program/Project	[]	[X]			

Information conforms to all applicable requirements. The above information is certified to be correct.

	Yes	No
References Available to Intended Audience	[X]	[]
Transmit to DOE-HQ/Office of Scientific and Technical Information	[]	[X]

Author/Requestor (Printed/Signature): R.D. Crowe/ [signature] Date: 5/28/92

Intended Audience

[] Internal [] Sponsor [X] External

Responsible Manager (Printed/Signature): M.H. Shannon/ [signature] Date

INFORMATION RELEASE ADMINISTRATION APPROVAL STAMP

Stamp is required before release. Release is contingent upon resolution of mandatory comments.

APPROVED FOR RELEASE — OFFICIAL DOCUMENT — V.B. — Date 7/24/92

Date Cancelled

Date Disapproved

BD-7600-062 (08/91) WEF074 Part 1

DISTRIBUTION SHEET

To: DISTRIBUTION

From: Waste Remediation Safety Programs

Date: 11/08/92

Project Title/Work Order:

Ferrocyanide Waste Tank Hazard Assessment - Interim Report

EDT No.:

ECN No.: 185093

Name	IN	With Attachment	EDT/ECN & Comment	EDT/ECN Only
R. T. Allemann	K7-15			
J. M. Atwood	S0-61			
H. Babad	R2-08			
D. B. Bechtold	T6-50			
J. B. Billetdeaux	R2-08			
G. L. Borsheim	R2-11			
S. A. Bryan	P7-25			
R. J. Cash (5)	R2-31			
R. F. Christensen (8)	A4-02			
M. D. Crippen	L5-31			
R. D. Crowe	H5-32			
C. DeFigh-Price	B4-55			
D. R. Dickinson	L5-31			
G. T. Dukelow	R2-32			
J. G. Flandro	R2-31			
C. J. Forbes	R1-08			
G. L. Fox	L5-01			
G. T. Frater	R1-51			
J. C. Fulton	R2-31			
K. A. Gasper	R2-08			
R. E. Gerton	A4-02			
J. M. Grigsby	H5-32			
T. W. Halverson	T5-49			
D. G. Hamrick	R1-51			
H. D. Harmon	R2-52			
D. L. Heer	H0-38			
J. D. Hopkins	R2-08			
R. D. House	A5-55			
L. L. Humphreys	R2-83			
M. N. Islam	R2-52			
D. W. Jeppson	R3-08			
J. R. Jewett	L5-31			
B. M. Johnson	K1-78			
N. W. Kirch	P8-38			
W. L. Knecht	T6-50			
A. G. Krasopoulos	R2-11			
C. A. Kuhlman	H0-34			
M. A. Lilga	B3-30			
J. D. McCormack	L5-31			
J. M. McLaren	H0-34			
N. J. Milliken	H5-34			
A. F. Noonan	R2-12			
R. S. Popielarczyk	R1-30			
R. E. Raymond	R1-80			
I. E. Reep	R2-08			
E. L. Renner	R2-08			
D. A. Reynolds	P8-38			
D. C. Richardson	R2-11			
R. D. Scheele	P7-25			
G. F. Schiefelbein	R2-31			
C. P. Schroeder	L7-06			
M. H. Shannon	H5-30			
N. L. Simon	R2-78			
B. C. Simpson	K2-38			
D. M. Strachan	R2-12			
H. Toffer	H0-38			
R. K. Welty	R1-80			
W. F. Zuroff	R2-14			
Central Files	L8-04			
EDMC	H4-22			
Information Release Administration	A1-65			
PNL Technical Files	K1-11			
Public Reading Room	A2-24			
RL Docket File	A3-11			
TFIC	R1-28			

DISTRIBUTION

Number of copies	
OFFSITE	
25	U.S. Department of Energy EM-35, Trevion II Washington, D.C. 20585 John C. Tseng
1	U.S. Department of Energy Idaho Operations Office 785 DOE Place Idaho Falls, Idaho 83402 P. Gene Woodall
1	U.S. Department of Energy Savannah River Operations Office P.O. Box A Aiken, South Carolina 29808 Thomas C. Temple
1	Charles S. Abrams 1987 Virginia Idaho Falls, ID 83404
1	David O. Campbell 102 Windham Road Oak Ridge, TN 37830
1	Fred N. Carlson 6965 North 5th West Idaho Falls, ID 83401
1	Donald T. Oakley 409 12th Street SW, Suite 310 Washington, DC 20024-2188
1	Arlin K. Postma 3640 Ballard Road Dallis, Oregon 97338
1	Air Products & Chemicals, Inc. 7201 Hamilton Blvd Allentown, PA 18195-1501 George E. Schmauch

DISTRIBUTION (cont)

Number of copies	
OFFSITE	
1	Battelle Columbus Laboratories 505 King Avenue Columbus, OH 43201-2693 James A. Gieseke
2	Brookhaven National Laboratory Upton, NY 11973 Kamal K. Bandyopadhyay Morris Reich
1	EG and G Idaho, Inc. P.O. Box 1625 Idaho Falls, Idaho 83415 William C. Schutte
1	Fauske and Associates, Inc. 16W070 W. 83rd St. Burr Ridge, IL 60521 Hans K. Fauske
1	Harvard University 295 Upland Avenue Newton Highlands, MA 02161 Melvin W. First
1	Lawrence Livermore National Laboratory P.O. Box 808, L-221 Livermore, CA 94550 Billy C. Hudson
4	Los Alamos National Laboratory P.O. Box 1663 Los Alamos, NM 87545 Steve F. Agnew Steve Eisenhawer Thomas E. Larson Harold Sullivan

DISTRIBUTION (cont)

Number of copies

OFFSITE

1	MIT/Department of Nuclear Engineering 77 Massachusetts Ave. Room 24-102 Cambridge, MA 02139 Mujid S. Kazimi
1	NUCON P.O. Box 29246 Columbus, OH 43229 Louis Kovach
3	Oak Ridge National Laboratory Emory D. Collins P.O. Box 2008 7930, MS-6385 Oak Ridge, TN 37831-6385 Charles W. Forsberg P.O. Box 2008 MS-6495 Oak Ridge, TN 37831-6495 Thomas S. Kress P.O. Box 2009 9108, MS-8088 Oak Ridge, TN 37831-8088
1	Oak Ridge National Laboratory David J. Pruett P.O. Box 2008 4501, MS-6223 Oak Ridge, TN 37831-6223
1	Rice University 5211 Paisley Houston, TX 77096 Andrew S. Veletsos
1	Sandia National Laboratory P.O. Box 5800 Albuquerque, NM 87185 Scott E. Slezak

DISTRIBUTION (cont)

Number of copies

OFFSITE

4	Science Applications International Corporation 12850 Middlebrook Road Trevion I, Suite 300 Germantown, MD 20874 Ray S. Daniels (3) John M. Saveland
1	West Valley Nuclear Services Co., Inc. Rock Springs Road (Box 191) West Valley, New York 14171 David K. Ploetz
1	Westinghouse Idaho Nuclear Co., Inc. 1955 Freemont Ave P.O. Box 4000 Idaho Falls, Idaho 83403-4000 Alan P. Hoskins
1	Westinghouse Savannah River Company P.O. Box 616, 703-H Aiken, South Carolina 29802 Paul d'Entremont